Design for the In- and Outlet Structure of the Energy Storage Lake within the Delta21 Plan

Y. Paasman

Technische Universiteit Delft

Ballast Nedam

TU Delft

Design for the in- and outlet structure of the Energy Storage Lake within the Delta21 plan

Yordi Paasman
4221346

B.Sc. in Civil Engineering, Delft University of Technology, 2017

Thesis Submitted in Partial Fulfillment of the
Requirements for the Degree of
Master of Science

To be presented publicly on Friday March 13th, 2020 at 15:30h.

Thesis committee:

Dr. ir. M. A. N. Hendriks	TU Delft, supervisor
Ir. L. J. M. Houben	TU Delft
Dr. ing. M. Z. Voorendt	TU Delft
Ing. G. F. van der Woerdt, MBA	Ballast Nedam

Structural Engineering
Hydraulic Structures
Delft University of Technology
The Netherlands

An electronic version of this thesis is available at `http://repository.tudelft.nl/`.

ABSTRACT

Yordi Paasman, Structural Engineering, University of Technology Delft
Abstract of Master's Thesis, Submitted 05 March 2020:
Design for the In- and Outlet Structure of the Energy Storage Lake within the Delta21 Plan.

This thesis aims to come up with a preliminary design for the in- and outlet structure, in which pump-turbines are housed, of the energy storage lake within the Delta21 plan. The goal is to come up with a feasible, cost-effective and lasting solution, that can store green energy, pump out 10 000 m^3/s of water and retain design storms, the classic design steps are followed.

The method followed, starts with an analysis of the problem, giving insight to the relevant stakeholders and functions that should be included. These elements lead to the Program of Requirements, which contains research into the tailor-made pump-turbine system and present-day water levels. The analysis ends in presenting the boundary conditions.

This thesis continues with several concepts that fulfil the functions and requirements. For those concepts, the possible construction methods are described, and checks are performed to verify the stability, including 1) piping, 2) rotational stability, 3) sliding, 4) bearing capacity and 5) (static) floating stability.

Using the evaluation criteria from the analysis, described after the Program of Requirements, and weighting factors, following from the stakeholder analysis, the value of the different alternatives is calculated via a Multiple-Criteria Decision Analysis and compared to each other, by including costs. The resulting alternative is presented in Figure 2 and Figure 3.

Lastly, one more iteration is made to check the strength of the walls and floors of the most desirable alternative.

It can be concluded that the most straightforward alternative, called 'Unity', is more cost-effective than an alternative integrated into the dune surrounding the energy storage lake. Also, the minimum width of that caisson, which is 53 m and follows from the pump-turbine system, can be achieved according to the stability checks. The author recommends checking the interaction between the spillway and the in- and outlet structure and model the foundation of the caisson more thoroughly.

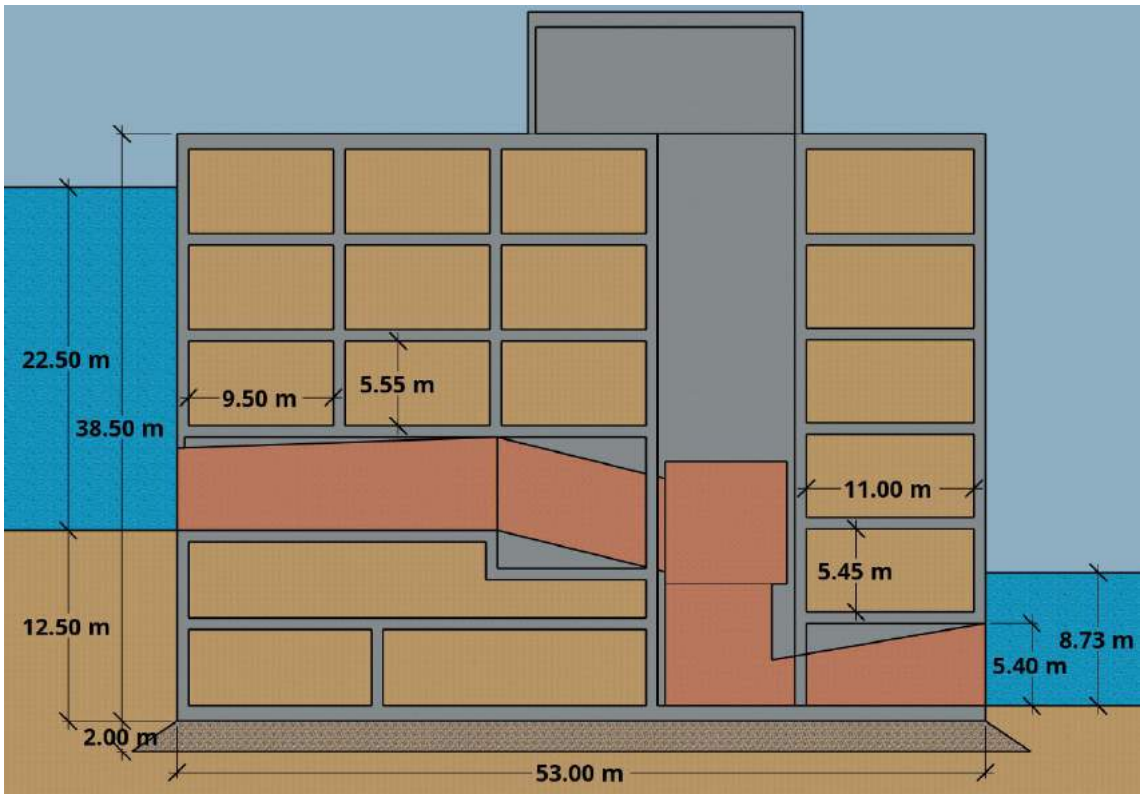

Figure 2: Final conceptual design in 2D.

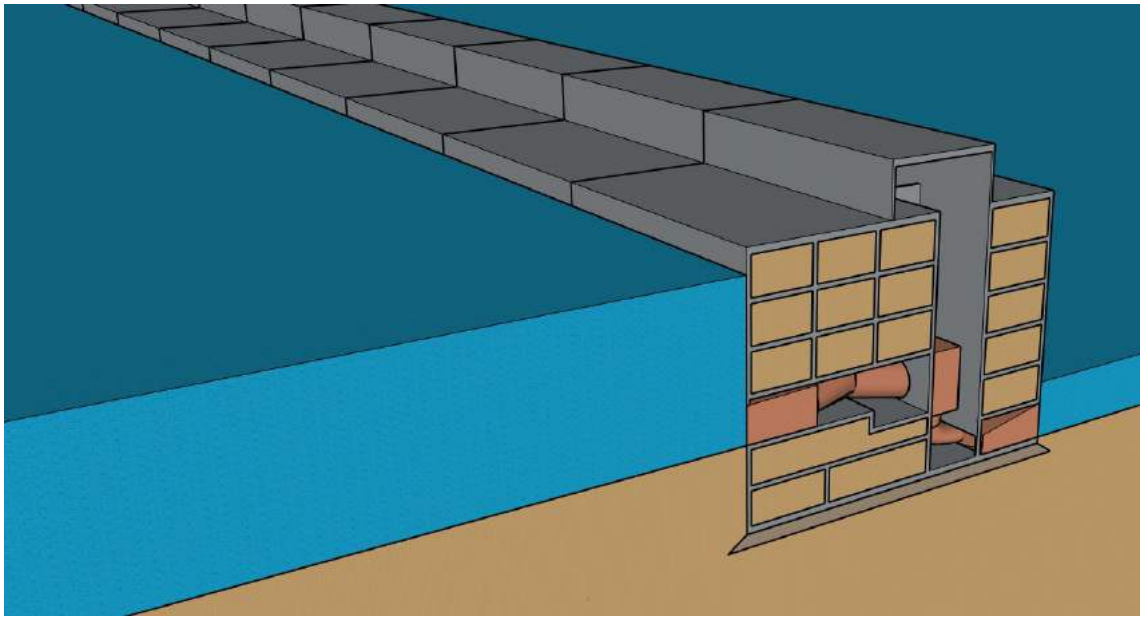

Figure 3: Final conceptual design in 3D.

Getting wisdom is the wisest thing you can do!
And whatever else you do, develop good judgment.

PROVERBS 4:7

PREFACE

This master's thesis followed by my interest in hydraulic structures. For over four years, I have worked as a tour guide at the Keringhuis, informing all kinds of people about the Delta Works and the Maeslant storm-surge barrier in particular.

It is with great pleasure that I can participate in a design that contributes to an expansion of the current Delta Works, within my field of study, namely the specialization of Hydraulic Structures in the master track Structural Engineering.

On a personal interest, I will try to combine the fields of hydraulic structures and structural engineering with sustainability. The latter is one of the most important subjects for the coming years, with many exciting challenges to solve.

This thesis is useful for everyone with interest in the Delta21 plan and in particular, interest in the pump-turbine design or the caisson closure of the energy storage lake. Furthermore, this thesis can be used to study an example of a standard design process in the field of Civil Engineering.

Special thanks for Ballast Nedam, in particular, Frank van der Woerdt and Bas Belfroid, for guiding me through the research for the thesis and offering a place to work at their office. Also, my thesis committee and Delta21 provided me with handy insights, knowledge, and feedback, for which I am grateful.

I want to thank my parents, Jan and Wilma, my sister Esmée and her boyfriend Danny, for the rest and support I find at their place and also my roommates, Thijmen and Mitchel, for the discussions and distractions I find with them.

Last, but certainly not least, my lovely girlfriend, Sophie, cannot remain unmentioned, for supporting me in all ways during this master's thesis.

Yordi Paasman
Delft, March 4, 2020

TABLE OF CONTENTS

LIST OF ABBREVIATIONS

CPT Cone Penetration Test

ESL Energy Storage Lake

FEM Finite Element Method

HAT highest astronomical tide

HR Hydraulische Randvoorwaarden primaire waterkeringen

KRM European Marine Strategy Framework Directive

LAT lowest astronomical tide

LCA Life Cycle Analysis

MCDA Multiple-Criteria Decision Analysis

MHWN mean high water neaps

MHWS mean high water springs

MLWN mean low water neaps

MLWS mean low water springs

MSL mean sea level

MW Megawatt

NAP Normaal Amsterdams Peil

PoR Program of Requirements

SLS Serviceability Limit State

TAW Technische Adviescommissie voor de Waterkeringen

ULS Ultimate Limit State

LIST OF SYMBOLS

The next list describes several symbols that will be later used within the body of the document.

Physics Constants

ρ_{sw}	Density of seawater (=1 025)	kg/m^3
g	Gravitational acceleration (=9,81)	m/s^2

Other Symbols

ρ	density
σ	stress
A	area
d	diameter
H	wave height
kg	kilogram
M	bending moment
m	meter
N	Newton (force)
V	shear force
W	Watt

CHAPTER 1

INTRODUCTION

The introduction presents the Delta21 plan, describes the motivation for this master's thesis and lastly, presents a reading guide for this report.

1.1 Overview Delta21

The Dutch Delta Works have been finished for a while now. Still, a delta commissioner is in function which is in charge of the Dutch Delta Programme. One of the new challenges for the Dutch flood protection is climate change, leading to sea-level rise, and the consequences it has on vulnerable cities like Dordrecht. The actual problem is further discussed in Subsection 2.2.1, but Delta21 promises to be part of the answer.

This master's thesis will be carried out following the Delta21 plan, a plan to increase the flood protection in the Haringvliet estuary.

As an overview: the Delta21 plan focuses primarily on flood protection, but also includes energy generation and storage, assures freshwater for Rotterdam and makes fish migration possible.

The main goal of Delta21 is to provide a future proof solution for the south-western delta of the Netherlands. The plan consists of an Energy Storage Lake (ESL) and a Tidal Basin and takes care of flood protection, energy storage and improving the ecology.

Figure 1.1 and Figure 1.2 provide an overview of Delta21.

The plan is to construct an energy storage lake, with an area of 20 km^2, off the coast of the Maasvlakte II. The pump-turbines within the energy storage lake will primarily be a way to pump out excess water from the Haringvliet, that will be necessary when the Delta Works are closed, and extreme river discharge is coinciding. However, those pump-turbines can also transform the energy storage lake into a battery via the principle of pumped hydro storage, which will be explained in Section 2.3. When the energy storage lake is realised, the old, salt, ecology and fish migration will be restored in the Haringvliet. The new salt ecology will be due to the permanently opening of the sluices of the Haringvliet.

Figure 1.1: Overview of Delta21.

Figure 1.2: Artist impression of the Energy Storage Lake and tidal lake.

1.2 Motivation for this Master's Thesis

This section gives an introduction to the origin and relevance of this master's thesis.

At this current date, the Netherlands is well prepared against flooding due to iconic projects like the Delta Works and the Dutch Room for the River Programme. However, we also observe a global sea-level rise that is accelerating "from 1,4 mm per year over the period 1901–1990 to 2,1 mm per year over the period 1970–2015 to 3,2 mm per year over the period 1993–2015 to 3,6 mm per year over the period 2006–2015 (high confidence)" (Oppenheimer et al. 2019).

According to (Deltacommissie 2008) the sea level rise that should be considered in the Netherlands is 0,65 to 1,30 m in 2100 and 2 to 4 m in 2200. Together with an expected increase in maximum discharge around 2100 of the Rhine (16 000 m^3/s to 18 000 m^3/s) and the Meuse (3 800 m^3/s to 4 600 m^3/s), the Dutch delta requires additional protection to high water levels.

More recent research, like (Deltares 2018a), show that the sea level rise can even reach levels of 2 to 3 meters in 2100 and 5 to 8 meters in 2200.

This master's thesis contributes to the broader Delta21 plan, to protect the Dutch delta against the combination of a storm surge on the sea and an extreme river discharge from the Rhine or the Meuse.

Furthermore, via the Delta21 plan, this in- and outlet structure will contribute to the Sustainable Development Goals (United Nations 2015). More specific to goal 7: "Affordable and Green Energy", by facilitating green energy storage in the form of Pumped Hydro Storage, and goal 9: "Industry, Innovation, and Infrastructure", since this innovation has potential to be applied all around the world.

1.3 Thesis Outline

This master's thesis follows a classic engineering design process, starting with an analysis in Chapter 2: 'Exploration of the Problem', Chapter 3: 'Basis of the Design' and Chapter 4: 'Boundary Conditions'.

The synthesis follows the analysis in Chapter 5: 'Functional Design' and the simulation in Chapters 6: 'Construction and Stability of Concept 'Unity' ', 7: 'Construction and Stability of Concept 'Duality' ', 8: 'Construction and Stability of Concept 'Integration' ' and Chapter 10: 'Strength Verification of the Most Favorable Alternative'.

The design process ends with Chapter 9: 'Evaluation of Alternatives', after which Chapter 12: 'Resulting Structure and Discussion' and Chapter 13: 'Conclusions and Recommendations' follows.

Part I

Analysis

CHAPTER 2

EXPLORATION OF THE PROBLEM

Firstly, this chapter gives an overview of the Dutch coastal protection, after it describes the Delta21 plan in more detail, followed by a more in-depth overview of the energy storage lake. Following that, a stakeholder analysis and function analysis will be performed. This chapter ends with the problem statement.

2.1 Overview of Dutch Coastal Protection

The Dutch delta has been exposed to many storm-surge floods in the past. A series of heavy storms and floods in the fourteenth and fifteenth centuries created the current geography of our delta (Meyer 2009). The massive storm of 1916, which caused extensive flooding (Lier and Steiner 1982), was perhaps the most decisive factor in closing off the Zuiderzee, currently 'IJsselmeer'. This enormous project, mainly consisting of constructing a large dam named the 'Afsluitdijk' that finished in 1932, land reclamation of the 'Wieringermeer', 20 000 ha, and a land reclamation project called 'Flevoland and the 'Noordoostpolder', 146 000 ha in total, that was finished in 1968 (Lier and Steiner 1982).

Now that the Zuiderzee delta was protected against storm surges, the Netherlands was still vulnerable in the south-western regions. The islands and estuaries of the province of 'Zeeland' and the province of 'Zuid-Holland' require many kilometres of dykes to protect the hinterland.

In 1953 the last major flooding, to this date, occurred in the Netherlands. This flood, with water heights up to almost four meters above Normaal Amsterdams Peil (NAP) or Amsterdam Ordnance Datum, the vertical datum used in large parts of Western Europe, resulted in a considerable loss of life, officially 1 836, and property due to breaches in approximately 180 km of coastal-defence dykes (Watson and Finkl 1992). The estimated damage was 1,5 billion guilders (Rijkswaterstaat 2019), currently 5,4 billion euro. It deserves notice that the disaster could have been much worse if the dykes in the 'Hollandse IJssel' would have collapsed and large parts of the 'Randstad', the economic and political centre of the Netherlands, would have been flooded. Please see Figure 2.1 for an overview of the flooded area.

Figure 2.1: Flooding of 1953, SOURCE: `https://nl.wikipedia.org/wiki/Watersnood_van_1953`.

To prevent such a disaster from happening again, the Delta Plan was put into effect trough a law in 1958. In that same year, the first Delta work was already finished building; namely, the storm surge barrier 'Hollandse IJssel', located at Krimpen aan den IJssel.

An overview of the constructed Delta Works and the construction types can be found in Table A.1 in appendix A.

A study of Rijkswaterstaat in 1970 of the environmental quality of the Scheldt-Rhine estuary was quite alarming (Meyer 2009). Repair of the estuary was considered necessary for the survival of the delta and the survival of many plants and fish in the area. Due to these findings, the decision was made to not fully damming the East Scheldt, but designing a flexible structure and maintaining the ecological balance in the estuary.

The Delta Project was completed in 1997 with the Maeslant storm-surge barrier, protecting the cities of Rotterdam and Dordrecht.

Currently, the Zuiderzee Works and the Delta Works are being looked at, concerning flood protection and ecology. At the time of writing of this master's thesis, the 'Afsluitdijk' is being renovated to make it future proof. Main reasons for this are the expected acceleration of the sea level rise and more extreme weather events. Details regarding climate change are not discussed in this thesis, and the policy from Rijkswaterstaat is followed, which means designing with the most extreme climate scenario from the KNMI (RWS-WVL Waterkeringen 2018) unless the design is adaptable.

Also, the Delta Works have to be looked at concerning rising sea levels, extreme weather events and ecology. The scope of this master's thesis is limited to the Haringvliet and hinterland.

2.2 Main Pillars of Delta21

The Delta21 plan, introduced in Chapter 1, focuses mainly on three aspects: flood protection, energy storage and ecology. These aspects are each described in this section.

2.2.1 Flood Protection

The Delta21 plan will influence the flood protection in a densely populated area, with cities like Rotterdam and Dordrecht. In this area, among others due to subsidence and expected climate change, the expectation is that, without action, in 2050 30% of all dykes will be too low and in 2100 even 50% (Lavooij 2018c).

The current Delta Works protect the Dutch coast against flooding from the sea, as was explained in Section 2.1. When these barriers are closed for a longer time, the river discharge will lead to higher water levels in the hinterland and consequently increases the risk of flooding via rising river water levels. The Maeslant storm-surge barrier closes when the water level reaches NAP + 3 m in the city of Rotterdam or NAP + 2,90 m in the city of Dordrecht, which is expected to occur once every 10 to 20 years. Combining this with a frequency of failure, stated by the minister, of once in every 100 closures, the total frequency of failure is once every 1 000 to 2 000 years.

Currently, when the Maeslant storm-surge barrier is closed for a longer time, the barrier can be raised during mean low water neaps (MLWN) and kept floating on the water, to allow for water to flow underneath the barrier to the sea. On average once every ten years a prolonged storm will occur, during which the Maeslant storm-surge barrier not necessarily closes.

The most critical period for the hinterland is when the Maeslant storm-surge barrier is closed for a longer time, and the river discharge lies around 5 000 to 7 000 m^3/s (Lavooij 2018c). Instead of raising the dykes in the hinterland, Delta21 suggests adding an extensive pumping system in the Haringvliet to pump out the excess water. These pumps need to be able to pump out 10 000 m^3/s of water and also function as a turbine to store energy in the ESL.

Due to the Delta21 plan, the saltwater will intrude further into the hinterland, and that could pose a problem to the freshwater inlet that is now located around the island of Tiengemeten. To assure freshwater supply to the hinterland, two new water inlets will be realised closer to Dordrecht, indicated with black circles in Figure 1.1.

These measures aim to increase the flood protection of the downstream area and provide a maximum target water level of NAP + 2,5 m at Dordrecht. Meaning the surrounding dunes on the seaside in the Delta21 plan will become part of the primary flood defence system and that the dykes in this area do not need to be raised.

2.2.2 Energy Storage and Generation

In the Netherlands, the supply of so-called green energy rises quickly, mostly from wind turbines and solar energy, which are heavily dependant on the weather.

This means that, increasingly, there is on one side overcapacity, which is during the day when most of the green energy, in the form of solar energy, is produced and the energy demand is lower. On the other hand, also temporary shortages, in the morning or evening when the energy demand is the largest and less solar energy is produced. The occurring shortages currently keep conventional energy sources to producing, not green, energy.

Currently, the continuity of supply is provided by maintaining the existing overcapacity and shutting down the clean energy, 'curtailment', (Lavooij 2018b), because of limited options to store energy.

Within Delta21 the energy storage lake can temporarily store electricity as pumped hydroelectric storage with a maximum water height difference of 17,5 m and an average head difference of 14 m. Utilising pump-turbines, it should be possible to pump out a total volume of 10 000 m^3/s of water.

2.2.3 Ecology

The third main goal of Delta21 is to return the saltwater in the western Haringvliet and to restore the fish migration (Lavooij 2018a). Special care has to be taken to ensure freshwater in the eastern Haringvliet for agricultural purposes and the production of drinking water.

By constructing the in- and outlet structure and tidal power plant, a continuous flow of saltwater is guaranteed in the Haringvliet, and the Haringvliet dam can permanently be opened.

These measures should all enlarge the effect of the Kierbesluit, a decision from Rijkswaterstaat, to partly open the Haringvliet sluices to return the salt tide and ecology into the Haringvliet.

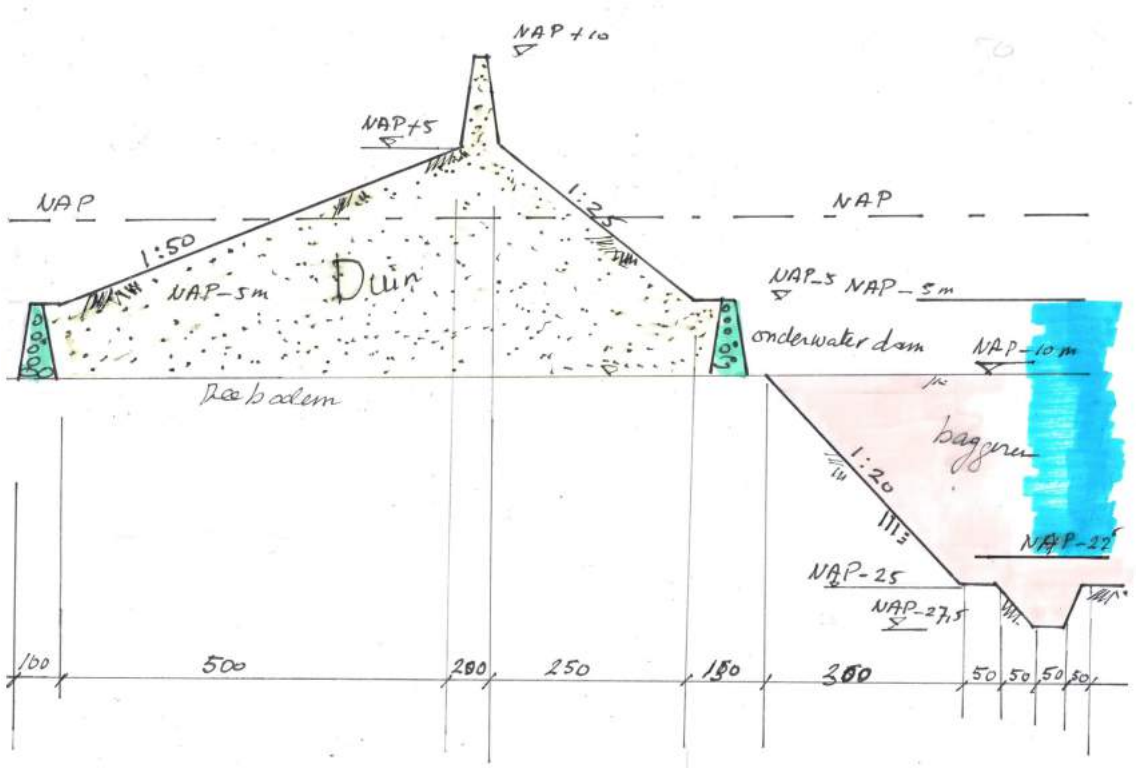

Figure 2.2: Overview of the sketched Delta21 sea dune, SOURCE: Delta21.

2.3 Energy Storage Lake

The energy storage lake will have a total volume of 350 mln m^3 (Lavooij 2018b). Sea dunes surround the energy storage lake with a gentle slope of approximately 1:30, a first global overview that requires further design and checks is given in Figure 2.2.

The in- and outlet structure will be located on the north side of the energy storage lake and the spillway on the south end. These structures consist of caissons with pump-turbines on the side of the North Sea and a spillway on the side of the Haringvliet. The bottom level of the energy storage lake will be situated between 25 m and 27,5 m below NAP and the lower, as a first estimate, and upper 5 m of the lake will not be used, because of pump requirements. This means that the water level within the energy storage lake can rise or fall with a maximum of 17,5 m and on average, 14 m will be utilized, also depending on the size of the pump-turbines. These levels are schematised in Section 4.1.4.

In the in- and outlet structure, several pump-turbines will be installed. With these pump-turbines, the ESL should be emptied in 12 hours. The bottom of the energy storage lake consists until NAP - 50 m of fine sand with some small layers of sand and silt. From NAP - 50 m until NAP - 60 m a ten-meter thick clay layer is present at the Maasvlakte II and it is assumed that this clay layer is also present underneath the energy storage lake.

More characteristics of Delta21 can be found in appendix B.

2.4 Existing Range Pump-Turbines

Existing pump-turbines, as will be used in the in- and outlet structure of the energy storage lake, are mostly applied in higher head areas. Figure 2.3 shows the application range of pump-turbines, according to Voith.

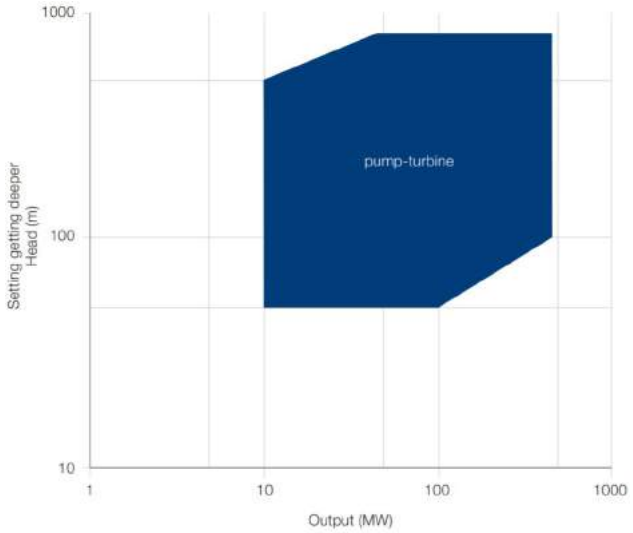

Figure 2.3: Application range of pump-turbines, SOURCE: Voith.

Some example project from General Electric (GE) run from the 72 m head project ALQUEVA II in Portugal (2 x 130 MW) to the 345 m head project SAMRANGJIN (2 x 340 MW) in South Korea.

2.5 Stakeholder Analysis

In this section, a stakeholder analysis is performed to identify what all the relevant wishes and requirements are. First, a list of stakeholders is created, then their involvement is analyzed to gain insight into their interest and power in the project. After that, their involvement in the project and the effect on the stakeholder is determined. Finally, all stakeholders are placed into a matrix, based on their interest and power, to be able to prioritize all wishes and requirements.

2.5.1 Stakeholder Inventory

In Table C.1 in Appendix C, an elaborate stakeholder list is presented. In the Appendix, the stakeholders who should be managed very carefully, meaning power and interest is minimal high, are described, except for the most important stakeholders. In this section, the stakeholders with both interest and power very high are described.

Rijkswaterstaat Rijkswaterstaat is the executive body of the Ministry of Infrastructure and Water Management and responsible for the design, construction, management and maintenance of the main infrastructure facilities in the Netherlands. According to their website, Rijkswaterstaat states: "We want to live in a country that is protected against flooding. A country where there is enough green and enough and clean drinking water. And where we can go from A to B quickly and safely."

This highlights the position of Rijkswaterstaat towards the project for flood protection and sustainability. Both the interest and power of Rijkswaterstaat are very high. Rijkswaterstaat will ultimately be the client of this project.

Ministry of Infrastructure and Water Management The Dutch Ministry of Infrastructure and Water Management, during the writing of this master's thesis, fall under the minister Cora van Nieuwenhuizen and state secretary Stientje van Veldhoven and is the ministry directing Rijkswaterstaat. As can be seen on their website: "The Ministry of Infrastructure and Water Management is committed to improving quality of life, access and mobility in a clean, safe and sustainable environment. The Ministry strives to create an efficient network of roads, railways, waterways and airways, effective water management to protect against flooding, and improved air and water quality." The Ministry also protects and manages the Natura 2000 areas.

According to the website of Natura 2000: "Natura 2000 is a network of core breeding and resting sites for rare and threatened species and some rare natural habitat types which are protected in their own right. It stretches across all 28 EU countries, both on land and at sea. The aim of the network is to ensure the long-term survival of Europe's most valuable and threatened species and habitats, listed under both the Birds Directive and the Habitats Directive."

Since the location of the energy storage lake is pointed out as a Natura 2000 area, both the interest and power of the Ministry are very high.

Port of Rotterdam As is stated on their website: "The objective of the Port of Rotterdam Authority is to enhance the port's competitive position as a logistics hub and world-class industrial complex. Not only in terms of size but also concerning quality. The core tasks of the Port Authority are to develop, manage and exploit the port in a sustainable way and to render speedy and safe services for shipping."

Because the energy storage lake will be built directly against the Maasvlakte II, the interest of the Port of Rotterdam is very high as well as their power.

Province of Zuid-Holland On the website of the province of Zuid-Holland it can be read that the province's five priorities are:

- Exploiting our economic potential;
- protecting the metropolitan delta;
- enabling the transition to a circular economy;
- ensuring a reliable and sustainable food supply;
- creating reliable and clean transport.

The first three bullets match with the goal and vision of Delta21, and since the project is proposed within the province's borders, the province has very high interest and very high power.

2.5.2 Stakeholder Matrix

Sorted on interest and power, the stakeholders can be categorized in a so-called stakeholder matrix, as is done below.

Interest ↑ / Power →	Low	Medium	High	Very High
Very High			*Hollandse Delta Water Authority*	*Rijkswaterstaat* *M-IenM: KWR + Natura 2000* *Port of Rotterdam* *Province of Zuid-Holland*
High		*Oyster and Mussel association* *Heat company Rotterdam*	*Delfland Water Authority* *Municipality of Dordrecht*	*M-IenM: Safety Against Flooding* *Delta Commissioner* *Municipality of Rotterdam*
Medium	*Milieudefensie*	*Evides* *WNF*	*Rivierenland Water Authority* *TenneT* *Ministry of Agriculture, Nature and Food Quality*	*Ministry of Economic Affairs*
Low	*Rijnland Water Authority* *Brabantse Delta Water Authority* *Municipality of Oostvoorne* *Fishermen's association* *Natuur & Milieu*	*Municipality of Goeree-Overflakkee* *Province of Noord-Brabant* *Sport Fishing Netherlands* *LTO Nederland*		

Figure 2.4: Stakeholder matrix.

The stakeholders in the upper right quadrant should be managed closely and in the upper left quadrant should be kept satisfied. The stakeholders in the lower right quadrant should be kept informed, and in the lower-left quadrant should be monitored.

2.5.3 Conclusion of Stakeholder Analysis

From the stakeholder analysis, it can be concluded that Rijkswaterstaat is the key player in this project as the future client, together with the Ministry of Infrastructure and Water Management, since it is a designated Natura 2000 area, the Port of Rotterdam and the Province of Zuid-Holland. From these four stakeholders, it follows that flood protection, sustainability, economic progress and ecological preservation and improvement are the main goals in designing a suitable in- and outlet structure for the energy storage lake.

Other important stakeholders, like the Water Authorities and Milieudefensie, support this conclusion. The outcome of the stakeholder analysis serves as a basis for the evaluation in Chapter 9.

2.6 Function Analysis

In this function analysis, the requirements from the client will be translated into solution-free functions, which can be distinguished in main functions and sub-functions. The Delta21 plan is primarily generated to increase the flood protection in the hinterland and has two more sub-functions, namely energy storage and ecology. These themes are also taken as the basis of the function analysis. The function tree, following these steps, is presented in Figure 2.5 for specifically the in- and outlet structure and in Figure 2.6 for the energy storage lake as a whole.

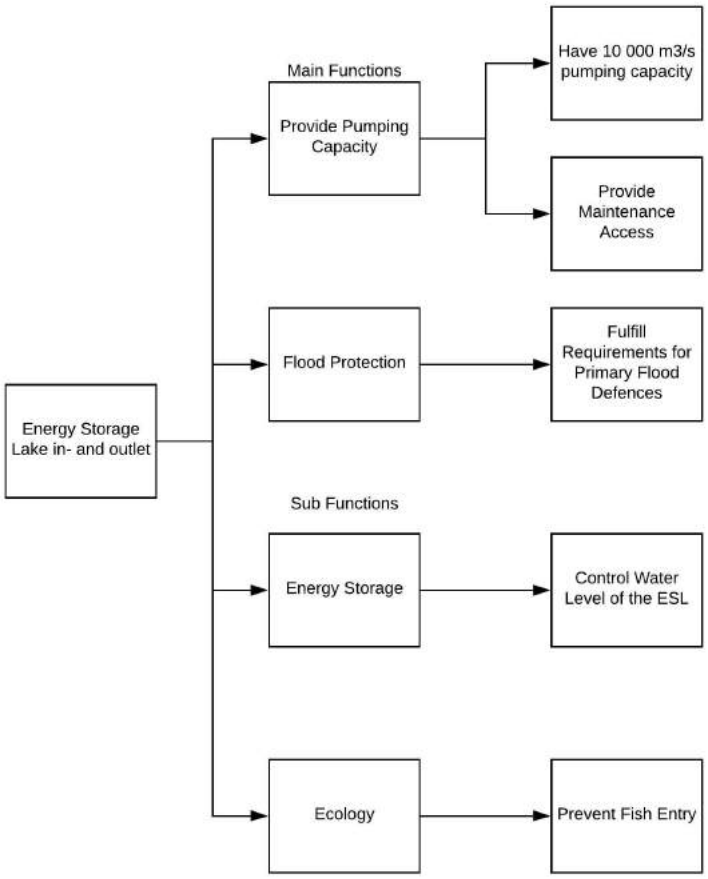

Figure 2.5: Function analysis tree of the ESL in- and outlet.

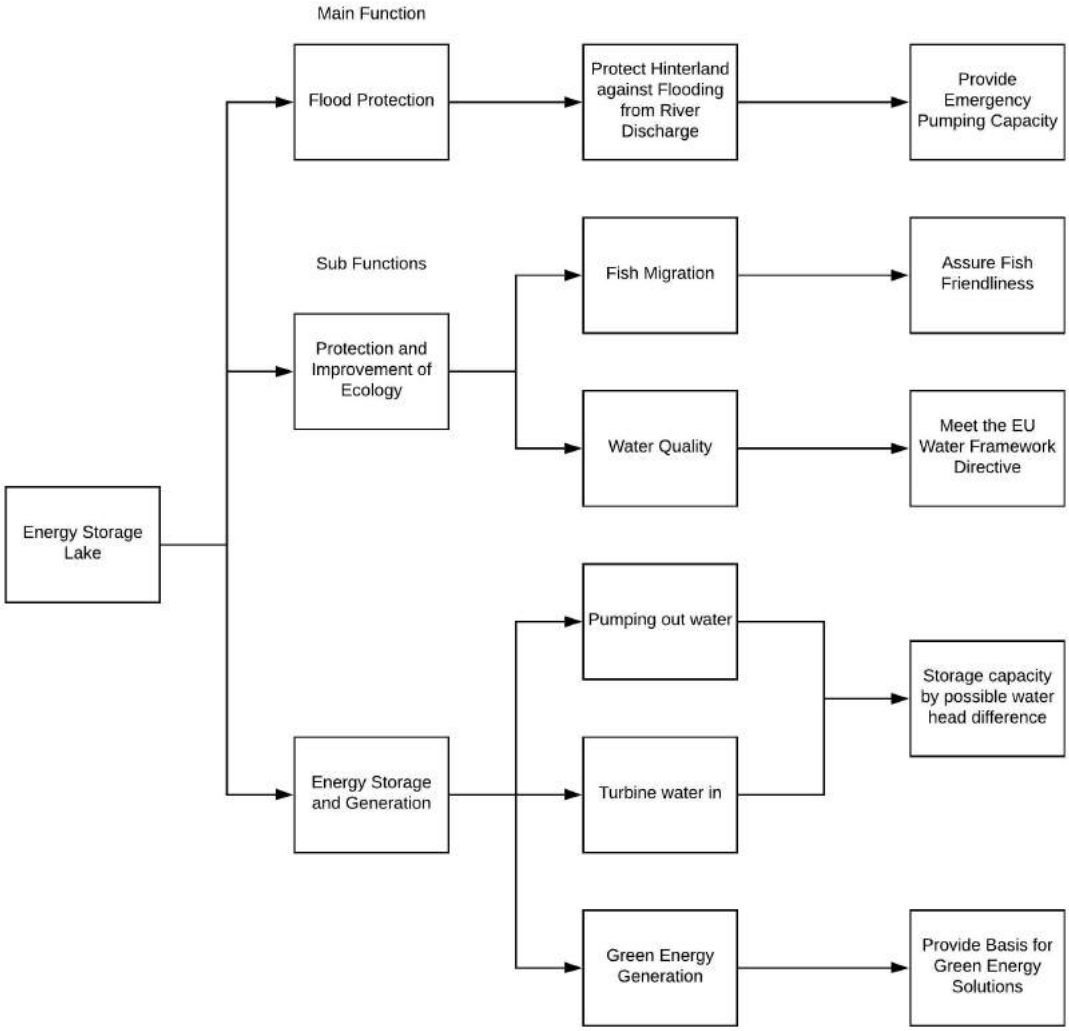

Figure 2.6: Function analysis tree of the energy storage lake.

2.7 Problem Statement

Currently, there is no designed solution for the energy storage lake that can reach the desired flood protection level, can store energy and preserve the ecology in the project area.

CHAPTER 3

BASIS OF THE DESIGN

The exploration of the problem, as described in Chapter 2, is taken as a basis to come up with the design objective. Secondly, the design method is described, and the scope is delimited, after which the Program of Requirements is compiled. Finally, the evaluation criteria are listed that will be used in Chapter 9: 'Evaluation of Alternatives'.

3.1 Design Objective

The objective of this study is to come up with a conceptual design for the in- and outlet structure of the Energy Storage Lake within the Delta21 plan and to provide input for the assessment of the feasibility of the project.

The design objective is to design a feasible, cost-effective and lasting solution, which can store energy, pump out excess water and retain design storms.

3.2 Design Method

The design method to address the problem statement and design objective, within the scope, will follow the regular design path that is taught in the bachelor study program of Civil Engineering via the lecture notes of 'Integraal Ontwerp en Beheer' (Hertogh, Bosch-Rekveldt, and Houwing 2018). These notes are based on a comparison between scientific research and engineering design (Eekels and Roozenburg 1991). This is systems engineering applied in civil engineering. That design method can be schematized as is done in Figure 3.1.

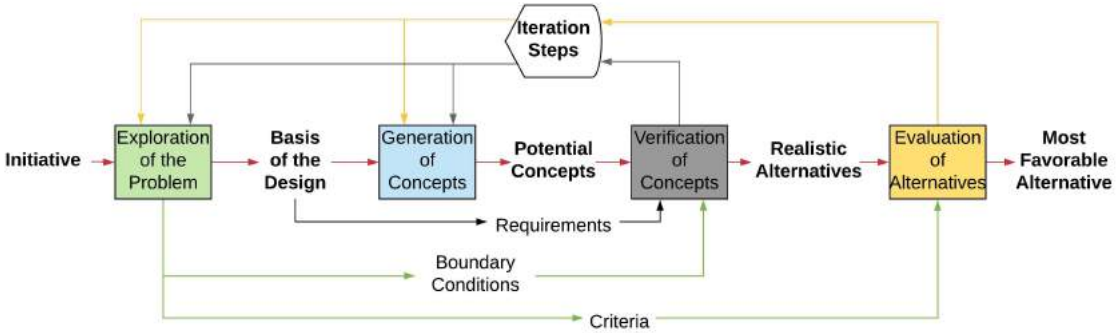

Figure 3.1: Flowchart design process.

In order to go through all the steps of the above-described design process, the following guideline of steps is used:

Firstly, for the exploration of the problem, presented in the previous chapter, the reports and expertise from Delta21 will be used. Interviews with, and reports from Pentair, a partner of Delta21, will be used to assess the pump-turbine installation and knowledge from the thesis committee and specialists within Ballast Nedam is used to come up with a stakeholder analysis, function analysis and the problem statement.

Secondly, the design objective, scope and program of requirements will follow naturally from the exploration of the problem. Relevant laws and regulations will be studied to determine all boundary conditions and then, the evaluation criteria will be listed, which also follows from Chapter 2: 'Exploration of the Problem'.

Thirdly, different concepts will be developed and presented graphically.

Fourthly, with a safety philosophy and determined failure mechanisms, the concepts will be verified, functionally and with regards to stability, also using available knowledge within the TU Delft and Ballast Nedam. This includes the main dimensions, the pump-turbine integration within the caisson, the construction methods and rough cost estimation, for which the budget department of Ballast Nedam will be used.

Finally, the alternatives that passed the verification will be evaluated using a multiple-criteria decision analysis (MCDA) and cost-value ratio. The most desirable alternative will undergo one more iteration, which will be a strength check of relevant walls and floors.

3.3 Scope

The outcome of this master's thesis is a conceptual design, so not all relevant aspects can be treated.

Please note that in the remainder of this master's thesis, the spillway between the energy storage lake and the tidal basin will not be considered.

In the generation of concepts, only caisson structures will be considered. This in- and outlet structure will need to facilitate several pump-turbines, resist the loads acting on the structure and provide sufficient protection against flooding of the hinterland. The pump-turbine installation will be designed by Pentair.

For the costs, only rough costs will be included, maintenance costs and project costs will be left out of the scope.

Outside the scope of this master's thesis will be:

- The design of the dune surrounding the energy storage lake;
- the connection between the dune and the in- and outlet structure;
- scour protection, due to turbulence and flow velocities;
- spillway design;
- interaction between the in- and outlet structure and the spillway;
- optimising the location of the in- and outlet structure;
- designing the closing mechanism on the seaside;
- the interconnection between the caissons.

Furthermore, the ecology is not treated, since that is part of the wider Delta21 plan. Also, the spatial integration of the concepts within the environment is left outside the design.

3.4 Program of Requirements

The program of requirements, described in this section, consists of functional requirements, such as pump-turbine properties, requirements coming from the primary flood defence system, technical requirements for reliability and availability, structural design requirements and requirements for retaining height and wave overtopping. This is in agreement with the old Dutch guideline for water barrier (Technische Adviescommissie voor de Waterkeringen 2003).

There are different types of technical requirements. A list of requirements, according to Rijkswaterstaat (Rijkswaterstaat 2005), is summarized in table 3.1.

Aspect	**Explanation**
Safety	Requirements concerning safety during realization and use phase of realized objects, for as well the user as for the surroundings.
Availability & Reliability	Requirements concerning availability, lifespan and reliability of realized objects.
Design	Requirements concerning the external design of realized objects.
Environmental hygiene	Requirements for dust, noise, vibrations and odour during realization and use phase.
Construction	Requirements to the construction of and adjustments to newly build and existing structures.
Maintenance	Requirements concerning required maintenance facilities and concerning maintenance processes (maintainability).
Sustainability	Requirements concerning the adaptation of realized objects to future expectations.
Demolition	Requirements concerning the demolition of objects to be demolished.

Table 3.1: Technical requirements, according to Rijkswaterstaat, SOURCE: (Rijkswaterstaat 2005).

Safety is treated in Section 6.3. Environmental hygiene is left out of the scope of this master's thesis, maintenance and construction are already covered in respectively Section 3.4.1 and 4.2. Sustainability is implemented in the design and verification phase, and demolition is not relevant for this project.

3.4.1 Functional Requirements

The functional requirements for the in- and outlet structure follow more or less directly from Section 2.6: 'Function Analysis'. The structure should be able to:

- Comply with the requirements for a primary flood defence;
  - Probability of failure, according to TAW 2003 guideline.
  - A closing mechanism on the seaside.
- Provide emergency pump capacity;
  - Minimum 10 000 m^3/s pump capacity.
- Be fish friendly;
  - Prevent fish entry.
- Store energy;
  - Include pump-turbine systems.
  - Empty the lake within 12 hours.
  - Crane-like structure and access for maintenance.
- Be structurally integer;
  - Stability.
  - Strength.
- Have a 100-year lifespan.

3.4.2 Primary Flood Defence System

The current primary flood defence system is shown in Figure 3.2. Since the Haringvliet barrier will be permanently opened and on the south side of the energy storage lake a spillway is located, the flood defence line will run over the in- and outlet structure of the energy storage lake, as indicated in Figure 3.3. The line cannot run over the spillway since the function prohibits it from closing.

Figure 3.2: Dutch norm frequencies, SOURCE: `https://waterveiligheidsportaal.nl/`.

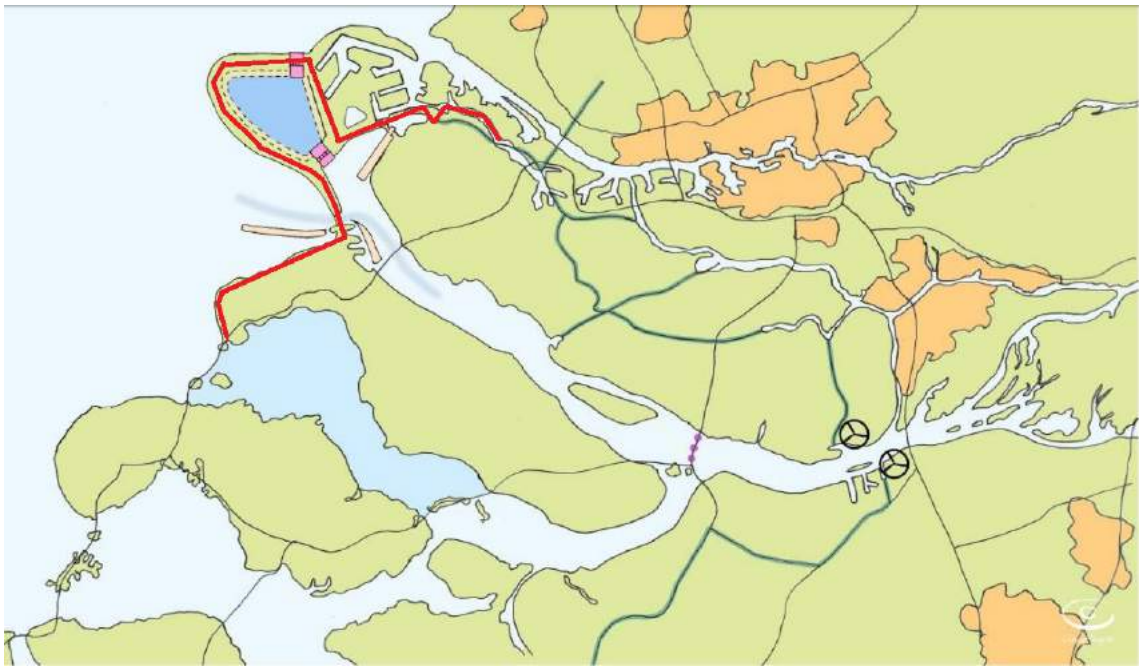

Figure 3.3: Primary flood defence line after the construction of Delta21.

3.4.3 Reliability and Availability

3.4.3.1 Reliability

Following the Water Act, that is summarized in (Rijkswaterstaat 2014a), the overall probability of failure for the in- and outlet structure should be 1/10 000 per year. Besides the resistance against possible failure mechanisms, also pumping capacity is considered in the reliability of the structure.

According to (Rijkswaterstaat 2014a) the probability of flooding of dyke ring 20 'Voorne-Putten' and dyke ring 25 'Goeree-Overflakkee' is respectively 1/100 per year and 1/340 per year, please refer to Appendix G, which is extremely low. Details can be found in Appendix G. The Delta21 plan, including this in- and outlet structure, directly affects the hinterland by protecting against a storm from the sea and lowering the water level in the estuary by pumping out excess water.

The latter also affects the dyke rings of 21: Hoekse Waard (1/170), 22: Eiland van Dordrecht (1/710) and 24: Land van Altena (1/160). Expected is that lowering extreme water levels will increase flood safety significantly.

The probability of flooding is defined as (RWS-WVL Waterkeringen 2018):

The probability of flooding is the chance of loss of water-retaining capacity of a dyke section so that the area protected by the dyke section floods in such a way that fatalities or substantial economic damage occur.

Since a probabilistic analysis is left out of the scope of this master's thesis, the old probability of exceedance approach is used in the design. So a water level that occurs once every 10 000 years.

Pump-turbines
For the replacement of a pump-turbine, approximately two weeks is needed. To assure the minimum discharge is always reached, 10% extra pump-turbines are assumed in the design.

Closure of Flood Defence According to (Technische Adviescommissie voor de Waterkeringen 2003) the reliability of closure for a flood defence is given as:

$$P_{fa} = P\{V_{open} > V_{acc}\} = P_{ns} \cdot N\{V_{open} > V_{acc}|ns\} = P_{ns} \cdot n_j < 0,1 \cdot norm \quad (3.1)$$

With: P_{fa} = probability of failure of the structure due to failure of closing mechanism [1/year]
P_{ns} = probability of failure closing process
$n_j = N\{V_{open} > V_{acceptable}|ns\}$ = frequency of exceeding acceptable inflow volume with opened structure [questions/year]
norm = the design or norm frequency, as stated in the Water Act.

To comply with the highest probability of failure allowed, a probability of failure of $0,1 \cdot 1/10\ 000 = 1/100\ 000$ per year is taken into account. A detailed calculation for acceptable inflow volume is left outside the scope since there are too many uncertainties in the Delta21 plan.

3.4.3.2 Restrictions

The Dutch storm season is defined from October 1 until April 15. In this season, all works regarding water barriers are prohibited by law, which is the Dutch Water Act.

It means no construction activities can go on in this period, and no maintenance activities can take place.

This had implications for the planning of the construction, which are out of the scope of this thesis. Also, for maintenance, this requires a strict scheme, with preventive maintenance measures.

3.4.4 Sustainability of Concrete

"Except for water, concrete is the most consumed material in the world by mass. With an estimated yearly consumption approaching 30 billion tonnes, concrete outpaces the per capita production of any other material, and the demand worldwide is ever-growing (Monteiro, Miller, and Horvath 2017)."

By producing one tonne of cement, approximately one tonne of CO_2 is released, making it responsible for 8-9% of the global anthropogenic CO_2 (Monteiro, Miller, and Horvath 2017). One solution to decrease the amount of cement used in the concrete mix is to partly replace the, generally used, Portland cement by industrial by-products. These products can be either coal fly ash or iron blast-furnace slag. Special care has to be taken that the properties of these products will only enhance the concrete properties, and not decrease them.

Another solution is to reduce the CO_2 emissions by adopting 'carbon capture and storage' or 'carbon capture and reuse' technologies in cement production, but this is still uneconomical (Monteiro, Miller, and Horvath 2017).

It is recommended to go with the first solution in this project to increase sustainability.

3.4.5 Structural Design

The structural requirements are the requirements for the structure to fulfil all functional requirements. For this project, the structural requirements are to:

- Resist all failure mechanisms;
  - Comply with the codes and guidelines.
- Carry the pump-turbine system and provide maintenance access;
- have a practical construction method.

Structurally, this master's thesis aims to consider different construction methods and give insight into the stability and strength of the concepts:

- Describe possible construction methods and split the individual construction steps to come up with different loading scenarios;
- determine the main dimensions of the concepts by doing several stability checks:
  - static floating stability,
  - shear criterion, or sliding,
  - turn-over criterion
  - bearing capacity subsoil.

The caisson alternative that is the most desirable after the evaluation will be iterated in the following steps:

- Execute strength verification in the governing load situation for the most favourable alternative, including:
  - shear strength,
  - bending moments
  - crack width.

3.5 Evaluation Criteria

The evaluation criteria that follow from Chapter 2 and 3 that will be used in Chapter 9, are listed below:

- Adaptability,
- ease of construction,
- ease of maintenance,
- energy efficiency,
- material use,
- risk.

For the evaluation, the created value, benefit, will be weighed against the costs in a cost-benefit analysis.

These criteria are not prioritized or weighted yet. It is done in Section 9.2: 'Weighting Factors'.

CHAPTER 4

BOUNDARY CONDITIONS

The boundary conditions are split up in three parts, namely:

1. **Functional** boundary conditions, such as transport access and pump-turbines;
2. **legal** boundary conditions, such as laws, codes, guidelines and destination plans;
3. **environmental** boundary conditions, such as water levels, wave heights and geotechnical conditions.

The end of the chapter gives a summary of the boundary conditions, to understand the remaindering chapters better.

4.1 Functional Boundary Conditions

4.1.1 Surroundings

As was indicated in Section 2.2.3, the proposed project location is Natura 2000 area, as is also indicated with green in Figure 4.1a, with accessory access restriction of the Voordelta in Figure 4.1b.

(a) Natura 2000 area. **(b)** Access restriction Voordelta.

Figure 4.1: Natura 2000, SOURCE: `https://www.noordzeeloket.nl/atlas-actueel/`.

Compensation for loss of Natura 2000 area is part of the bigger Delta21 plan and shortly described in Section 2.2.1. Broadly, returning the salt tide in the Haringvliet and creating two new freshwater inlets acts as compensation. The access restriction for relevant areas is recorded in the legal decision 'Toegangsbeperkingsbesluit Bollen van de Ooster en Bollen van het Nieuwe Zand'.

Furthermore, an electrical cable and telecom cable run across the project location as can be seen in Figure 4.2. Dealing with these cables is left outside the scope since the proposed structure is not located around the cables.

Figure 4.2: Electrical and telecom cables, SOURCE: `https://www.noordzeeloket.nl/atlas-actueel/`.

Other, less relevant, functional boundary conditions are given in Appendix E, Section E.6.

4.1.2 Requirements for Pump-Turbines

The pump-turbines that are assumed to be Francis turbines, 'mixed flow', with pumping function. Detailed pump-turbine calculations, checked by Pentair, can be found in Appendix F, but results are discussed below. When the total width of all pump-turbines, directly placed beside each other, without partition walls, necessary for the emergency pump capacity, which is 10 000 m^3/s, is plotted on the x-axis and the discharge Q is plotted on the y-axis, Figure 4.3a is the result. When the discharge is plotted against the power, both per pump-turbine, the result is Figure 4.3b.

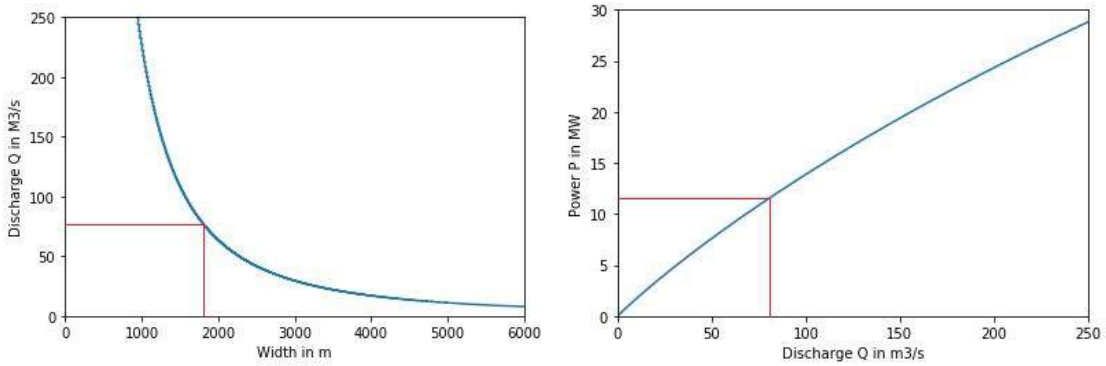

(a) Total width versus discharge.

(b) Discharge versus power.

Figure 4.3: Discharge Q versus total width and power.

Other important factors in the determination of the pump-turbine size are the total generated energy and the costs. The total generated energy, combining all required pump-turbines, depends on the size and number of applied pump-turbines. By plotting the discharge per pump-turbine against the total generated energy of all required pump-turbines, taking the emergency pump capacity as the starting point, the result is shown in Figure 4.4a. The energy generated by all applied pump-turbines is plotted against the discharge capacity of one pump-turbine.

Assuming a fixed price per generated kW of €500, which is an assumption from Pentair, the total costs can be estimated as is done in Figure 4.4b, where the total costs of all required pump-turbines are plotted against the discharge of one pump-turbine. That both figures are scattered at higher discharges can be explained because the number of required pump-turbines is a rounded number, only depending on the emergency pump capacity.

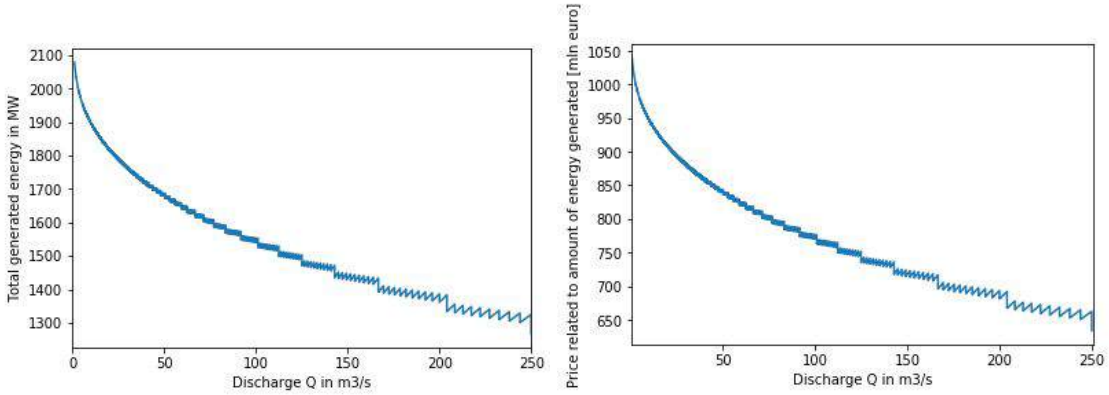

(a) Discharge versus generated energy.

(b) Discharge versus costs in mln euro.

Figure 4.4: Discharge Q versus generated energy and costs.

From those graphs, a pump-turbines discharge capacity of 80 m^3/s is chosen, since then one enters the steep region of the total width versus discharge graph and the discharge versus cost graph enters the, more or less, linear region. It means a corresponding power per pump-turbine of 11,47 MW. Then, looking at the requirement for emergency pump capacity, some $\frac{10\,000}{80} = 125$ pump-turbines are needed, which will generate 1 583 MW of energy, considering 10% extra pump-turbines for maintenance purposes, making 138 numbers in total.

The 11,47 MW pump-turbine comes with an inlet impeller diameter of 4,92 m, which requires an outlet impeller diameter of 6,11 m. Estimated costs of pump-turbines lay around €500/kW, which is added to €5,7 mln for a single 11,47 MW pump-turbine and €791,5 mln in total.

4.1.3 Pump-Turbine Dimensions

The dimensions of the in- and outlet of the pump-turbines are determined according to (U.S. Army Corps of Engineers 1994). The dimensions followed are shown in Figure 4.5a and Figure 4.5b

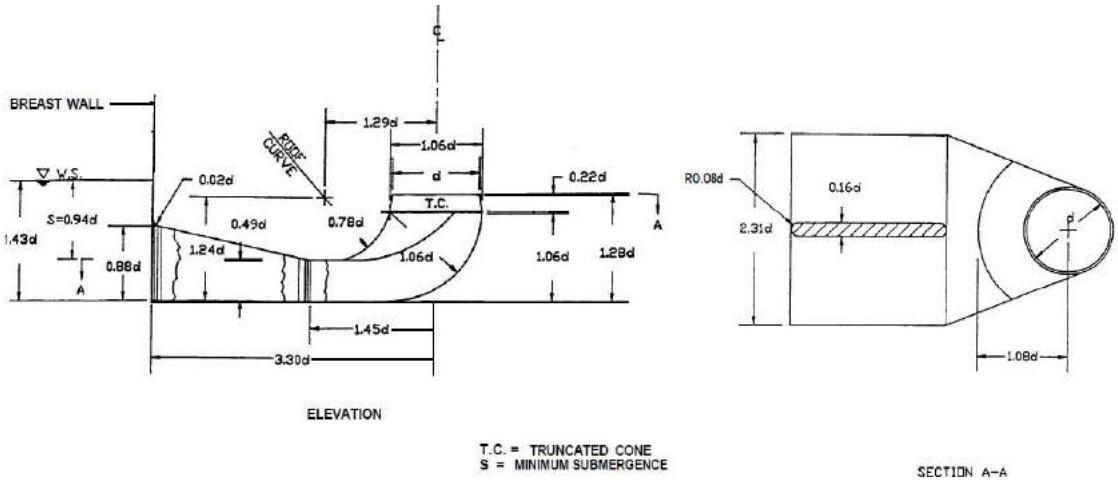

(a) Overview of pump-turbine dimensions. **(b)** Cross-section AA of Figure 4.5a

Figure 4.5: Pump-turbine dimensions, SOURCE: (U.S. Army Corps of Engineers 1994).

This means that the rectangular inlet will have dimensions (width x height) 11,37 x 4,33 m and the outlet will have dimensions 14,11 m x 5,38 m.

The outlet needs at least 21 m length and the inlet needs at least 17 m length. Both will function as inlet and outlet, so a minimum required length on both sides is considered as 21 m. The pipe in between requires at least 11 m to overcome the height difference. These values added, lead to a minimum length of 53 m, in the width aspect of the caisson, and so perpendicular to the flow direction.

4.1.4 Visualisation of Water Levels

Following the previous Section, 4.1.2, the minimum water level on the energy storage lake is NAP - 18,8 m, the outlet should be submerged with 1,43 times the outlet pipe diameter. Consequently, the average head difference is 12,13 m. An overview can be found in Figure 4.6.

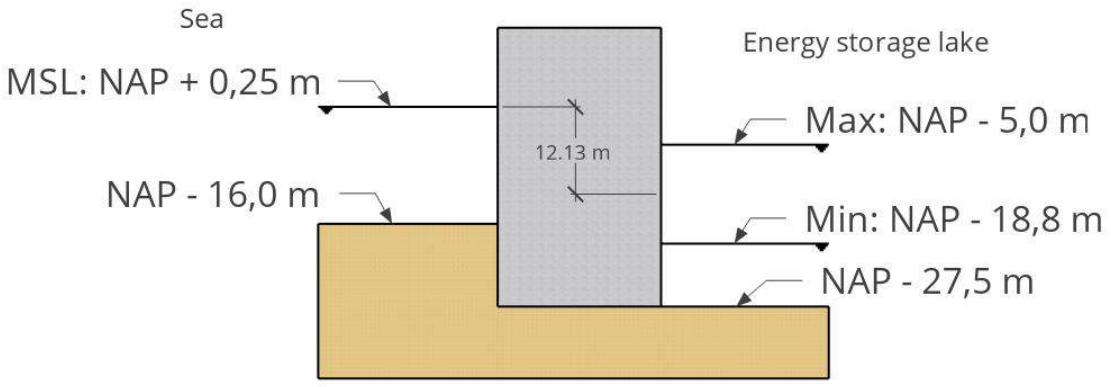

Figure 4.6: Overview of acting water levels.

4.1.5 Restrictions in Dimensions

Structurally, caissons can be dimensioned as large as is needed. Restricting factors in caisson design are floating capacity, building limitations or stability during transport. The largest caisson found volume-wise is 180 meters long, 88 meters wide and 47 meters high, which is a prestressed concrete chamber and is used as an offshore LNG terminal in the Adriatic Sea off the coast of Venice. The caisson was constructed in Algeciras and sailed for 21 days through the Mediterranean Sea to reach its final destination.

4.2 Legal Boundary Conditions

Like any civil project, this project needs to comply with Dutch laws and regulations. Firstly, the project falls directly under the Water Act from 2017. Also the in 2021 expected Environment & Planning Act will play a significant role in the project.

Overall, the Eurocode does not cover hydraulic structures, but where required, the Eurocode will be used as the leading guideline. For the design of hydraulic structures, also the British Code BS-06349 can be used.

There are, however, guidelines for designing hydraulic structures and storm surge barriers. Two of them, which will be used, are the TAW, 'Technische Adviescommissie voor de Waterkeringen / Technical Advisory committee for Water barriers', 2003 and the HR 2007, 'Hydraulische Randvoorwaarden primaire waterkeringen / Hydraulic boundary conditions primary water barrier'.

An overview of the relevant laws, regulations and guidelines is listed on the next page:

- Water Act, or 'Waterwet', 2017,
- European Floods Directive, incorporated in the Water Act,
- Spatial Planning Act, or 'Wet ruimtelijke ordening', 2006,
- Environmental Management Act, or 'Wet milieubeheer', 1993,
- Nature Conservation Act, or 'Natuurbeschermingswet', 1998,
- Flora and Fauna Act, or 'Flora- en faunawet', 1998,
- Environmental Licensing (General Provisions) Act, or 'Wet algemene bepalingen omgevingsrecht', 2010,
- Environment & Planning Act, or 'Omgevingswet', expected in 2021,
- Eurocode or other relevant codes,
- TAW 2003,
- HR 2007.

The most crucial legal boundary condition for the determination of hydraulic boundary conditions and the safety assessment is the 'Waterwet 2017', or the law on water 2017. In this law, the management and usage of all water systems are described. A ministerial regulation on the Waterwet is the 'Regeling veiligheid primaire waterkeringen 2017', Primary flood defence safety regulations 2017, where more details regarding the determination of hydraulic boundary conditions and strength assessment are given. An example is that for all dyke rings in the Netherlands, the probability of failure is determined, expressed in a signal value and a lower limit.

4.3 Environmental Boundary Conditions

Environmental boundary conditions consist out of:

- Meteorological boundary conditions, such as wind;
- hydraulic boundary conditions, such as water levels, wave heights and currents;
- geotechnical boundary conditions, such as soil layers and properties.

Morphological boundary conditions, which influences the need for dredging, are not considered in this design and are left out of the scope.

4.3.1 Meteorological Boundary Conditions

The governing wind directions and speeds are determined as meteorological boundary conditions. As can be seen in Figure 4.7, the governing wind direction is not perpendicular to the proposed in- and outlet structure.

According to the KNMI, the superstorm that could occur at the North Sea once in ten thousand years has a wind speed of 170 km/h, being 47,22 m/s. If one takes climate change into account, the KNMI predicts that the 170 km/h would occur every thousand years and the 1 / 10 000 years superstorm would have a wind speed of 200 km/h, converted 55,56 m/s. These values of the KNMI are average wind speeds over 12 hours at the height of two kilometres.

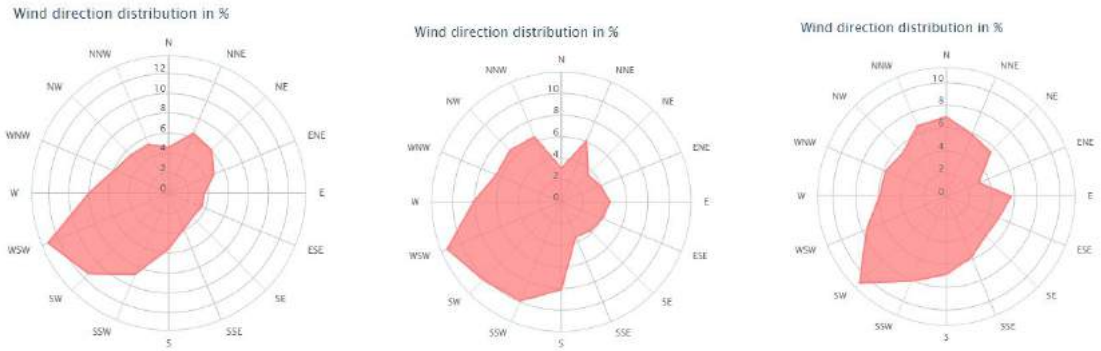

Figure 4.7: Wind distribution respectively in Lichteiland Goeree/Renesse, Hoek van Holland and Ouddorp, SOURCE: `https://www.windfinder.com/`.

For hydraulic calculations like, for example, wave conditions, the wind speed at the height of 10 meters above ground, or water, should be used. Converting the wind speed that is estimated at two kilometres height to 10 meters height, a wind speed of 34 m/s is found. Calculations and methods used to derive this wind speed can be found in Appendix D.

4.3.2 Hydraulic Boundary Conditions

Various hydraulic events have an influence on the in- and outlet structure of the energy storage lake. The events that will be explored are **water levels**, including the design storm, **wave conditions** and **currents**.

4.3.2.1 Water levels

Current water levels

The water levels on the North Sea near the Haringvliet are continuously being measured by the measuring station 'Haringvliet10', which is located on the location indicated in Figure 4.8.

These measurements have been analyzed by Rijkswaterstaat for the period between 1982 and 2010 (Rijkswaterstaat 2013) and are shown in table 4.1 and 4.2. These tables are based on (Dillingh 2013).

The project office 'Veiligheid Nederland in Kaart', or 'Safety of the Netherlands mapped', from Rijkswaterstaat analyzed the safety of all Dutch waterworks according to the risk approach (Rijkswaterstaat 2014a), following the Water Act. In other words, looking at the different failure mechanisms and calculating a combined risk of failure per dyke ring. Elements of this risk approach that will also be applied in this design are looking at the different failure mechanisms and taking the exceedance probability as one of the assumptions for the water level.

According to the Water Act, the lowest probability of failure at the surrounding dyke ring is 1 / 10 000, as can be seen in Figure 3.2. As has been stated in Section 3.4.3.1, an exceedance frequency of 1 / 10 000 will be used.

It means a water level of NAP + 5,00 m. This is higher than the water level the Haringvliet barrier is designed for, which is NAP + 4,80 m.

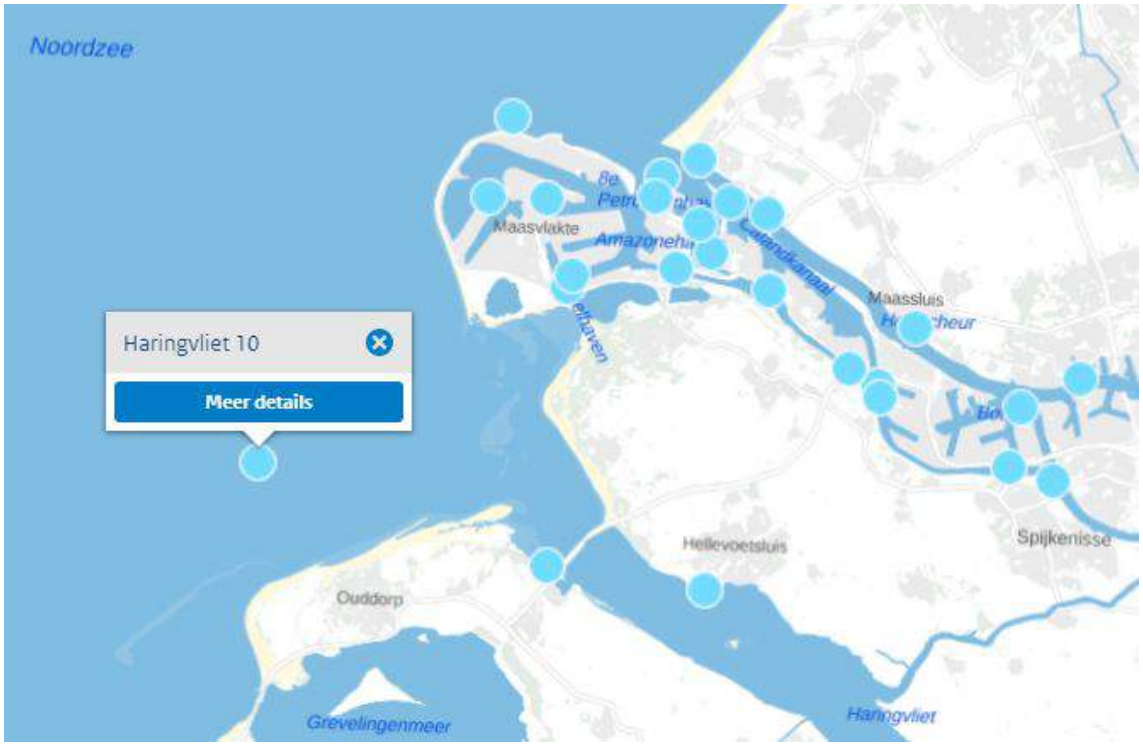

Figure 4.8: Measuring station Haringvliet10, SOURCE: `https://waterinfo.rws.nl/`.

	Final averages			Values lunar course	
Tidal type / quantity	**MHWN level**	**MLWN level**	**Tidal head**	**MHWN**	**MLWN**
Avg. springtide	145	-92	237	1:14	6:44
Avg. tide	124	-86	210	1:14	7:05
Avg. neap tide	93	-77	170	1:13	7:32
Avg. duration of rising				6:34	
Avg. duration of decrease				5:51	
Avg. water level		0			

Table 4.1: Water levels in cm compared to NAP from measuring station Haringvliet10, SOURCE: (Dillingh 2013).

Average exceeding and falling frequencies		
Frequency	**Exceeding high water levels**	**Fall below low water levels**
Once every 10 000 years	500	
Once every 5 000 years	480	
Once every 4 000 years	480	
Once every 2 000 years	450	
Once every 1 000 years	430	
Once every 500 years	410	
Once every 200 years	390	
Once every 100 years	370	
Once every 50 years	350	
Once every 20 years	320	
Once every 10 years	300	-205
Once every 5 years	280	-200
Once every 2 years	260	-185
Once a year	245	-170
Twice a year	230	-165
Five times a year	210	-150
LAT		-127

Highest known value	306 cm 9 Nov 2007	Period 1982 - 2010
Lowest known value	-215 cm 12 Mar 1996	Period 1982 - 2010

Particularities:
- 1 May 1981: Start of observations

Table 4.2: Exceeding and falling water levels in cm compared to NAP, the starting point is the measuring station Haringvliet10, SOURCE: (Dillingh 2013).

As has been stated in Section 2.3, the water level on the energy storage lake will vary between NAP - 22,5 m and NAP - 5 m.

sea-level rise
From 1890 to 2017, the Dutch relative sea-level rose with 24 cm, which is 1,9 mm per year (CBS et al. 2018). The trend in the data seems to have a linear pattern over the whole period.

Furthermore, subsidence of the sea bottom occurs along the Dutch coast with a speed of 0,2 mm per year (Barends et al. 2008), so the corrected value of the absolute sea-level rise can be set at 1,7 mm per year.

Lastly, (CBS et al. 2018) expects a corrected sea-level rise at the Dutch coast of 2,3 mm per year, due to the melting of ice caps at Greenland. In conclusion, the speed of sea-level rise that will be used in the remainder of this report is 2,3 mm per year, which means 23 cm in 2119, assuming a 100 year lifetime.

Global trends in sea-level rise show an acceleration nowadays. The Dutch sea-level rising does not show this acceleration, and it is not clear why this difference exists. The acceleration in global sea live rise is not taken into account in this report.

According to the KNMI climate scenarios (Hurk et al. 2014), the lowest sea-level rising expected around 2071-2100 is +25 cm to +60 cm, and for the highest predicted scenario, this is +45 cm to +80 cm.

Estimating the water levels, according to Hydra-NL [P.1] and Riskeer [P.2], used for designing and examining existing structures, gives values indicated in Table 4.3.

Riskeer

	h [m + NAP]
Dyke segment 25-1	5,44
Dyke segment 20-1	5,40

Hydra-NL	Climate scenario G	Climate scenario W+
Haringvliet barrier	h [m + NAP]	h [m + NAP]
1 / 10 000	5,639	6,139
Maasvlakte	h [m + NAP]	h [m + NAP]
1 / 10 000	5,287	5,787
Dyke ring 25-1	h [m + NAP]	h [m + NAP]
1 / 10 000	5,503	6,003

Table 4.3: Expected water levels according to Hydra-NL and Riskeer.

Wind set down

A quick check for the wind set down in the energy storage lakeside is performed. For an open system the following basic formula is valid:

$$\frac{\delta h_1}{\delta x} = \frac{k \cdot u^2 \cdot cos\,(\phi)}{g \cdot h} \tag{4.1}$$

For a closed lake, like the energy storage lake, the formula can be rewritten as (Jonkman et al. 2018):

$$\delta h_1 = 0,41 \cdot k \cdot \frac{u^2}{g \cdot h} \cdot F \cdot cos\,(\phi) \tag{4.2}$$

The factor 0,41 is determined from the shape of the lake, which is assumed to be an isosceles trapezoid. Details are worked out in Appendix E.

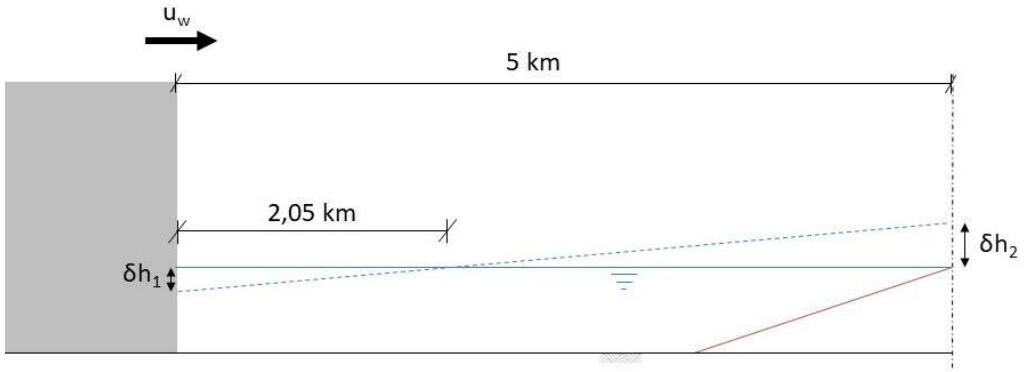

Figure 4.9: Wind set up and set down.

The lowest water height is 7,83 m, and the highest level is 22,5 m. By filling in all the parameters, the wind offset equals 0,10 m at the structure with the lowest water height (negligible) and 0,03 m at high water, which was expected to be lower.

On the side of the North Sea, the design water level is governing, since this already includes wind setup.

Design extreme water levels

Assuming a sea-level rise of + 80 cm in 2085, using climate scenario W+ from the KNMI is advised in designing new structures (Rijkswaterstaat 2014b). The design water level of NAP + 6,50 m in 2100, the highest value from Hydra-NL with added short-term atmospheric depressions of 0,30 m, is assumed as governing high water level (GHW). The most extreme water level difference is sketched in image 4.10. It is the most extreme scenario: that the design storm occurs at the side of the North Sea and the water level on the lakeside is the lowest possible, including wind set down.

Furthermore, the highest possible water level in the energy storage lake, NAP - 5,0 m, and the lowest possible water level on the seaside, NAP - 2,0 m, see Table 4.2, are indicated. The wave height is given as the significant wave height.

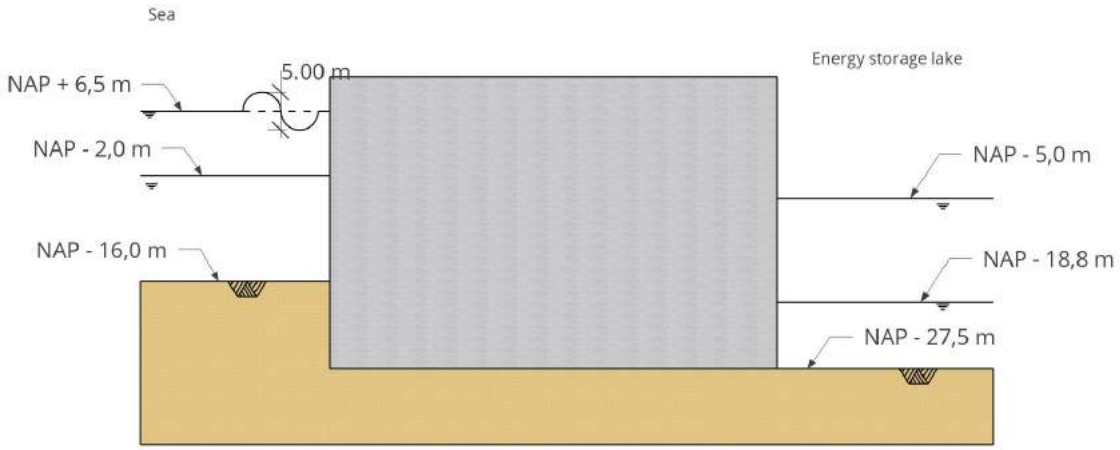

Figure 4.10: Most extreme water level difference.

4.3.2.2 Waves

To determine the governing wave conditions at the location of the in- and outlet structure, three methods are compared to each other. Namely via **existing reports and literature**, via **modelling software** and via **hand calculations**. In this section, only the results of these studies are presented, more details are given in Appendix E, Section E.2.

Existing reports and literature
For various measuring stations on the North Sea, the present wave conditions are presented, and predictions have been made to a once every 10 000 year scenario. An overview of these results is given in Table 4.4.

Location	Depth [m]	Hm0 [m]	Tm-1,0 [s]	Tm02 [s]	Tp [s]
MPN	18	7,96	12,7	9,46	15,3
EUR	32	8,19	11,3	8,74	12,7
LEG	21	8,08	11,2	8,56	12,9
SWB	20	7,06	10,8	8,15	12,3

Table 4.4: Data which is obtained from wave measuring stations, SOURCE: (Heijer et al. 2006).

Modelling software
Two types of modelling software have been used to predict the wave conditions at several points across the Dutch shoreline. The software is discussed in Appendix P, and detailed information about the followed procedure can be found in Appendix E, Section E.2. The obtained results are summarised in Table 4.5.

Riskeer

	Hs [m]
Dyke segment 25-1	5,44
Dyke segment 20-1	3,46

Hydra-NL	Climate scenario G	Climate scenario W+
Haringvliet barrier	Hs [m]	Hs [m]
2023	3,402	3,402
2050	3,414	3,490
2100	3,490	3,666
Maasvlakte	Hs [m]	Hs [m]
2023	8,926	8,926
2050	8,914	8,985
2100	8,985	9,147

Table 4.5: Wave data from Riskeer and Hydra-NL

Hand calculations

Lastly, hand calculations are performed according to Bretschneider:

$$\widetilde{H} = 0,283 \cdot \tanh\left(0,53 \cdot \tilde{d}^{\,0,75}\right) \cdot \tanh\left(\frac{0,0125 \cdot \widetilde{F}^{\,0,42}}{\tanh\left(0,53 \cdot \tilde{d}^{\,0,75}\right)}\right) \tag{4.3}$$

$$\widetilde{T} = 7,54 \cdot \tanh\left(0,833 \cdot \tilde{d}^{\,0,375}\right) \cdot \tanh\left(\frac{0,077 \cdot \widetilde{F}^{\,0,25}}{\tanh\left(0,833 \cdot \tilde{d}^{\,0,375}\right)}\right) \tag{4.4}$$

A water depth of 22,5 m is taken, which is NAP + 6,5 m storm setup. The results are presented in Table 4.6.

Wind Direction [Degrees N]	**Wind Speed (1/10 000 yrs) [m/s]**	**Fetch F [km]**	**Significant wave height Hs [m]**	**Peak wave period Tp [s]**
0	34	430	5,0	9,8

Table 4.6: Wave calculations, according to Bretschneider.

Design wave conditions

For the significant wave height, the calculated wave height, according to Bretschneider, is taken a starting point in the design, as these values correspond roughly to the reports and models. Due to this, a H_s of 5,0 m is assumed as significant wave height in extreme conditions. Peak wave period T_p will be 9,8 s. It also falls within the limitations of:

$$H_s \leq 0,5 \cdot d \quad : \quad 5,0 \leq 0,5 \cdot 22,5 = 11,3m \tag{4.5}$$

Wavelength
To determine the wavelength, the depth characteristic, $\frac{h}{L}$, should be determined, according to Table 4.7 from (Molenaar and Voorendt 2019).

Relative depth **Characteristics**	**Shallow water** $\frac{h}{L} < \frac{1}{20}$	**Transitional water depth** $\frac{1}{20} < \frac{h}{L} < \frac{1}{2}$	**Deepwater** $\frac{h}{L} > \frac{1}{2}$
Wavelength (L)	$L = T \cdot \sqrt{g \cdot h}$	$L = \frac{g \cdot T^2}{2\pi} \cdot \tanh(k \cdot h)$	$L = L_0 = \frac{g \cdot T^2}{2\pi}$
$k = \frac{2\pi}{L}$			

Table 4.7: Wavelength table, SOURCE: (Molenaar and Voorendt 2019).

It is an iterative process, with the result that the wavelength is 122 m and it is a transitional water depth, with characteristic $\frac{1}{20} < \frac{h = 22{,}5\ m}{L = 122\ m} = 0,18 < \frac{1}{2}$.

4.3.2.3 Currents

There is very little to say about currents at the proposed project location, due to the changing morphology of the area after the realisation of Delta21. Also, the proposed in- and outlet structure will be located in the shelter of the Maasvlakte II, and the dunes of the energy storage lake and the structure will impose currents itself from the pumping of the water. For these reasons, currents are left out of this project.

Currents through the caisson can be determined by dividing the discharge over the area of the outlet. This results into a flow velocity of $\frac{80\ \text{m}^3/\text{s}}{14{,}11\ \text{m} \cdot 5{,}38\ \text{m}}$ = 1,05 m/s.

4.3.3 Geotechnical Boundary Conditions

The DINOloket web application is used to determine the geotechnical boundary conditions. Cross-sections, presented in Appendix E, Section E.3, are used for the global positioning of different soil layers and data from three Cone Penetration Test (CPT) locations, indicated in Appendix E, Section E.4, are used to determine the soil properties.

The cross-sections confirm the clay layer around NAP - 50 m, but it seems the clay layer is slightly smaller than 10 m in thickness.

The CPT's show that the structure will be directly located on gravely sand. From these data, the soil parameters are summarized in Table 4.8.

Name	**Admixture**	**Consistency**	γ **[**kNm^3**]**	γ_{sat} **[**kNm^3**]**	q_c **[MPa]**	C'_p	C'_s	C_c / $(1 + e_0)$	C_α	$C_s w$ / $(1 + e_0)$	E_{100} **[MPa]**	ϕ' **[°]**	**c' [kPa]**	c_u **[kPa]**
Gravel	Weak silty	fixed/solid	19 or 20	21 or 22	30	1 200 or 1 400	∞	0,001 9 or 0,001 6	0	0,000 6 or 0,000 5	90 or 105	37,5 or 40	0	na
Gravel	Weak silty	Mediocre	18	20	25	1 000	∞	0,002 3	0	0,000 8	75	35,0	0	na
Sand	Clean	Loose	17	19	5	200	∞	0,011 5	0	0,003 8	15	30,0	0	na
Clay	Clean	Mediocre	17	17	1,0	15	160	0,153 3	0,006 1	0,051 1	2	17,5	5	50

Table 4.8: Soil parameters, SOURCE: Table 2.b (NEN-EN 1997-1+C1+A1/NB 2016).

A visualization of the subsoil from CPT S36H00032-01 is made in Appendix Section E.5. That CPT is chosen is because the three CPT's do not differ that much from each other and this one is the closest to the proposed project location. The soil profile is shown in Figure 4.11. Please note that the thickness and position of the solid clay layer are very uncertain and the assumption from Delta21 is used, meaning that the clay layer has a thickness of 10 meters and begins and NAP - 50 m. What can be concluded is that the caisson's foundation will be on gravely sand.

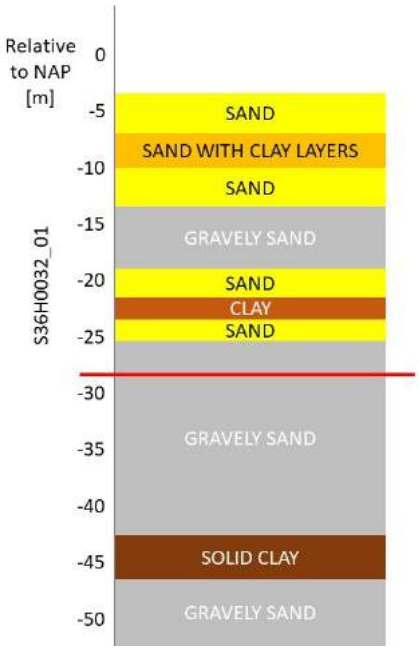

Figure 4.11: Soil profile of CPT S36H0032-01.

4.4 Overview of Relevant Boundary Conditions

In this section, a brief overview is given of relevant boundary conditions. Table 4.9 can be used as reference work for the remainder of this master's thesis.

Parameter	Symbol	Value	Unit
Pump-Turbine Discharge	Q	80	m^3/s
Number of Pump-Turbines	$N_{pump-turbines}$	138	No.
Sea Bottom Level	SBL	NAP - 16	m
Mean sea-level	MSL	NAP + 0,25	m
Maximum Water Level ESL	Max ESL	NAP - 5,0	m
Minimum Water Level ESL	Min ESL	NAP - 18,8	m
ESL Bottom Level	BESL	NAP - 27,5	m
Average Pumping Head Difference	ΔH	12,13	m
Wind speed	u_{10}	34	m/s
Governing High Water	GHW	NAP + 6,5	m
Significant Wave Height	H_s	5,0	m
Wavelength	L	122	m
Saturated Volumetric Weight of Gravely Sand	$\gamma_{sat;s}$	20	kN/m^3
The Angle of Internal Friction of Gravely Sand	$\phi'_{s;k}$	35,0	°
Saturated Volumetric Weight of Ballast Sand	$\gamma_{sat;bs}$	19	kN/m^3
The Angle of Internal Friction of Ballast Sand	$\phi'_{bs;k}$	30,0	°

Table 4.9: Overview of relevant boundary conditions.

As parameters, the averaged values of gravely sand are chosen.

Part II

Development of Concepts

CHAPTER 5

FUNCTIONAL DESIGN

This chapter, 'Functional Design', describes the required components all concepts should include. Also, the main dimensions are determined, following the requirements for minimum retaining height and the dimensions of the pump-turbine system. After describing these elements, different concepts will be generated and presented. The stability of these concepts will be considered in the following chapters. Lastly, a check of the functional requirements is performed for all generated concepts.

5.1 Required Components

Various components have been described before in this report, which the final solution at least should possess. Since the structure is a primary water barrier, the retaining height should be sufficient to comply with the Dutch Water Act. The structure is located in Natura 2000 area, so the concepts should impose the least hindrance to the surroundings as possible. It means, for example, fitting into the environment and being as compact as possible.

The caisson structure should also house the pump-turbine system and provide maintenance access to it. Lastly, there should be space on top of the caisson for a road, either for solely maintenance purposes or recreational traffic.

Lastly, scour protection will be required in front of and behind the structure. The design of the scour protection will not be treated in this thesis.

To enumerate the required components, the concepts should:

- house the pump-turbine system;
- allow for ballast rooms;
- provide space for a maintenance crane;
- include a road;
- have scour protection.

Based on these components, the concepts are generated and, to some extent, evaluated.

5.2 Main Dimensions

The visual interpretation of the main dimensions in terms of height, width and length are shown in Figure 5.1.

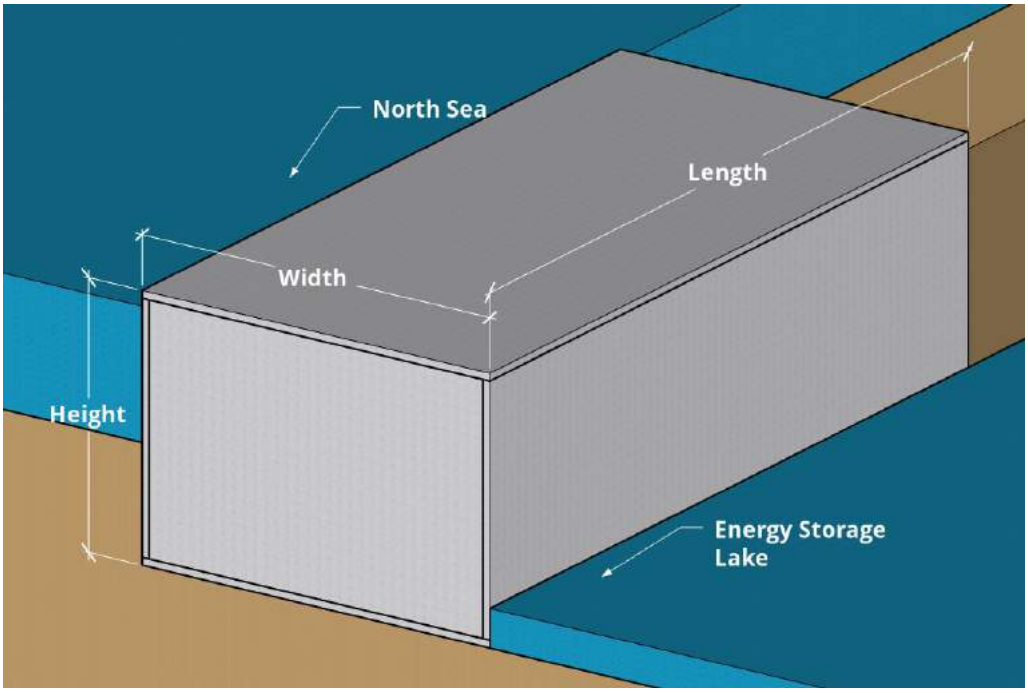

Figure 5.1: Interpretation of caisson dimensions.

The different dimensions are treated separately below.

5.2.1 Height Aspect

The height of the structure follows from the allowed overtopping discharge. An elaboration on the calculation procedure is presented in Appendix H. This section presents the results.

The equation that is used to determine the minimum retaining height, that follows from the crest height above the still water level of NAP + 6,50 m, the most extreme situation, is:

$$R_c = \frac{1}{2,12} \cdot H_s \cdot \left[-\ln \left(\frac{q}{0,054\sqrt{g \cdot H_s^3}} \right) \right]^{1/1,3} \tag{5.1}$$

From the EurOtop manual (EurOtop 2018), valid for vertical seawalls in cases without influencing foreshore. According to the EurOtop manual, “a practical definition of an influencing foreshore is shallow or intermediate-depth water, i.e. not deep water, at the structure toe, but also depends on whether the foreshore is horizontal or sloping (1:50 and steeper).” At the projected location the seabed is near horizontal and no influencing foreshore is present. An overtopping discharge of 0,174 m^3/s/m is used, as is obtained from Appendix H, leading to a freeboard of 4,85 m.

Applying a bullnose on the seaside reduces the freeboard to 3,50 m.

Top of Structure Level
The minimum freeboard, without a bullnose, is 4,60 m, leading to a minimum, top of structure level of NAP + 11,10 m.

Including a bullnose, the freeboard becomes 3,5 m, leading to the minimum, top of structure level becomes NAP + 10 m.

5.2.2 Width Aspect

The width of the pump-turbine outlet, perpendicular to the flow direction, is governing as the maximum width of the pump-turbine structure, in this case, that is 14,11 m. As described in 4.1.3, the minimum length of the pump-turbine system, parallel to the flow direction and so in the width direction of the caisson, is 53 m.

5.2.3 Length Aspect

The number of applied pump-turbines is 138. This number is obtained in Section 4.1.2: three pump-turbine rooms per caisson are chosen, so 46 caissons are required. Three pump-turbine rooms per caisson are beneficial for the construction of the caisson.

One caisson will then have a length of 44,33 m, assuming 0,5 m thick walls.

5.3 Graphical Overview of Concept 'Unity'

Visually, the most basic and simple design for a caisson can be found in Figure 5.2. The concept with a single caisson is named 'Unity' in the remainder of the report. The Governing Low Water (GWL) level follows from Table 4.2.

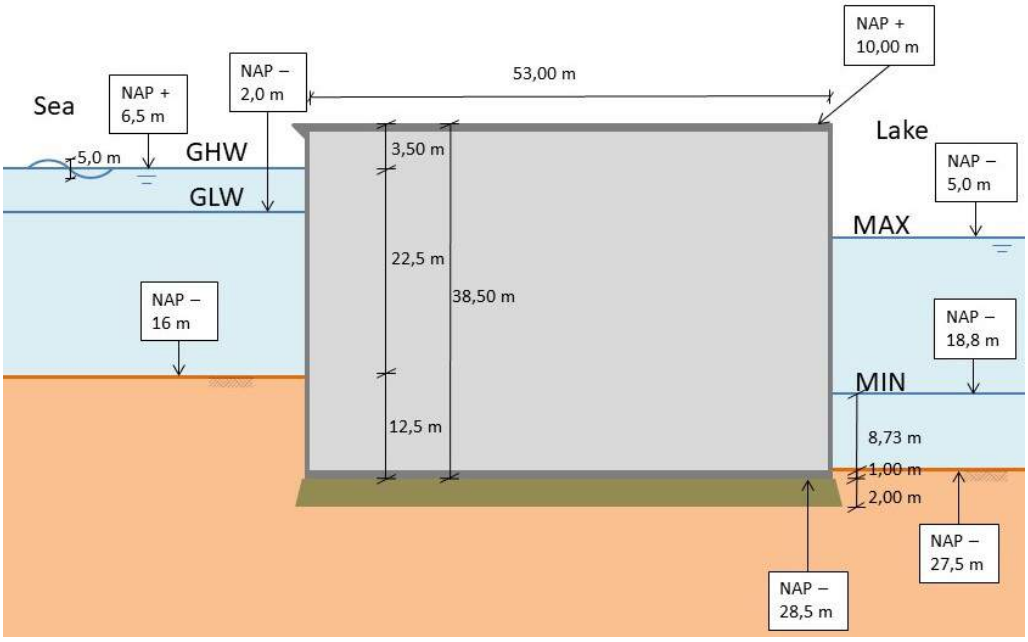

Figure 5.2: Conceptual layout of the concept 'Unity', with bullnose.

With internal dimensions that can be found in the cross-section in Figure 5.3:

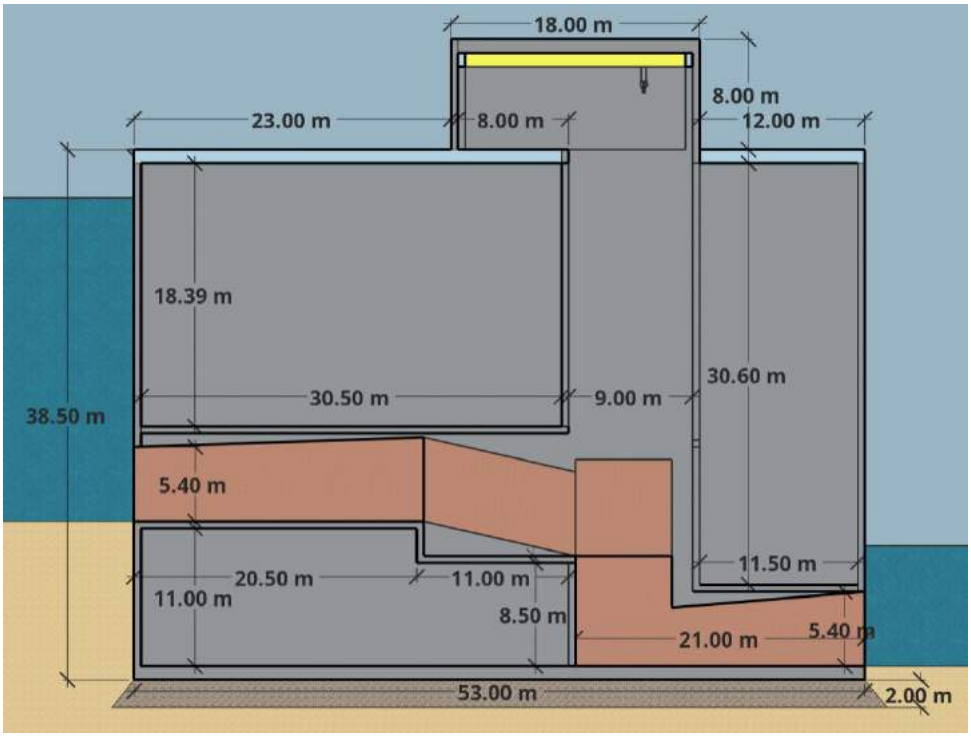

Figure 5.3: Internal dimensions of concept 'Unity'.

With the corresponding plan view in Figure 5.4.

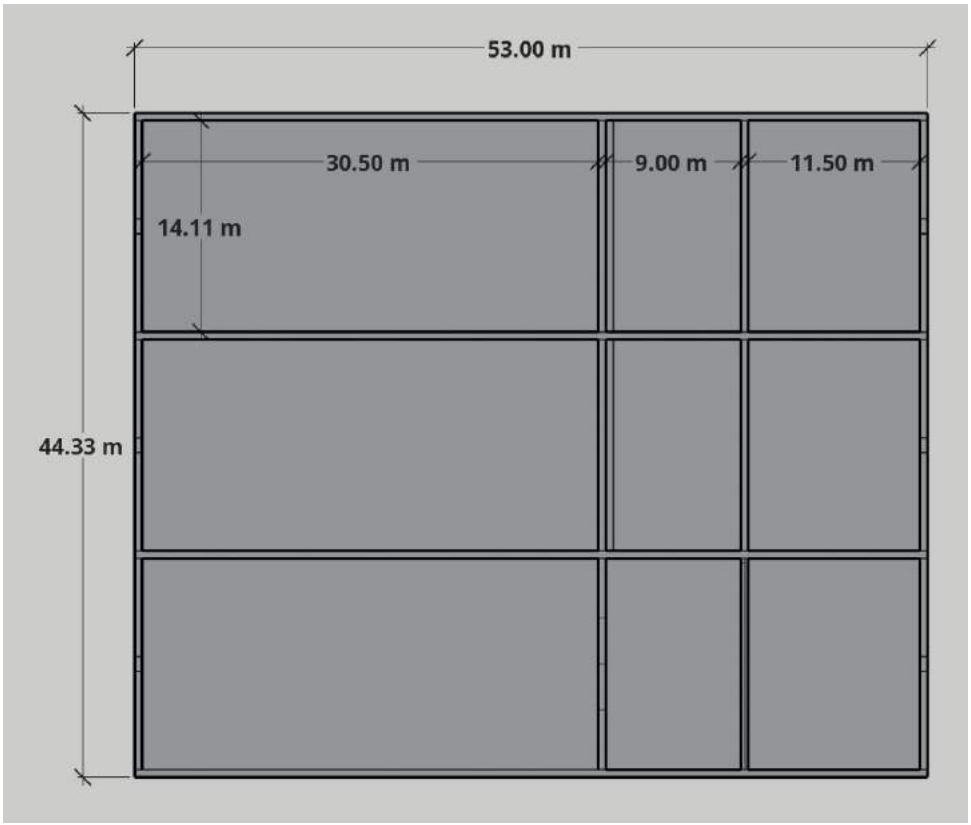

Figure 5.4: Plan view of a three pump-turbine room section of concept 'Unity'.

5.4 Graphical Overview of Concept ‘Duality’

Further concepts could consist of a double layer, as in stacked caissons. Special care should be taken in the connection of the caissons. Two caisson units stacked on top of each other are shown in Figure 5.5.

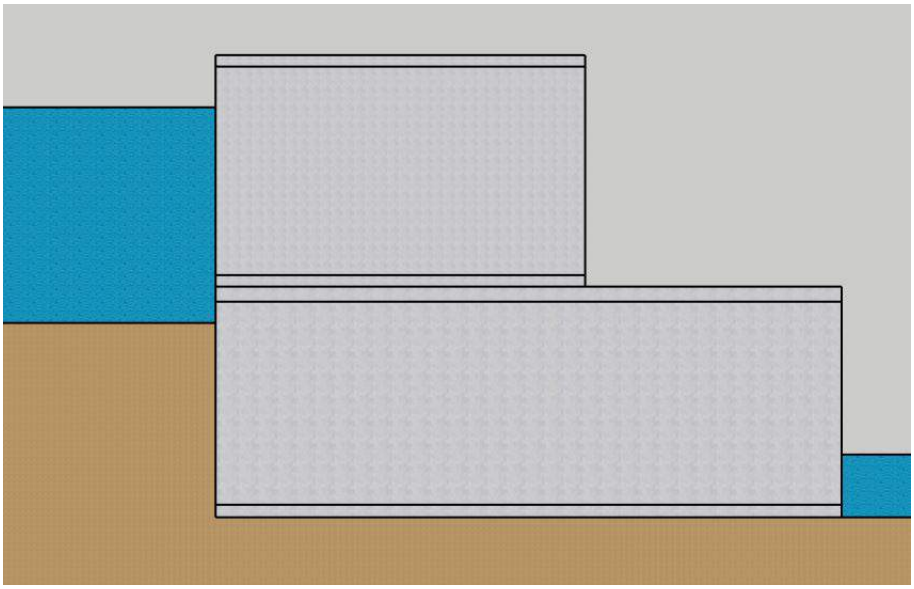

Figure 5.5: Concept ‘Duality’.

With internal dimensions shown in Figure 5.6.

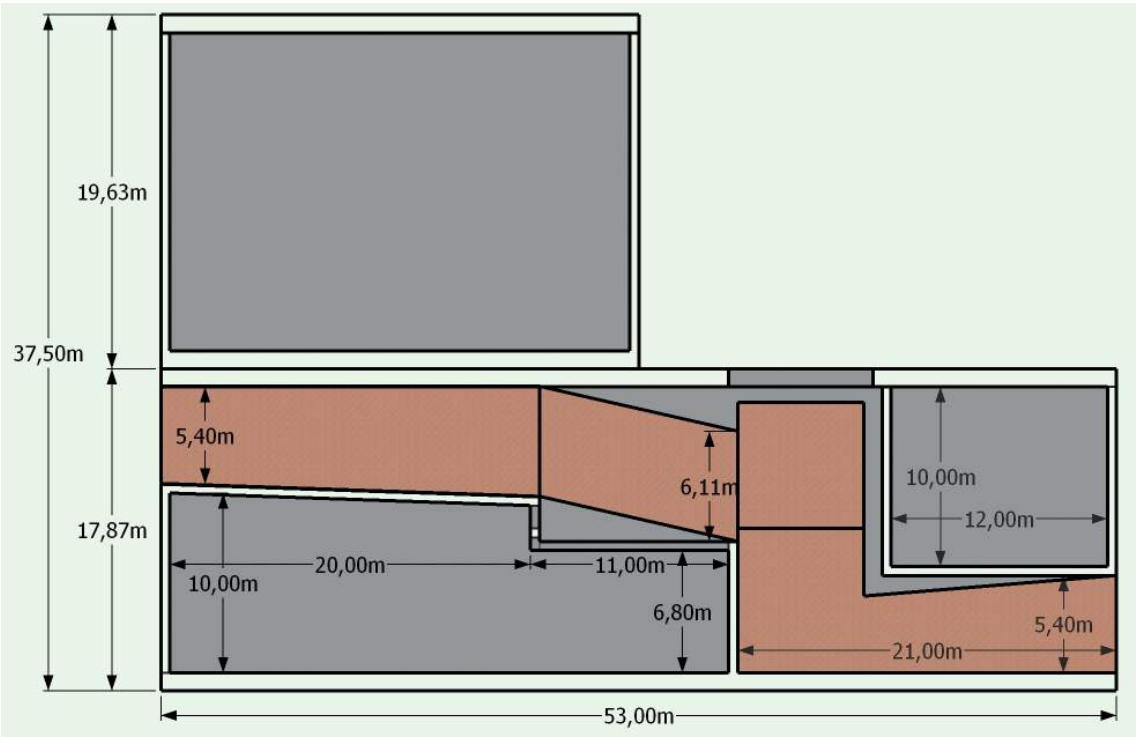

Figure 5.6: Internal dimensions of concept ‘Duality’.

5.5 Graphical Overview of Concept 'Integration'

Instead of closing of the energy storage lake with a full concrete structure, it is also possible to integrate the pump-turbine structure within the dune section, described in Section 2.3. An overview of that concept can be found in Figure 5.7 and is named 'integration' since it is integrated into the dune structure.

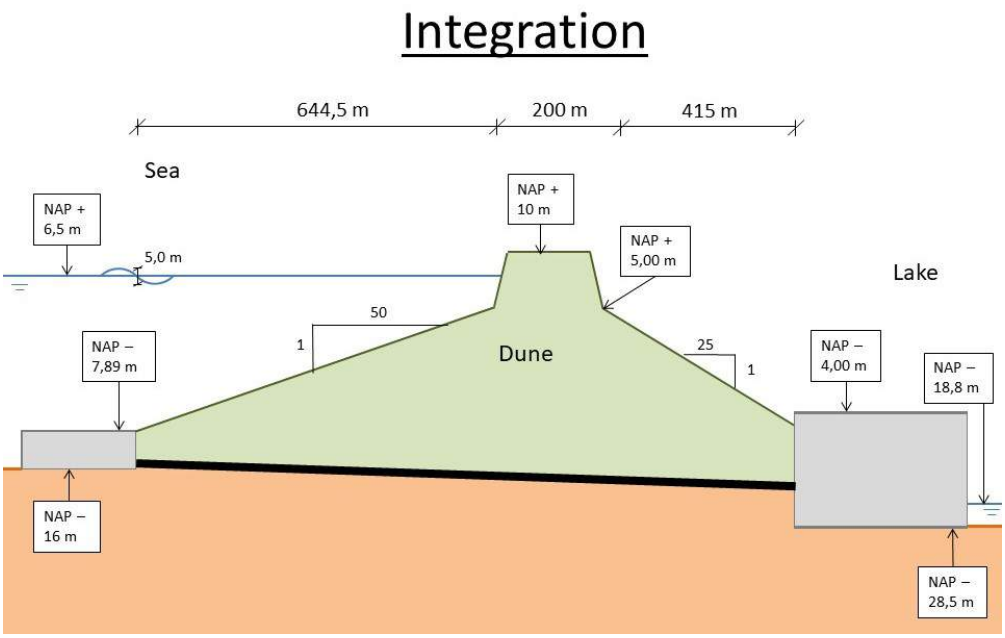

Figure 5.7: Concept 'Integration'.

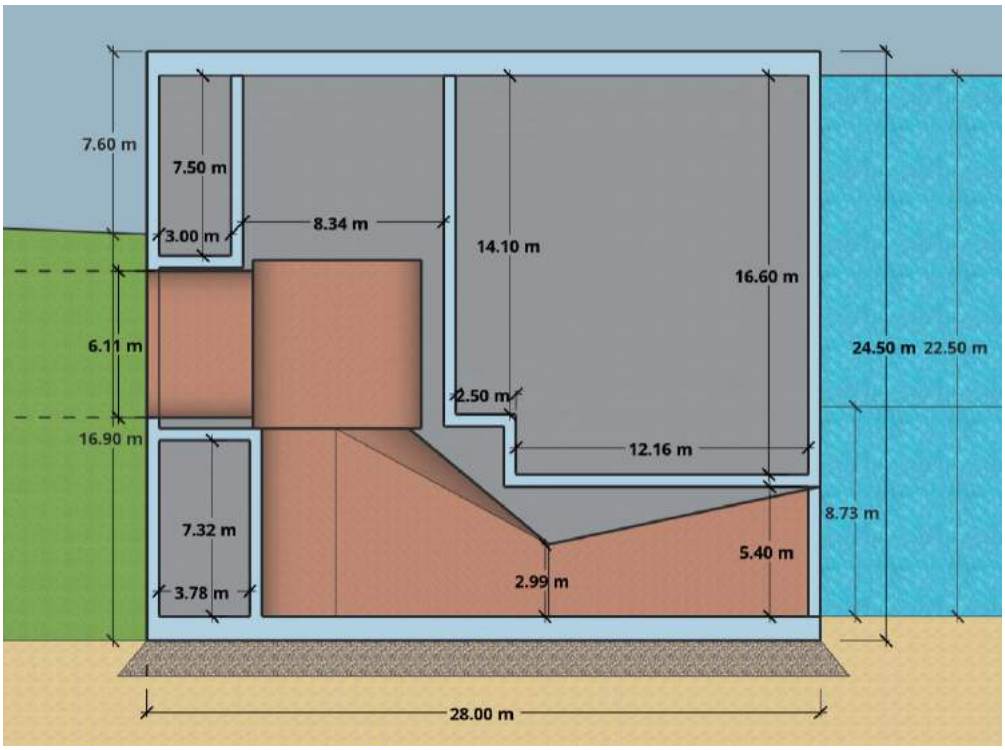

Figure 5.8: Cross-section of the inlet.

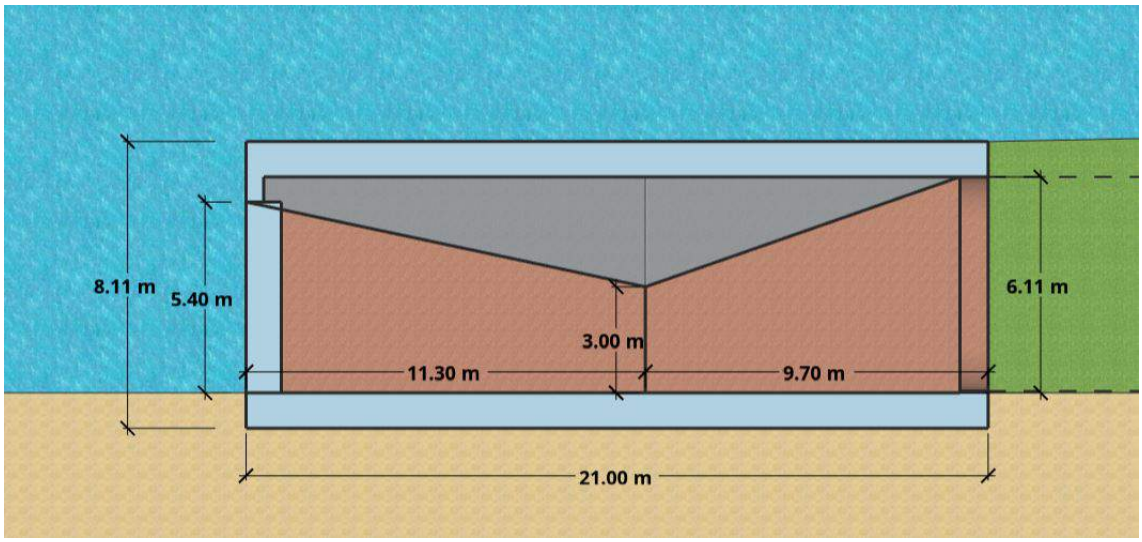

Figure 5.9: Cross-section of the outlets.

5.6 Functional Requirement Check

In short, all concepts contain the components described in Section 5.1. The concepts all contain the pump-turbine system and fulfil the retaining height criterion. Also, there is enough space for the construction of a road.

Maintenance access
In concept 'Unity' there is an overhead crane system integrated within the concept if required ballast weight allows for it. Combined with the opening in the roof and the flat layout of the roof, maintenance is relatively easy.

For concept 'Duality', maintenance is only possible during low water on the energy storage lake. Since that water level is fully controlled, maintenance can be performed safely. A road can be present on the top caisson since that will always be above the water level. A road on the lower caisson is possible, space-wise, but it will be located underwater for half of the time.

In the last concept, 'Integration', a recreational road can be located on top of the dune and a work-purpose road can be located on top of the lake-side caisson. Also, an overhead crane system is present within the concept, on the condition that enough ballast weight can be obtained.

5.7 Gravel sill

Applying a gravel sill under the caisson, with a consistency of 65% gravel and 35% sand, according to The Rock Manual (CIRIA, CUR 2007), Chapter 5, the internal angle of friction of well-graded angular particles is 39° assuming the compaction is loose since the stones could be dumped in the water. The weight of the sill material then becomes: 0,65x21 + 0,35x19 = 20,3 kN/m^3. All relevant angles of friction are summarized in Table 5.1. Furthermore, the ratio $\delta = 2/3 \cdot \phi^{'}$ and $\tan(\phi_d^{'}) = \frac{\tan\left(\phi_k^{'}\right)}{1,2}$.

Angle of Friction	Value	Unit
$\phi_{soil;k}^{'}$	35	°
$\phi_{soil;d}^{'}$	30,3	°
$\delta_{soil;k}$	23,5	°
$\delta_{soil;d}$	19,9	°
$\phi_{sand;k}^{'}$	30	°
$\phi_{sand;d}^{'}$	25,7	°
$\delta_{sand;k}$	20,1	°
$\delta_{sand;d}$	17	°
$\phi_{sill;k}^{'}$	39	°
$\phi_{sill;d}^{'}$	34	°
$\delta_{sill;k}$	26,1	°
$\delta_{sill;d}$	22,2	°

Table 5.1: Various angles of the sill material.

Part III

Verification of the Concepts

CHAPTER 6

CONSTRUCTION AND STABILITY OF CONCEPT 'UNITY'

Following the previous chapter, where concepts are generated, the different concepts will be verified. Firstly, the possible construction methods are discussed, and after that, the structural verification will take place. The latter consists of defining the failure mechanisms, describing the governing loading per failure mechanism and checking whether the dimensions hold. After a concept is verified structurally, it will be called an alternative.

6.1 Construction Methods

There are two main types for a caisson. The first is to prefabricate the caisson and then transport the floating caisson to the final location, which was dredged and prepared at the required depth. The second is a pneumatic caisson, which it digs itself into the ground to the required depth. Another structure that is considered is an in situ build in- and outlet structure.

Constructing in situ can be done in several ways. The methods described further are a construction pit and a cofferdam. Both methods can be either constructed as a caisson at the required level or as a pneumatic caisson at existing sea bottom level.

Prefabricated construction consists of only one building method, depending on the dimensions of the construction pit, and has to be transported as a floating caisson. Usually, this is done either partially self-propelled, meaning the caisson is floating on its own and is transported by towing vessels, or transported by floating cranes, where the caisson is not or partially floating and requires an extra lifting force. This latter method seems not suitable for these sizes of caissons. The prefabrication method does require an onshore or near-shore construction pit that can be flooded, existing or new to be built.

The caisson foundation can be either shallow, thus directly on the subsoil, or using piles. For this master's thesis, only shallow foundations will be considered since the underwater connection between the piles and the structure requires a specialised solution.

The pneumatic caisson is a special kind of in situ construction. The pneumatic caisson will be constructed at the final location, and it will lower itself to the required depth. This method will not be considered, for the method being technically challenging.

6.1.1 Foundation

The caisson will be constructed directly on the seabed, that has to be well prepared, to prevent undesirable settlements and for positioning, if prefabricated. A sill can be applied to spread the loads more evenly to the subsoil and to allow for some flow if required.

6.1.2 Prefabrication

While the 'in-situ' construction has been described in Appendix J, the prefabricated caisson will be discussed below.

6.1.2.1 Construction Dock

When considering a construction dock to prefabricate the caissons, there are two options, either re-use an existing construction dock or build a new construction dock at a suitable location. Suitable, existing locations, were inventoried by Rijkswaterstaat in (Rijkswaterstaat 1992) for the construction of tunnel elements. Of all named locations only the construction dock Barendrecht is still available, with dimensions of 150x350 m^2 at a depth of NAP - 10 m.

The research into finding or designing a suitable construction dock can be very elaborate. Thus the Barendrecht construction dock is chosen as the starting point. The limitations of this construction dock are imposed by its dimensions, the depth of the transport route and the available height under crossing infrastructure. The dimensions are named before and are 150x350 m^2 at a depth of NAP - 10 m, the limitation in water depth is NAP - 10 m in the river 'Oude Maas'. Two bridges will cross the water on the route to the final location, namely the 'Spijkenisserbrug' with a clearance, in opened condition, of NAP + 45,0 m and the 'Botlekbridge' with the same clearance in opened condition.

Another option is to create a building dock near the final location of the in- and outlet structure. That can be constructed like the in-situ building method described in Appendix J, only with a shallower building pit.

The draught, which is 13,5 m, see Section 6.3.5, exceeds the limitations for the Barendrecht building-dock. Also, the clay layer is not able to withstand bursting for the in situ case, see Appendix J, so a building-dock nearby the final location might provide the best option.

A building-dock can be created, making use of the dune defence of the energy storage lake, as is showed in Figure 6.1. To be able to sail out during governing low water, which is NAP - 2 m, the bottom of the building pit should be located at NAP - 17 m and the water level should be kept below NAP - 17,5 m. Since the dunes should be able to lower the water level to NAP - 22,5 m, this should impose no problems.

Figure 6.1: Possible location of the building dock.

6.1.2.2 Transport

For transport of the caisson, there are two main options. Namely as a floating caisson using towing boats or crane-carried transport. During transport, four caissons will be coupled together, creating a total length of 177,32 m. This length is beneficial for navigability and submerging.

6.2 Construction Steps

In this section, the constructability will be discussed. In other words, the different building phases of the caisson, where external forces will act on the caisson, will be shown and based on that, the loading situation will be inventoried.

6.2.1 Building Phases

The construction of the caisson is advised to do in a building dock near the final location. The building process is assumed to consist roughly of six main phases, which are visually described in Appendix J. The technically challenging phase, this will be checked in the strength verification, is indicated below.

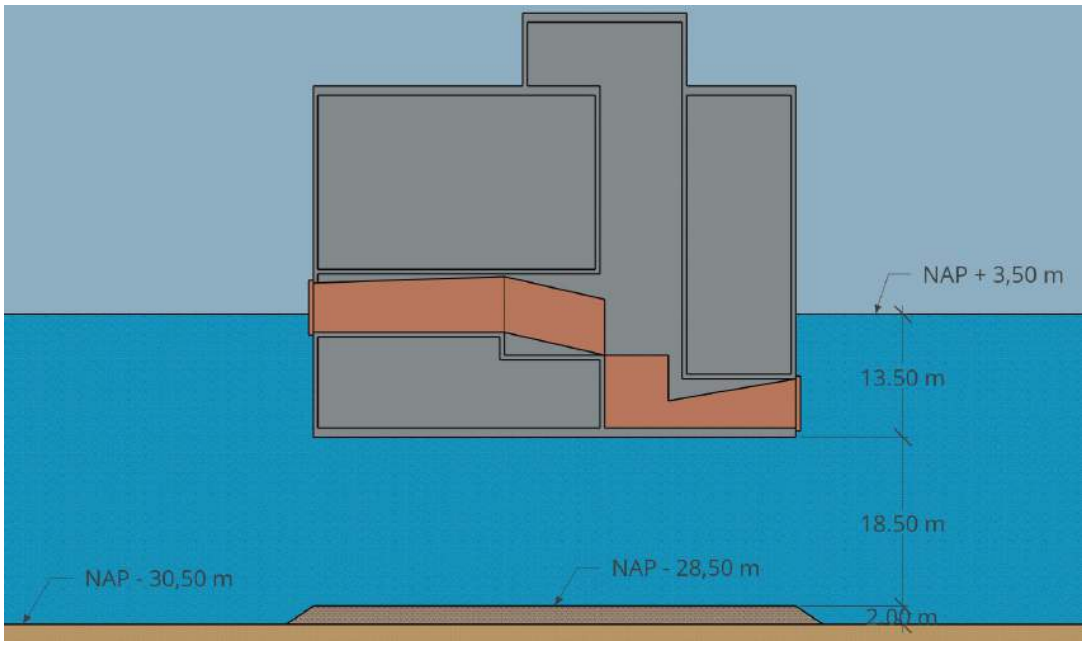

Figure 6.2: Construction phase 4 of the concept 'Unity'.

In construction phase 4 the prefabricated caisson has been transported trough open water to its final location. Figure 6.2 shows the draught and required sinking depth, with a water level of NAP + 3,50 m.

6.2.2 Inventory of Loads

Different loads act on the concepts. First, there are permanent loads:

- Self-weight,
- pump-turbine weight,
- permanent water pressure,
- ballast weight,
- soil pressure.

The variable loads that can occur are:

- (Still) variable water pressures,
- wave pressures,
- currents due to pumping,
- temperature loads,
- wind pressures,
- snow loads,
- ice loads.

Also, some special loads are named in (Technische Adviescommissie voor de Waterkeringen 2003), namely:

- Collision,
- explosion,
- fire,
- current due to non-closure,
- vandalism and sabotage.

Collision with a ship is excluded for concept 'Integration', but in other concepts, the likelihood of ship collision is almost zero. The project is located out of shipping routes and also in the shelter of the Tweede Maasvlakte. Collision loads will therefore not be considered.

According to Eurocode NEN-EN 1997-1-7 (2015), "Explosions must be taken into account in the designing and calculating of all parts of the building, and other civil engineering works where gas is burned or regulated, or where explosive material such as explosive gases, or liquids that form explosive vapour or gas is stored or transported (for example, chemical installations, ships, tankers, pipelines, homes with gas installations, energy pipes, car and train tunnels)." These elements are not present in this project, so explosion loads are not considered.

Loads due to ice are barely mentioned in the Eurocode. In the NEN-EN 1997-1-7 NB (2011), as an addition to the Eurocode, an extra paragraph 5.4 is added. This paragraph, in Chapter 5: 'Explosions in constructions', only states that loads due to ice should be considered and that a method is described in Jessberger H.L. *Bodenfrost und Eisdruk*. The British Standard (BS 06349-1-2-2016) mentions ice loads and states that: "In the recent past, loading from floating sea ice has not been a problem around the British Islands and need not be considered for structures whose design life is of the order of 50 years". Ice loads are left out of the design for this structure.

Currents due to non-closure are possible to occur in this structure. In Chapter 10, this will be further elaborated, if required.

Neither the Eurocode nor the British Standard covers loading due to vandalism and sabotage. So in this project, these loads are also not considered.

6.3 Failure Mechanism Checks

The five failure mechanism checks in ULS that will be performed are:

1. Piping,
2. rotational stability,
3. sliding resistance,
4. vertical bearing capacity,
5. (static) floating stability.

The adopted safety philosophy is from the 'Leidraad Kunstwerken 2003' from the 'Technische Adviescommissie voor de Waterkeringen'. On page 187, the partial safety factors are summarised. For the dominant loading, the following factors are assumed:

PERMANENT:

- Own weight: (1,35 or 1,2 or 1,0 or 0,9) F_{rep}
- Soil pressure: (1,2 or 1,0 or 0,9) F_{rep}
- Groundwater pressure: (1,2 or 1,0 or 0,9) F_{rep}

When the own weight is the only source of loading, the safety factor of γ_G = 1,35 is used. For loading, due to permanent fluid pressure, a factor γ_f of 1,2 (unfavourable) can be used. If the permanent loading is combined with other loads a factor $\gamma_{G;unf}$ = 1,2 (unfavourable) or $\gamma_{G;fav}$ = 0,9 (favourable) must be used.

For permanent loading, due to ground pressure, a partial safety factor of γ_g = 1,0, favourable and unfavourable, should be used.

VARIABLE:

- Pressure differences due to:
  - Water levels: 1,25 F_{norm},
  - Wind waves: 1,25 F_{norm}.

The variable water pressure is calculated by determining the governing high water level and the corresponding inland water level. With those values, the representative value of the pressure difference is determined. That value should be multiplied with a safety factor γ_H = 1,25.

Furthermore, the guideline (Technische Adviescommissie voor de Waterkeringen 2003) states on page 201 that in the loading combination, in the case of a correlation between high water and wind waves via wind, they must be considered as simultaneously. Also, on the upward water pressures under a structure, which are associated with the outside water level, the safety factor of 1,25 does not have to be used, but instead, a factor γ_{H0} of 1,0 can be used.

Lastly, the angle of internal friction has to be adjusted with a parameter $\gamma_{\phi'}$ = 1,2, following from Eurocode 7 (2016) NB Table A.1. This safety factor should be applied to $\tan\left(\phi_k^{'}\right)$.

6.3.1 Piping

Piping is visually presented in the Eurocode as in Figure 6.3. The difference with our case is that the sheet pile wall in the example is a caisson, and so significantly wider. The governing loading situation for piping is with the extreme water level event on the seaside and low water on the energy storage lake.

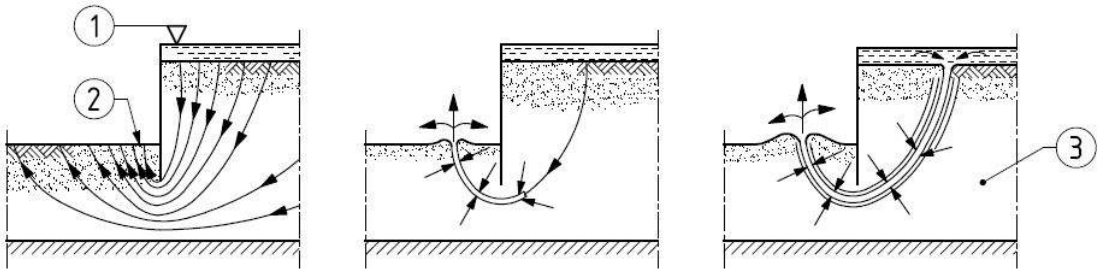

Figure 6.3: Piping development example, SOURCE: NEN-EN 1997-1, Eurocode 7.

According to Bligh and Lane (1993), the limit state function for piping is:

$$Z_p = L - c \cdot \Delta H \tag{6.1}$$

In which L stands for the seepage length, c is the percolation factor and Δ H is the head difference. The percolation factor for coarse sand (d_{50} = 300 − 2 000 μm) is 12, and the maximum head difference is 25,27 m.

They also found that vertical paths offered a three times higher resistance than horizontal ones. Introducing the length of a seepage screen as L_{spw} the seepage length on the seaside is $L_1 = 3 \cdot h_{seasoil} + 3 \cdot L_{spw}$ = 3*12,5 + 3*L_{spw} m.

The seepage length on the lake side is $L_2 = 3 \cdot L_{spw} + W + 3 \cdot h_{lakesoil} = 3 * L_{spw} + 53 + 3 * 1$ m.

Setting the seepage screen length to 35 m, the loading becomes 12 x 25,27 m = 303,24 m. The resistance equals $L_1 + L_2$ = 303,50 m.

As can be seen from the soil investigation, most probably there is a 10 m thick clay layer at NAP - 50 m. It means that the sheet pile wall 'only' has to reach that depth, which equals a minimum length of 22,5 m. No research has been performed to check whether this is possible, furthermore, also since a sheet pile wall is favourable in the distribution of water pressures when placed at the side of the highest pressure, a sheet pile wall is not considered in the remaining calculations.

6.3.2 Rotational Stability

The rotational stability check that will be performed is around the foot of the structure on the lakeside. The sum of design destabilising moments ($M_{dst,d}$) will be compared to the sum of design stabilising moments ($M_{stb,d}$).

$$\Sigma M_{dst,d} \leq \Sigma M_{stb,d}$$

The line of action of resultant force can be calculated and from that value, the eccentricity of actions from the centre line of the base. The eccentricity will be used to determine the effective width of the base, which is needed to calculate the bearing resistance. A sketch of this failure mechanism can be found in Figure 6.4.

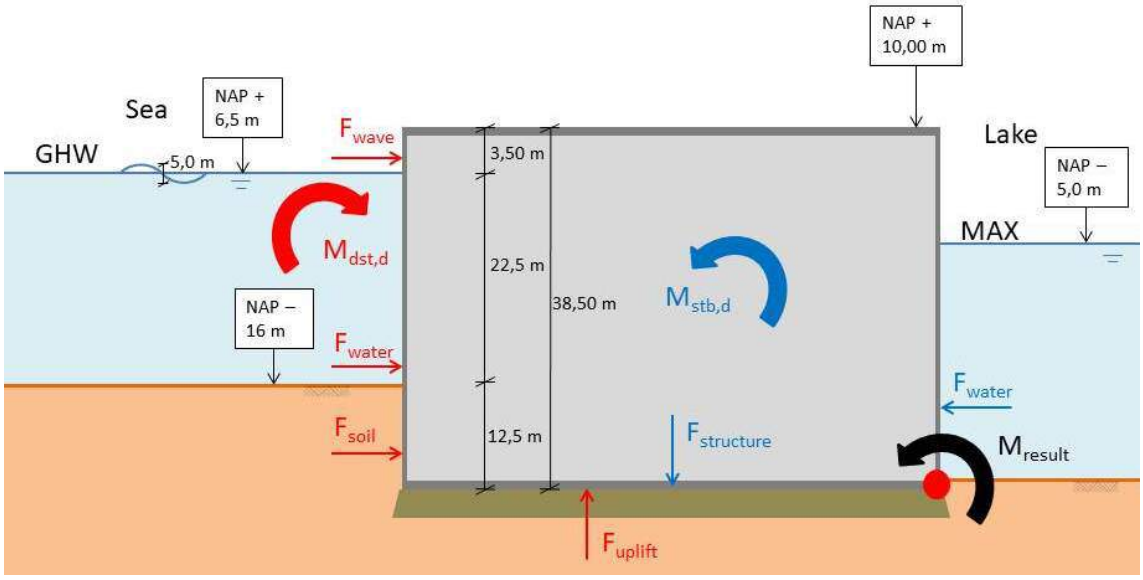

Figure 6.4: Rotational stability of the concept 'Unity'.

The governing loading situation for the rotational stability check is with the extreme water level event on the seaside and high water on the energy storage lake. Detailed calculations can be found in Appendix K. The caisson is assumed to be filled with a ballast material, included in $M_{concrete,G}$.

Unity check
The acting destabilising moments equal $M_{dst,d}$ = 622 320 kNm/m. The total stabilising moment $M_{stb,d}$ = 838 064 kNm/m.

The unity check for the governing loading situation becomes $uc = \frac{M_{dst,d}}{M_{stb,d}}$ = 0,74.

Eccentricity
The line of action of the resultant force is a distance from the toe of the structure: x = 16,21 m. For the eccentricity, the loading combination with the extreme water level event on the seaside and low water on the energy storage lake is governing. Namely, the biggest eccentricity gives the smallest effective width.

The e_d = 10,29 from the centre line of the base.

6.3.3 Resistance against sliding

This failure mechanism is sketched in Figure 6.5 and described in detail in Appendix K.

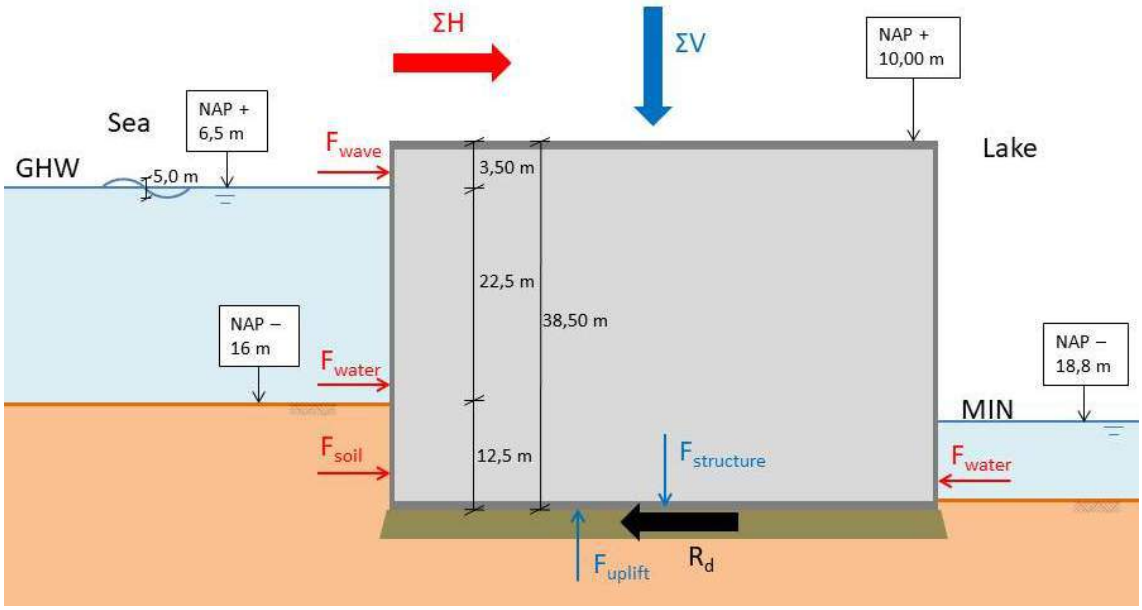

Figure 6.5: Sliding resistance of concept 'Unity'.

Which is based on the principle of:

$$\Sigma H \leq f \cdot \Sigma V$$

or

$$\Sigma H \leq R_d = V_d \cdot \tan(\delta_d)$$

The governing loading situation for sliding is with the extreme water level event on the seaside and low water on the energy storage lake. The resulting horizontal force from external loads ΣH = 9 536 kN/m and the vertical force downwards equals ΣV = 16 748 kN/m. When the roughness between the concrete and the sill is improved, consequently increased, a higher friction angle can be used in determining the sliding resistance. When ϕ_d instead of δ_d can be used, the horizontal sliding resistance R_d = 11 302 kN/m, which gives a unity check of 0,84. In order to obtain a unity check of 1,0, the friction angle should become 29,65°.

The angle of repose of the sill is a parameter with huge uncertainty since the sill will be placed underwater. The sill can be placed and left loosely or can be compacted afterwards. In Figure 6.6, the angle of repose is varied against the horizontal sliding resistance. In the two lines, either the design value of the angle of repose is used or the reduced design delta value.

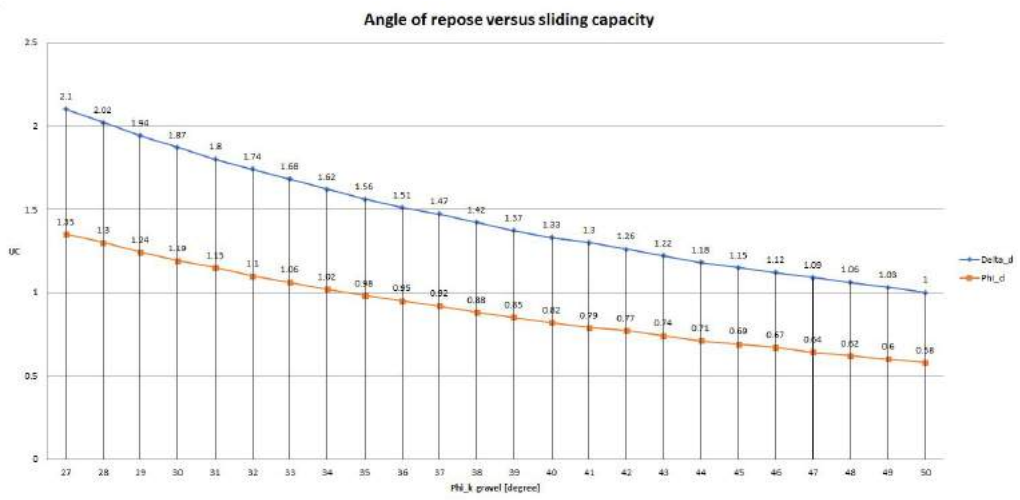

Figure 6.6: Sensitivity of the angle of repose versus the sliding resistance.

6.3.4 Bearing resistance

The bearing capacity of the soil is described by NEN-EN 1997-1, Eurocode 7:

$$\sigma^{'}_{max;d} = \sigma^{'}_{v;z;d} \cdot N_q \cdot s_q \cdot b_q \cdot i_q + 0,5 \cdot \gamma^{'}_{average} \cdot b' \cdot N_{\gamma'} \cdot s_{\gamma'} \cdot b_{\gamma} \cdot i_{\gamma'} \tag{6.2}$$

The first part in Equation 6.2 describes the influence of the loading of the higher sand layer. The second part describes the behaviour of the slip circle.

The bearing capacity will be described for two interfaces: the first interface is the caisson directly on the sill and the second interface is between the sill and the native soil. It is sketched in Figure 6.7. The governing load situation is GHW on the seaside and the minimum water level on the lakeside since this gives the lowest effective width.

Detailed calculations are performed in Appendix K. For stability, the exerted pressure on the soil should be lower than the pressure the soil can take up:

$$q_d \leq \sigma^{'}_{max;d} \tag{6.3}$$

For the first interface, between the caisson and the sill, the bearing capacity of the sill $\sigma'_{max;d}$ = 639 kN/m^2 and the maximum acting stress q_d = 517 kN/m^2, leading to a unity check of 0,81. For the second interface, between the 2 m high sill and the native soil, the bearing capacity of the soil $\sigma'_{max;d}$ = 560 kN/m^2 and the maximum acting stress q_d = 498 kN/m^2, leading to a unity check of 0,89.

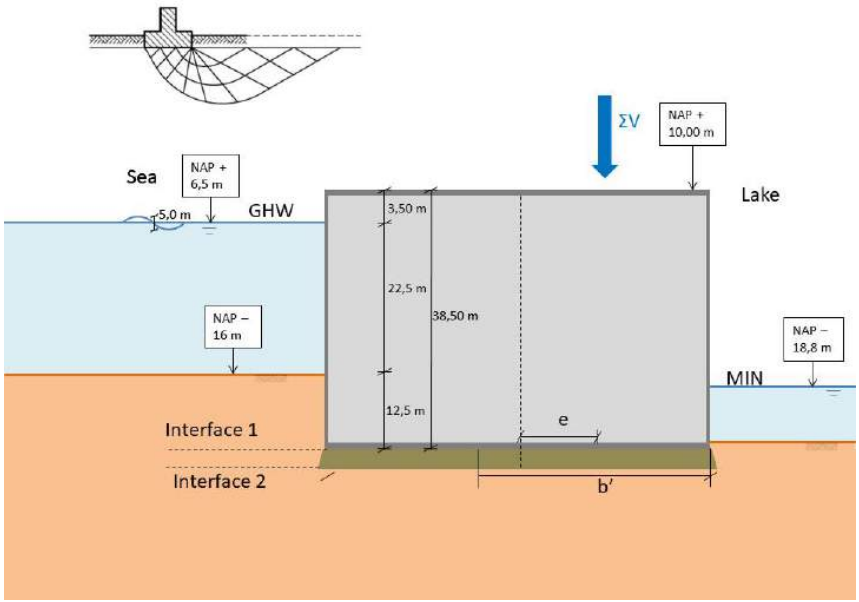

Figure 6.7: Bearing capacity of concept 'Unity'.

A significant influence on the bearing capacity is the internal angle of repose of the sill. Especially since the sill is placed underwater, the variance can be significant. The sensitivity is shown in Figure 6.8, where the angle of repose is varied, and the resulting unity check for the bearing capacity of the sill is displayed. The angle of repose presented is the characteristic value, while the calculations are performed with the design value.

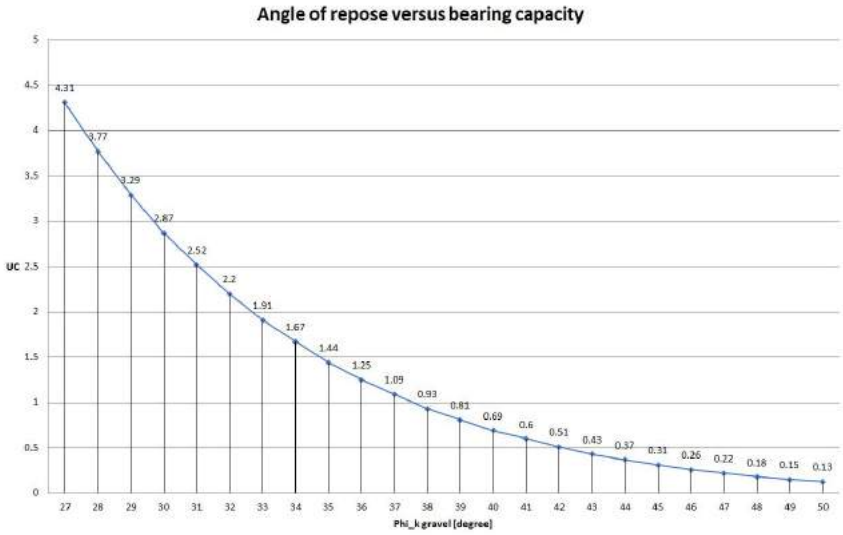

Figure 6.8: Sensitivity of the angle of repose versus the bearing capacity.

The course of the sensitivity analysis is exponential, meaning the influence of a smaller angle of repose has a relatively significant influence on the bearing capacity.

6.3.5 Floating stability

Assuming a prefabricated caisson that should be transported to the site, the draught and floating stability will be discussed in this section. This section is based on the lecture notes of Hydraulic Structures - Caissons (2016).

The static stability is handled according to Figure 6.9.

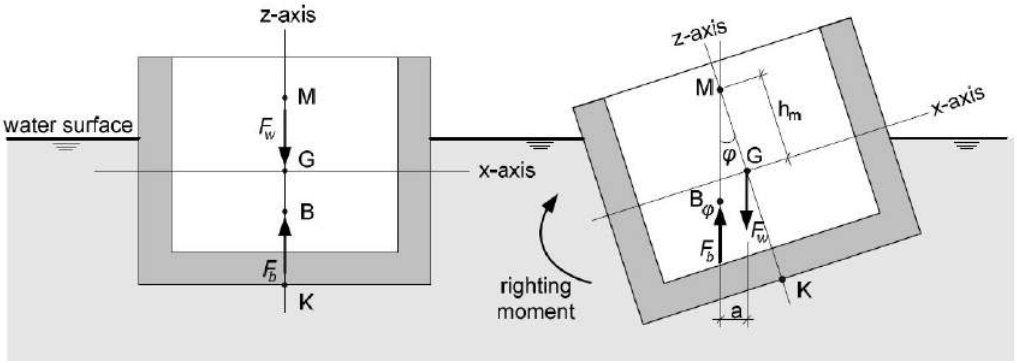

Figure 6.9: Static stability of a floating element, SOURCE: (Molenaar and Voorendt 2019).

The caisson is, statically, stable when the metacentric height, h_m is positive, i.e. greater than zero. For practical reasons, the metacentric height should be kept above 0,5 m. The rule is:

$$h_m = \overline{KB} + \overline{BM} - \overline{KG} \geq 0,5\text{m}$$

The result for an empty caisson is that h_m = 3,95 m and is very stable.

Another useful result from this analysis is that the draught of the caisson is 13,52 m.

6.4 Stability Overview of Alternative 'Unity'

In Table 6.1, an overview of the checked stability conditions is given.

Stability component	**Value**	**Requirement / capacity**	**U.C.**
Rotational Stability	$M_{overturning}$ = 622 320 kNm/m	$M_{resisting}$ = 838 132 kNm/m	0,74
Sliding: Prefabricated	H_{Ed} = 9 536 kN/m	H_{Rd} = 6 836 kN/m	1,39
Sliding: In-situ	H_{Ed}= 9 536 kN/m	H_{Rd} = 11 302 kN/m	0,84
Bearing Capacity: Interface 1	q_d = 517 kN/m^2	$\sigma'_{max;d}$ = 639 kN/m^2	0,81
Bearing Capacity: Interface 2	q_d = 498 kN/m^2	$\sigma'_{max;d}$ = 560 kN/m^2	0,89
Static Floating Stability	h_m = 3,95 m	$h_m \geq$ 0,0 m (0,5 m)	0,13

Table 6.1: Overview of the checked stability conditions for alternative 'Unity'.

CHAPTER 7

CONSTRUCTION AND STABILITY OF CONCEPT ‘DUALITY’

Since the checks on concept ‘Unity’ are just within limits, there is not much to gain by creating two separate caissons and stacking them upon each other. The idea was to gain resistance against rotating, but concept ‘Unity’ can be constructed with the minimum required width, and having unity checks for bearing capacity just under 1,0. It means that by reducing the area of the upper caisson and leaving the height equal, the caisson will fail on sliding, plus the eccentricity will be larger, consequently reducing the effective width. It also leads, without measures, to failing on the bearing capacity.

The conclusion is that this concept will be rejected.

CHAPTER 8

CONSTRUCTION AND STABILITY OF CONCEPT 'INTEGRATION'

In the same way concept 'Unity' was treated in Chapter 6, here the construction method and stability of concept 'Integration' will be treated. The seaside caisson and the lakeside caisson will be assessed separately. First, for the whole concept, the construction methods and construction steps are discussed. Then, the failure mechanisms undermining the stability of the caisson located on the sea are assessed. Lastly, these failure mechanism checks are performed for the caisson located on the lakeside, which contains the pump-turbine system.

The same checks, as with concept 'Unity', will be performed, and the safety factors will be used. These can be found in Section 6.3.

8.1 Construction Method

Just as with concept 'Unity' the initial foundation of concept 'Integration' will be directly on the subsoil, without the use of piles. Referring to the same considerations used in the construction method of concept 'Unity', it is, for now, advised to prefabricate the caissons in a building dock nearby the final location.

8.2 Construction Steps

The construction steps are separated for the seaside caisson and the lakeside caisson. All construction steps are showed and explained in Appendix L. Only relevant or interesting construction situations, for strength verification, are showed in the next section.

After the caisson have been placed at their position, the soil can be filled until the bottom level of the pipe that connects the two caissons. Then, while underwater, the steel pipe has to be welded to a transition piece on either side. After, the dune can be constructed.

Seaside caisson
The highlighted building phases of the seaside concept are shown below.

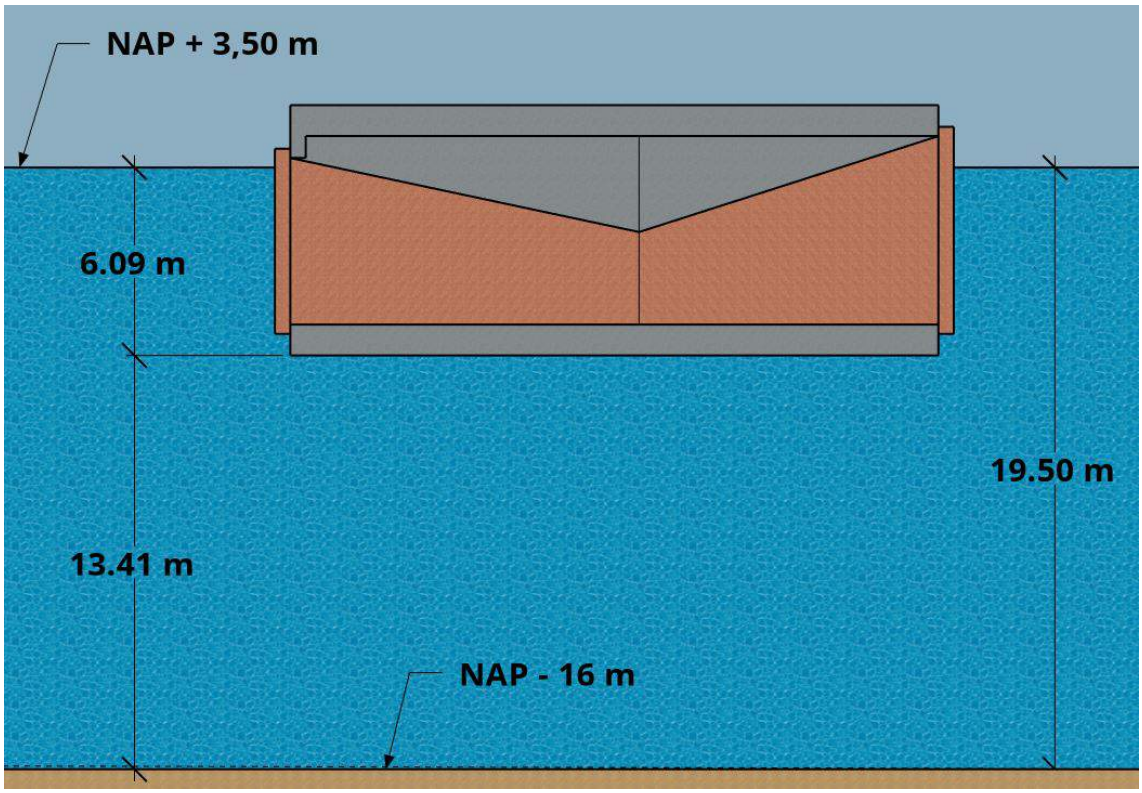

Figure 8.1: Highlighted construction phase (4) of the seaside caisson, concept 'Integration'.

Figure 8.1 shows the seaside caisson at the final location before sinking to the sea bottom. The figure shows the draught of the caisson and the distance to the bottom, in the governing water level situation, which is NAP + 3,50 m, just as with concept 'Unity'. Figure 8.2 shows the caisson in the final position, fully immersed to the sea bottom.

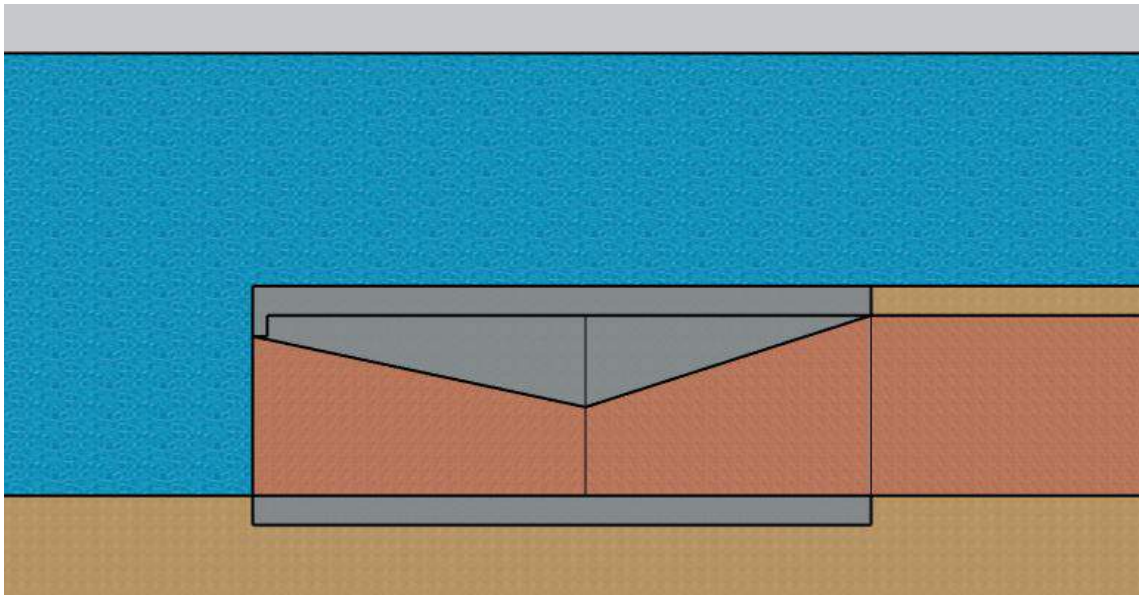

Figure 8.2: Final construction phase of the seaside caisson, concept 'Integration'.

Lakeside caisson
The highlighted construction phases of the lakeside caisson are shown below.

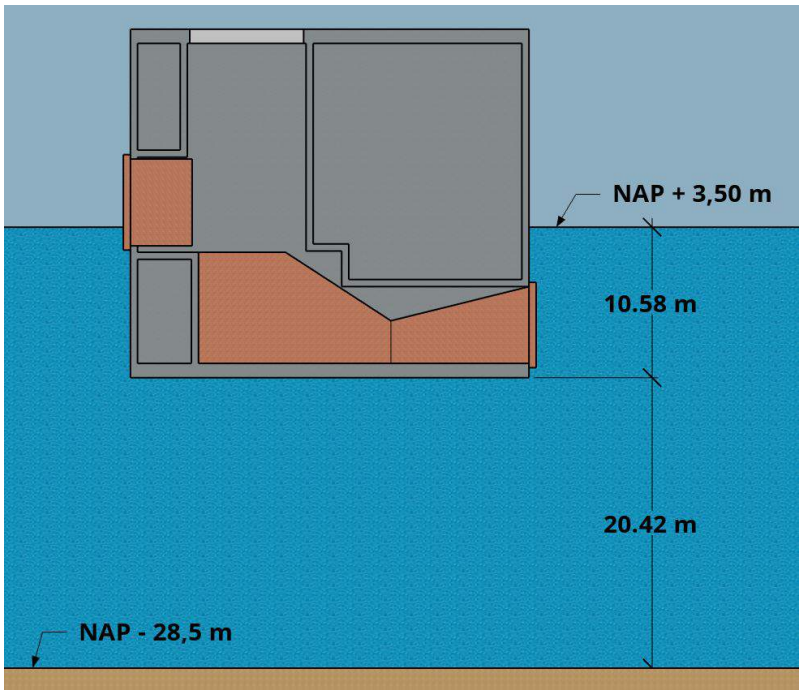

Figure 8.3: Highlighted construction phase (4) of the lakeside caisson.

Figure 8.3 shows the situation just before immersion, at the final location. While Figure 8.4 shows the immersed position, entirely below the waterline. Care has to be taken that the caisson is able to immerse below the waterline. The yellow pole above the caisson is mainly to indicate the position of the caisson, below water level.

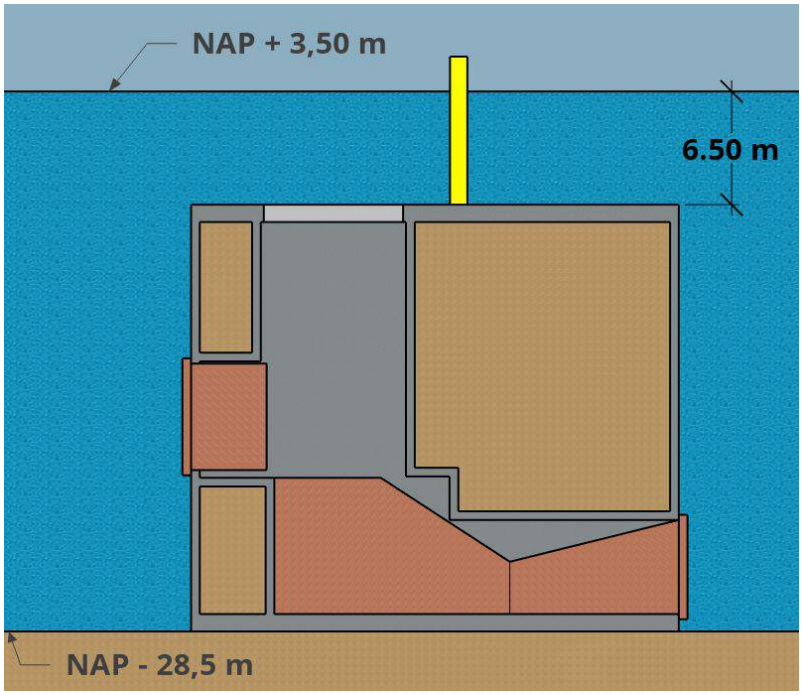

Figure 8.4: Highlighted construction phase (5) of the lakeside caisson.

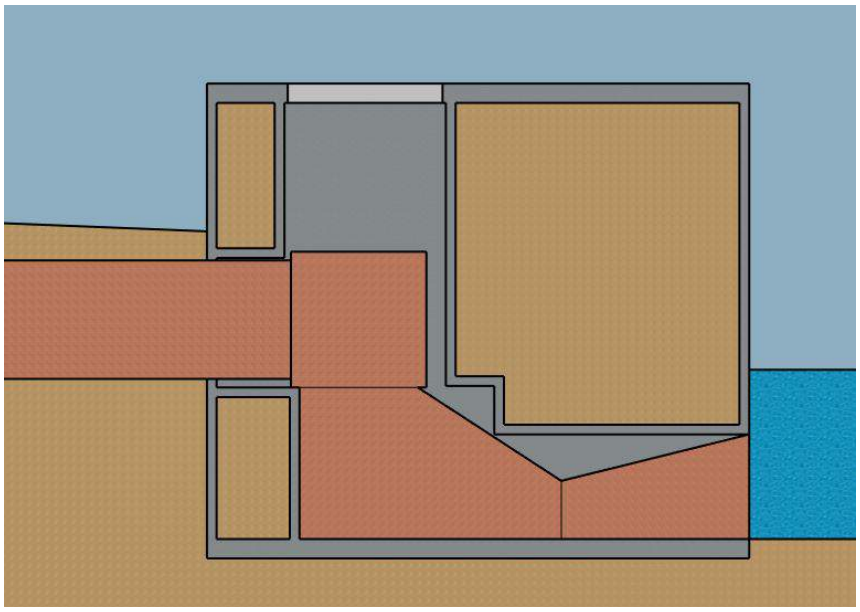

Figure 8.5: Final construction phase of the lakeside caisson, concept 'Integration'.

Figure 8.5 shows the final construction situation of the lakeside caisson.

8.3 Piping Check for the Structures Combined

As described in Chapter 6, piping is described by:

$$Z_p = L - c \cdot \Delta H \tag{8.1}$$

Where the water level difference is still the 25,27 m. Now the horizontal piping length is significantly longer due to the dune in between, see Figure 8.6, not to scale.

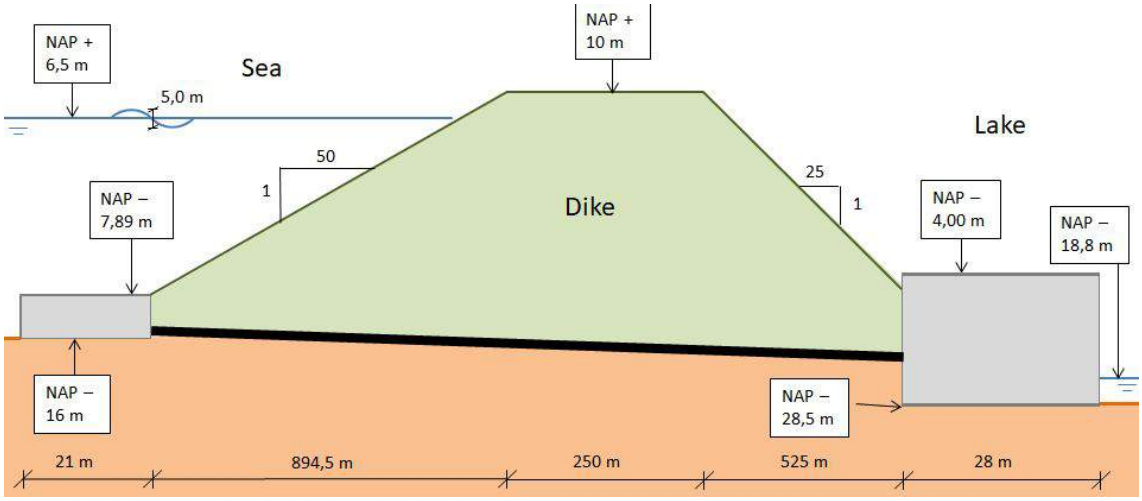

Figure 8.6: Piping length for concept 'Integration'.

The percolation factor, c, is 12 and the total piping length, horizontally approximated, is 1 718,5 m.

The Z_p value in ULS is then 1 415,3 m, which equals a unity check of 0,18. So no additional requirements are necessary.

8.4 Failure Mechanism Checks of the Seaside Caisson

8.4.1 Rotational Stability

The rotational stability check that will be performed is around the foot of the structure on the seaside, on the far end from the dune. The sum of design destabilising moments ($M_{dst,d}$) will be compared to the sum of design stabilising moments ($M_{stb,d}$).

$$\Sigma M_{dst,d} \leq \Sigma M_{stb,d}$$

The line of action of resultant force can be calculated and from that value, the eccentricity of actions from the centre line of the base. The eccentricity will be used to determine the effective width of the base, which is needed to calculate the bearing resistance. This failure mechanism for this caisson can be found in Figure 8.7.

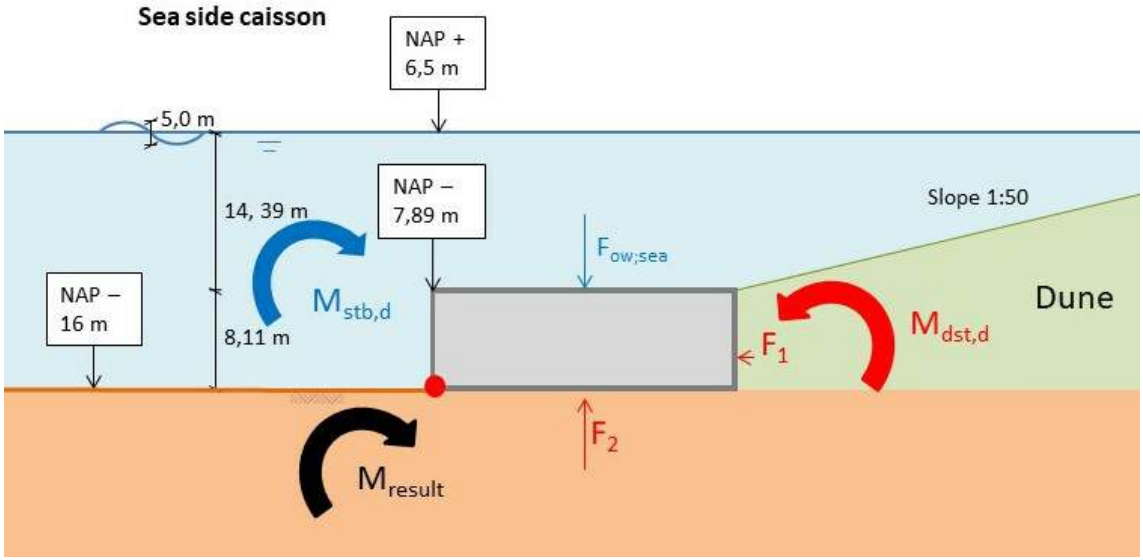

Figure 8.7: Rotational stability failure mechanism for seaside caisson.

The sum of destabilising moments equals 18 387 kNm/m, and the sum of stabilising moments equals 23 569 kNm/m. It leads to a unity check of 0,78.

The eccentricity is 6,6 m from the centre line of the base.

8.4.2 Resistance against sliding

This failure mechanism is sketched in Figure 8.8 and based on the principle of:

$$\Sigma H \leq f \cdot \Sigma V$$

or

$$\Sigma H \leq R_d$$

The resulting horizontal load equals ΣH = 143 kN/m and the resulting vertical load Σ V = 303 kN/m.

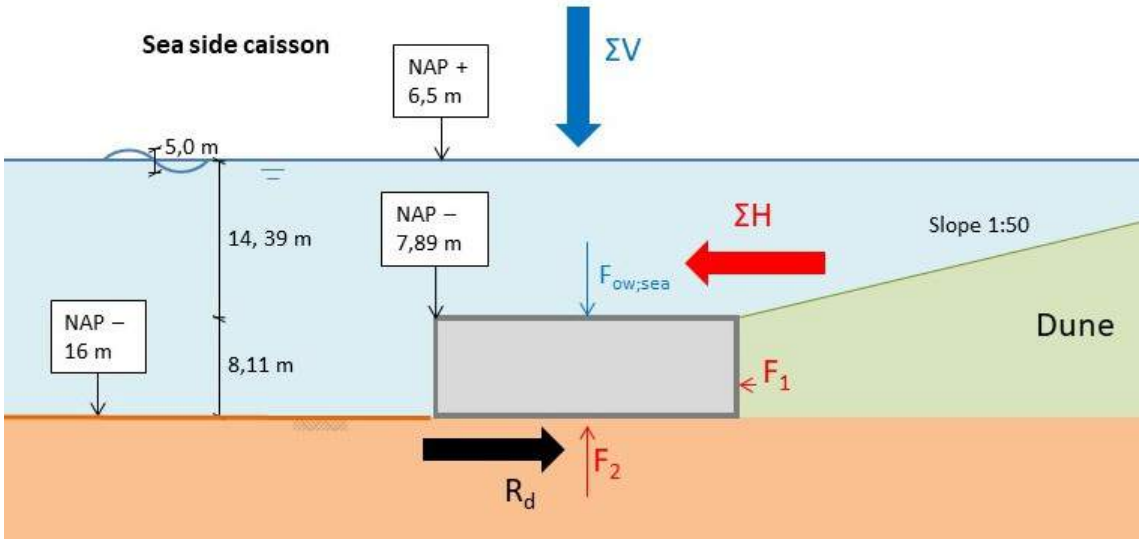

Figure 8.8: Sliding resistance for seaside caisson.

Sliding resistance
The resistance against sliding is given, in Eurocode 7, as:

$$R_d = V_d^{'} \cdot \tan \delta_d \tag{8.2}$$

Where δ_d = 19,9° for the present soil. Consequently, the sliding resistance is R_d = 110 kN/m, which is 33 kN/m short.

Increasing the resistance
When the reduced δ_d can be increased to $\phi_k^{'}$, the sliding resistance becomes R_d = 277 kN/m, which is 34 kN/m overcapacity.

This can be achieved by roughening the bottom surface of the caisson.

Also, the caisson is connected to a large steel pipe, which, for sure, can take 33 kN/m.

8.4.3 Bearing resistance

The bearing capacity of the soil is described by NEN-EN 1997-1, Eurocode 7:

$$\sigma_{max;d}^{'} = \sigma_{v;z;d}^{'} \cdot N_q \cdot s_q \cdot b_q \cdot i_q + 0,5 \cdot \gamma_{average}^{'} \cdot b' \cdot N_{\gamma'} \cdot s_{\gamma'} \cdot b_\gamma \cdot i_{\gamma'} \tag{8.3}$$

It will be described for the interfaces between the caisson and the native soil, as is sketched in Figure 8.9.

For stability, the exerted pressure on the soil should not exceed the pressure the soil can take up:

$$q_d \leq \sigma_{max;d}^{'} \tag{8.4}$$

The bearing capacity of the subsoil $\sigma_{max;d}^{'}$ = 181 kN/m^2 and the maximum vertical stress equals q_d = 39 kN/m^2. It results in a unity check of 0,22.

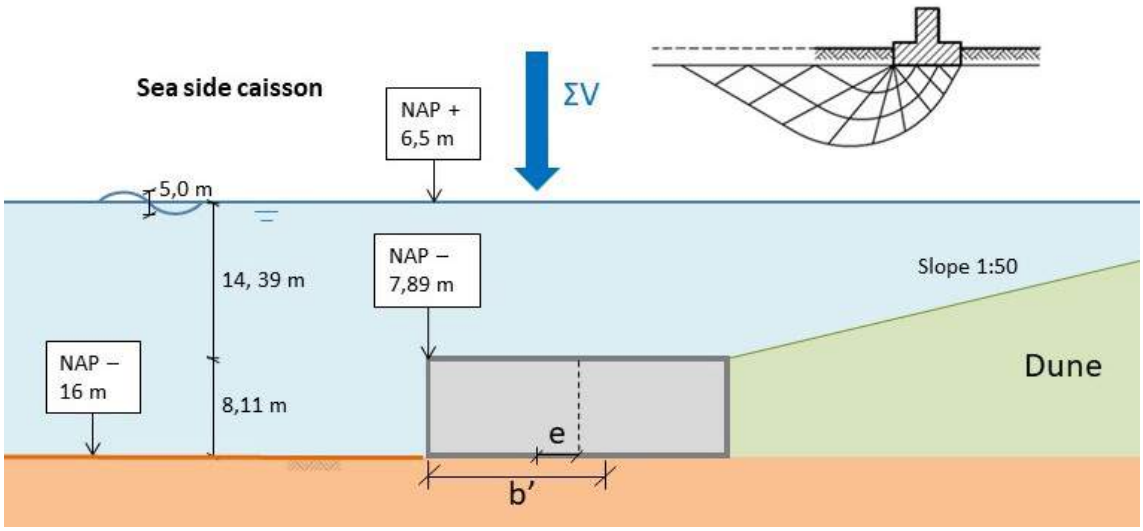

Figure 8.9: The bearing capacity for the seaside caisson.

8.4.4 Floating Stability

The same calculation procedure, as described in Section 6.3.5, is followed, and in Appendix M, detailed calculations are presented. The following statement must be true for the caisson to be statically stable, floating in the water:

$$h_m = \overline{KB} + \overline{BM} - \overline{KG} \geq 0,5\ m \tag{8.5}$$

For the seaside caisson, the metacentric height equals 4,90 m, and the draught is 6,09 m.

8.5 Failure Mechanism Checks of the Lakeside Caisson

8.5.1 Rotational Stability

The rotational stability check that will be performed is around the foot of the structure on the lakeside, on the far end from the dune. The sum of design destabilising moments ($M_{dst,d}$) will be compared to the sum of design stabilising moments ($M_{stb,d}$). The line of action of resultant force can be calculated and from that value, the eccentricity of actions from the centre line of the base. The eccentricity will be used to determine the effective width of the base, which is needed to calculate the bearing resistance.

The failure mechanism of the rotational stability of the lakeside caisson is sketched in Figure 8.10. The rule is:

$$\Sigma M_{dst,d} \leq \Sigma M_{stb,d}$$

The resulting destabilising moment, described in detail in Appendix M, is 85 706 kN/m and the stabilising moment equals 107 834 kN/m. It gives a unity check of 0,79.

The eccentricity, in this case, is 5,17 m from the centre line of the base.

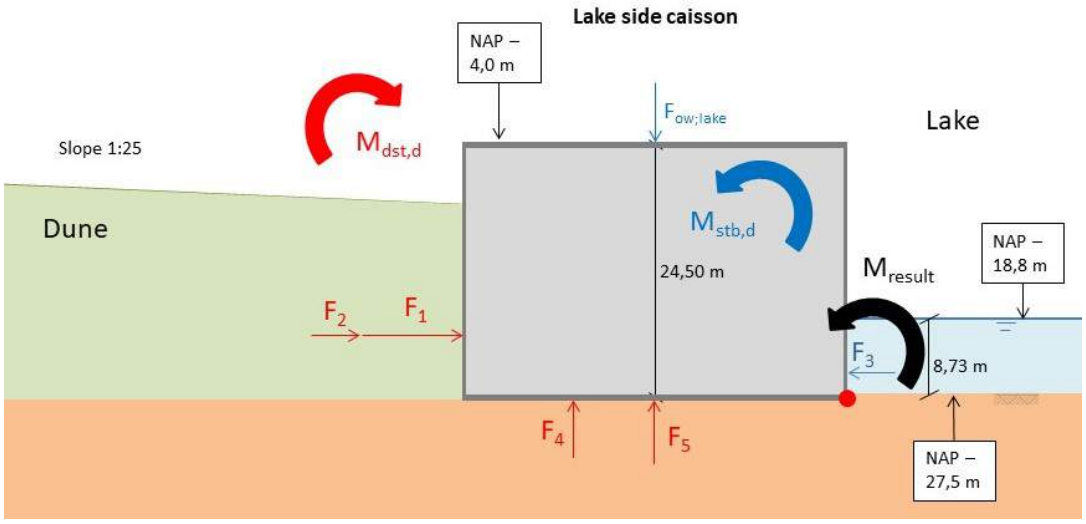

Figure 8.10: Failure mechanism rotational stability of the lakeside caisson.

8.5.2 Resistance against sliding

This failure mechanism is indicated in Figure 8.11, which is based on the principle of:

$$\Sigma H \leq f \cdot \Sigma V$$

or

$$\Sigma H \leq R_d$$

The resulting horizontal load equals Σ H = 2 036 kN/m and the resulting vertical load Σ V = 4 152 kN/m.

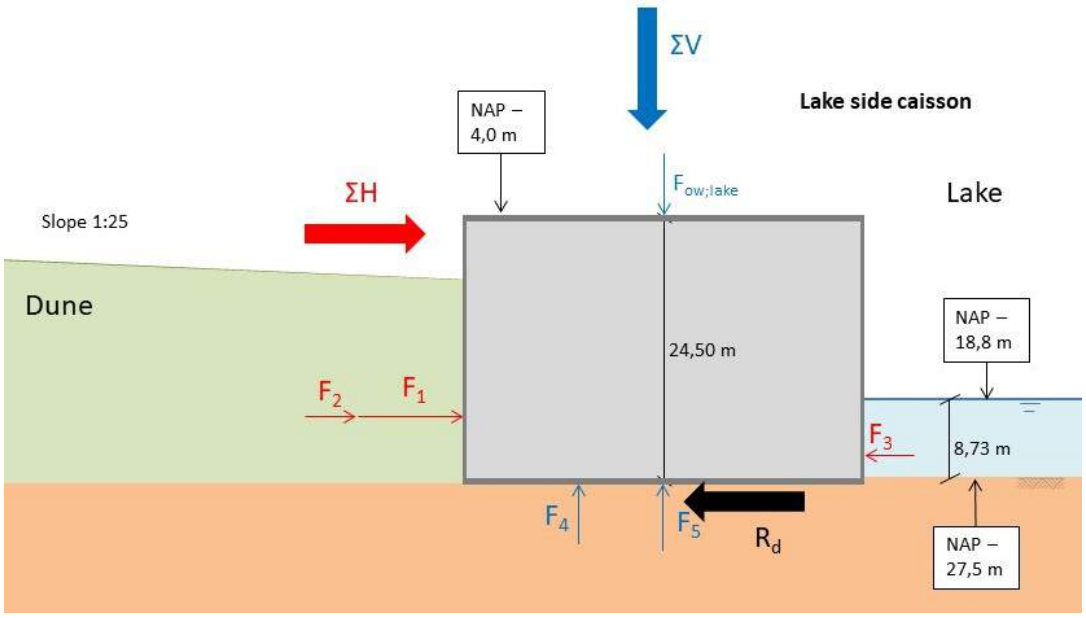

Figure 8.11: Sliding resistance of the lakeside caisson.

Sliding resistance
The resistance against sliding is given, in Eurocode 7, as:

$$R_d = V_d^{'} \cdot \tan \delta_d \tag{8.6}$$

Where δ_d = 22,2° for the present sill. Consequently, the sliding resistance is R_d = 1 695 kN/m, which is 341 kN/m short.

Increasing the resistance
When the reduced δ_d can be increased to $\phi_k^{'}$, the sliding resistance becomes R_d = 2 802 kN/m, which is 766 kN/m overcapacity. The unity check then becomes 0,73.

This can be achieved by roughening the bottom surface of the caisson.

8.5.3 Bearing resistance

The bearing capacity of the soil is described by NEN-EN 1997-1, Eurocode 7:

$$\sigma_{max;d}^{'} = \sigma_{v;z;d}^{'} \cdot N_q \cdot s_q \cdot b_q \cdot i_q + 0,5 \cdot \gamma_{average}^{'} \cdot b' \cdot N_{\gamma'} \cdot s_{\gamma'} \cdot b_\gamma \cdot i_{\gamma'} \tag{8.7}$$

It will be described for the interface between the caisson the native soil, as showed in Figure 8.12.

For stability, the exerted pressure on the soil should not exceed the pressure the soil can take up:

$$q_d \leq \sigma_{max;d}^{'} \tag{8.8}$$

The acting stress q_d = 174 kN/m^2 and the bearing capacity is 191 kN/m^2, resulting in a unity check of 0,91.

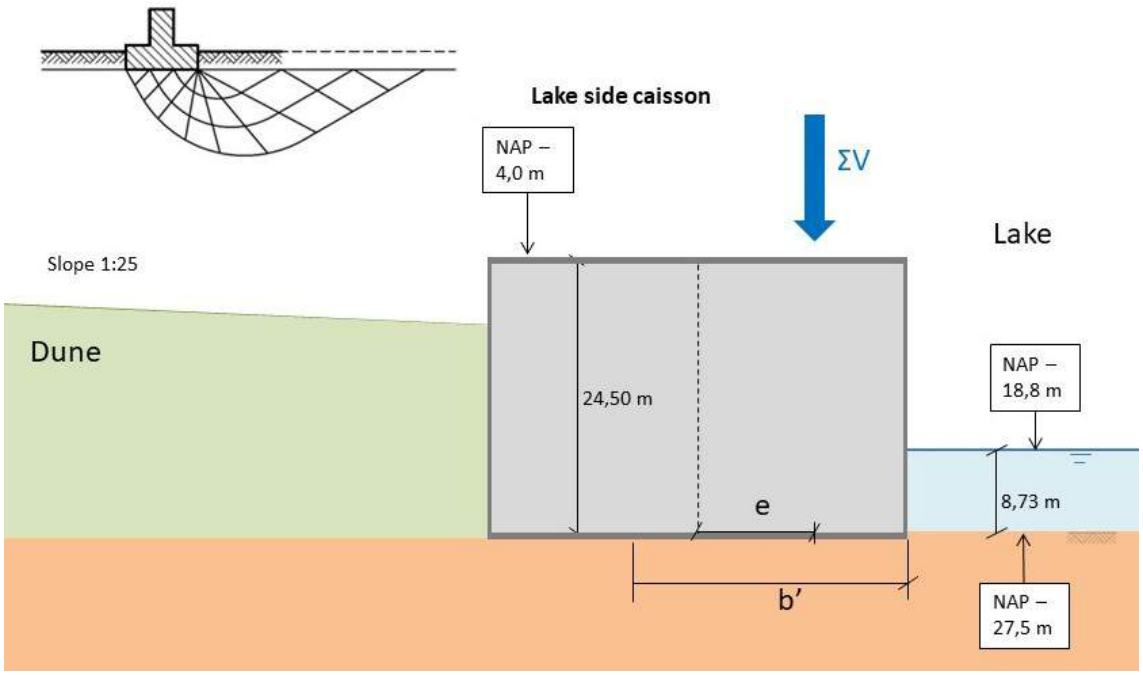

Figure 8.12: Bearing capacity for the lakeside caisson.

8.5.4 Floating Stability

The same calculation procedure, as described in Section 6.3.5, is followed, and in Appendix M, detailed calculations are presented. Again, the stability is described by;

$$h_m = \overline{KB} + \overline{BM} - \overline{KG} \geq 0,5\ m \tag{8.9}$$

Leading to a metacentric height of 5,5 m and a draught of 10,58 m.

8.6 Stability Overview of Alternative 'Integration'

In Table 8.1, an overview of the checked stability conditions is given.

Stability component	**Value**	**Requirement / capacity**	**U.C.**
Seaside Caisson			
Rotational Stability	$M_{overturning}$ = 18 387 kNm/m	$M_{resisting}$ = 23 569 kNm/m	0,78
Sliding: Prefabricated	H_{Ed} = 143 kN/m	H_{Rd} = 110 kN/m	1,30
Sliding: In-situ	H_{Ed}= 143 kN/m	H_{Rd} = 277 kN/m	0,52
Bearing Capacity	q_d = 181 kN/m^2	$\sigma'_{max;d}$ = 39 kN/m^2	0,22
Static Floating Stability	h_m = 4,90 m	$h_m \geq$ 0,0 m (0,5 m)	0,10
Lakeside Caisson			
Rotational Stability	$M_{overturning}$ = 85 706 kNm/m	$M_{resisting}$ = 107 834 kNm/m	0,79
Sliding: Prefabricated	H_{Ed} = 2 036 kN/m	H_{Rd} = 1 695 kN/m	1,20
Sliding: In-situ	H_{Ed} = 2 036 kN/m	H_{Rd} = 2 802 kN/m	0,73
Bearing Capacity: Interface 1	q_d = 235 kN/m^2	$\sigma'_{max;d}$ = 296 kN/m^2	0,79
Static Floating Stability	h_m = 5,50 m	$h_m \geq$ 0,0 m (0,5 m)	0,09

Table 8.1: Overview of the checked stability conditions for alternative 'Integration'.

Part IV

Evaluation of the Alternatives

CHAPTER 9

EVALUATION OF ALTERNATIVES

In this chapter, the evaluation of alternatives, the alternative 'Unity' will be weighed against the alternative 'Integration'. First, the evaluation criteria will be treated, and scores will be assigned per alternative. Then, the weighting factors are described, followed by the Multiple-Criteria Decision Analysis. After that, the costs will be set against the value and, finally, conclusions will be drawn.

9.1 Evaluation Criteria

The different evaluation criteria have already been set in Section 3.5, but for convenience are listed again below, in alphabetical order;

1. Adaptability,
2. ease of construction,
3. ease of maintenance,
4. energy efficiency,
5. material use,
6. risk.

On each evaluation criterion, an alternative can score either 0, 1 or 2. A score of 0 is given when an alternative score relatively low, a score of 1 is given when an alternative score relatively average and a score of 2 is given when an alternative score relatively good on an evaluation criterion.

9.1.1 Adaptability

Adaptability means, in this case, the possibilities of expansion or other changes in the future, especially concerning uncertainties in sea level rise.

Alternative 'Unity' - 1
It is relatively easy to alter the shape or higher the alternative 'Unity'. A possible road on top of the structure can set limitations, but even then there are most likely enough options to higher the caisson.

Alternative 'Integration' - 2
Since a dune is chosen, the adaptability is very high. There will be much space to increase the height of a dune in the future. A side note is that when a dyke structure is chosen, the adaptability will be significantly lower.

9.1.2 Ease of Construction

The ease of construction for the different alternatives is the amount and complexity of steps that have to be taken.

Alternative 'Unity' - 1
The most challenging part of the construction of alternative 'Unity' is most probably, looking at the delta works, the final closure of the caissons. Assumed that the dunes are constructed first and the in- and outlet structure is constructed lastly. The rest of the construction is mostly straightforward prefabrication, submerging and filling of the soil, including scour protection.

Alternative 'Integration' - 0
For alternative 'Integration' more steps are required since the pipe between the caissons should be attached underwater, and the dune body has to be constructed. It can make things quite complicated.

9.1.3 Ease of Maintenance

The ease of maintenance of the pump-turbine system is equal for both alternatives. In both alternatives, one can place an overhead crane on top of the caisson. The only difference is that the pipe in between the caisson for alternative 'Integration' cannot be reached that easily.

Alternative 'Unity' - 2 / alternative 'Integration' - 1

9.1.4 Energy Efficiency

Alternative 'Unity' has the most ecient pump-turbine system, without additional width. The 'Integration' alternative has a quite long pipe in between, which creates friction, and additional research should be carried out to determine the exact eect on the energy storage capacity.

Alternative 'Unity' - 2 / alternative 'Integration' - 0

9.1.5 Material Use

Alternative 'Unity' requires more concrete than alternative 'Integration', but the latter requires more sand or clay for the dune. Since concrete has a bigger effect on the sustainability of the project, this is considered dominant.

Alternative 'Unity' - 1 / alternative 'Integration' - 2

9.1.6 Risk

Usually, in Dutch hydraulic engineering, the risk is defined as a probability times a consequence. Here, potential high-risk factors are compared.

Alternative 'Unity' - 2
Alternative 'Unity' is designed to resist large water level differences, where vertical bearing capacity is governing in ULS.

Alternative 'Integration' - 0
In terms of external loading, the probability of failure is very low, since the dune body is embedded between two caissons. The risk comes mostly from the pipe within the dune, that can cause liquefaction of the dune when leakage occurs. Furthermore, the pipe has to be connected underwater, which also imposes enormous risks, and there are two times more caissons, which have to be immersed.

9.2 Weighting Factors

To the different evaluation criteria, an individual weighting factor of 1, 2 or 3 is given. This value is based on the stakeholder analysis in Section 2.5. When the evaluation criteria meet the requirements set by a stakeholder, placed in the upper right quadrant of table C.1, it is given a weighting factor of 3. When an evaluating criterion meets the requirements of a different stakeholder, it is given a score 2. Lastly, when it is a general evaluation criterion, a score of 1 is given. The results are summarized in Table 9.1.

Criteria	**Weighting Factor**
Adaptability	3
Ease of Construction	1
Ease of Maintenance	2
Energy Efficiency	1
Material Use	2
Risk	3

Table 9.1: Allocation of Weighting Factors.

9.3 Multiple-Criteria Decision Analysis

All the previously described evaluation criteria will now be multiplied by the weighting factor, from the previous section. Those values are added to each other to come up with the total value of an alternative. The obtained results are presented in Table 9.2.

Criterion	Weighting Factor	Score of Alternative 'Unity'	Score of Alternative 'Integration'
Adaptability	3	x 1 = 3	x 2 = 6
Ease of Construction	1	x 1 = 1	x 0 = 0
Ease of Maintenance	2	x 2 = 4	x 1 = 2
Energy Efficiency	1	x 2 = 2	x 0 = 0
Material Use	2	x 1 = 2	x 2 = 4
Risk	3	x 2 = 6	x 0 = 0
Total	-	**18**	**12**

Table 9.2: Multiple-Criteria Decision Analysis.

As can be seen from Table 9.2, the alternative 'Unity' creates more value, without looking at the costs.

9.4 Cost-Value Analysis

For the cost-value analysis, first, the costs for both alternatives should be determined.

The cost build-up for alternative 'Unity' and alternative 'Integration' are presented in Appendix N. Total construction costs for alternative 'Unity', for purely the caisson structure, are €386,6 mln and for dredging and sand refill works the costs are €49,4 mln. The costs of the pump-turbines have already been described in Section 4.1.2. The result is a total of direct project costs of €1 350,3 mln, and this includes 10% uncertainty.

Comparing the value, previously described, against the costs, expressed in billion euros, the cost-value ratio of alternative 'Unity' is $\frac{18}{1,3503}$ = 13,3.

The total costs for purely the caissons of the concept 'Integration' are €238,0 mln. For the dredging works, dune construction and steel pipe in between, €2 422,0 mln, combined leading to a total direct project cost of €3 796,5 mln, including 10% uncertainty. This leads to a cost-value ratio of $\frac{12}{3,7965}$ = 3,2.

Graphically, the cost-value ratios are presented in Figure 9.1.

Included in the costs are the concrete works, including formwork, reinforcement and casting, and the ballast material. Also, the dredging works and sand refill costs are included. Not included are the costs for project management, costs for the construction phase, including building pit, floating the caissons, sinking them, and engineering costs.

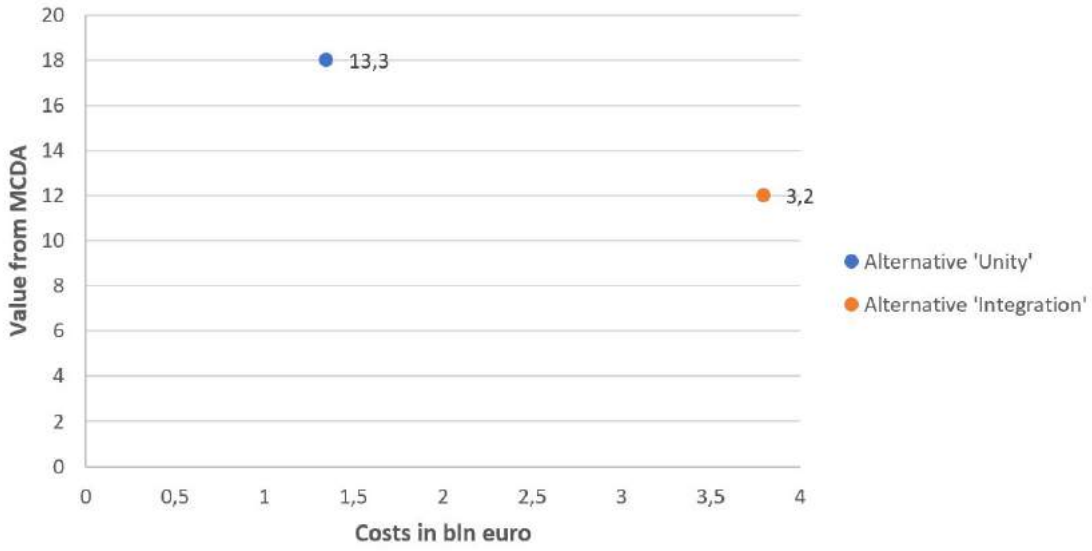

Figure 9.1: Cost-value graph.

9.5 Conclusions of the Evaluation

It can be seen from both the Multiple-Criteria Decision Analysis and the cost-value ratio that concept ‘Unity’ gives the most value for money, even more since the construction of the dune in between the caissons for the ‘Integration’ alternative.

For other reasons, i.e. when additional criteria like aesthetics are included, the alternative of ‘Integration’ could be chosen, but for now, only the alternative ‘Unity’ will be iterated structurally.

Part V

Strength Verification and Stability Iteration

CHAPTER 10

STRENGTH VERIFICATION OF THE MOST FAVORABLE ALTERNATIVE

In this chapter, the floors and walls of the caisson of alternative ‘Unity’ will be checked against the imposed loads. Per governing element the loading situation is described, the ULS bending moment check is performed, the ULS shear force resistance is determined, and the SLS crack width requirement is assessed, which is according to the list presented in Section 3.4.5.

In Figure 10.1, the relevant floors and walls are numbered, and the leading dimensions are presented. From left to right these are called ‘Outer wall 1’, ‘Inner floor 1’, ‘Inner wall 1’, ‘Inner wall 2’, ‘Inner floor 2’ and ‘Outer wall 2’.

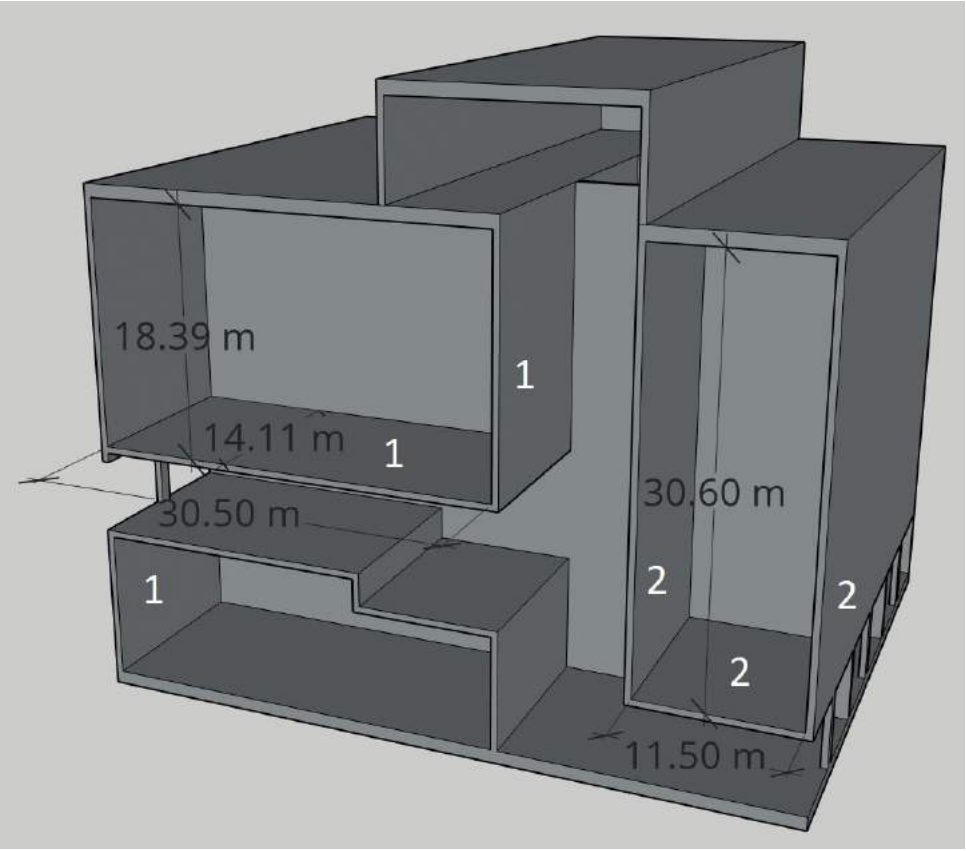

Figure 10.1: Cross-section, 3D, of the alternative ‘Unity’.

All the elements are worked out in more detail in Appendix O: ‘Strength Verification’. Here, the headline is presented.

10.1 Proposed Spatial Improvement

In Appendix O, it can be seen that the first proposed ballast rooms are too large, as they impose huge bending moments in the concrete slabs. To optimise the design and in this way, the bending moment distributions, the proposed spatial improvement can be found in Figure 10.2.

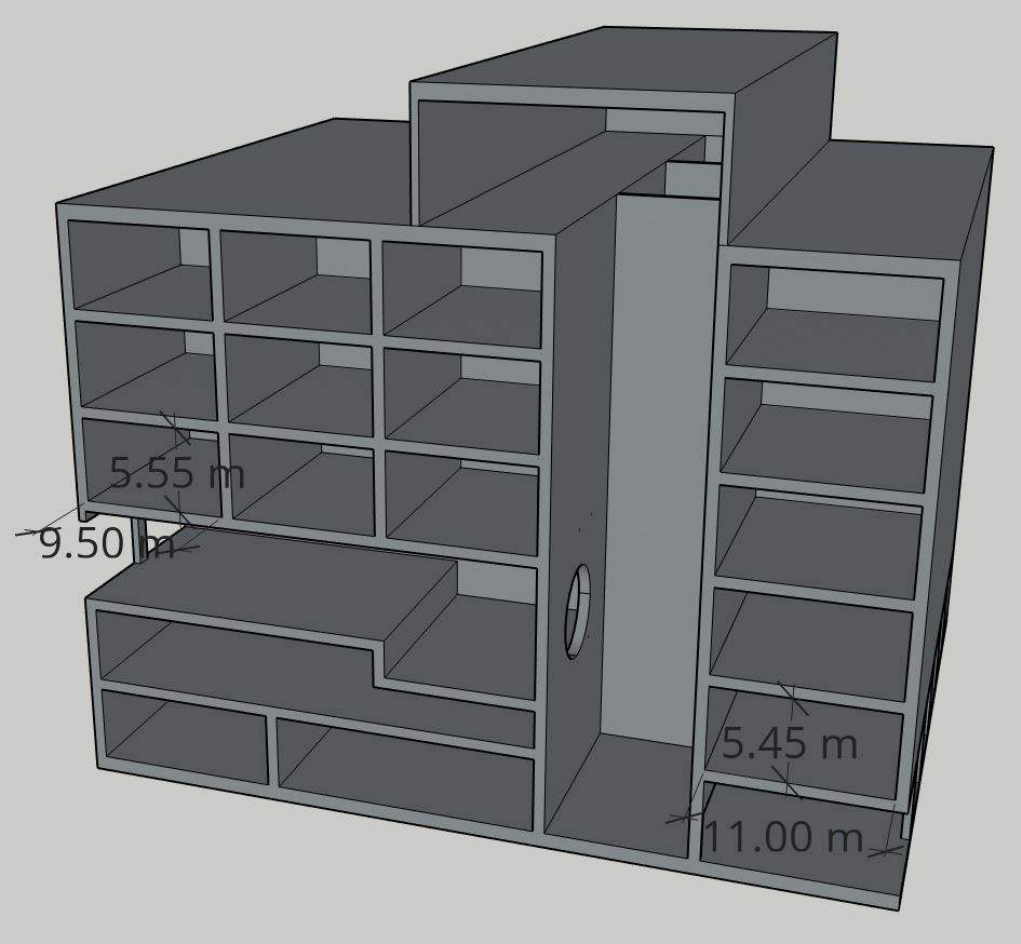

Figure 10.2: Proposed spatial improvement for alternative 'Unity'.

The difficulty for this spatial system is to get the ballast material into the different ballast compartments. This process is not the goal of this chapter and will not be treated anymore in this master's thesis.

Other options to improve the design are to prestress the concrete or to increase the concrete height more effectively, like applying I-beams. These options are not treated in this master's thesis.

10.2 Inner Floor 1

With the divided ballast rooms, the loading situation of one of the inner floors of the upper left ballast room is described in this section. First, the ultimate limit state (ULS) is checked in terms of bending moment capacity and shear force resistance. Then, in the serviceability limit state (SLS), the crack width requirement is checked.

10.2.1 Loading situation

The characteristic loading situation is presented in Figure 10.3.

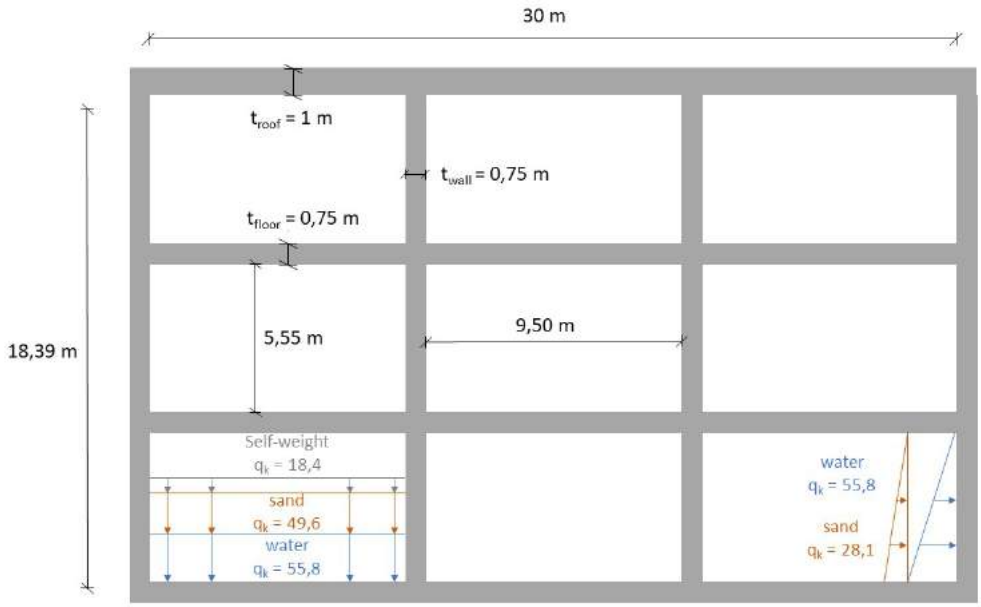

Figure 10.3: Loading situation of compartmentalised inner floor 1.

The assumption is that all the ballast rooms are filled to the top with wet sand, volumic weight 19 kN/m^3, see Table 4.8, and K_0 factor of 0,566, see Appendix K. The water inside is assumed salt since it is dredged from the sea bottom. The volumic weight of reinforced concrete is taken as 24,53 kN/m^3, where concrete class C50/60 is chosen.

For the determination of the bending moment distribution, the old Dutch norm NEN6720 is used, Table 18 to be specific. Figure 10.4 is taken from that table. The supports of the plate will be somewhere between free line supports and fully clamped line supports. For a first estimation of the acting bending moments, plate types I, II, IV A and IV B will be assessed and the maximum bending moments will be checked.

For the ULS checks, the design load is the characteristic loads summarised and multiplied with γ_G = 1,35, since all loads are permanent and no variable loads are present. In SLS, the design load equals the characteristic load.

Lastly, the build-up of a 1 m wide cross-section of the floor is presented in Figure 10.5. The nominal cover on the reinforcement is 50 mm since the exposure class is XS2 and the structural class that should be used is S5.

The top reinforcement is chosen as ϕ32 mm, and the inner reinforcement on the top side is ϕ25 mm. Resulting in a reinforcement area of $A_{s,top}$ = 8 042 mm^2 and $A_{s,bottom}$ = 5 400 mm^2. Combined the reinforcement area is A_s = 13 442 mm^2.

	l_y/l_x	1.0	1.2	1.4	1.6	1.8	2.0	2.5	3.0
I	$m_{vx} = 0.001\ p_d l_x^2$	41	54	67	79	87	97	110	117
	$m_{vy} = 0.001\ p_d l_x^2$	41	35	31	28	26	25	24	23
II	$m_{vx} = 0.001\ p_d l_x^2$	18	26	32	36	39	41	42	43
	$m_{vy} = 0.001\ p_d l_x^2$	18	16	12	10	10	10	10	10
	$m_{sx} = -0.001\ p_d l_x^2$	51	63	72	78	81	82	83	83
	$m_{sy} = -0.001\ p_d l_x^2$	51	54	55	54	54	53	51	49
	$a_x / l_x =$	0.18	0.19	0.19	0.19	0.19	0.19	0.19	0.19
	$a_y / l_y =$	0.18	0.16	0.15	0.13	0.11	0.10	0.07	0.06
III	$m_{vx} = 0.001\ p_d l_x^2$	25	36	45	53	58	62	67	69
	$m_{vy} = 0.001\ p_d l_x^2$	25	23	20	19	18	17	17	17
	$m_{sx} = -0.001\ p_d l_x^2$	68	84	97	106	113	117	122	124
	$m_{sy} = -0.001\ p_d l_x^2$	68	74	77	77	77	76	73	71
	$a_x / l_x =$	0.20	0.22	0.22	0.22	0.23	0.23	0.24	0.24
	$a_y / l_y =$	0.21	0.19	0.17	0.16	0.13	0.12	0.09	0.09
IV A	$m_{vx} = 0.001\ p_d l_x^2$	16	28	42	56	69	80	100	112
	$m_{vy} = 0.001\ p_d l_x^2$	29	32	32	30	27	24	20	18
	$m_{sy} = -0.001\ p_d l_x^2$	69	85	97	105	110	112	112	112
	$a_y / l_y =$	0.19	0.19	0.17	0.17	0.16	0.15	0.12	0.11
IV B	$m_{vx} = 0.001\ p_d l_x^2$	29	34	38	40	42	42	42	42
	$m_{vy} = 0.001\ p_d l_x^2$	16	14	13	13	13	13	13	13
	$m_{sx} = -0.001\ p_d l_x^2$	69	76	80	82	83	83	83	83
	$a_x / l_x =$	0.19	0.20	0.20	0.21	0.21	0.21	0.21	0.21

Figure 10.4: Plate moment distributions, SOURCE: NEN6720, Table 18.

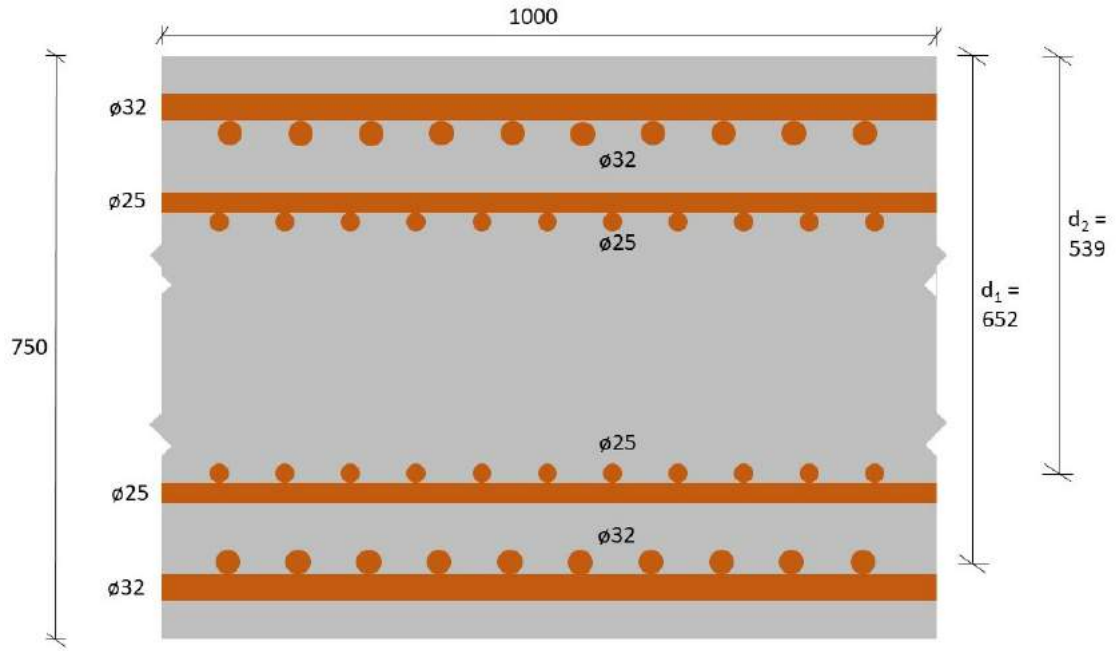

Figure 10.5: Cross-section of a 0,75 m thick floor element.

10.2.2 ULS check

The design load in ULS equals $q_d = 1,35 \cdot (55,8 + 49,6 + 18,4) = 167,1$ kN/m^2.

Bending moment
To determine the maximum bending moment, using Figure 10.4 with a l_y/l_x ratio of 1,49, it occurs in a simply supported plate (I) and has as value $m_{vx,I}$ = 1 078 kNm/m. The maximum negative bending moment occurs in plate type IV A and has as a value $m_{sy,IV\,A}$ = 1 529 kNm/m.

The bending moment resistance of the slab presented in Figure 10.5 can be determined by using:

$$M_{Rd} = A_s \cdot f_{yd} \cdot z = A_s \cdot f_{yd} \cdot d \cdot \left(1 - 0,52 \cdot \rho \cdot \frac{f_{yd}}{f_{cd}}\right) \tag{10.1}$$

The bending moment resistance of the two reinforcement layers is determined by calculating them individually and then adding them to each other. The inner reinforcement layer, when considering both reinforcement directions, the closest to the concrete edge, is taken, since this gives the lowest bending moment resistance.

The bending moment resistance of the ϕ32-100 mm layer is 2 090 kNm/m and of the ϕ25-100 mm is 1 180 kNm/m, combined M_{Rd} = 3 270 kNm/m.

Resulting in an unity check of $\frac{1\,529}{3\,270}$ = 0,52.

Shear force
The shear force is acting at the place of the line support, so at the connection with the wall, it is determined via $V_{Ed} = \frac{q_d \cdot l_x}{2}$ = 794 kN/m.

Without shear reinforcement, the shear capacity $V_{Rd,c}$ = 583,7 kN/m. The shear force resistance, for elements including shear reinforcement, is given by the smallest value of Equation 10.2 and 10.3.

$$V_{Rd,s} = \frac{A_{sw}}{s} \cdot z \cdot f_{ywd} \cdot \cot(\theta) \tag{10.2}$$

$$V_{Rd,max} = \frac{\alpha_{cw} \cdot b_w \cdot z \cdot \nu_1 \cdot f_{cd}}{\cot(\theta) + \tan(\theta)} \tag{10.3}$$

Assuming the angle between the pressure diagonal of concrete and the axis of the beam perpendicular to the shear force, θ, as 45°, and since no pre-tension force is present $\alpha_{cw} = 1$, the value for $V_{Rd,max}$ = 5 100 kN/m and most probably not governing.

Having a centre to centre spacing, s, of 200 mm, a reinforcement area, of the cross-section of the shear reinforcement, of A_{sw} = 750 mm^2/m should be present to reach a shear resistance V_{Rd} = 832 kN/m.

It translates to five, since the spacing is 200 mm, double-edged vertical brackets ϕ10-200 mm per meter slab, giving a steel area of $5 * 2 * 0,25 * \pi * 10^2$ = 785 mm^2/m.

10.2.3 SLS requirement

The load in SLS equals q_k = 55,8 + 49,6 + 18,4 = 123,8 kN/m^2, leading to a bending moment of $m_{sy;IV\,A}$ = 1 133 kNm/m.

According to Eurocode 1992-1-1, Table 7.1N with exposure class XS2, the requirement for allowed crack width is $w_{max} \leq 0,20$ mm. The crack width can be calculated according to:

$$w_k = s_{r,max} \cdot (\epsilon_{sm} - \epsilon_{cm}) \tag{10.4}$$

Where;

$$\epsilon_{sm} - \epsilon_{cm} = \frac{\sigma_s - k_t \cdot \frac{f_{ct,eff}}{\rho_{p,eff}} \left(1 + \alpha_e \cdot \rho_{p,eff}\right)}{E_s} \geq 0,6 \cdot \frac{\sigma_s}{E_s}$$

And;

$$s_{r,max} = k_3 \cdot c + k_1 \cdot k_2 \cdot k_4 \cdot \phi \,/\, \rho_{p,eff} \leq \text{MAX}\{(50 - 0,8 \cdot f_{ck}) \cdot \phi; 15 \cdot \phi\}$$

Calculation details are provided in Appendix O, but for the applied loading situation, the crack width equals w_k = 0,188 mm < 0,20 mm.

10.3 Other Relevant Elements Check

For the other described elements, the acting moments and shear forces are summarized in Table 10.1.

Element	l_x **[m]**	l_y **[m]**	l_x/l_y **[-]**	q_d **[kN/m^2]**	M_{Ed} **[kNm/m]**	V_{Ed} **[kN/m]**
Inner floor 1	9,5	14,11	1,49	167,1	1 529	794
Outer wall 1	5	14,11	2,82	376,8	1 078	**942**
Inner wall 1	5,55	14,11	2,54	68,0	235	189
Inner wall 2	5,45	14,11	2,59	55,6	185	152
Inner floor 2	11,00	14,11	1,28	164,4	**1 550**	905
Outer wall 2	5,45	14,11	2,59	146,2	657	538

Table 10.1: Overview of the relevant distributions for various concrete elements.

As can be seen in Table 10.1, the shear reinforcement, A_{sw}, should be increased to 900 mm^2/m, with a centre to centre spacing of 200 mm, in order to reach a shear capacity of 999 kN/m.

The SLS bending moment of 'inner floor 2' equals 1 148 kN/m^2, resulting in a maximum crack width of 0,186 mm < 0,20 mm. Further iteration is not required.

CHAPTER 11

STABILITY ITERATION

11.1 Draught Check

After the previous chapter, the draught has to be checked once more, since the weight has been increased.

The total weight of the empty caisson, so also of the concrete structure, is per 3 pump-turbine rooms, F_w = 541 395 kN.

The draught of the caisson can be determined according to:

$$d = \frac{F_w}{W \cdot L \cdot \rho_{sw}} = \frac{541\ 395}{53 * 44,33 * 10,06} = 22,91 \text{ m}$$

The bottom of the building pit should now be located at NAP - 26,4 m and the water level at NAP - 26,9 m. It is significantly more than what the surrounding dunes are designed for, which is NAP - 22,5 m but falls within the limitations imposed by the clay layer, which is presented in Appendix J.

Since the weight is higher since more concrete is used, less ballast material is required so that extra optimisations can be performed. To reduce weight and further improve the design, it would be more attractive to use prestressing in order to reduce the amount of concrete used. Alternatively, an option would be to use a different concrete slab shape, like I- or T- sections, in order to use the concrete more efficiently.

11.2 Stability Check

The total structure length now becomes $(3 * 14,11 + 4 * 0,75) * \frac{138}{3}$ = 2 085,18 m. In Table 11.1, an overview of the stability checks is shown. The caisson still fulfils the criteria. Worked out calculations can be found in Appendix O, Section O.7. For the roughened design in the sliding component, the friction angle between the caisson floor and sill should be at least 27,74°.

Stability component	**Value**	**Requirement / capacity**	**U.C.**
Rotational Stability	$M_{overturning}$ = 622 320 kNm/m	$M_{resisting}$ = 885 784 kNm/m	0,70
Sliding: Prefabricated, not roughened	H_{Ed} = 9 536 kN/m	H_{Rd} = 7 400 kN/m	1,29
Sliding: In-situ	H_{Ed}= 9 536 kN/m	H_{Rd} = 12 230 kN/m	0,78
Sliding: Prefabricated, roughened	H_{Ed} = 9 536 kN/m	H_{Rd} = 9 536 kN/m	1,00
Bearing Capacity: Interface 1	q_d = 515 kN/m^2	$\sigma'_{max;d}$ = 850 kN/m^2	0,81
Bearing Capacity: Interface 2	q_d = 499 kN/m^2	$\sigma'_{max;d}$ = 549 kN/m^2	0,91
Static Floating Stability	h_m = 0,89 m	$h_m \geq$ 0,0 m (0,5 m)	0,56

Table 11.1: Overview of the improved caisson's stability conditions.

Part VI

Discussion, Conclusions and Recommendations

CHAPTER 12

RESULTING STRUCTURE AND DISCUSSION

In this chapter, the final design of the most favourable alternative is presented by showing the design, summarising the construction method and providing an overview of the stability requirement. Lastly, the design process is discussed.

12.1 Proposed Conceptual Design

From Chapter 9, it follows that alternative 'Unity' is most favourable and so, alternative 'Unity' has been optimised in Chapter 10. In this section, the design is shown, the construction method is repeated, and the stability requirements are summarised.

12.1.1 Design of the Conceptual Solution

The resulting structure is presented in Figure 12.1, including an overview of the energy storage lake of the Delta21 plan. A white circle highlights the location of the structure.

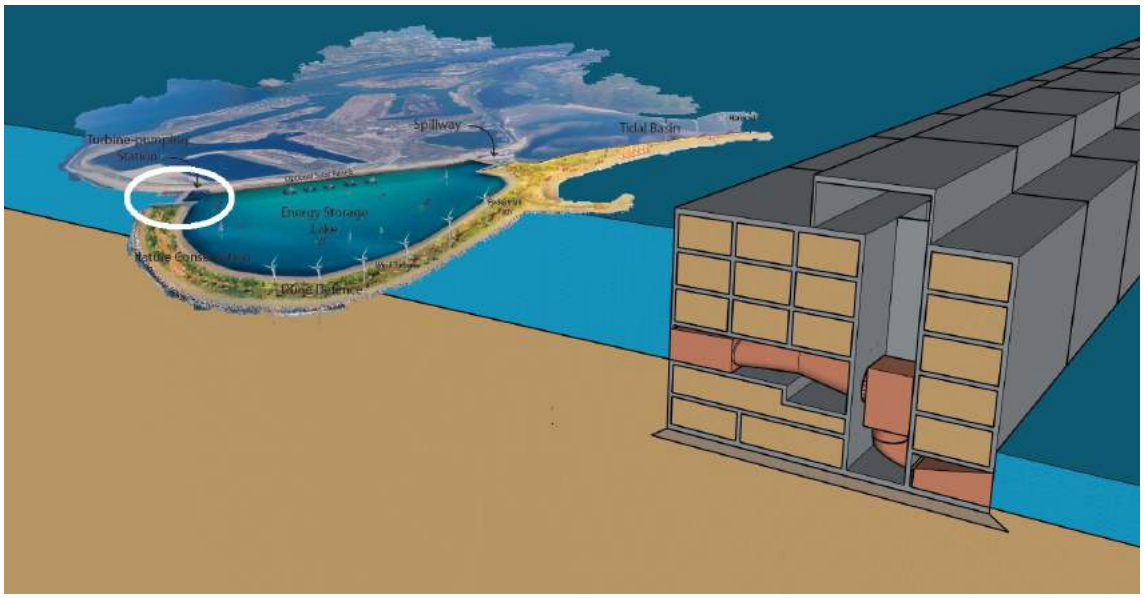

Figure 12.1: Overview cross-section of the conceptual solution.

Components that have been left outside the scope are a piping screen and scour protection.

The walls have a thickness of 0,75 m, and the caisson consists of three pump-turbine rooms that each have a width of 14,11 m. The complete in- and outlet structure has a total of 138 pump-turbines, leading to a total length of 2 085 m. The structure width can be kept at the minimum required, following the pump-turbines, 53 m. The height of the caisson is 38,5 m, running from NAP - 28,5 m until NAP + 10 m.

For a better insight into the layout of the caissons, a 2D cross-section is presented in Figure 12.2, and a 3D view from a different perspective is presented in Figure 12.3.

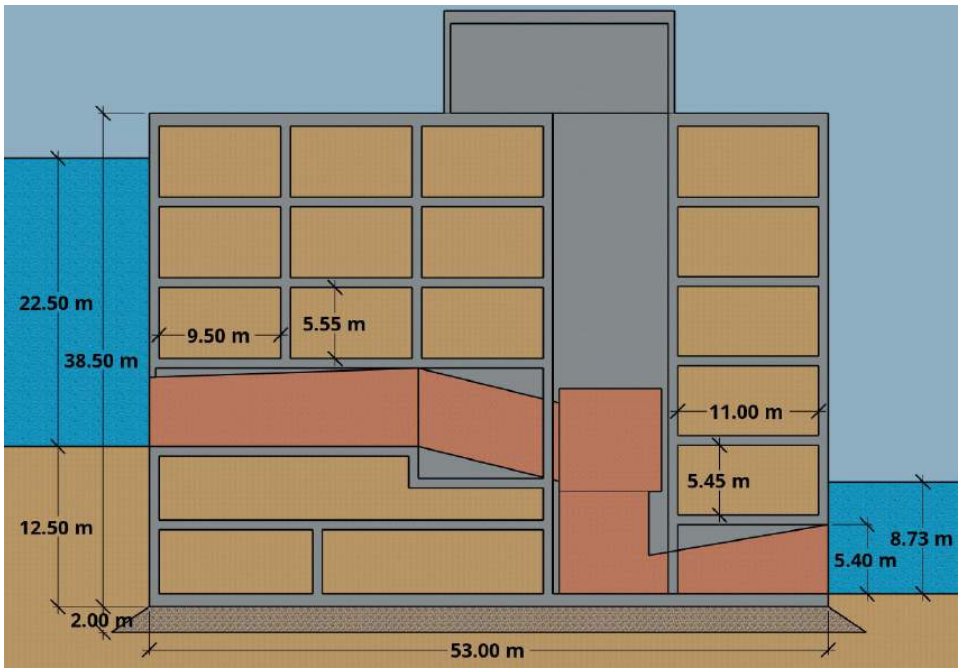

Figure 12.2: 2D cross-section of the conceptual solution.

The main components that can be distinguished are the compartmentalised ballast rooms, the pump-turbine system running through the caisson, the shaft along which the pump-turbine generator can be transported for maintenance reasons, including the optional crane housing on top, and the sill below the caisson.

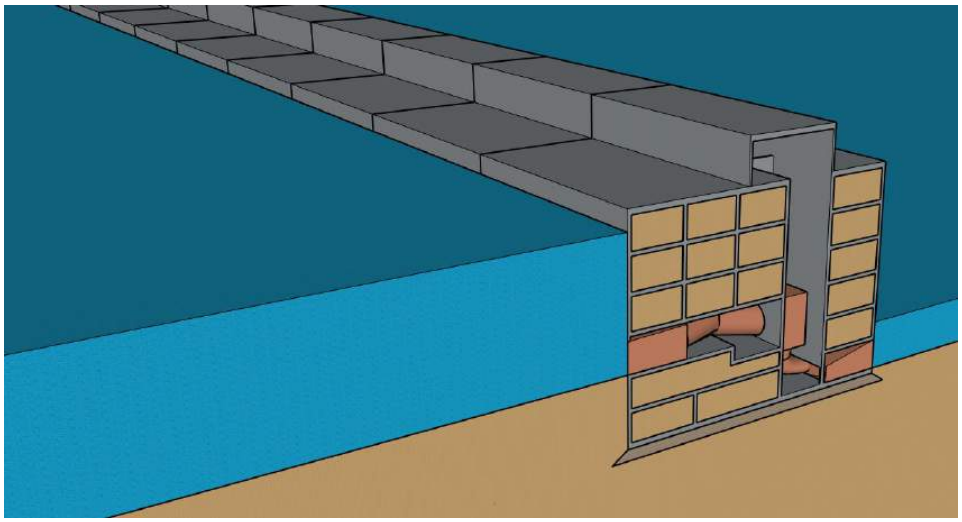

Figure 12.3: 3D cross-section of the conceptual solution.

12.1.2 Construction Method

The proposed construction method is to build the caisson in a building dock that is constructed inside the energy storage lake after the surrounding dunes have been made. Starting from the draught of the iterated caisson, which is 22,91 m, the bottom of the building-dock should be located at NAP - 26,4 m and the water level inside the building-dock should be kept at NAP - 26,9 m.

The caisson is consists of three pump-turbine rooms with 0,75 m thick walls and 1,0 m thick floor or deck elements. The total length of a caisson then becomes 45,33 m and per four caissons they will be floated out to the final location, obtaining a total length of 181,32 m. To couple the caissons during transport, prestressing cables will be used. For transporting the caissons to the final location, a trench has to be dredged out to be able to sail the caisson there.

At the final location, with the sill, the caissons are sunk by pumping in sand into the ballast compartments. After settling at the bottom, the prestressing cables are removed, and the caissons are acting as individual caissons again.

12.1.3 Stability Overview

In this report, various stability checks are performed, which are summarised in Table 12.1. The original unity checks are compared to the unity checks of the improved design.

Stability component	**U.C. Original**	**U.C. Improved**
Rotational Stability	0,74	0,70
Sliding: Prefabricated, not roughened	1,39	1,29
Sliding: In-situ	0,84	0,78
Sliding: Prefabricated, roughened	1,00	1,00
Bearing Capacity: In-situ	0,81	0,81
Bearing Capacity: Prefabricated	0,89	0,91
Static Floating Stability	0,13	0,56

Table 12.1: Comparison of the checked stability conditions for alternative 'Unity'.

For the sliding component, the roughness between the caisson floor and the sill should be 29,65° for the original design and at least 27,74° for the improved design.

An optimisation regarding most stability checks can be performed. Since the roughness between the sill and the caisson is the decisive factor between the unity check of 'sliding: prefabricated' and 'sliding: in-situ' and more research needs to be done, this optimisation is not part of this master's thesis.

12.2 Discussion of the Design Process

Before the conclusions can be stated, first, the design process is discussed. In this section, the considerations regarding the design process will be considered. Per element of the design process, e.g. the analysis and the design, the results and used methods are discussed to validate the outcomes.

The parts that will be discussed are the analysis, focusing on Chapters 2 and 3, the boundary conditions, consisting of Chapter 4, the design, consisting of functional design and the construction, and stability), including Chapters 5, 6, 7 and 8, and the evaluation and iteration, which are the remaining Chapters 9 and 10.

12.2.1 Discussion of the Analysis

The analysis covers Chapter 2: 'Exploration of the Problem' and Chapter 3: 'Basis of the Design'. The analysis starts with a description of the Delta21 plan and more specific the energy storage lake, wherein the in- and outlet structure is situated. Section 2.3 presents the dunes around the energy storage lake, but these are not validated nor researched yet. Especially for alternative 'Integration', this can have significant effect in order to reduce costs.

Furthermore, the stakeholder analysis provides an overview of the stakeholders, but no interviews with representatives from these stakeholders have been conducted. The views and interests of these stakeholders are drawn from the knowledge provided by Delta21 and their publicly stated visions. Therefore, since this analysis is the base of the function analysis, evaluation criteria and the Program of Requirements, this PoR can be subdued to changes or additions/subtractions in requirements. With great certainty, it can be stated that this will not have a considerable influence on the structural systems underlying the alternatives. Most probably, the layout of the alternative would be altered.

The design of the pump-turbine system could have a significant impact on the structure since it is governing for the main dimensions of the caisson. When the existing range pump-turbines is chosen, significantly smaller pump-turbine systems are integrated into the caissons. For the feasibility of this master's thesis, it was assumed that the pump-turbines could be scaled up accordingly to the theoretical framework provided by Pentair. The chosen type of pump-turbine is based on the design graphs in Appendix F.

12.2.2 Discussion of the Boundary Conditions

The boundary conditions are determined in Chapter 4: 'Boundary Conditions' and were split up in three categories: **legal**, **environmental** and **functional** boundary conditions.

In the section about the legal boundary conditions, mostly the Dutch Water Act is treated. Changes can be expected at the time of construction of this project, but much is uncertain about that now. A minor change could be the transition to the Environment & Planning Act, or in Dutch 'Omgevingsvergunning', but that is mostly a difference in the permit process.

The environmental boundary conditions cover the meteorological, hydraulic and geotechnical boundary conditions.

For the meteorological boundary conditions, the starting point is a superstorm, that could occur once every 10 000 years, with a, 12 hours averaged, wind speed of 200 km/h at the height of two kilometres. It is translated to a 10-meter height, which is required for the wave calculations, and it is assumed that this wind speed can occur perpendicular to the structure.

The hydraulic boundary conditions are obtained by comparing three methods, namely existing reports/literature, forecasting software, like Hydra-NL, and for waves, hand calculations. For the design water level, the, currently, most extreme climate scenario W+ from the KNMI is used. There are many uncertainties in sea level rise predictions, so it is wise to design for the upper boundary of the predictions. However, the obtained NAP + 6,50 m is 1,50 m more than what the Haringvliet was designed for and 1,0 m more than the Oosterschelde barrier can resist.

For wave generation, there is a lot more uncertainty. The wave data that can be found in existing literature, or is obtained from forecasting software and those which have been calculated, dier to some extent. Wave measuring stations in the deeper areas of the North Sea predict significant wave heights, from the energy spectrum, once every 10 000 years of 7,1 to 8,2 meters. Prediction software can only calculate for points along the Dutch shore, with an exception for the Maasvlakte shipping trench, with a depth over 20 m. The latter gives a significant wave height of 9,1 m, where the other points give values between 3,4 m and 5,4 m. Lastly, Bretschneider hand calculations result in the significant wave height of 5,0 m, which is a good average value and is used as a starting point. Bigger or smaller wave height has quite some impact, for example, on the acting wave pressure on the caisson or the overtopping requirement. This significant wave height is used directly in overtopping calculations and is converted by a standard rule for the stability checks.

The last category of the environmental boundary conditions is the geotechnical boundary conditions. There are many uncertainties here, since only a few cone penetration test results are available, some distance away from the in- and outlet structure location. Many failure mechanisms for stability depend on the soil type. Currents have not been included since the construction of the energy storage lake will alter the flow patterns of the North Sea.

The boundary conditions finish off with the functional boundary conditions in Section 3.4.1. Many of the possible implications lay outside the scope of this Master's thesis.

12.2.3 Discussion of the Design

The design of the in- and outlet structure is covered in multiple chapters, namely Chapter 5: 'Functional Design', Chapter 6: 'Construction and Stability of Concept 'Unity'', Chapter 7: 'Construction and Stability of Concept 'Duality'' and Chapter 8: 'Construction and Stability of Concept 'Integration''. The functional design and the 'construction and stability are discussed in different paragraphs.

Functional Design
The main components of the functional design follow from previous chapters. Though new research is carried out in the form of the required retaining height, mostly worked out in Appendix H. In these calculations, starting points are the extreme water level, significant wave height and the allowed overtopping discharge, depending on storage capacity. The first two have been discussed in the previous subsection, leaving the allowed overtopping discharge.

The used formula is taken from the EurOtop 2018 manual, in which the average discharge is increased with one standard deviation compared to the previous manual. Much research has been done on this subject, so the input parameters are the main subject of discussion. The allowed overtopping discharge depends on the available storage capacity behind the structure, in this case, the energy storage lake. Assumed is that the water level can safely increase by 0,75 m. As a comparison: when the overtopping discharge of 10 l/s/m is used, the same as applies to the dunes, the structure becomes almost 5,5 m higher.

Construction and Stability Checks
For the construction, the most significant uncertainty is the presence of a clay layer between NAP - 50 m and NAP - 60 m, which could be utilised to keep a building pit dry. Appendix E shows that it is likely, but to be sure, tests have to be performed at the exact location. Also, use was made of the presence of the dunes before constructing the caissons for the in- and outlet structure. Research into these dunes and whether they can keep the building pit as good as dry to NAP - 22,5 m and design for the dykes surrounding the building pit at the other sides are outside the scope of this Master's thesis. Also, outside the scope is the foundation of the caisson on piles, applying a pneumatic caisson and describing the construction of the caisson itself.

For the stability, five failure mechanisms have been checked; 1) piping, 2) rotational stability, 3) horizontal sliding, 4) vertical bearing capacity and 5) static floating stability. The checks are mainly based on the Eurocode, except for piping, for which a relatively coarse check has been performed based on Bligh & Lane. For the other checks, the safety philosophy of the old 'Leidraad Kunstwerken 2003' has been adopted, which, in combination with the extreme events, will lead to conservative estimations.

Rotational stability and static floating stability are in none of the alternatives governing. For horizontal sliding, the friction between the sill and the concrete floor has to be increased to reach sufficient sliding resistance. Also, compaction of the sill has much potential in increasing the sliding resistance, as is shown in the sensitivity analysis.

For the bearing capacity of the subsoil, two interfaces have been checked without modelling it using suitable software, namely, between the caisson and the sill and between the sill and the subsoil.

12.2.4 Discussion of the Evaluation and Strength Verification

The last two chapters that require a discussion are Chapter 9: 'Evaluation of Alternatives' and Chapter 10: 'Strength Verification of the Most Favorable Alternative' and they are discussed in separate paragraphs below.

Evaluation
The evaluation consists of two main elements, a Multiple-Criteria Decision Analysis and a cost indication. Input for the MCDA comes mainly from the stakeholder analysis. Namely, the evaluation criteria and the weighting factors are based on this analysis, which is already discussed in Subsection 12.2.1.

The indicated costs are for the majority based on expertise from the budgeting department of Ballast Nedam and mostly based on the concrete works alone. When a more detailed construction planning is drafted, additional costs for the construction process can be included to give a complete overview of the costs.

Furthermore, including costs for the construction phase will also contribute to cost differences. For alternative 'Integration' twice as much, but smaller, caissons have to be constructed and transported to and immersed at the final location.

A better evaluation based on costs can be made using a cost-benefit analysis. For this, the benefits of the different alternatives should be budgeted and compared to each other.

Strength Verification
The strength verification is performed without an extensive Finite Element Model (FEM), but has been performed using simplified plate configurations.

This simplification can, on the one hand, mean that very conservative estimations are made for the plate configuration. In this way, higher bending moments follow from the calculation then will be present. On the other hand, passing on of the bending moments between the plates has not to be considered and that can either amplify or reduce the occurring bending moments.

After this strength verification, many more optimizations can be performed. Since the weight of the caisson (empty and filled with ballast) has now increased, the resistance against overturning and sliding has increased, but the bearing capacity will be lower. Consequently, less ballast material has to be used and less loading will be present on the inner floors and inner walls. It means that measures such as reducing the thickness of the walls or the amount of reinforcement can be applied.

CHAPTER 13

CONCLUSIONS AND RECOMMENDATIONS

The last chapter of the main body of this master's thesis consists of the conclusions of the design process and recommendations for potential future research.

13.1 Conclusions of the Design Process

This master's thesis aimed to come up with a preliminary design for the in- and outlet structure of the energy storage lake within the Delta21 plan and to give insight into possible bottlenecks of the design.

The main conclusions of this master's thesis are:

1. To meet the pumping requirement of 10 000 m^3/s, a tailor-made pump-turbine must be made.

2. For an in-situ construction pit at NAP - 30,5 m, the clay layer cannot resist bursting. A building pit till NAP - 26,4 m in the energy storage lake will work.

3. The minimum width of 53 m, following from the pump-turbine system, passes all performed stability checks.

4. For alternative 'Integration' the dune and pipe, for the pump-turbine, in between the caissons is a costly addition to the construction costs, making it significantly more expensive than the alternative 'Unity'.

Following the requirements and boundary conditions, presented in this thesis, an alternative for the in- and outlet structure of the energy storage lake has been presented. This conceptual solution measures up to those requirements and conditions and fulfils the requirements for a primary water barrier, is stable against an extreme event, i.e. a water level of NAP + 6,50 m and a significant wave height of 5,0 m, and a suitable construction method is described.

13.2 Recommendations

The recommendations have been split up into two parts, recommendations that can be included in the design process and recommendations that are generally useful to work out in more detail for the Delta21 project itself.

13.2.1 Recommendations for the Design Process

- **Interaction between the spillway and the in- and outlet structure**; investigate how the spillway should be designed to make sure the water height on the energy storage lake can vary between the specified levels, and still the extreme discharge capacity of 10 000 m^3/s can be utilised when required;
- **Foundation of the caisson**; whether a foundation on piles can be advantageous compared to the foundation on a sill, also with regards to create additional horizontal sliding resistance, and to make a foundation model for the caisson to give a better insight in the soil behaviour;
- **Application of a Pneumatic caisson**; consider whether it is cheaper or possible to apply a pneumatic caisson in order to prevent excavation works at the location;
- **Currents around the energy storage lake**; the construction of the energy storage lake will influence the currents flowing along the Dutch coast. Additional research will have to be performed to predict current patterns and whether it influences the in- and outlet structure.

13.2.2 General Recommendations for the project

- **Solution for the dune - structure connection**; The connection between the caisson and the dune should be designed since it requires a unique solution;
- **Soil investigation**; decrease the uncertainty in the soil parameters and verify the presence of a clay layer around NAP - 50 m;
- **Wave energy spectrum analysis**; since swell waves, with a long period, can often contain higher energy, or arrive from a different direction, than shorter period higher waves within the energy spectrum - from British Standard [BS 06349-1-2 (31)];
- **Construction planning**; to work out in more detail a phased schedule, so costs can be included for the required time for building the structure;
- **Waterproofing of concrete**; since the ballast compartments are filled with wet sand and the caisson is in direct contact with the seawater, and the energy storage lake water and concrete is naturally not waterproof;
- **Strength iteration**; in order to reduce the draught of the caisson, it could be advantageous to explore the prestressing of the concrete slabs or to alter the shape of the concrete cross-section, as in applying, for example, I-profiles, to optimise the use of material. Furthermore, it is recommended to make a Finite Element Model of the caisson for checking the bending moments and shear forces.

REFERENCES

Barends, F.B.J. et al. (2008). *Bodemdaling langs de Nederlandse kust*. ISBN: 978-90-5199-521-3.

Bjerkseter, Catho and Anders Agotnes (2013). "Levelised Costs of Energy for Offshore Floating Wind Turbine Concepts". PhD thesis. Norwegian University of Life Sciences.

CBS et al. (2018). *Zeespiegelstijging langs de Nederlandse kust en mondiaal, 1890-2017*. URL: www.clo.nl.

CIRIA, CUR, CETMEF (2007). *The Rock Manual. The use of rocks in hydraulic engineering (2nd edition)*. C863, CIRIA, London. ISBN: 978-0-86017-683-1.

Deltacommissie (2008). *Samen werken met water*. Tech. rep.

Deltares (2018a). *Mogelijke gevolgen van versnelde zeespiegelstijging voor het Deltaprogramma*. Tech. rep. URL: https://www.deltares.nl/app/uploads/2018/08/Deltares%7B%5C_%7DMogelijke-gevolgen-van-versnelde-zeespiegelstijging-voor-het-Deltaprogramma.pdf.

— (2018b). *Werkwijze Bepaling Hydraulische Ontwerprandvoorwaarden*. Tech. rep.

Dillingh, D (2013). *Kenmerkende waarden kustwateren en grote rivieren*. Tech. rep. 1207509-000. Deltares.

Eekels, J. and N. F.M. Roozenburg (1991). "A methodological comparison of the structures of scientific research and engineering design: their similarities and differences". In: *Design Studies* 12.4, pp. 197–203. ISSN: 0142694X. DOI: 10.1016/0142-694X(91)90031-Q.

EurOtop (2018). *EurOtop manual*. Tech. rep.

Heijer, F. den et al. (2006). *Achtergrondrapport HR 2006 voor de Zee en Estuaria*. Tech. rep.

Hertogh, Prof.dr.ir. M.J.C.M., Dr.ir. M.G.C. Bosch-Rekveldt, and Dr. E.J. Houwing (2018). *Dictaat CTB1220 Integraal Ontwerp en Beheer*.

Hurk, Bart van den et al. (2014). *KNMI ' 14 : Climate Change scenarios for the 21st Century*. Tech. rep. May. DOI: 10.1007/s00382-009-0721-6. URL: http://www.klimaatscenarios.nl/brochures/index.html.

Jonkman, S.N. et al. (2018). *Flood Defences Lecture Notes CIE5314*.

Kloosterman, Herman et al. (2002). *Hoge molens vangen veel wind*. Tech. rep. Rijksuniversiteit Groningen.

Lavooij, Huub (2018a). *01-Deelrapport Natuurherstel*.

— (2018b). *03-ENERGIE-deelrapport-18 sept*.

— (2018c). *05-Waterveiligheid,21 sept*.

Lier, Hubert N. van and Frederick R. Steiner (1982). "A review of the Zuiderzee reclamation works: An example of Dutch physical planning". In: *Landscape Planning* 9.1, pp. 35–59. ISSN: 03043924. DOI: 10.1016/0304-3924(82)90010-7.

Meyer, Han (2009). "Reinventing the Dutch Delta: Complexity and Conflicts". In: *Built Environment* 35.4, pp. 432–451.

Molenaar, W.F. and M.Z. Voorendt (2018). *Hydraulic Structures - General Lecture Notes*.

— (2019). *Manual Hydraulic Structures - TU Delft*.

Monteiro, Paulo J M, Sabbie A Miller, and Arpad Horvath (2017). "Towards sustainable concrete". In: *Nature Materials* 16.7, pp. 698–699. ISSN: 1476-4660. DOI: 10.1038/nmat4930. URL: https://doi.org/10.1038/nmat4930.

NEN-EN 1997-1+C1+A1/NB (2016). *National Annex to NEN-EN 1997-1 Eurocode 7: Geotechnical design - Part 1: General rules*. Tech. rep.

Oppenheimer, Michael et al. (2019). "Sea Level Rise and Implications for Low Lying Islands, Coasts and Communities." In: *IPCC Special Report on the Ocean and Cryosphere in a Changing Climate* 355.6321. ISSN: 10959203. DOI: 10.1126/science.aam6284.

Rijkswaterstaat (1992). *Bouw tunnel elementen : locatie bouwdok tunnelelementen (BTE 92010) : inrichtingsvarianten bouwdok (BTE 92008) : bouwmethoden tunnellelementen (BTE 92009)*. Tech. rep.

— (2005). *Guideline on Functional Specification*. Tech. rep. september. URL: http://www.coinsweb.nl/downloads/Handreiking%7B%5C_%7Dfunctioneel%7B%5C_%7Dspecificeren.pdf.

— (2013). *Characteristic values tidal area*. Tech. rep.

— (2014a). *De veiligheid van Nederland in kaart*. Tech. rep.

— (2014b). *Handreiking ontwerpen met overstromingskansen*. Tech. rep.

— (2019). *Watersnoodramp 1953*. URL: https://www.rijkswaterstaat.nl/water/waterbeheer/bescherming-tegen-het-water/watersnoodramp-1953/index.aspx.

RWS-WVL Waterkeringen (2018). *Werkwijzer Ontwerpen Waterkerende Kunstwerken – Ontwerpverificaties voor de hoogwatersituatie*. Tech. rep.

Stichting On'Wijs (2003). *Deltawerken - Haringvlietdam*. URL: http://www.onwijsnat53.nl/sporen/deltawerken/haringvlietdam/bouw.htm.

Technische Adviescommissie voor de Waterkeringen (2003). *Leidraad Kunstwerken*. Tech. rep.

U.S. Army Corps of Engineers (1994). *Mechanical and Electrical Design of Pumping Stations*. Tech. rep.

United Nations (2015). *Sustainable Development Goals*. URL: https://www.un.org/sustainabledevelopment/sustainable-development-goals/.

Voorendt, M.Z., W.F. Molenaar, and K.G. Bezuyen (2016). *Hydraulic Structures - Caissons: TU Delft lecture notes*. February. DOI: 10.1061/9780784406724.

Watson, Ian and Charles W Finkl (1992). "Simplified Technical Summary of the Complete Delta Works, Including the Eastern Scheldt / Eenvoudige technische samenvatting van de gehele deltawerken, inclusief de Oosterschelde / Vereinfachte technische Darstellung des gesamten Deltaplans, einschliessli". In: *Journal of Coastal Research*, pp. 1–56. ISSN: 07490208, 15515036. URL: http://www.jstor.org/stable/44864117.

Appendices

APPENDICES TABLE OF CONTENTS

APPENDIX A

OVERVIEW DELTA WORKS

In this appendix an overview of the constructed Delta Works is given.

DATE		MAJOR PROJECT COMPONENTS	TYPE	CONSTRUCTION	PURPOSE
1	1958	HOLLANDSE IJSSEL BARRIER Drop barrier	P*	Guillotine steel-gate drop barrier Navigation lock	Open Mode: Facilitates navigation and Rhine discharge (a 250 m3/s) Closed Mode: Storm-surge flood protection
2	1960	ZANDKREEK DAM Tidal-Control Dam	S	Caisson-core and dredged-sand embankment dam and Navigation lock	Reduced tidal-current velocity for construction of primary Veerse barrier Provides navigation to stagnant Lake Veerse
3	1961	VEERSE DAM Fixed Barrier	F	Caisson-core and primary dredged-sand embankment dam, with asphalt cover	Storm-surge estuary closure (with Zandkreek Dam creates Lake Veerse)
4	1965	GREVELINGEN DAM Tidal-Control Dam, Lock and Siphon Sluice	S	Combination cableway block and caisson core, with dredged-sand dam; Artificial island for navigation lock and Flushing siphon sluice	Reduced tidal-current velocity for construction of Brouwers barrier Facilitates navigation access to Lake Grevelingen Siphon helps flush Lake Grevelingen
5	1970	VOLKERAK DAM Waterway Dam and Navigation Locks	S	Artificial-island and coffer-dam construction on large lock complex (two locks for commercial traffic, one lock for pleasure craft)	Reduced tidal-current velocity for construction of Haringvliet barrier Contributes to Scheldt-Rhine non-tidal waterway link
6	1971	HARINGVLIET DAM Sluice-Gate Barrier and Navigation Lock	P	Artificial-island and coffer-dam construction on piled piers, for pivot-gate sluice barrier Also cableway block-core embankment section	Closed Mode: Storm-surge barrier Part Closed and Open: Rhine discharge (fresh-water management) Shipping access to North Sea
7	1972	BROUWERS DAM Fixed Barrier	F	South Channel: Cableway block core with dredged-sand embankment dam Central: Dredge-improved sand bank North Channel: Caisson core and sand embankment	Fixed storm-surge estuary closure, sluice and crest road

8	1983	MARQUISATE QUAY DAM Waterway Closure Dam	S	Core of riprap and gravel placed by barge and truck dump Core partially replaced by dredged-sand fill	Closure forms part of the Scheldt-Rhine waterway link Reduced tidal velocity for Oester dam construction and Controls salt-water intrusion to the east
9	1986	EASTERN SCHELDT BARRIER Lift-Gate Barrier	P	Two dredged-improved artificial islands Three sections of pier-and-lift-gate sluice barrier	Closed Mode: Storm-surge flood protection Open Mode: Tidal flushing for preservation of salt-water estuary Shipping access to North Sea
10	1987	PHILIPS WATERWAY DAM and KRAMMER NAVIGATION LOCKS	S	Large-scale artificial-island and coffer-dam construction of Krammer Lock Complex Dredged-sand embankment closure	Contributes to non-tidal conditions in the Scheldt-Rhine waterway Krammer Locks provide shipping access to Eastern Scheldt, but preserves salt-water eastern Scheldt and fresh-water waterway
11	1987	OESTER WATERWAY Closure Dam and Navigation Lock	S	Artificial-island and coffer-dam construction of navigation lock Dredged-sand embankment closure	Part of Scheldt-Rhine compartmentalization closure Facilitates shipping access between waterway and the Eastern Scheldt Controls salt-water intrusion to the east

* P = Primary storm-surge barrier; F = Primary storm-surge fixed embankment dam; S = Secondary tidal-control and/or waterway embankment

Table A.1: Overview of Delta Works.

APPENDIX B

CHARACTERISTICS DELTA21

An overview of the original characteristics of Delta21 is provided in Table B.1.

Delta21	**Characteristics**
Content size	350 – 400 million m^3
Tidal Basin + Haringvliet area	120 km^2
Power pumps / turbines ESL	1 860 MW
Max. emergency discharge to sea ESL + Tidal Basin	10 000 m^3/s
Water level in the ESL	NAP - 5 m to NAP -22,5 m (17,5 m difference)
Filling time / idle time at full load	12 hours
Average height difference	14 m (0,25 m + 13,75 m)
Power per pump / turbine	5 MW
Minimal idle time	12 hours (pumping)
Useful turbine power ESL	1 012 MW
Required pump power ESL	1 401 MW
Pump consumption at 100% utilization	6 136 GWh/yr
Turbine output at 100% utilization	4 443 GWh/yr
ESL installed power	60 MW
Tidal turbines Tidal Basin - output	550 GWh/yr

Table B.1: Characteristics Delta21.

APPENDIX C

STAKEHOLDER TABLE

In Table C.1 all the relevant stakeholders regarding the project are listed. The stakeholders are based on interest and power. Furthermore, their position towards the project and the effect of the project on them are shown.

Stakeholder	Involvement in subject	Primary or Secundary	Interest in subject (L-M-H-VH)	Influence/ power (L-M-H-VH)	Position	Effect of subject on actor
Rijkswaterstaat	Client	Primary	Very High	Very High	Flood protection, sustainability and drinking water.	Increase in flood protection and sustainability. Risk in fresh water supply. Costly project.
Natura 2000	Project Location is protected Natura 2000 area	Primary	Very High	Very High	Retaining and improving ecology.	Risk in loss of flora and fauna.
Havenbedrijf Rotterdam	Maasvlakte II	Primary	Very High	High	Shipping and project location.	Change in shipping routes and loss of expansion possibilities.
Vitens	Fresh water inlet	Primary	Very High	Medium	Fresh water supply.	Risk in fresh water supply from Haringvliet.
Ministry of Infrastructure and Water Management	Client (above Rijkswaterstaat)	Primary	High	Very High	A clean, safe and sustainable environment. Directing Rijkswaterstaat.	Increase in flood protection and sustainability. Costly project.
Delta Commissioner	Delta Structures (Haringvliet Dam)	Primary	High	High	Flood protection, fresh water supply, climate-proof and water-resilient country.	Expansion of Delta works, increase of activities.
Milieudefensie	Ecology	Primary	High	High	A clean, healthy, sustainable and fair world.	Risk in loss of flora and fauna. An increase of sustainability.
Province of Zuid-Holland	Spatial Planning Environmental Protection	Primary	High	Medium	Smart use of space, innovative economy, attractive living environment and clean energy.	Increase of area, possible expansion of infrastructure.
Delfland Water Authority	Water Management	Primary	High	Medium	Water management.	Risk in loss of fresh water supply. Change in water management.
Schieland en de Krimpenerwaard	Water Management	Primary	High	Medium	Water management.	Risk in loss of fresh water supply. Change in water management.
Hollandse Delta Water Authority	Water Management	Primary	High	Medium	Water management.	Risk in loss of fresh water supply. Change in water management.
Rivierenland Water Authority	Water Management	Primary	High	Medium	Water management.	Risk in loss of fresh water supply. Change in water management.

Brabantse Delta Water Authority	Water Management	Primary	High	Medium	Water management.	Risk in loss of fresh water supply. Change in water management.
Municipality of Goeree-Overflakkee	Spatial Planning	Primary	High	Low	Connection to land.	Change in area, possible infrastructural changes.
Municipality of Rotterdam	Spatial Planning Flood Protection	Primary	High	Low	Flood protection of the city.	Increased flood protection.
Municipality of Dordrecht	Spatial Planning Flood Protection	Primary	High	Low	Flood protection of the city.	Increased flood protection.
Province of Noord-Brabant	Environmental Protection	Primary	Medium	Low	Flood protection around the Volkerak-Zoomlake.	Increased flood protection.
Municipality of Westvoorne	Spatial Planning	Primary	Medium	Low	Connection to land.	Change in area, possible infrastructural changes.
Media	Informs the society	Secundary	High	Medium		

Table C.1: List of Stakeholders.

In this part all the stakeholder that were not discussed in the main report are listed and elaborated on.

Delta Commissioner "The Delta Commissioner, a special government commissioner, is in charge of the Delta Program. The Delta Program is in place to protect the Netherlands from flooding, to ensure a sufficient supply of fresh water, and to contribute to achieving a climate-proof and water-resilient spatial design in the Netherlands."

The interest and power of the Delta Commissioner are both high.

Municipality of Rotterdam Since the municipality of Rotterdam directly owns the land of the 'Tweede Maasvlakte', against which the energy storage lake will be build, they are too an important stakeholder. On their website they distinguish five perspectives in their environmental vision; circular city, compact city, healthy city, inclusive city and productive city. The first and last perspective are directly connected to the Delta21 plan.

Hollandse Delta Water Authority "The water authority of Hollandse Delta protects the islands of Zuid-Holland against flooding, manages the surface water, purifies the waste water, manages the (water)ways and makes an active contribution to the spatial design of it's area." The four mission of the water authority can be categorised in four groups; flood risk, enough water, clean water and water chain.

Delfland Water Authority Water authority Delfland has no direct borders with the Delta21 project plan, but has fresh water intakes in the Haringvliet, which will become mostly salt again. This could create problems for this water authority, so a fresh water inlet should be realised in the Delta21 plan.

Municipality of Dordrecht The main goal of Delta21 is to protect the hinterland, where Dordrecht lays, against flooding. According to the report of 'Veiligheid Nederland in kaart' (Rijkswaterstaat 2014a), the island of Dordrecht has a probability of flooding of 1/170, which is quite high. Also the group risk table in Appendix G is quite horizontal, which means that the consequences, in terms of victims, are relatively high.

Others Other important stakeholders for the Delta21 project are the Oyster and Mussel association and Heat company Rotterdam (should be kept satisfied) and the Rivierenland Water Authority, TenneT, the ministry of Agriculture, Nature and Food Quality and the ministry of Economic Affairs (should be kept informed).

Stakeholders that should be monitored are Evides, the World Nature Fund (WNF), Mileudefensie (Friends of the earth Netherlands), the municipality of Goeree-Overflakkee, the province of Noord-Brabant, Sport Fishing Netherlands, LTO Netherlands, Rijnland Water Authority, Brabantse Delta Water Authority, the municipality of Oostvoorne, the Fishermen's Association and Natuur&Milieu.

APPENDIX D

WIND SPEED CALCULATIONS

To be able to calculate the significant wave height, the wind speed has to be known. In this appendix the wind speed that can occur once every 10 000 years at a height of 2 km (obtained from the KNMI) will be translated to a wind speed at 10 m height above the water level. This wind speed can be used as input in the wave height calculations. The heaviest wave attack follows from a wind direction north to south.

The super storm that the KNMI expects once every 10 000 years had a wind speed of 200 km/h or 55,56 m/s, which is averaged over 12 hours and estimated at a height of two kilometers. As has been stated in the main report in Section 4.3.1, the wind speed at a height of 10 meters above ground / water level is needed. To convert this wind height, two different methods are used. Both methods describe the height profile as logarithmic.

The first method follows from Eurocode NEN-EN 1991-1-4: Wind actions. An important note to this method is that the input should be the basic wind speed v_b, which is determined as a function of the wind direction and season on a height of 10 meters above terrain category II (see Table D.1) and should be with the expression $v_b = c_{dir} \cdot c_{season} \cdot v_{b,0}$. Parameter c_{dir} is the wind direction factor (recommended value is 1,0), c_{season} is the seasonal factor (recommended value is 1,0) and $v_{b,0}$ is the fundamental value of the basic wind speed (the characteristic 10 minute averaged wind speed, independent of wind direction and time of the year, at 10 meters height above ground level in an open area with low vegetation, like grass, and freestanding obstacles with a spacing of at least 20 obstacle heights). To get an estimation for the wind speed at 10 meters height, the formula for the average wind speed v_m (which ought to be determined with basic wind speed v_b, which is dependant on the wind climate) at height z is rewritten:

$$v_m z = c_r z \cdot c_o z \cdot v_b \tag{D.1}$$

$$v_b = \frac{v_m z}{c_r z \cdot c_o z} \tag{D.2}$$

In which $c_r z$ is the roughness factor and $c_0 z$ is the orography factor, which is 1,0 at sea.

The roughness factor can be determined from:

$$c_r z = k_r \cdot \ln\left(\frac{z}{z_0}\right) \qquad for \qquad z_{min} \leq z \leq z_{max} \tag{D.3}$$

$$c_r z = c_r z_{min} \qquad for \qquad z \leq z_{min} \tag{D.4}$$

In which: z_0 is the roughness length and k_r is the terrain factor, dependent on the roughness length z_0, calculated according to:

$$k_r = 0,19 \cdot \left(\frac{z_0}{z_{0,II}} \right)^{0,07} \tag{D.5}$$

In which:
$z_{0,II}$ = 0,05 m (terrain category II: Table D.1);
z_{min} is the minimum height as described in Table D.1;
z_{max} equals 200 m and;
z_0 is described in Table D.1.

Terrain category		$\mathbf{z_o}$ **[m]**	$\mathbf{z_{min}}$ **[m]**
0	Sea or coastal area with wind approaching over open sea	0,003	1
I	Lakes or flat and horizontal area with negligible vegetation and without obstacles	0,01	1
II	Area with low vegetation, like grass, and free standing obstacles (trees, building) with a spacing of at least 20 obstacle heights	0,05	2
III	Area with regular vegetation or buildings or free standing obstacles with a spacing of at least 20 obstacle heights (like villages, suburban terrain, permanent forest)	0,3	5
IV	Area where at least 15% of the surface is covered with buildings with an average height above 15 meters	1,0	10
The terrain categories are highlighted in NEN-EN 1991 1-4 - Windbelasting A.1.			

Table D.1: Terrain categories and terrain parameters.

Starting with the terrain factor, $k_r = 0,19 \cdot \left(\frac{0,003}{0,05}\right)^{0,07} = 0,156$. Since the height described by the KNMI is two kilometers and z_{max} is 200 meters the z_max value is taken, because wind speeds higher than 200 meters can be assumed equal.
So $c_r200 = 0,156 \cdot \ln\left(\frac{200}{0,003}\right) = 1,733$.

Finally, $v_b = \frac{2003,6}{1,733 \cdot 1,0} = 32,06$ m/s.

The second method is found in (Kloosterman et al. 2002) and describes the gradient of the wind speed over the height as:

$$v_h = \frac{v_{10} \cdot \log \frac{h}{z}}{\log \frac{10}{z}} \tag{D.6}$$

Which describes the wind speed v_h at a height h, with a standard wind speed v_{10} at a height of 10 meters. Parameter z is the roughness height of the landscape (see Table D.1). In here no height restrictions are given, so the 2 kilometer height is used.

Rewriting the equation gives: $v_{10} = \frac{v_h \cdot \log\left(\frac{10}{z}\right)}{\log\left(\frac{h}{z}\right)} = \frac{\frac{200}{3,6} \cdot \log\left(\frac{10}{0,003}\right)}{\log\left(\frac{2\,000}{0,003}\right)} = 33,61$ m/s.

Since the values of the two methods are quite similar, a wind speed of 34 m/s will be used. Please note that these formulas are not intended to be used to calculate the basic wind speed, but rather uses this value as input. Since this is a preliminary study, this result will be used as starting point.

APPENDIX E

BOUNDARY CONDITIONS

In this appendix, some of the boundary conditions are worked out in more detail, like the wind set down, significant wave height and geotechnical data.

E.1 Wind set down

The wind set down has be be determined directly behind the structure (on the side of the energy storage lake). Following from the main report, the following formula can be used:

$$\delta h_1 = 0,41 \cdot k \cdot \frac{u^2}{g \cdot h} \cdot F \cdot cos\,(\phi)$$

The factor 0,41 is determined from the shape of the lake, which is assumed to be an isosceles trapezoid. See the sketch in Figure E.1 for the determination of the center of gravity.

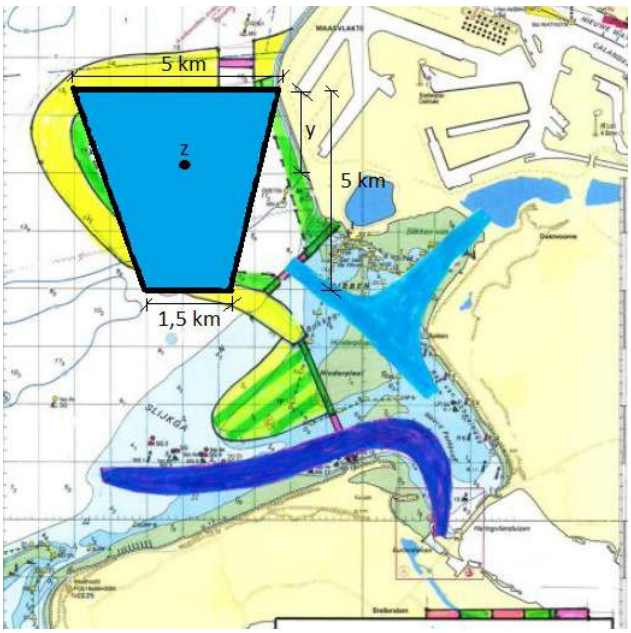

Figure E.1: Center of Gravity ESL.

To determine the center of gravity, the formula: $y = \frac{h}{3} \cdot \frac{b+2a}{b+a}$ where a is the short side, b is the long side and h is the height. Filling in the formula: $y = \frac{5}{3} \cdot \frac{5+2 \cdot 1,5}{5+1,5} = 2,05$ km. To determine the factor in the formula for the wind setup the position of the center of gravity is taken relative to the height of the lake, and is 0,41 (see Figure E.2).

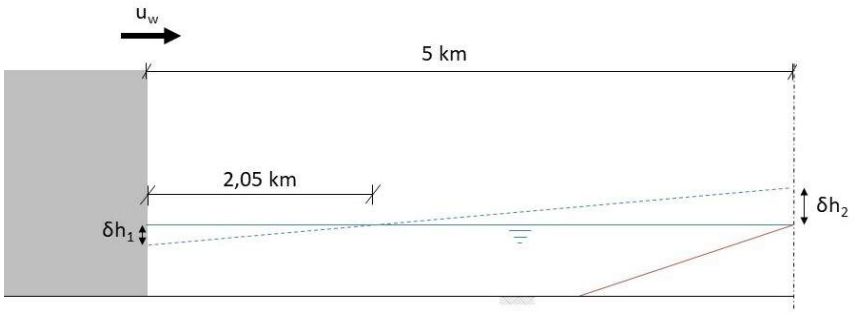

Figure E.2: Wind setup and set down.

With the order of magnitude for the constant k = $3,2 * 10^{-6}$ and assuming the oblique angle of wave attack $\phi = 0$, perpendicular to the structure, meaning the fetch is approximately 5 km. Assuming the lowest water level (7,83 m water depth on the lake side) and the most extreme wind speed of 34 m/s, the wind offset equals 0,10 m at the structure (negligible). It would be unwise to check the higher water level, since the water height is included in the denominator of the fraction. When it is done (high water is 22,5 m), the wind set down equals 0,03 m.

E.2 Waves

For determining the significant wave height and peak period, three methods will be used, namely; researching existing reports and observations, using software like Ringtoets and Hydra-NL and making estimations using the Bretschneider method.

From reports and observations the wave height H_{m0} is listed for several measuring stations on the North Sea (Heijer et al. 2006). The location of the measuring stations is indicated in Figure E.3 and the corresponding wave heights are listed in table E.1. In this report the measured data spans from 1979-2002 and for each station a conditional Weibull-distribution is made and the wave heights expected once every 10 000 years are calculated. For the fetch the distance from each station to the 'Doggersbank' is estimated.

Figure E.3: Locations of wave measuring stations.

Location	Depth [m]	Hm0 [m]	Tm-1,0 [s]	Tm02 [s]	Tp [s]
MPN	18	7,96	12,7	9,46	15,3
EUR	32	8,19	11,3	8,74	12,7
LEG	21	8,08	11,2	8,56	12,9
SWB	20	7,06	10,8	8,15	12,3

Table E.1: Data from wave measuring stations.

Software from Rijkswaterstaat, like Riskeer and Hydra-NL, gives the significant wave height that occurs once every 10 000 years. The results are summarized in table E.2. Dyke segment 20-1 is from dyke ring Voorne-Putten and is the segment between the Haringvlier barrier and the Maasvlakte. Dyke segment 25-1 is from dyke ring Goeree-Overflakkee and is the part between the Haringvliet barrier and the Oosterschelde barrier. The climate scenarios that are used in Hydra-NL are those of the KNMI (Hurk et al. 2014). The measured points in Hydra-NL are indicated by green dots in fig E.4.

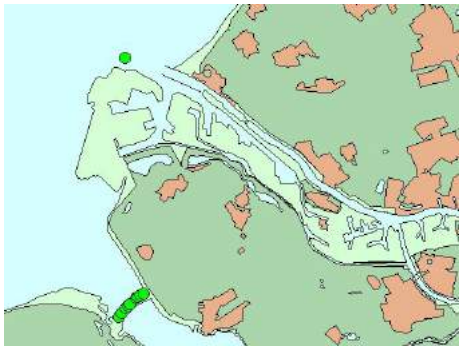

Figure E.4: Measuring points in Hydra-NL.

Riskeer

	Hs [m]
Dyke segment 25-1	5,44
Dyke segment 20-1	3,46

Hydra-NL	Climate scenario G	Climate scenarion W+
Haringvliet barrier	Hs [m]	Hs [m]
2023	3,402	3,402
2050	3,414	3,490
2100	3,490	3,666
Maasvlakte	Hs [m]	Hs [m]
2023	8,926	8,926
2050	8,914	8,985
2100	8,985	9,147

Table E.2: Wave data from Riskeer and Hydra-NL

Lastly, wave estimations according to the Bretschneider method (Voorendt, Molenaar, and Bezuyen 2016) are indicated in table E.3. According to Bretschneider the significant wave height can be calculated as follows:

$$\widetilde{H} = 0,283 \cdot \tanh\left(0,53 \cdot \tilde{d}^{\,0,75}\right) \cdot \tanh\left(\frac{0,0125 \cdot \tilde{F}^{\,0,42}}{\tanh\left(0,53 \cdot \tilde{d}^{\,0,75}\right)}\right) \tag{E.1}$$

$$\widetilde{T} = 7,54 \cdot \tanh\left(0,833 \cdot \tilde{d}^{\,0,375}\right) \cdot \tanh\left(\frac{0,077 \cdot \tilde{F}^{\,0,25}}{\tanh\left(0,833 \cdot \tilde{d}^{\,0,375}\right)}\right) \tag{E.2}$$

$$\widetilde{H} = \frac{g \cdot H_s}{u_{10}^2} \tag{E.3}$$

$$\widetilde{T} = \frac{g \cdot T_p}{u_{10}} \tag{E.4}$$

$$\widetilde{F} = \frac{g \cdot F}{u_{10}^2} \tag{E.5}$$

$$\tilde{d} = \frac{g \cdot d}{u_{10}^2} \tag{E.6}$$

As water depth a depth of 22,5 m is taken (NAP + 6,5 m storm setup).

Wind Direction [Degrees N]	Wind Speed (1/10 000 yrs) [m/s]	Fetch F [km]	Significant wave height Hs [m]	Peak wave period Tp [s]
0	34	430	5,0	9,8

Table E.3: Wave calculations according to Bretschneider.

The Fetch for the proposed location of the in- and outlet structure is indicated in Figures E.5. The Doggerbank is chosen, since this is a shoal in the North Sea. Furthermore, a longer fetch has a very minor impact on the significant wave height.

Figure E.5: Fetch to the Doggersbank.

E.3 Soil Cross Sections

In this section four different cross sections of the soil layers around the Haringvliet can be found, at the locations according to Figure E.6.

Figure E.6: Cross sections in DINOloket.

E.3.1 REGIS cross section 1

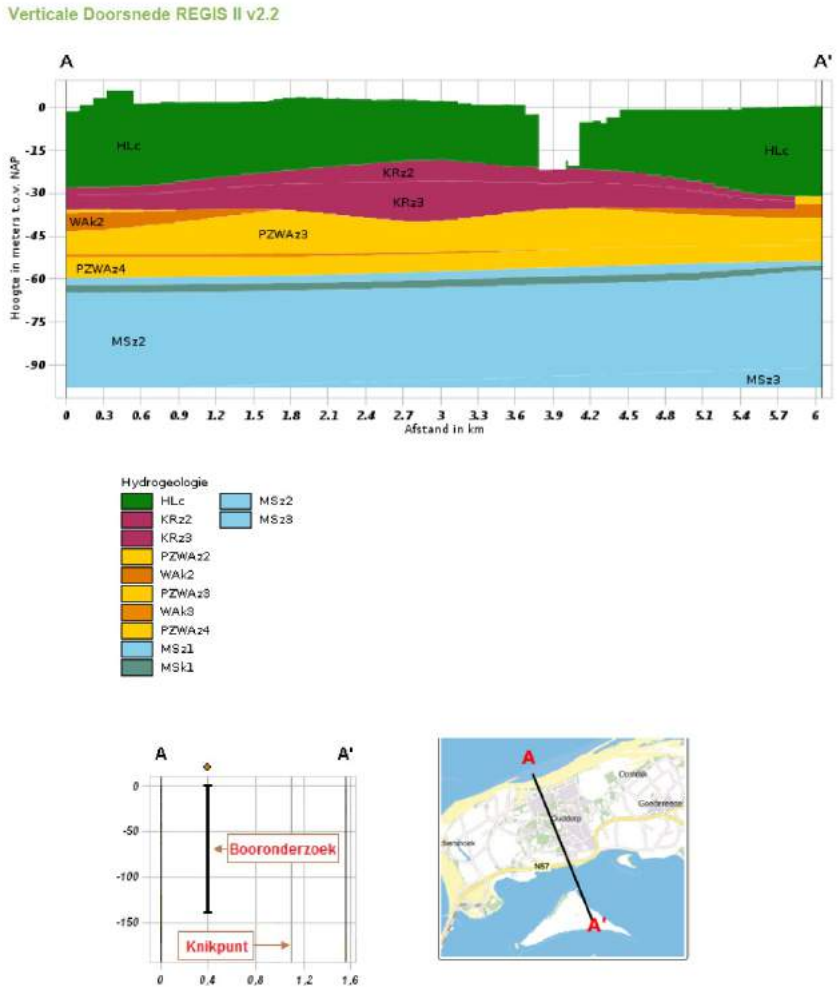

Figure E.7: REGIS cross section 1.

E.3.2 REGIS cross section 2

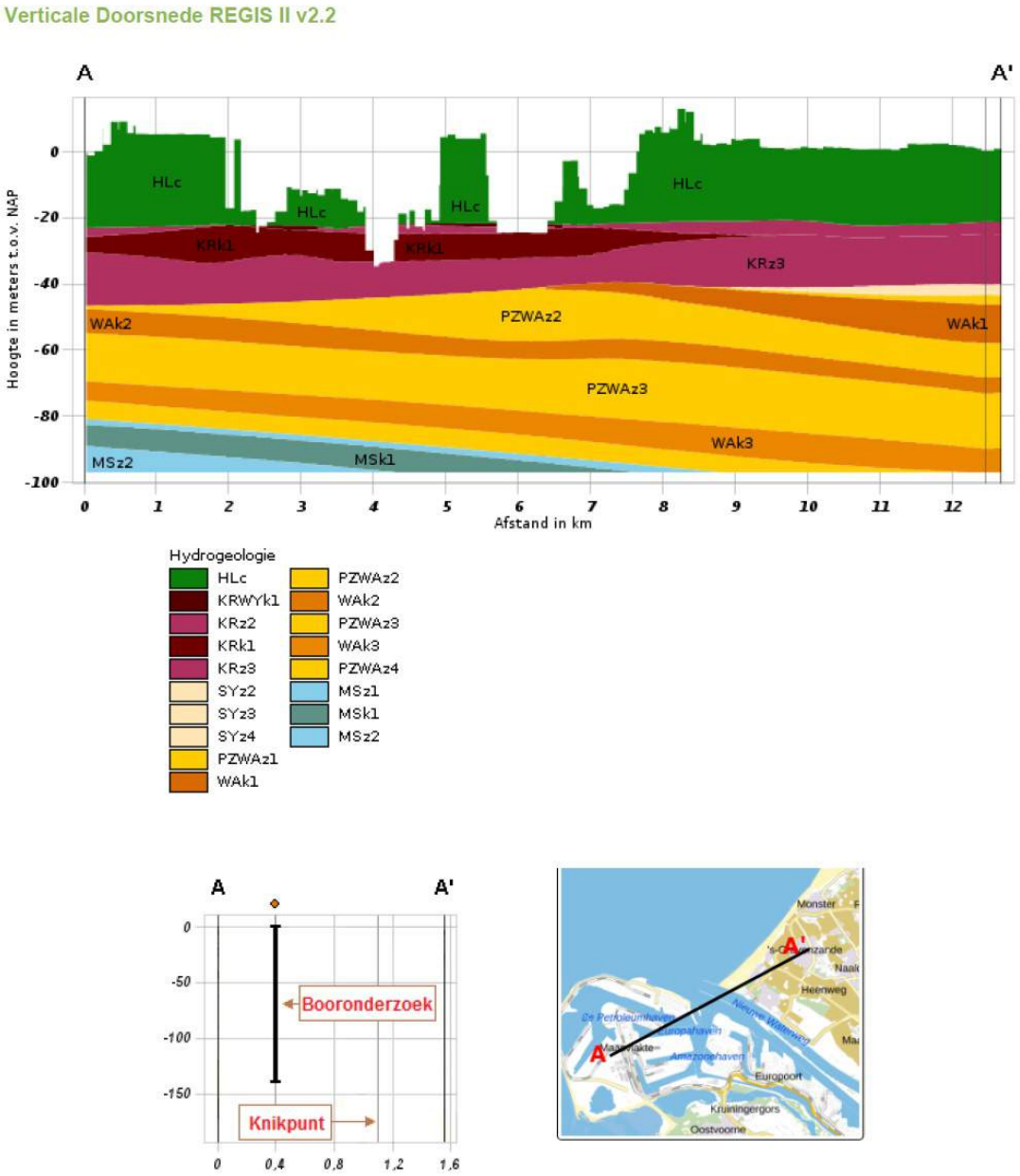

Figure E.8: REGIS cross section 2.

E.3.3 REGIS cross section 3

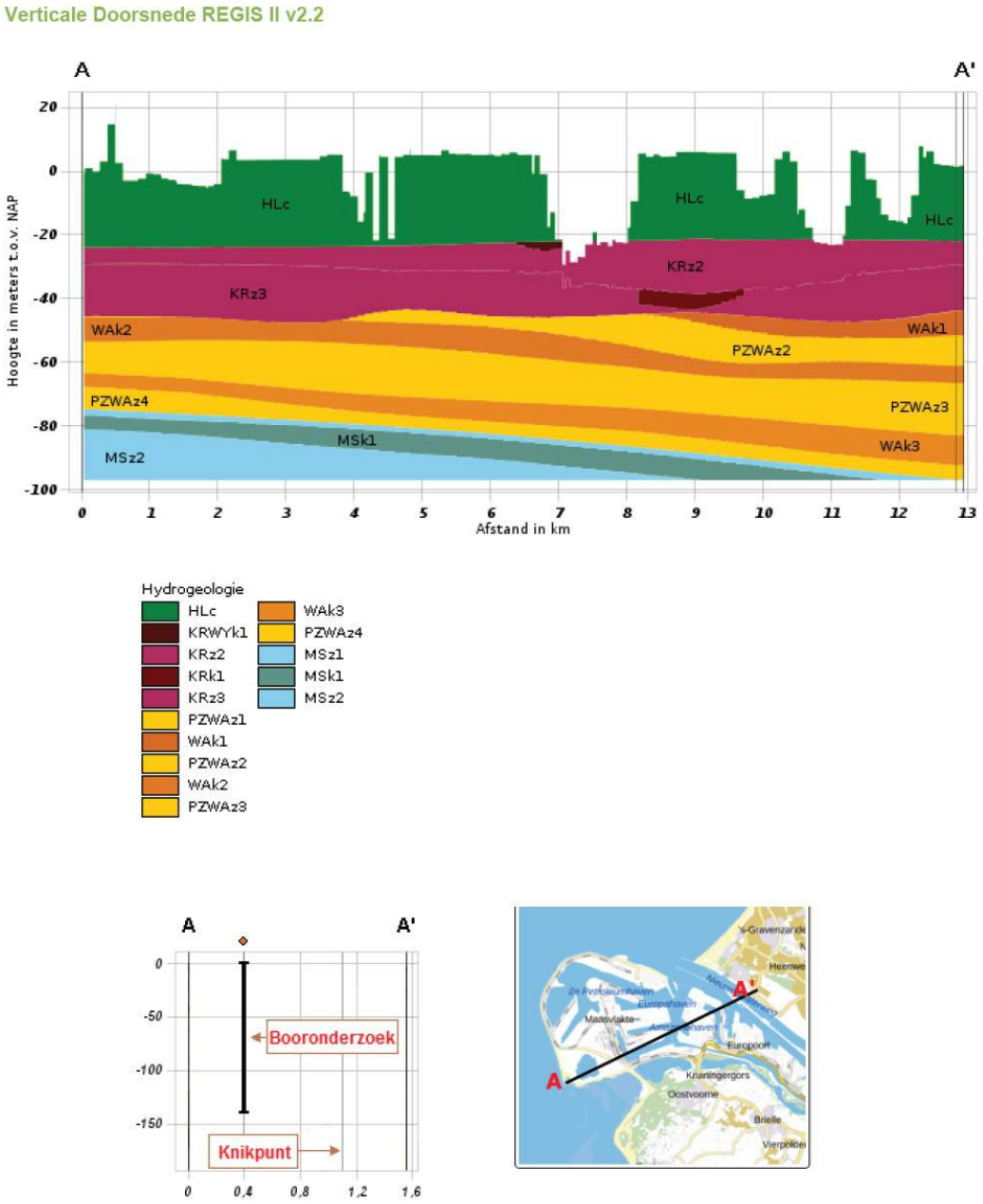

Figure E.9: REGIS cross section 3.

E.3.4 REGIS cross section 4

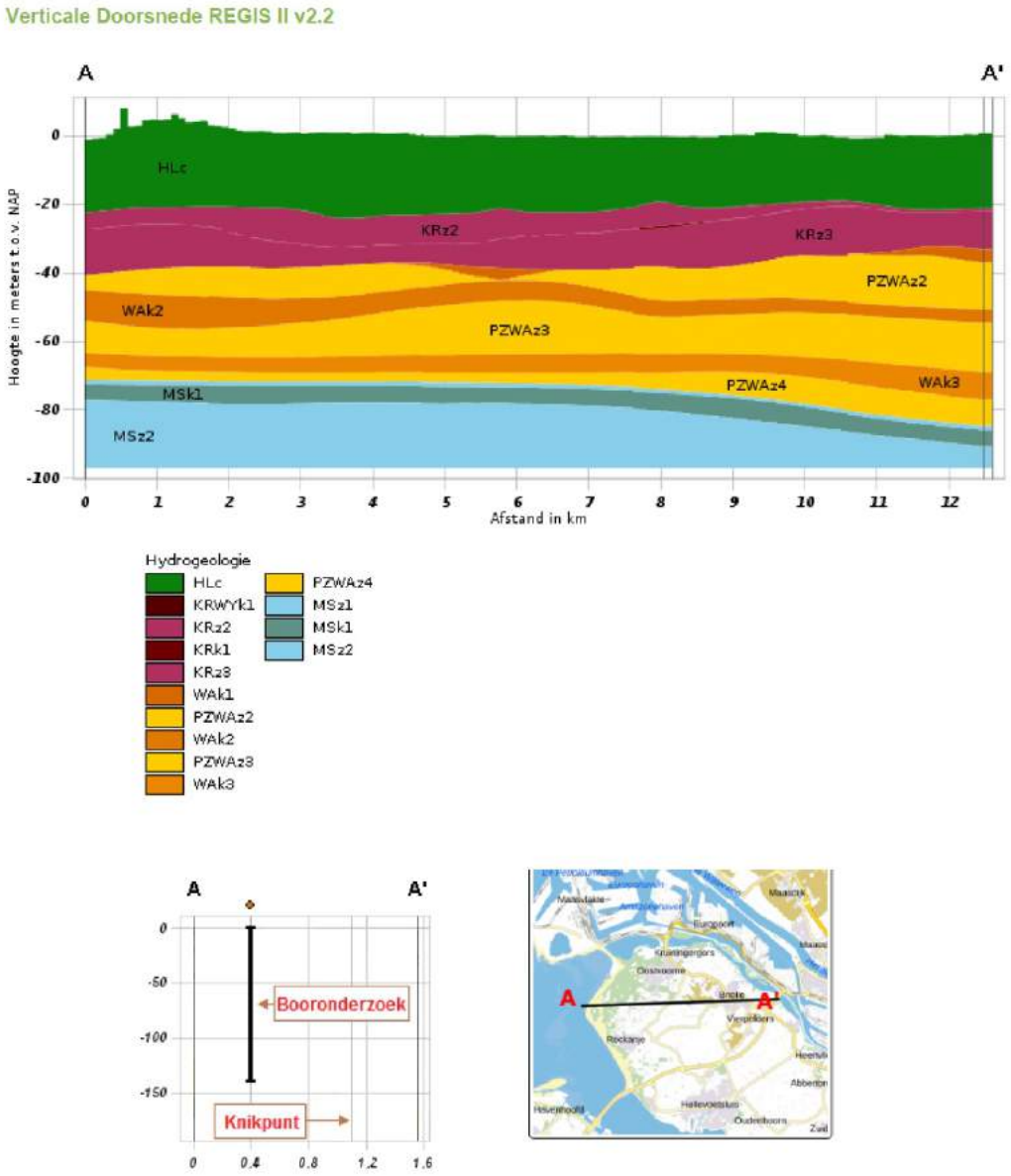

Figure E.10: REGIS cross section 4.

E.4 Cone Penetration Test Results

At the locations shown in Figures E.11, E.12 and E.13, CPT results are presented in this section.

Figure E.11: CPT S36H00032-01.

Figure E.12: CPT S36H00033-00.

Figure E.13: CPT S36H00035-01.

E.4.1 S36H00032-01

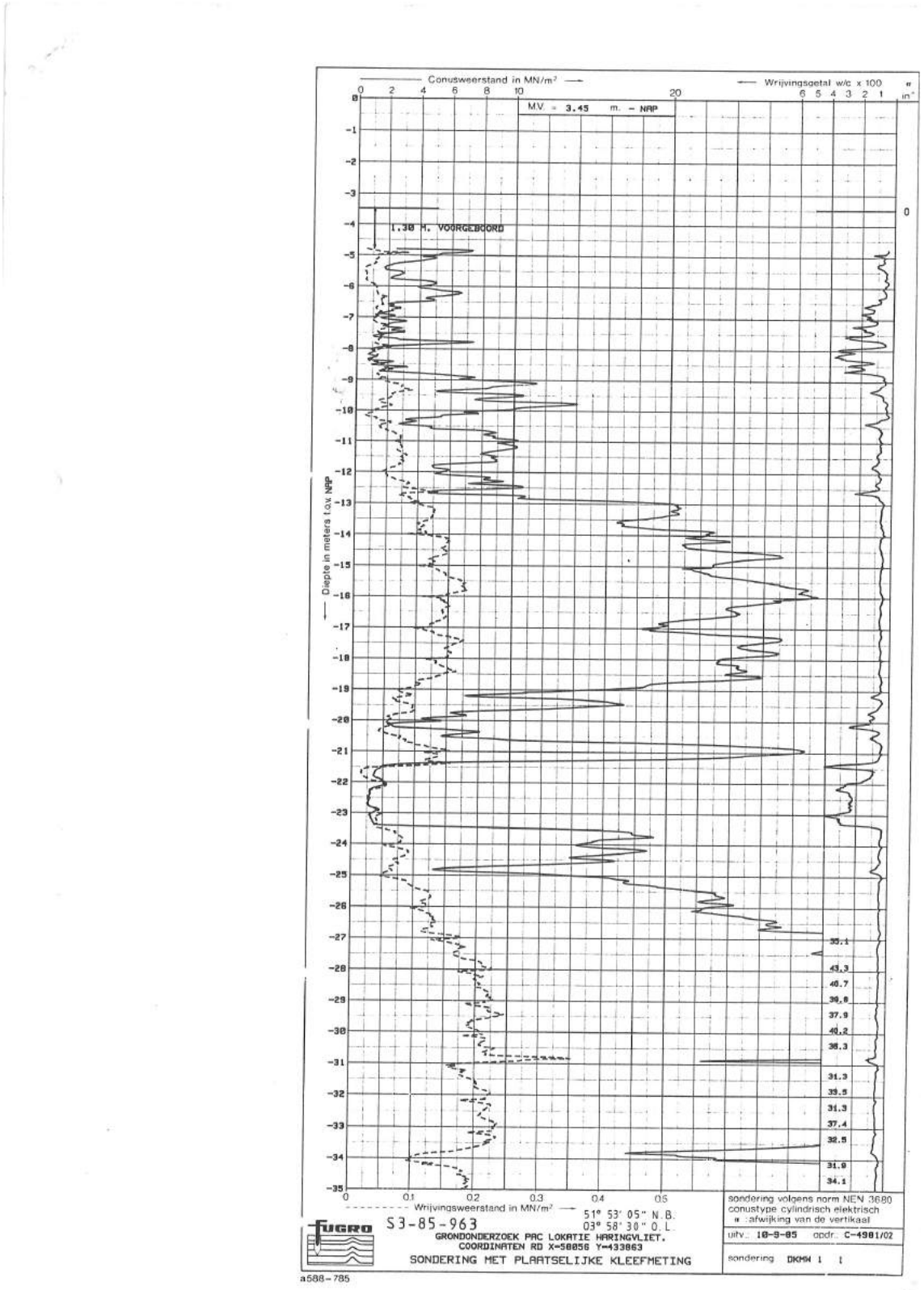

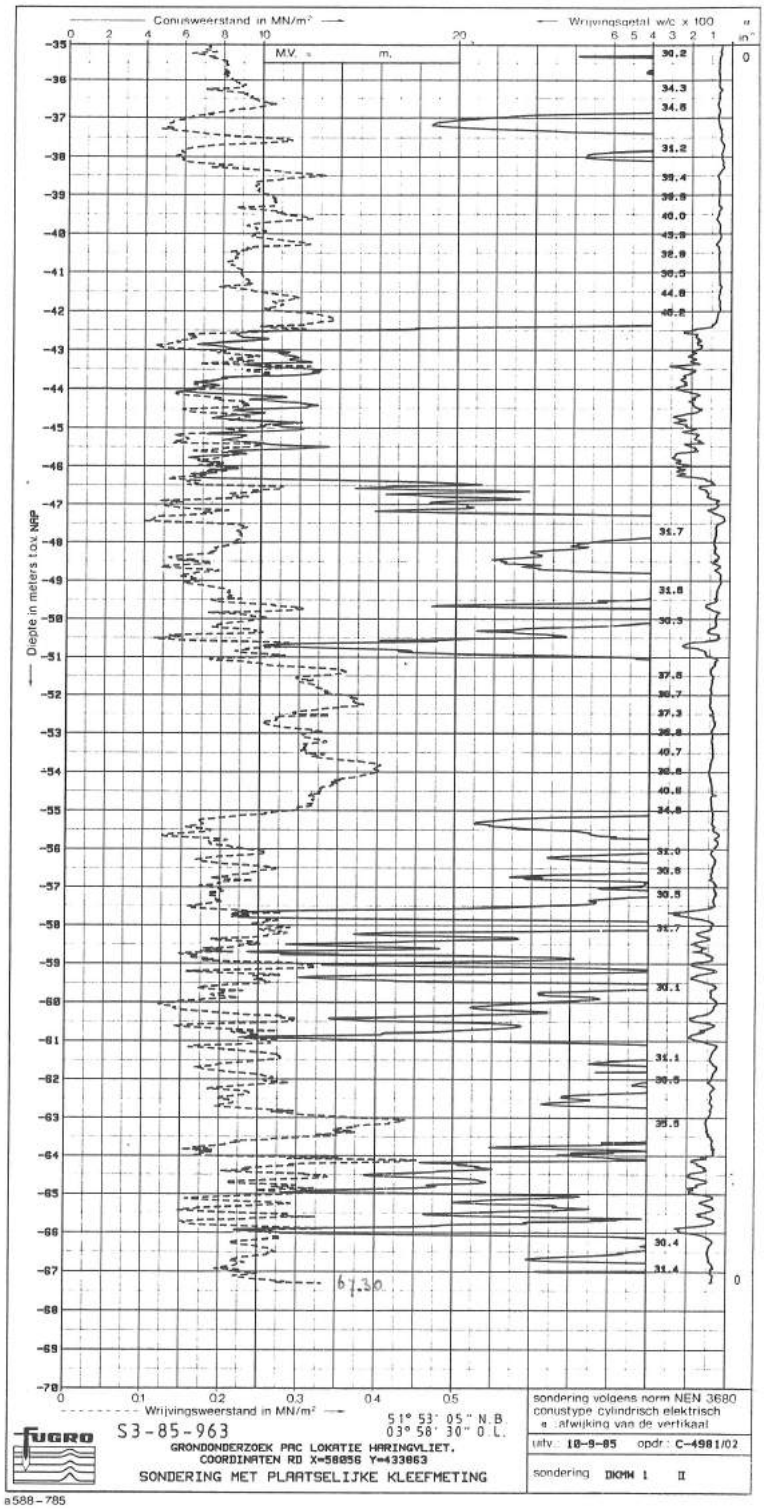
Conusweerstand in MN/m²
Wrijvingsgetal w/c x 100
M.V. = m.
Diepte in meters t.o.v. NAP
Wrijvingsweerstand in MN/m²
S3-85-963
51° 53' 05" N.B
03° 58' 30" O.L.
GRONDONDERZOEK PRC LOKATIE HARINGVLIET.
COORDINATEN RD X=58056 Y=433863
SONDERING MET PLAATSELIJKE KLEEFMETING
sondering volgens norm NEN 3680
conustype cylindrisch elektrisch
α : afwijking van de vertikaal
uitv.: 10-9-85 opdr.: C-4981/02
sondering DKMM 1 II
a588-785

E.4.2 S36H00033-00

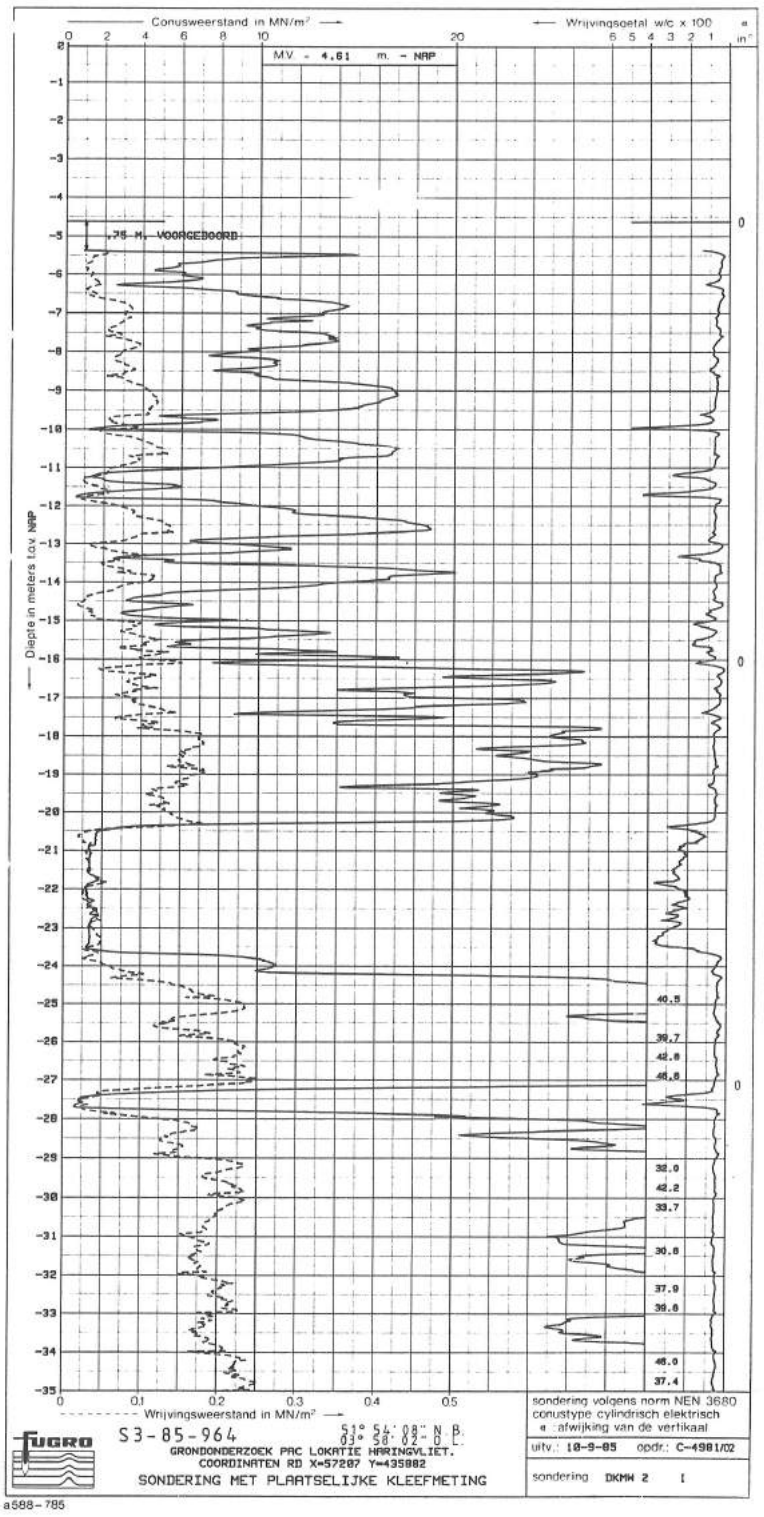

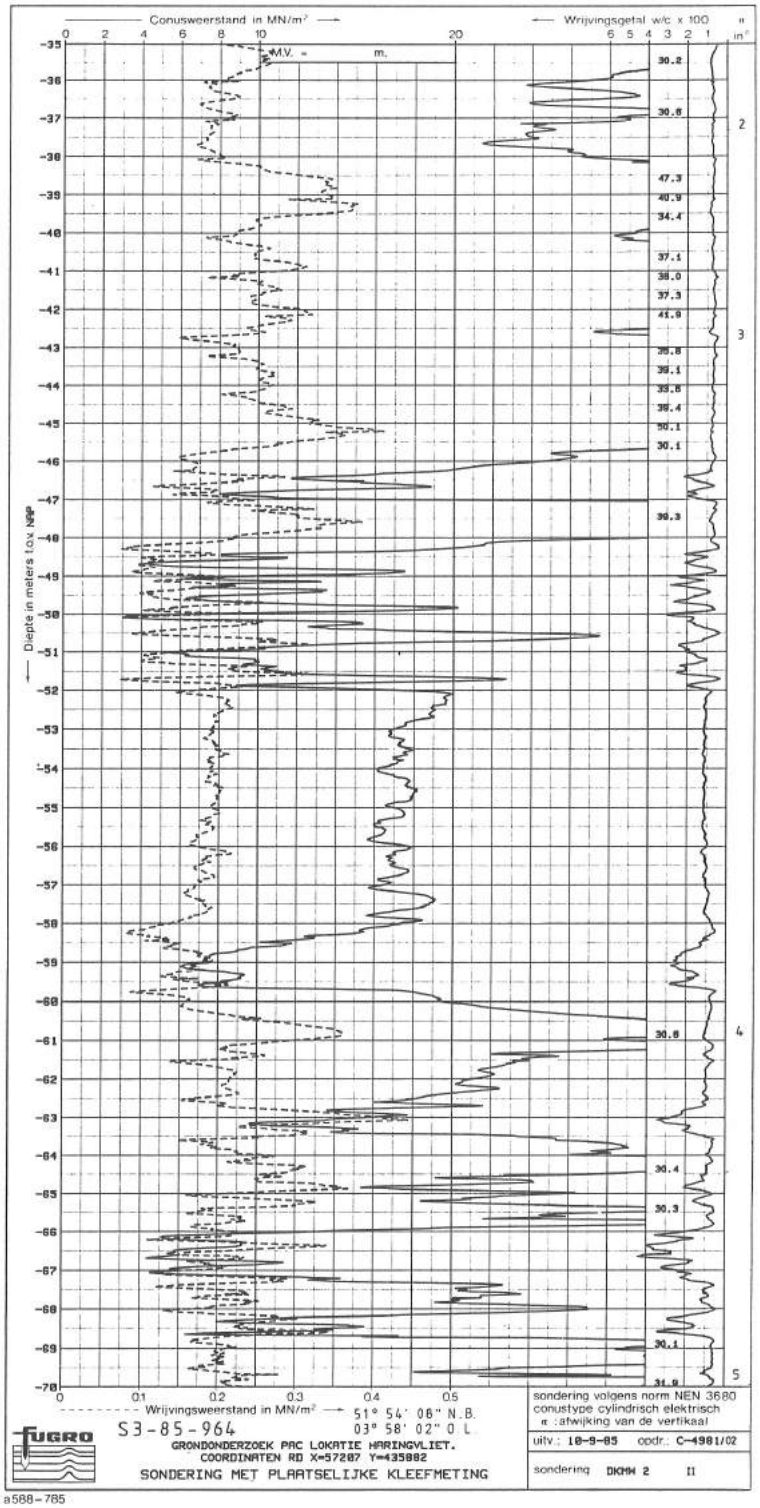
Conusweerstand in MN/m²
Wrijvingsgetal w/c x 100
M.V. = m.
Diepte in meters t.o.v. NAP
Wrijvingsweerstand in MN/m²
51° 54' 06" N.B.
03° 58' 02" O.L.
S3-85-964
GRONDONDERZOEK PAC LOKATIE HARINGVLIET.
COORDINATEN RD X=57207 Y=435882
SONDERING MET PLAATSELIJKE KLEEFMETING
FUGRO
sondering volgens norm NEN 3680
conustype cylindrisch elektrisch
α : afwijking van de vertikaal
uitv.: 18-9-85 opdr.: C-4981/02
sondering DKMM 2 II
a588-785

E.4.3 S3600035-01

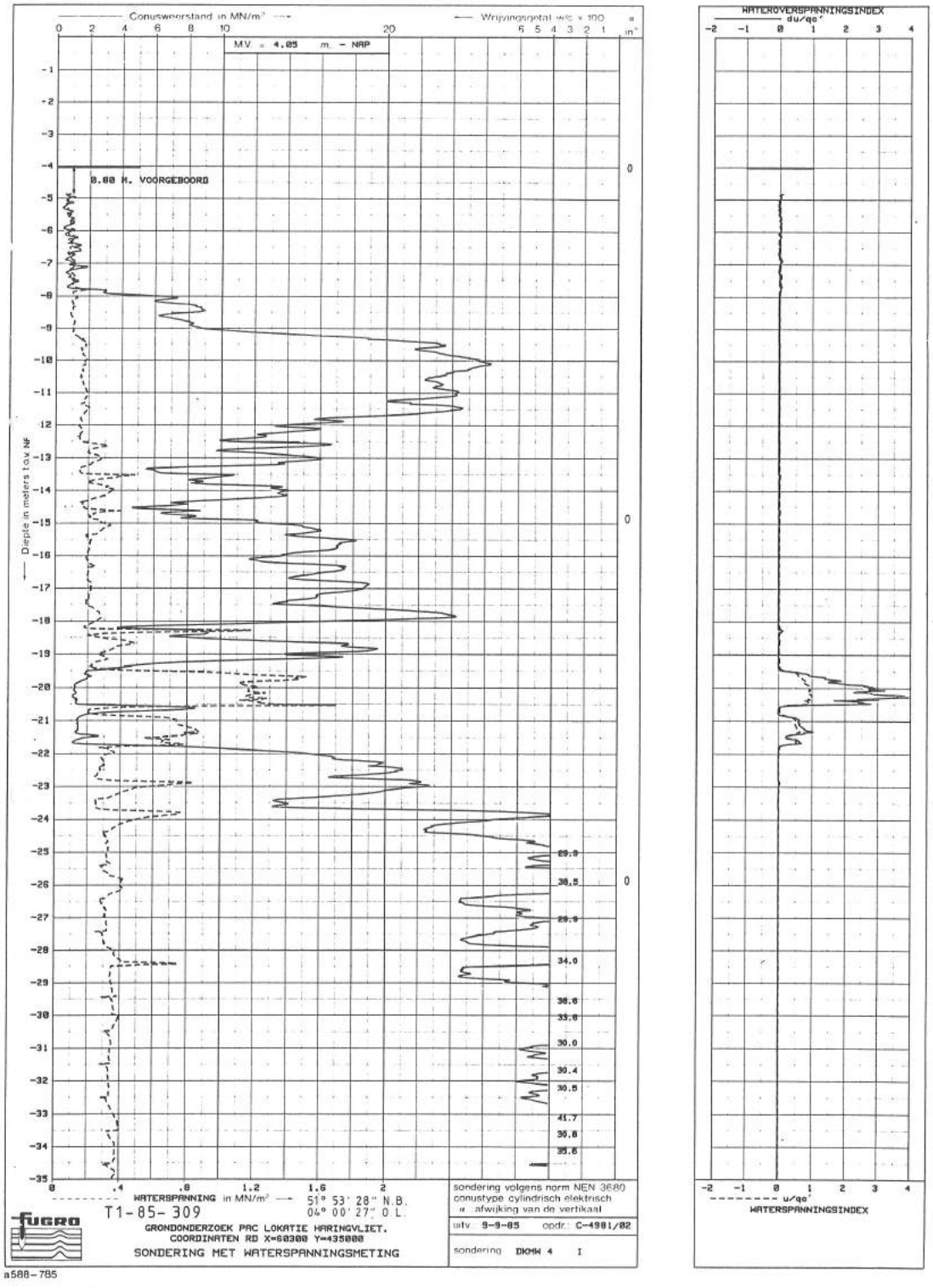

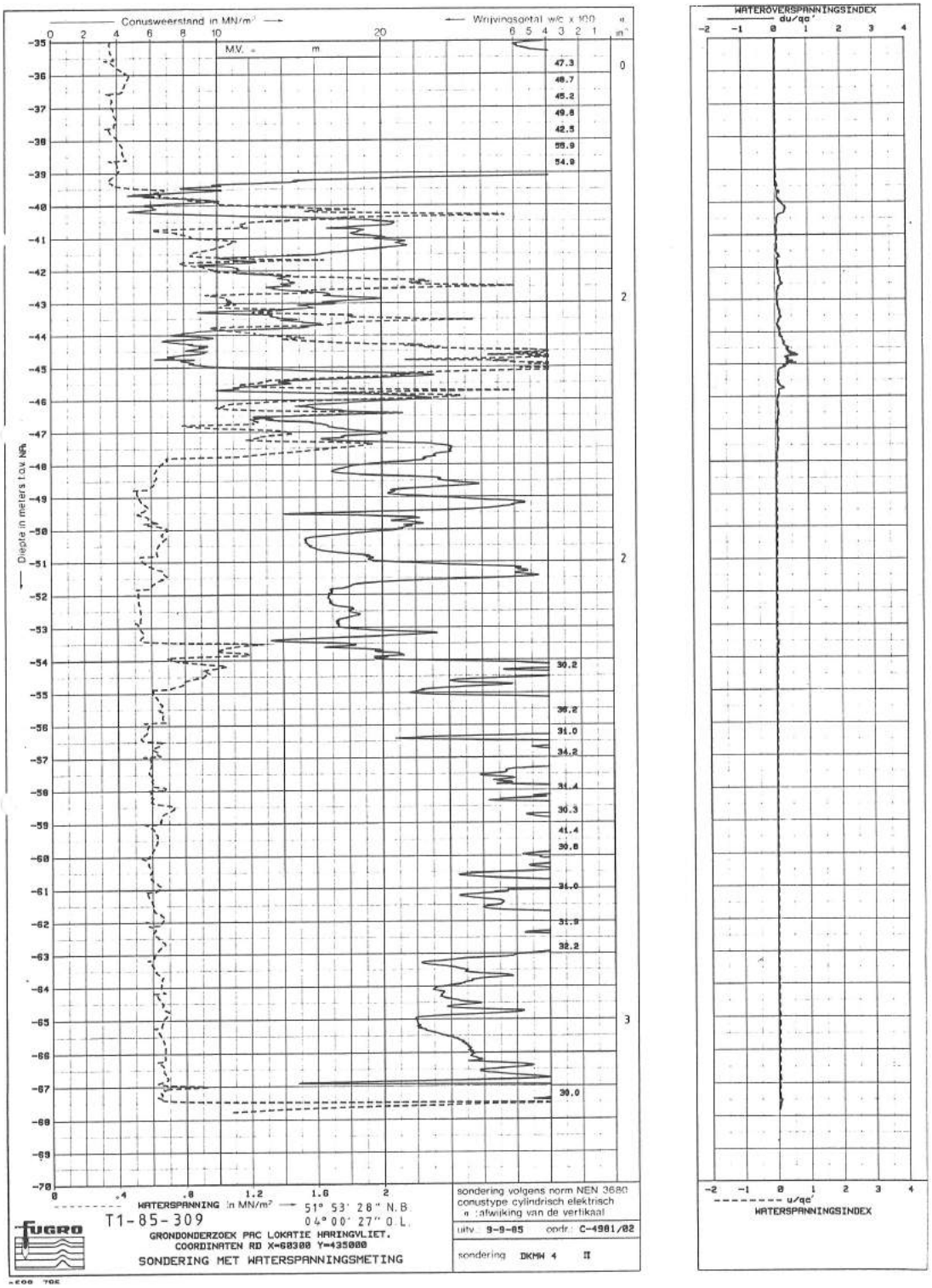
Conusweerstand in MN/m²
Wrijvingsgetal w/c x 100
Diepte in meters t.o.v. NAP
WATERSPANNING in MN/m²
T1-85-309
51° 53' 28" N.B.
04° 00' 27" O.L.
GRONDONDERZOEK PAC LOKATIE HARINGVLIET.
COORDINATEN RD X=68300 Y=435000
SONDERING MET WATERSPANNINGSMETING
sondering volgens norm NEN 3680
conustype cylindrisch elektrisch
α : afwijking van de vertikaal
uitv. 9-9-85
opdr.: C-4981/02
sondering DKMH 4 II
FUGRO
WATEROVERSPANNINGSINDEX
du/qc'
u/qc'
WATERSPANNINGSINDEX

E.5 Soil Profile

The soil profile is presented in two ways in Figure E.14.

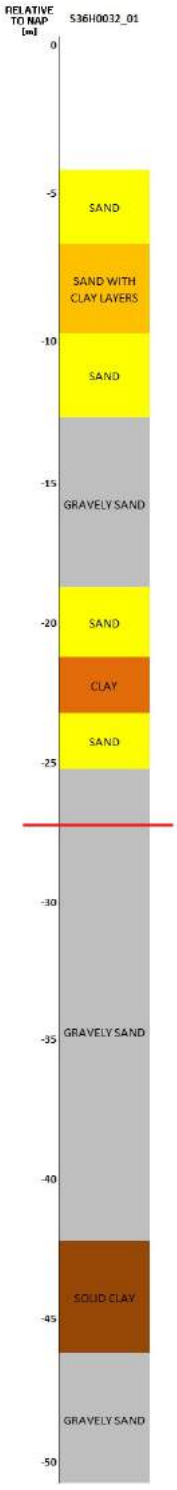

(a) Soil profile of S36H0032-01 (1/2).

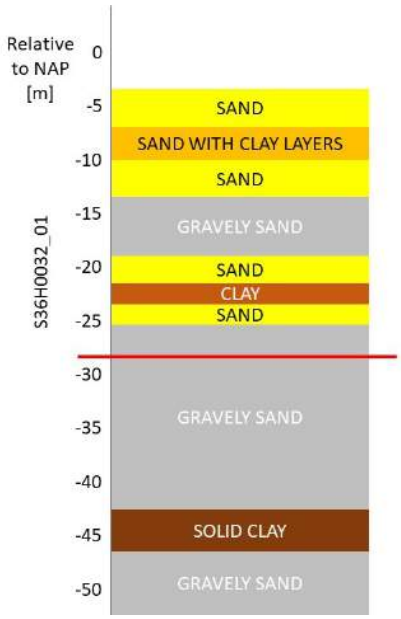

(b) Soil profile of S36H0032-01 (2/2).

Figure E.14: Soil build-up

E.6 Functional Boundary Conditions

Due to the Natura 2000 area, certain locations are also indicated as European Marine Strategy Framework Directive (KRM) and are indicated in Figures E.15a and E.15b.

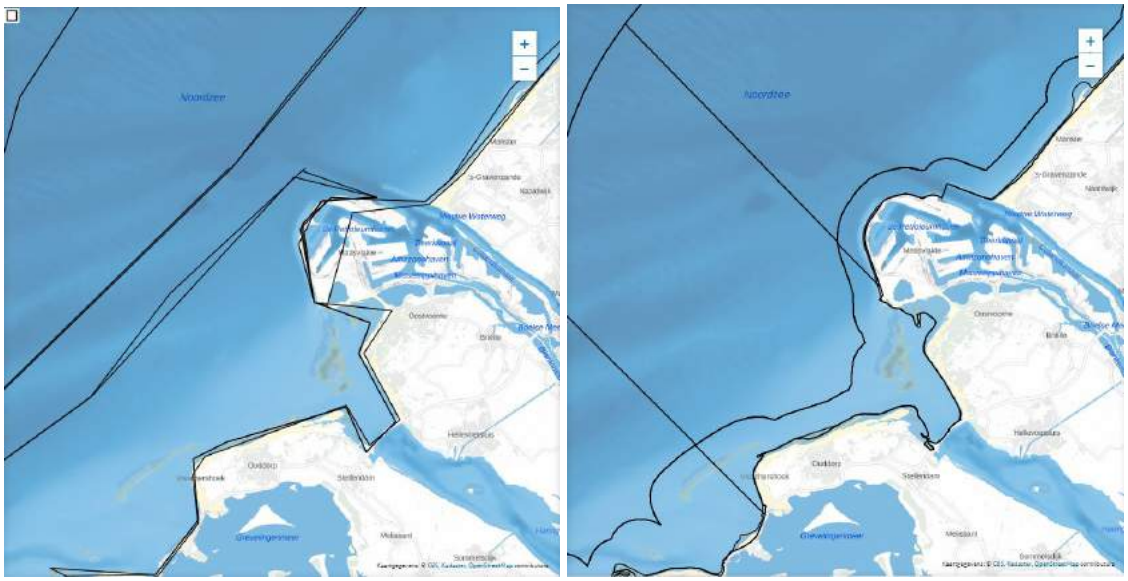

(a) KRM areas. **(b)** KRM reporting units.

Figure E.15: KRM.

Other designated areas at the project location are a shell extraction area and sand extraction areas, which are indicated in Figures E.16a and E.16b. These areas can probably be shifted to somewhere else.

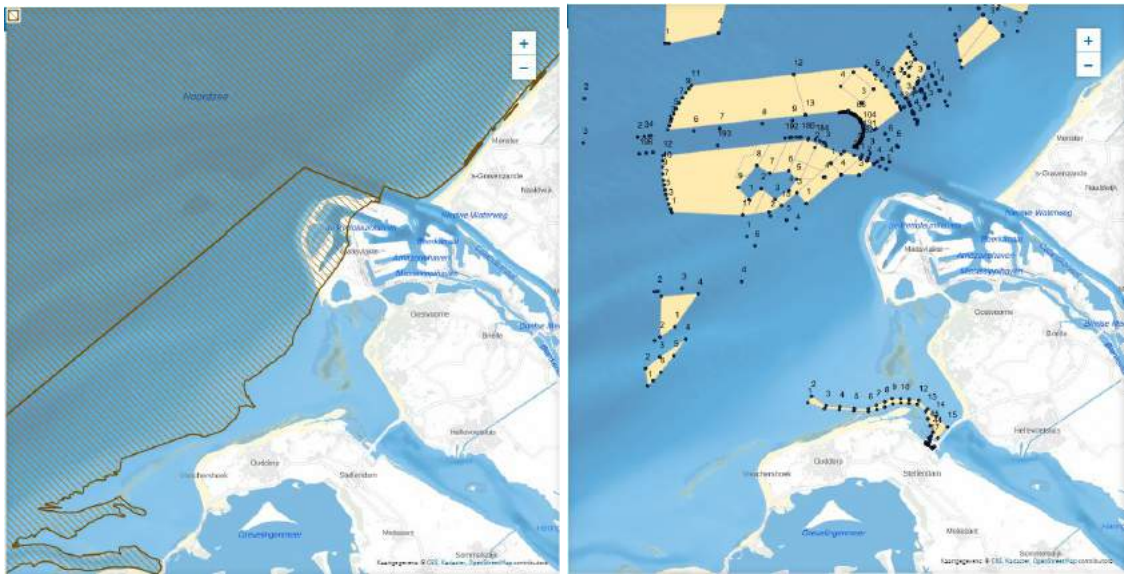

(a) Shell extraction area. **(b)** Sand extraction areas.

Figure E.16: Shell and sand extraction.

APPENDIX F

PUMP-TURBINE CALCULATIONS

The aim of this appendix is to calculate the power and required width of a pump-turbine, given the discharge as input value. The average water head for this project H = 14 m and the relative density of seawater ρ_{sw} =1 025 kg/m^3. First two characteristic values can be calculated, namely the specific speed of the impeller (Ω_s) and the hub to shroud ratio (λ).

$$\Omega_s = \frac{15}{H^{3/4}} \quad [-] \tag{F.1}$$

$$\lambda = 0,5 \cdot [1 - \exp(-\Omega_s)] \quad [-] \tag{F.2}$$

These values are unrelated to the discharge Q and remain constant for this specific project. Corresponding values are $\Omega_s = \frac{15}{14^{3/4}} = 2,07$ and
$\lambda = 0,5 \cdot [1 - \exp(-2,05)] = 0,44$. The next calculations are dependant on the discharge and can be adjusted according to project requirements.

Rotation speed

$$\Omega = \frac{\Omega_s \cdot (g \cdot H)^{3/4}}{\sqrt{Q}} \quad \text{[rad/s]} \tag{F.3}$$

Efficiency

$$\eta \approx 0,95 - 0,05 \cdot Q^{-1/3} - 0,125 \cdot [\log(\Omega_s)]^2 \quad [-] \tag{F.4}$$

Power

$$P = \frac{\rho_{sw} \cdot g \cdot Q \cdot H}{\eta} \quad \text{[W]} \tag{F.5}$$

Impeller inlet diameter

$$D_{s1} \approx 2 \cdot \left(\frac{1}{1 - \lambda^2}\right)^{1/3} \cdot \left[\frac{Q}{\Omega}\right]^{1/3} \quad \text{[m]} \tag{F.6}$$

Number of pump-turbines required

$$N = \frac{10\ 000}{Q} \quad \text{[-]} \tag{F.7}$$

Keeping the discharge variable a number of graphs can be plotted. In Figure F.1 the discharge is plotted against the power, in Figure F.2 the discharge is plotted against the number of turbines required and in Figure F.3 the discharge is plotted against the impeller inlet and outlet diameter.

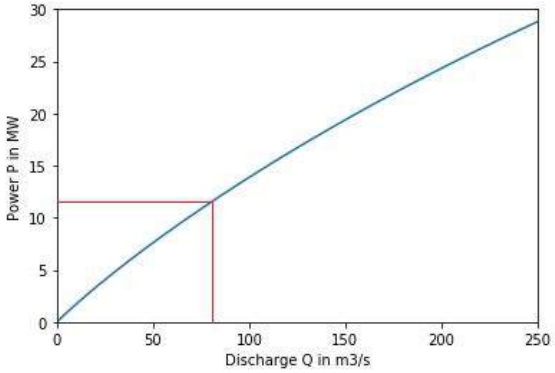

Figure F.1: Pump-turbine discharge versus power.

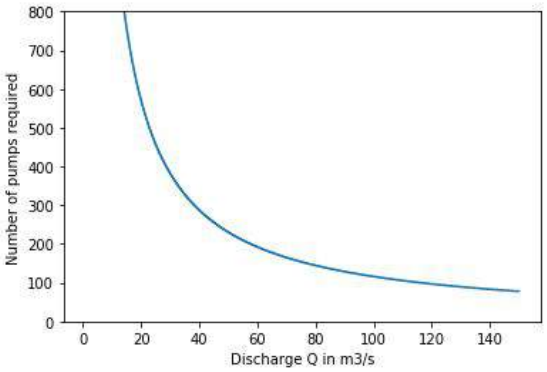

Figure F.2: Pump-turbine discharge versus number required.

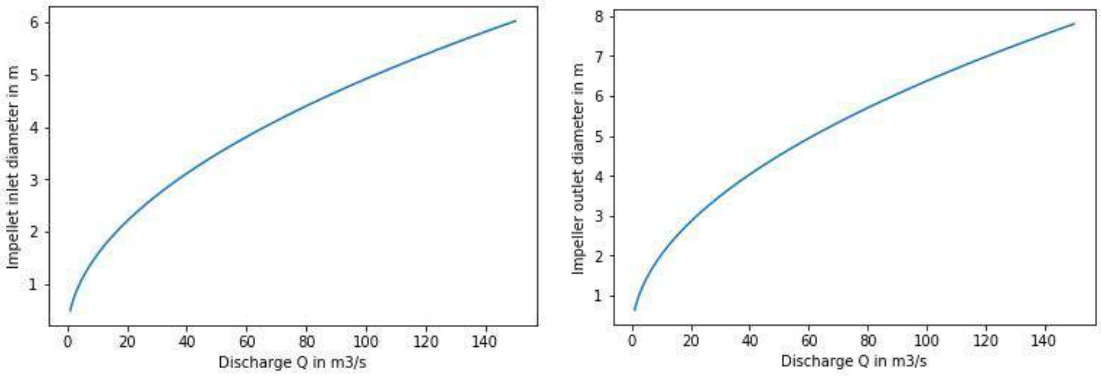

(a) Inlet.

(b) Outlet.

Figure F.3: Pump-turbine discharge versus impeller diameter.

With this information, also the total required width of the pump-turbines can be plotted against the power in Figure F.4a and discharge in Figure F.4b. In these plots the pump-turbines are placed directly next to each other, without any wall or anything in between. It is not realistic, but it offers a first insight in the required width of the structure.

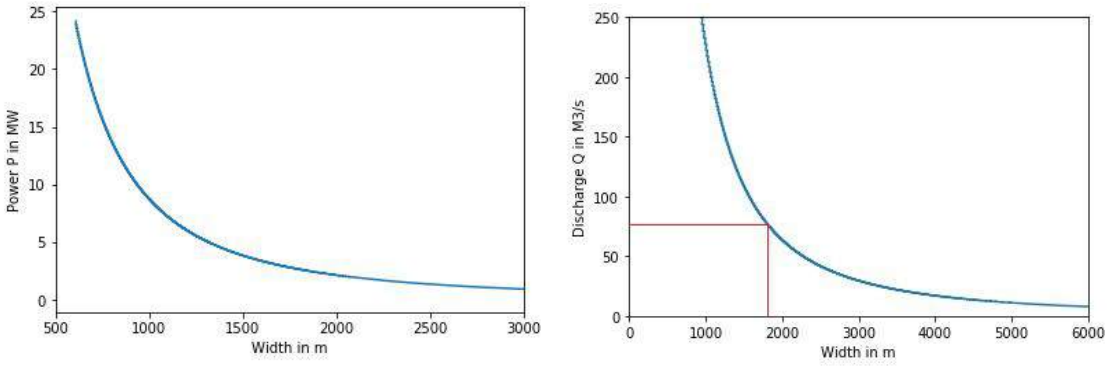

(a) Power.

(b) Discharge.

Figure F.4: Minimum width of the structure.

APPENDIX G

FLOOD RISKS PER DYKE RING

In this appendix the flood risk per dyke ring of the affected dyke rings is indicated. All information and figures are taken from (Rijkswaterstaat 2014a).

G.1 dyke Ring 20 Voorne-Putten

In Table G.1 the characteristics and probabilities of flooding are listed for dyke ring 20.

dyke ring 20: Voorne-Putten	
Characteristics	
Barrier administrator(s)	Water authority Hollandse Delta
Length of barriers category a	71,0 km
Number of structures	22
Area	19 500 ha
Inhabitants	155 400
Risk of flooding	
Probability of flooding per year	1/100
Economic risk per year	€12,9 mln
Avg. damage per flooding	€1,3 bln
Risk of victims per year	1,2
Avg. number of victims per flooding	120

Table G.1: Characteristics and probability of flooding for dyke ring 20.

The probability per of failure per dyke section (per year) and the local individual risk (per year) is shown in Figure G.1.

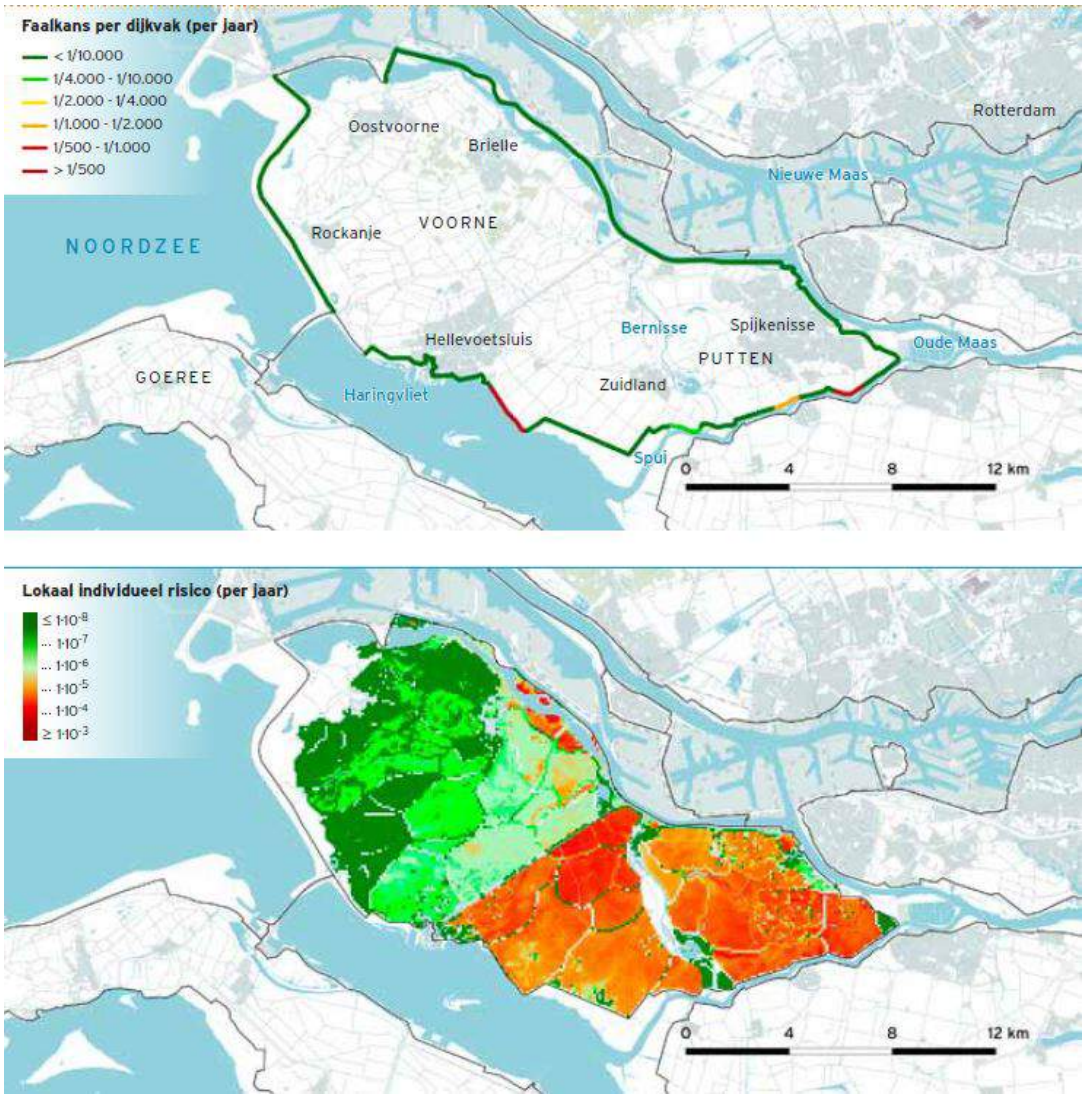

Figure G.1: dyke ring 20.

G.2 dyke Ring 21 Hoekse Waard

In Table G.2 the characteristics and probabilities of flooding are listed for dyke ring 21.

dyke ring 21: Hoekse Waard	
Characteristics	
Barrier administrator(s)	Water authority Hollandse Delta
Length of barriers category a	69,4 km
Number of structures	31
Area	24 500 ha
Inhabitants	83 100
Risk of flooding	
Probability of flooding per year	1/170
Economic risk per year	€0,6 mln
Avg. damage per flooding	€110 mln
Risk of victims per year	0,1
Avg. number of victims per flooding	10

Table G.2: Characteristics and probability of flooding for dyke ring 21.

The probability per of failure per dyke section (per year) and the local individual risk (per year) is shown in Figure G.2.

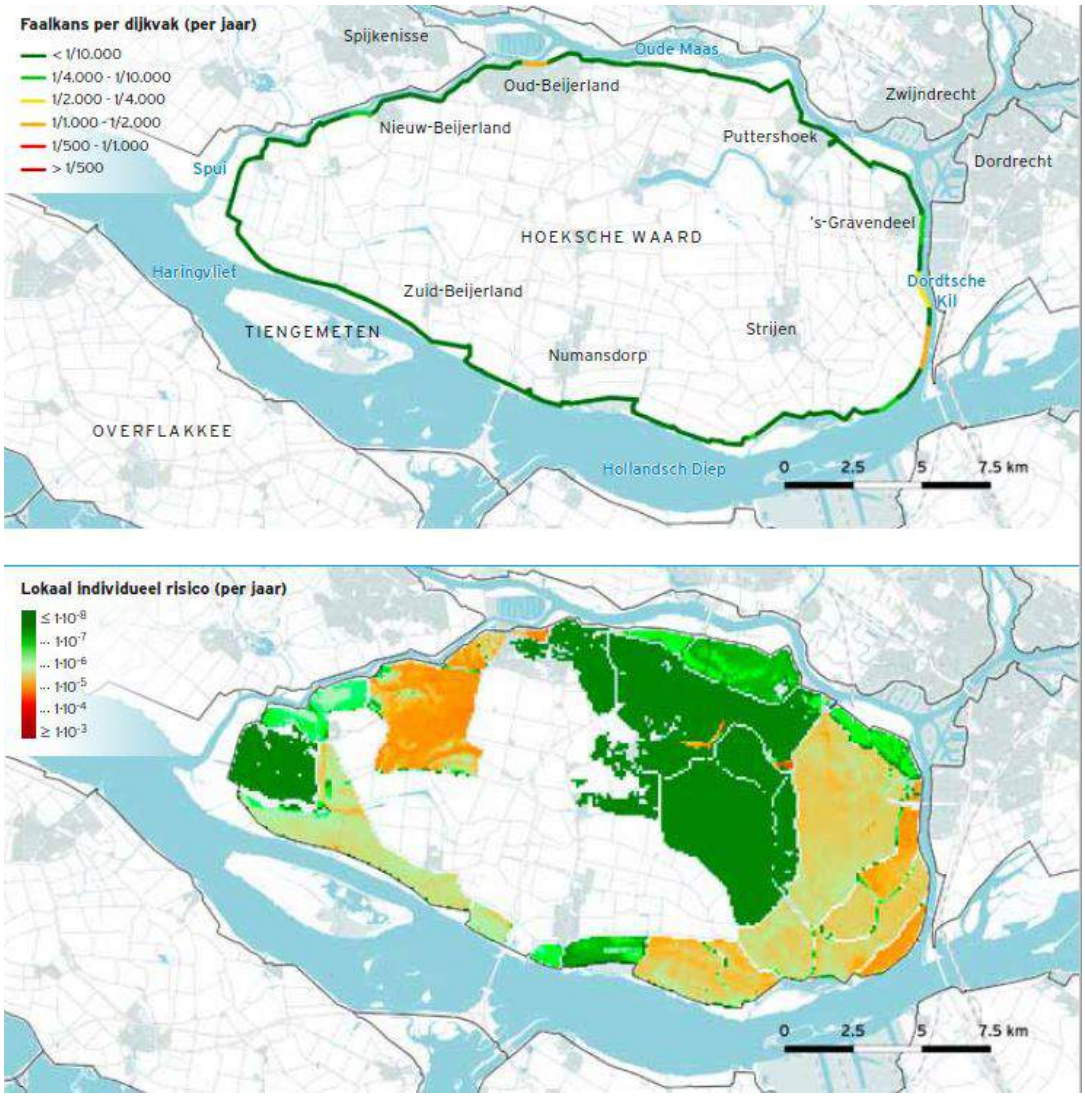

Figure G.2: dyke ring 21.

G.3 dyke Ring 22 Eiland van Dordrecht

In Table G.3 the characteristics and probabilities of flooding are listed for dyke ring 22.

dyke ring 22: Eiland van Dordrecht	
Characteristics	
Barrier administrator(s)	Water authority Hollandse Delta
Length of barriers category a	37,1 km
Number of structures	18
Area	4 920 ha
Inhabitants	104 800
Risk of flooding	
Probability of flooding per year	1/710
Economic risk per year	€0,1 mln
Avg. damage per flooding	€80 mln
Risk of victims per year	0,02
Avg. number of victims per flooding	12

Table G.3: Characteristics and probability of flooding for dyke ring 22.

The probability per of failure per dyke section (per year) and the local individual risk (per year) is shown in Figure G.3.

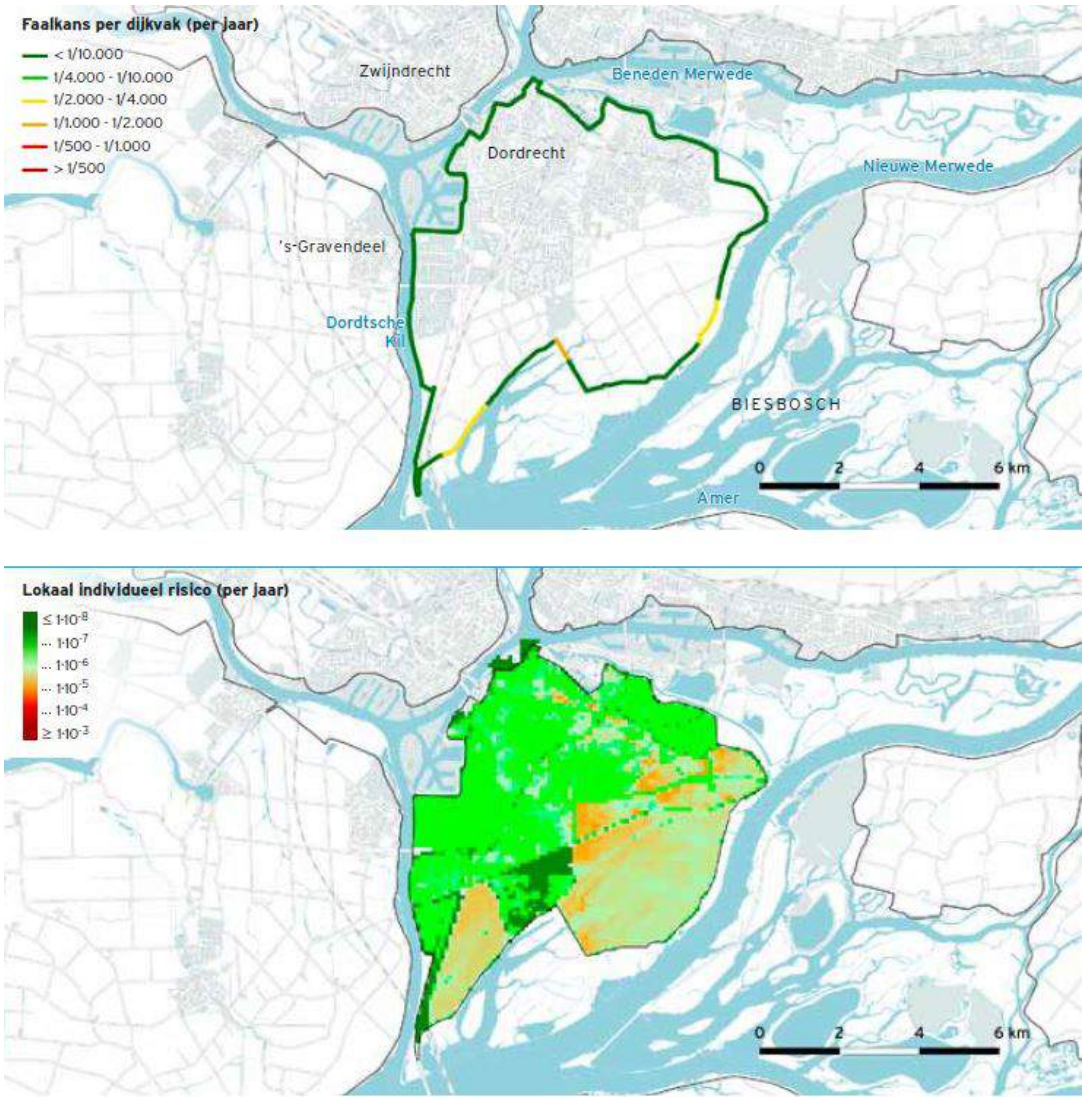

Figure G.3: dyke ring 22.

G.4 dyke Ring 24 Land van Altena

In Table G.4 the characteristics and probabilities of flooding are listed for dyke ring 24.

dyke ring 24: Land van Altena	
Characteristics	
Barrier administrator(s)	Water authority Rivierenland
Length of barriers category a	46,3 km
Number of structures	13
Area	16 300 ha
Inhabitants	51 100
Risk of flooding	
Probability of flooding per year	1/160
Economic risk per year	€17,5 mln
Avg. damage per flooding	€2,8 bln
Risk of victims per year	0,6
Avg. number of victims per flooding	88

Table G.4: Characteristics and probability of flooding for dyke ring 24.

The probability per of failure per dyke section (per year) and the local individual risk (per year) is shown in Figure G.4.

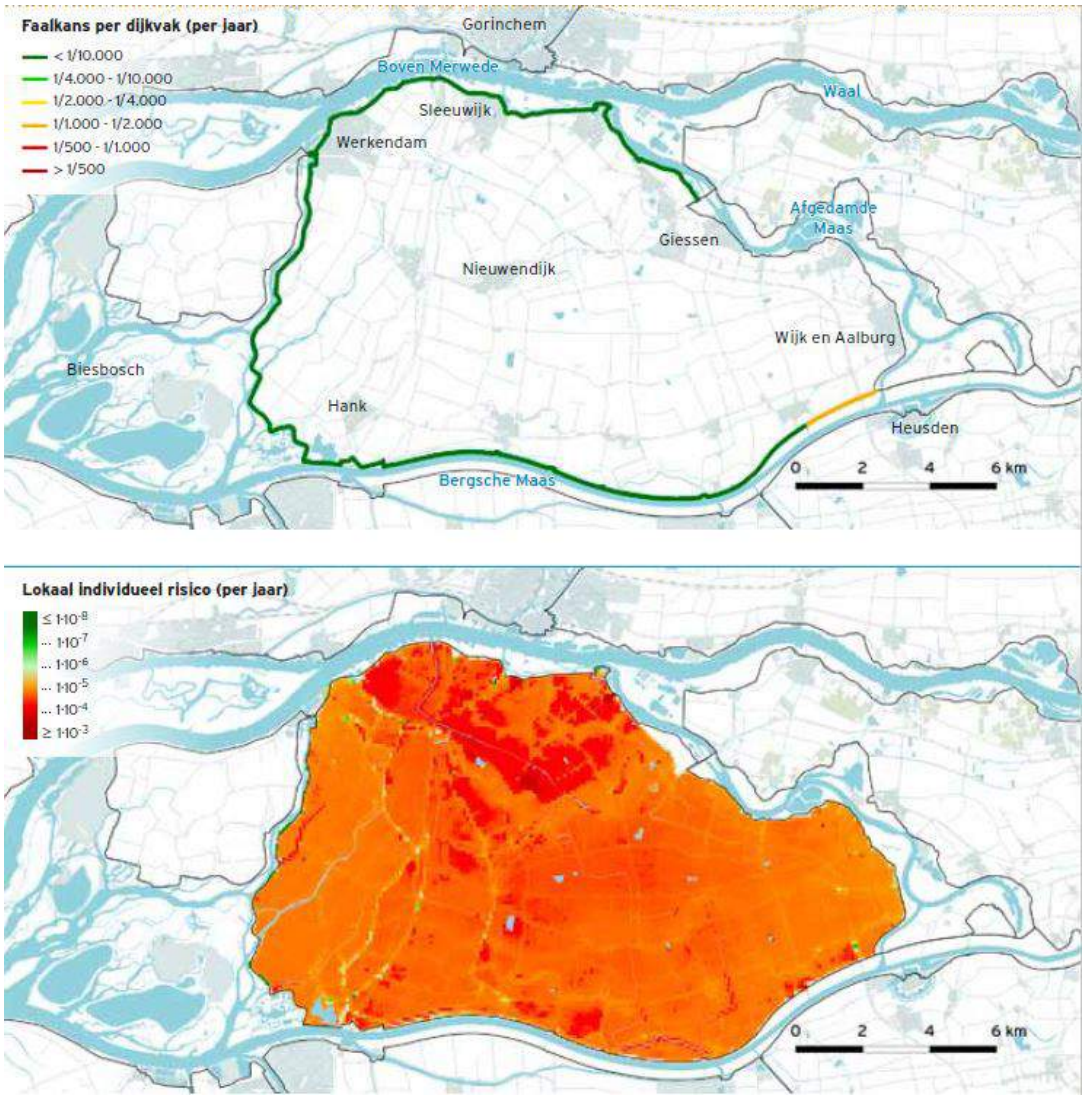

Figure G.4: dyke ring 24.

G.5 dyke Ring 25 Goeree-Overflakkee

In Table G.5 the characteristics and probabilities of flooding are listed for dyke ring 25.

dyke ring 25: Goeree-Overflakkee	
Characteristics	
Barrier administrator(s)	Water authority Hollandse Delta
Length of barriers category a	44,4 km
Number of structures	7
Area	22 600 ha
Inhabitants	46 500
Risk of flooding	
Probability of flooding per year	1/340
Economic risk per year	€0,03 mln
Avg. damage per flooding	€10 mln
Risk of victims per year	0,001
Avg. number of victims per flooding	< 1

Table G.5: Characteristics and probability of flooding for dyke ring 25.

The probability per of failure per dyke section (per year) and the local individual risk (per year) is shown in Figure G.5.

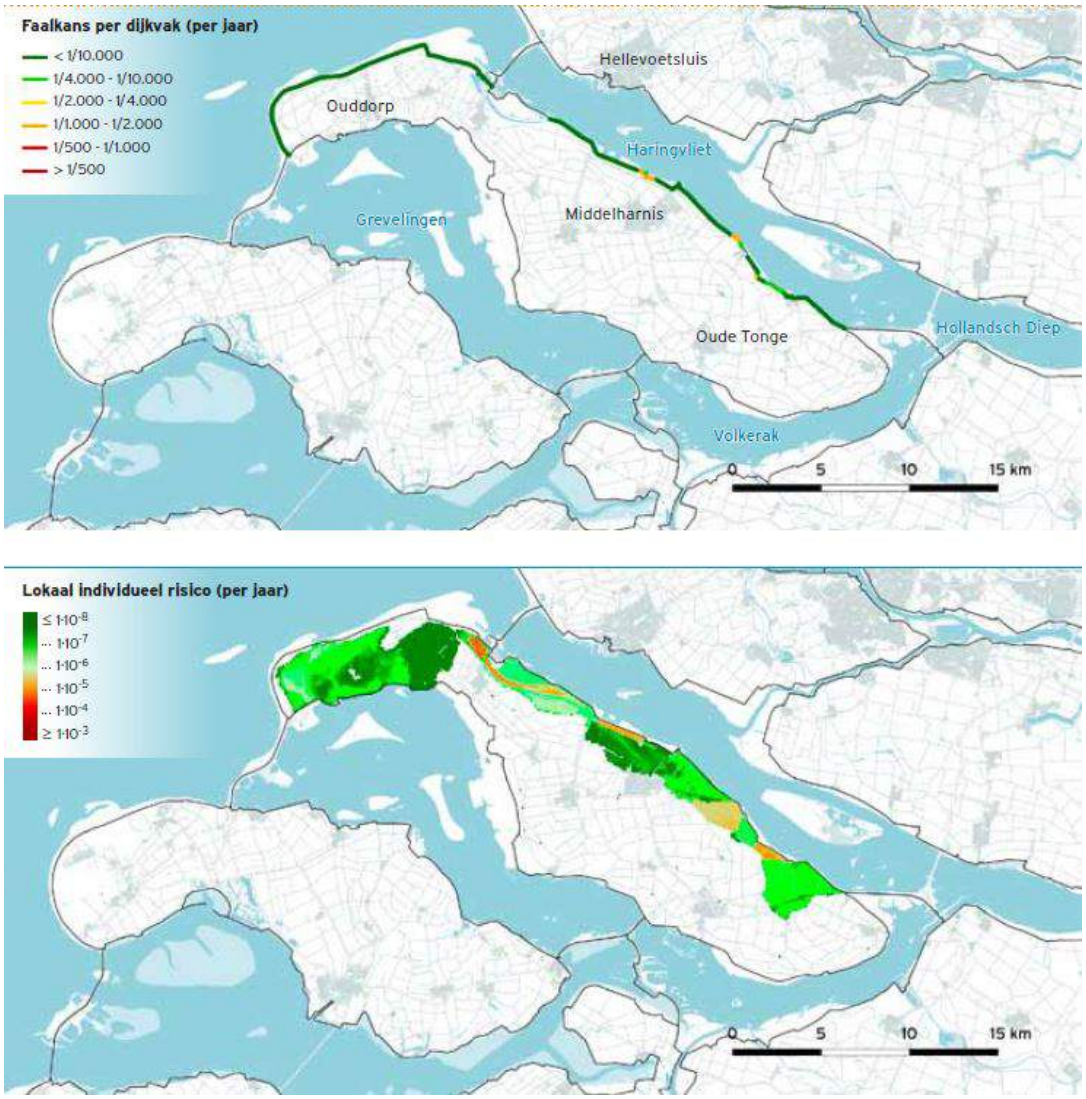

Figure G.5: dyke ring 25.

APPENDIX H

RETAINING HEIGHT

The retaining height of the in- and outlet structure is determined following the design procedure as described in (Technische Adviescommissie voor de Waterkeringen 2003). The design scheme presented in Figure H.1 is copied (but translated) from there.

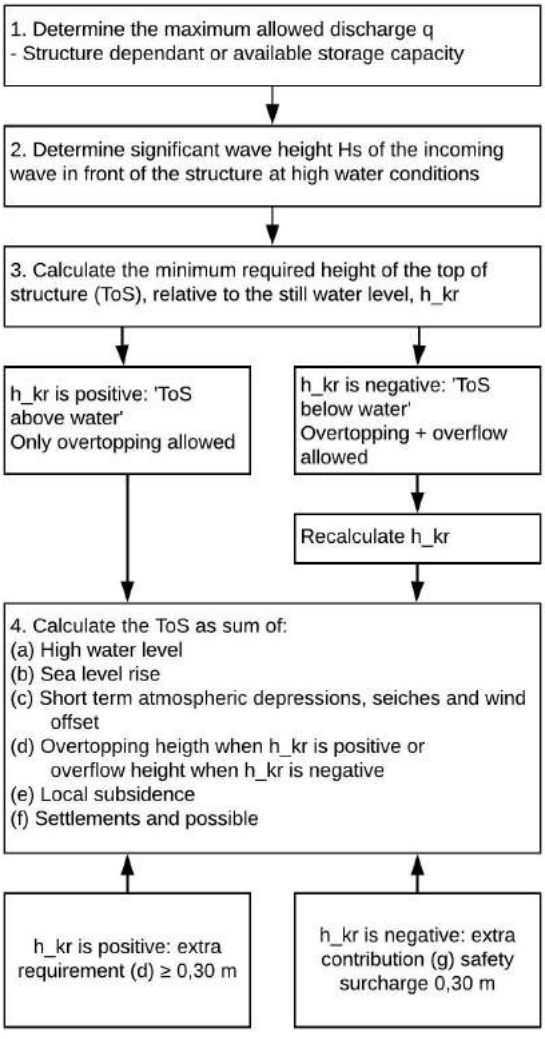

Figure H.1: Design scheme for the retaining height.

H.1 Design Procedure

In step 4 in Figure H.1 the contributions of High water level, Sea level rise, Short term atmospheric depressions and Settlements are already combined in the governing high water level (GHW) of NAP + 6,50 m and the contribution of Settlements is kept on 0 as a start. So the value of h_{kr} can directly be added onto the storm surge water level.

As calculated before the significant wave height in front of the structure, Hs, is 5,0 m. The overtopping formula as given in (Technische Adviescommissie voor de Waterkeringen 2003) for determining the average overtopping discharge, valid for non-breaking waves (as is the case here) is:

$$q = 0,13\sqrt{g \cdot H_s^3} \cdot \exp\left(-3,0 \cdot \frac{h_{kr}}{H_s}\frac{1}{\gamma_\beta \gamma_n}\right) \tag{H.1}$$

With: q = average overtopping discharge [m^3/s/m]
g = gravitational acceleration [m/s^2]
H_s = significant incoming wave height in front of the structure [m]
h_{kr} = Top of Structure above still water level [m]
γ_β = influence factor for oblique wave attack [-]
γ_n = influence factor for nose structure [-]

The most extreme wave condition is also the wave direction perpendicular to the structure and so γ_β is 1,0. As for an initial design, no nose structure is assumed and γ_n equals also 1,0.

The value 0,13 is a characteristic value and only valid for deterministic calculations. For probabilistic calculation a mean value of 0,34 should be used with standard deviation 0,09. This overtopping formula has changed slightly for several times over the years. All formulas have the same shape, which can be found in Equation H.2 (Rc is the freeboard and the same as h_{kr} in Equation H.1).

$$\frac{q}{\sqrt{g \cdot H_s^3}} = a \cdot \exp\left[-\left(b \cdot \frac{R_c}{H_s}\right)^c\right] \quad for\ R_c \geq 0 \tag{H.2}$$

An overview of the parameters for a, b and c is given in Table H.1.

	TAW [2003]		**EurOtop [2007]**		**Van der Meer and Bruce [2014]**	
	a	**b**	**a**	**b**	**a**	**b**
Mean value	0,34	-	-	2,6	-	-
Standard Deviation	0,09	-	-	0,8	-	-
Characteristic value	0,13	3,0	0,04	1,8	0,2	4,3

Table H.1: Coefficient values overtopping.

The new EurOtop 2018 manual (EurOtop 2018) has further developed the tuning of the parameters and will be used as governing. The new overtopping formula then becomes, for cases without influencing foreshores:

$$\frac{q}{\sqrt{g \cdot H_s^3}} = 0,047 \cdot \exp\left[-\left(2,35 \cdot \frac{R_c}{H_s}\right)^{1,3}\right] \tag{H.3}$$

Furtermore, the EurOtop [2018] manual strongly recommend for a design approach to increase the average discharge by about one standard deviation. So it becomes:

$$\frac{q}{\sqrt{g \cdot H_s^3}} = 0,054 \cdot \exp\left[-\left(2,12 \cdot \frac{R_c}{H_s}\right)^{1,3}\right] \tag{H.4}$$

And rewritten:

$$R_c = \frac{1}{2,12} \cdot H_s \cdot \left[-ln\left(\frac{q}{0,054\sqrt{g \cdot H_s^3}}\right)\right]^{1/1,3} \tag{H.5}$$

The only unknown, to be determined, parameter in the formula is the critical overtopping discharge q.

H.2 Allowed Overtopping Discharge

The overtopping discharge requirement follows either from an available storage capacity in the energy storage lake or, when that is not allowed, a value following from the literature.

Storage capacity
Looking at the permissible water level increase on the energy storage lake, there is a pumping overcapacity of 13 extra pumps x 80 m^3/s per pump = 1 040 m^3/s. Care should be taken to utilize this capacity, because it is meant to be back-up capacity for maintenance of the pump-turbines. During a design storm, lasting approximately 12 hours, if the energy storage lake (with an area of 20 km^2) can rise with a maximum of 0,75 meter, the storage capacity K = 15 mln m^3.

Allowed overtopping discharge over the structure
Taking the total length of the caissons as the number of pump-turbines times the governing width of the outlet plus walls with a thickness of 0,5 m gives a length of W = 138 · (14,11 m + 0,5 m) ≈ 2 km. Consequently, the permissible volume of water that goes over the structure, per unit width of the structure V_B = K / W = 7 500 m^3/m. During a 12 hours storm that means the maximum allowed overtopping discharge q = V_B / t = $\frac{7\,500}{12 \cdot 3600}$ = 0,174 $m^3/s/m$ = 174 l/s/m.

Overtopping over the surrounding dykes
For the overtopping discharge allowed at the surrounding dykes, following (Jonkman et al. 2018), there is some consensus that a value for q between 5 - 10 l/s/m is a good lower bound for the stability of grass covered inner slopes of dykes. Meaning a critical overtopping discharge q of 10 l/s/m or 0,01 $m^3/s/m$ is chosen. Approximating the length of dykes in contact with the sea as 12 000 m, a volume of $Q_{overtopping}$ = 0,01 · 12 000 + 0,174 · 2 000 = 468 m^3/s will flow into the lake during extreme conditions.

Combined overtopping discharge
Over the structure a maximum of 0,174 m^3/s/m · 2000 m = 348 m^3/s flows into the lake and over the dykes a maximum of 468 m^3/s flows into the lake, combined that is 816 m^3/s. For this scenario, 11 out of the 13 extra pump-turbines need to be utilized, or can be stored into the energy storage lake without any problems, when the water level in the lake is below the NAP - 5 m.

H.3 Minimum Retaining Height

Filling in Equation H.5, the freeboard relative to the governing high water level is $R_c = \frac{1}{2,12} \cdot H_s \cdot \left[-ln\left(\frac{q}{0,054\sqrt{g \cdot H_s^3}}\right)\right]^{1/1,3} = \frac{1}{2,12} \cdot 5,0 \cdot \left[-ln\left(\frac{0,174}{0,054\sqrt{9,81 \cdot 5,0^3}}\right)\right]^{0,77} = 4,60$ m.

H.3.1 Height reduction due to bullnose

When a bullnose is applied, the wave overtopping can be reduced by deflecting back seaward up-rushing water (EurOtop 2018). The mechanisms behind the application of a bullnose are complex and not yet fully described, but a first estimate is made here, based up existing guidance in the Netherlands and physical model studies.

The concept is based on three regimes:

1. a regime in which the bullnose / wave return wall has little or no influence upon the overtopping, with this being typical of lowest relative freeboard conditions, where the bullnose / wave return wall may simple become submerged in the overtopping water;
2. an intermediate regime in which the bullnose / wave return wall is increasingly effective as the relative freeboard increases;
3. a high-relative freeboard regime where the bullnose / wave return wall offers its maximum performance in being successful in deflecting up-rushing water back seawards.

Existing guidance is provided in Figure H.2.

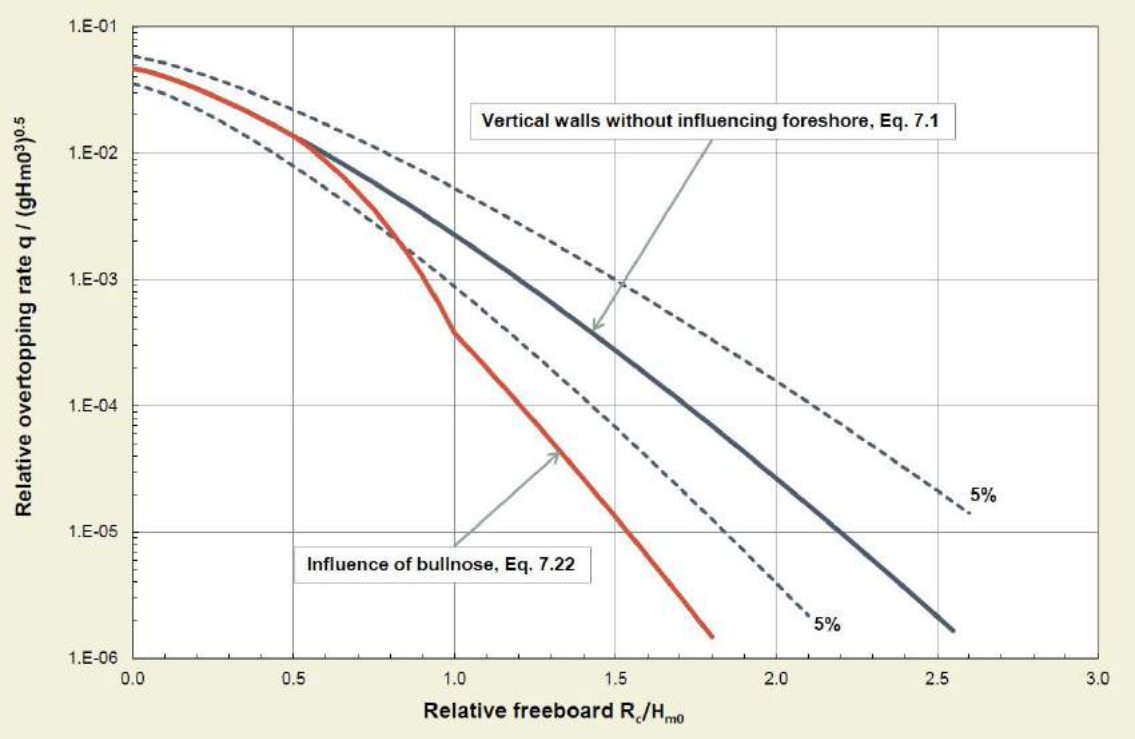

Figure H.2: Graph showing the three regimes of effectiveness of a bullnose / wave return wall (TAW, 2003).

The lines are described by:

$$\begin{aligned} \gamma_n &= 1,0 && \text{for } R_c \,/\, H_{m0} \leq 0,5 \\ \gamma_n &= 1,3 - 0,6 \cdot R_c \,/\, H_{m0} && \text{for } 0,5 < R_c \,/\, H_{m0} \leq 1,0 \\ \gamma_n &= 0,7 && \text{for } R_c \,/\, H_{m0} > 1,0 \end{aligned} \tag{H.6}$$

For a freeboard of 4,85 m and a wave height of 5,0 m the relative freeboard $R_c \,/\, H_{m0} = 0,97$, so $\gamma_n = 1,3 - 0,6 \cdot 0,97 = 0,72$. This leads to a freeboard of $\gamma_n \cdot R_c \approx 3,5$ m, which is NAP + 10 m.

APPENDIX I

GODA WAVE MODEL

The wave pressure can be calculated in two different ways, following Goda or following Sainflou. Sainflou has the advantage over Goda that it is simpler calculation work and less input is required. Disadvantages are that it is a conservative estimation and only valid for non-breaking waves (Technische Adviescommissie voor de Waterkeringen 2003). To get a proper estimation of the wave pressure, the model of Goda is used.

The model of Goda assumes full reflection of waves ($\chi = 1$) and in the model the unreflected wave height $H_D = 2,2 \cdot H_s$ should be entered, since reflection is discounted for in the expressions for wave pressures. Figure I.1 gives an overview of the used parameters in the model of Goda.

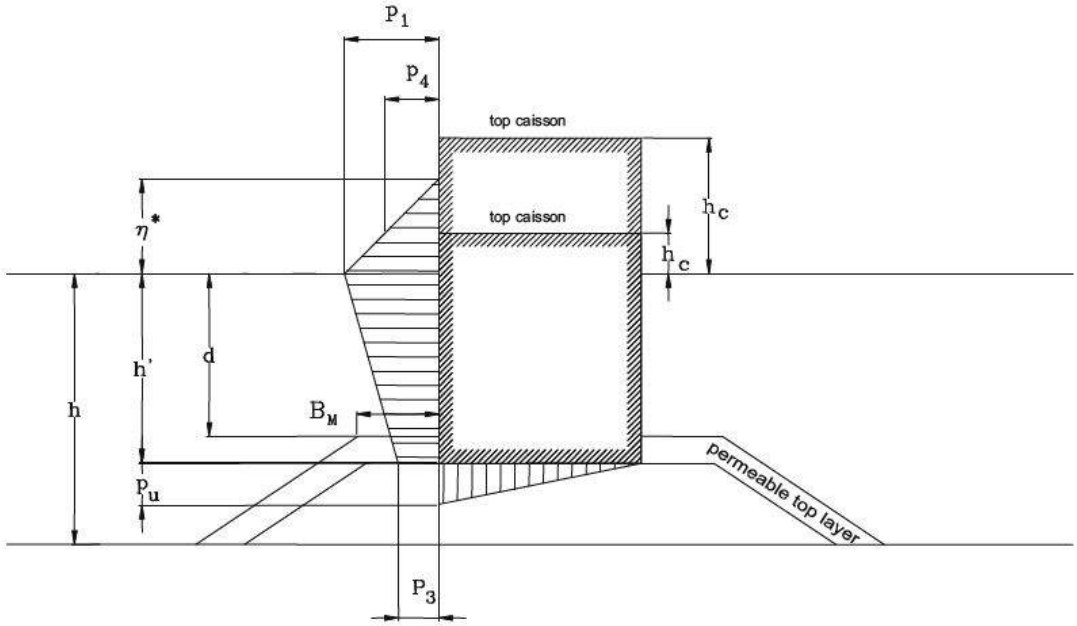

Figure I.1: Goda (modified by Tanimoto): wave pressure.

On the sea side there is no sill, so $h = h^{'} = d$ and $B_m = 0$. Furthermore, the maximum wave pressures are:

$$\begin{aligned} p_1 &= 0,5 \cdot (1 + \cos(\beta)) \cdot \left(\lambda_1 \alpha_1 + \lambda_2 \alpha_2 \cos^2(\beta)\right) \cdot \rho_{sw} \cdot g \cdot H_D \\ p_3 &= \alpha_3 \cdot p_1 \\ p_4 &= \alpha_4 \cdot p_1 \\ p_u &= 0,5 \cdot (1 + \cos(\beta)) \cdot \lambda_3 \alpha_1 \alpha_3 \cdot \rho_{sw} \cdot g \cdot H_D \end{aligned} \tag{I.1}$$

In which:

β = the angle of the incoming wave

$$\eta^* = 0,75 \cdot (1 + \cos(\beta)) \cdot \lambda_1 H_D$$

$$\alpha_1 = 0,6 + 0,5 \cdot \left(\frac{4\pi h \,/\, L_D}{\sinh(4\pi h \,/\, L_D)}\right)^2$$

$$\alpha_2 = \min\left(\frac{(1 - d \,/\, h_b)\,(H_D \,/\, d)^2}{3}, \frac{2d}{H_D}\right)$$

$$\alpha_3 = 1 - \left(h^{'} \,/\, h\right) \cdot \left(1 - \frac{1}{\cosh(2\pi h \,/\, L_D)}\right) \approx \frac{1}{\cosh(kd)} \text{(without sill)}$$

$$\alpha_4 = 1 - \frac{h_c^*}{\eta^*}$$

$$h_c^* = \min(\eta^*, h_c)$$

$\lambda_1, \lambda_2, \lambda_3$ = factors dependant on the shape of the structure and on wave conditions; (vertical wall and non-breaking waves: $\lambda_1 = \lambda_2 = \lambda_3 = 1$)

h_b = water depth at a distance $5H_D$ from the wall

APPENDIX J

CONSTRUCTION OF CONCEPT 'UNITY'

In this appendix the in-situ construction method and all construction steps of the concept 'Unity' are discussed.

J.1 In Situ Construction

The two main construction methods considered here are a construction pit and a cofferdam. The difference between these is that a construction pit consists of (earthen) slopes and a cofferdam is enclosed by walls, most frequently sheet pile walls or combi-walls.

The choice between an construction dock and cofferdam depends on many factors, including available space, costs and local conditions. Generally, a construction dock is less expensive than a cofferdam, which will most probably be the case with the scale of this project. Generally cofferdams are used for projects like bridge piers.

J.1.1 Construction Pit

At the location of the in- and outlet structure of the Delta21 plan, a construction pit can be made. This method has also been applied to construct the Haringvliet barrier. To construct a construction pit, globally the following steps have to be performed;

- Installation of the dewatering system;
- excavation;
- installation of piles from the bottom of the construction pit, if it is not possible to use a shallow foundation;
- installation of seepage screens to prevent piping, if necessary.

It is also possible to excavate the construction pit by dredging. This choice depends on the accessibility of the construction pit to floating or demountable dredging equipment, the availability of sufficient room for depots and sedimentation basins in the immediate area, the available construction time, the dewatering time and the combination of time and costs.

Other aspects that should be considered are dimensions, supply (access to the site and cranes for lifting), slope stability and dewatering.

Another option is to use the dykes surrounding the energy storage lake and only come up with a solution that closes off the opening where the in- and outlet structure is located. In that case a huge construction pit can be created, with dykes that can already handle big water level differences.

Dimensions
The depth of the construction pit depends on the level of the underside of the structure, in this case NAP - 27,5 m plus the thickness of the floor slab plus the required sill height. Leading to NAP - 30,5 m, including the 1 m floor thickness and 2 m sill. The horizontal dimension of the bottom of the construction pit equals the sum of the external dimensions of the finished structure, the space required for the formwork with supports, the space for work roads (if required), crane tracks and storage space (Molenaar and Voorendt 2018). For the construction of the Haringvliet dam also an in situ construction pit was build, which was 600 m wide (Stichting On'Wijs 2003). This width is also used as a starting point in this design.

The retaining height of the construction pit depends on the allowed probability of failure. For the construction pit of the Haringvliet sluices a frequency of failure of 0,02 per year was used, which is once every 50 years (Molenaar and Voorendt 2019). According to Table 4.2 that corresponds to a water height of NAP + 3,50 m.

For the surrounding dykes a slope of 1V/4H is assumed, since these slopes are generally not problematic (Jonkman et al. 2018). Since the top of the dyke is located at NAP + 3,50 m and the bottom of the construction pit at NAP - 30,5 m, the dyke requires a width of 136 m on either side, leaving 328 m (when the width is 600 m) for the construction of the caissons, supply routes and storage.

The combined length of the caissons is around 2 020 m (with 138 pump-turbines and 0,5 m thick walls). Adding the slopes of the dyke and allowing for transport around the caissons a total length of 2,5 km seems suitable for the construction pit.

Summarized the construction pit will have dimensions of W x L = 600 x 2 500 m with a height between NAP + 3,50 m and NAP - 30,5 m.

Supply
Special care needs to be taken to make transport of all construction material possible to the construction pit. Preferable there is one driving direction, so that all vehicles can follow the same line. This is especially handy for concrete carrying vehicles. The most probable transport route is via the Maasvlakte II. Furthermore, a detailed plan of the required amount of cranes, with the radius and maximum lift load, should be made, which could influence the dimensions of the construction pit.

Dewatering
In order to keep a dry site, constant phreatic drainage is required. Circa 0,50 m beneath the bottom is necessary to ensure that no part of the work site is softened (Molenaar and Voorendt 2019). Also, to ensure operational reliability it is, usually, preferable to use a number of smaller infiltration wells than a few larger ones.

Special care has to be taken to make sure the building pit can be sealed off, to prevent too much inflow of water. An option is to place a sheet pile wall into the clay layer to create a seal.

Taking the NAP + 3,50 m on the sea side and the assumption that the bottom of the clay layer lies at NAP - 60 m, the pressure at the bottom of the clay layer equals 63,5 · 10,06 = 639 kN/m^2.

The bottom of the pit lies at NAP - 30,5 m (water level at NAP - 31 m) and the clay layer starts at NAP - 50 m. This results in a total pressure (including weight of the clay and sand layer) of 590 kN/m^2, which is not enough to resist the outside pressure. Options to mitigate the up-bursting of the clay layer are installing vertical drainage and relieving the pressure or increasing the weight in the building pit by casting a, tremendously expensive, underwater concrete floor.

For further iterations in the design, having the bottom of the building pit at NAP - 27,5 m and the water level at NAP - 28 m, the clay layer is sufficient. Of course, additional research is required to check the actual position and thickness of the clay layer.

J.2 Construction Phases

The prefabrication starts in a building dock near the final location, as shown in Figure 6.1. The caisson is build-up per three pump-turbine rooms, as indicated in Figure 5.4

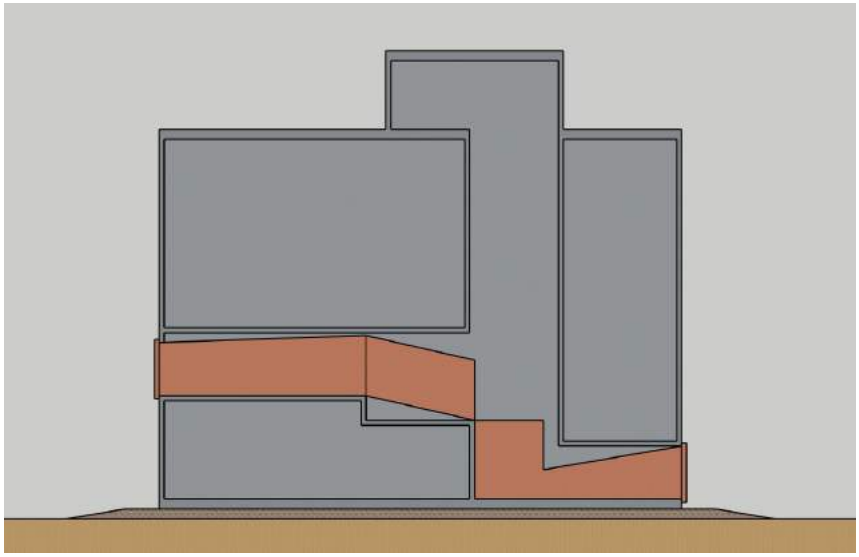

Figure J.1: Construction phase 1 of concept ‘Unity’.

Construction phase 1 is when the building of the (empty) caisson is finished in the building dock and the openings of the pump-turbine are closed off. Phase 2 is when the caisson is floating in the water. As we see in Appendix K, the draught is 13,5 m.

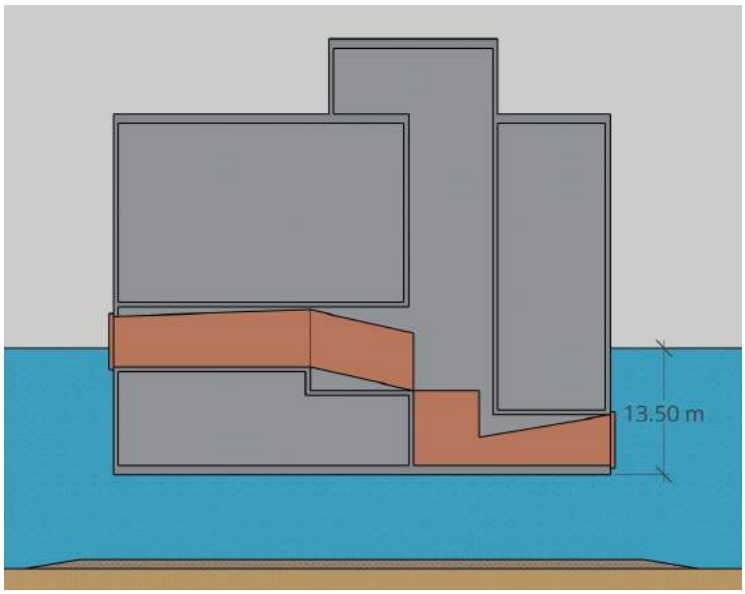

Figure J.2: Construction phase 2 of concept 'Unity'.

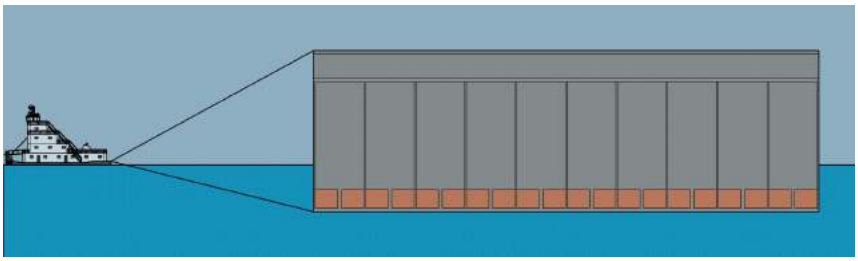

Figure J.3: Construction phase 3 of concept 'Unity'.

Construction phase 3 is when the caisson is being transported by towing boats to it's final location.

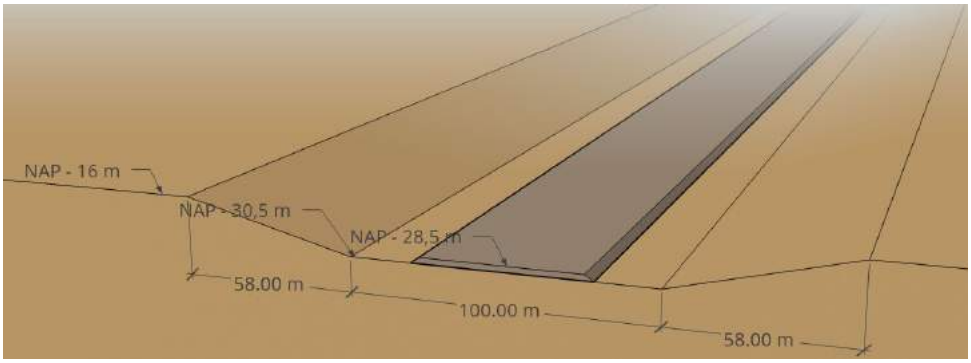

Figure J.4: Overview of dredging works of concept 'Unity'.

An overview of required dredging works at the final location are showed in Figure J.4 and J.5. For a stable slope a slope of 1V:4H is assumed. Most probably, the dredging works for the whole energy storage lake will take place at once, but to find the costs for this project a trench of 100 m width is considered, after which the trench slopes back up to NAP - 16 m. This means that, with a length of 2,5 km, a volume of sand of 5,73 mln m^3 should be dredged out.

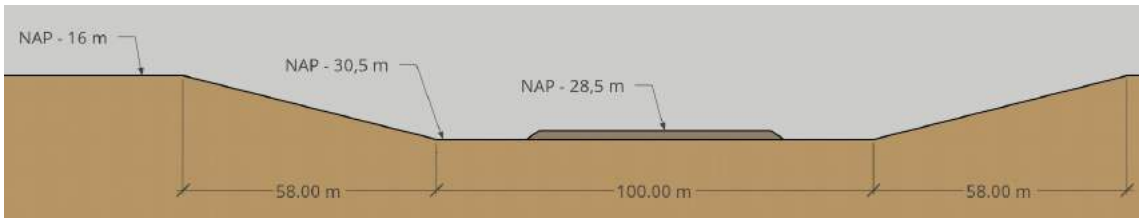

Figure J.5: Side view of dredging works of concept 'Unity'.

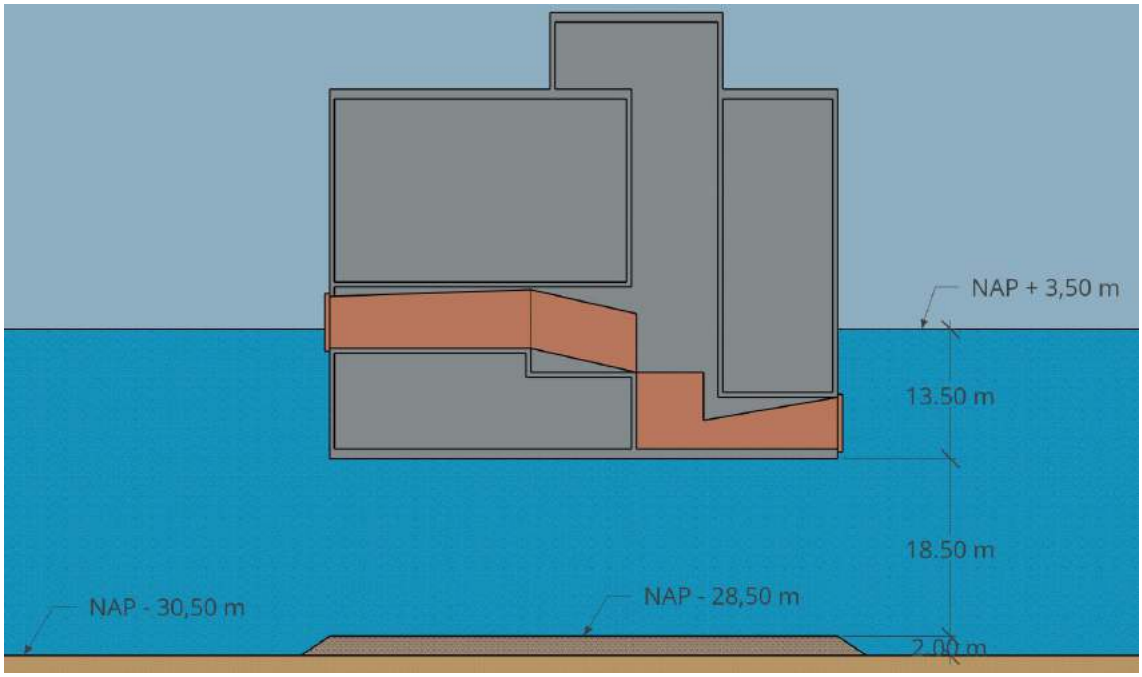

Figure J.6: Construction phase 4 of concept 'Unity'.

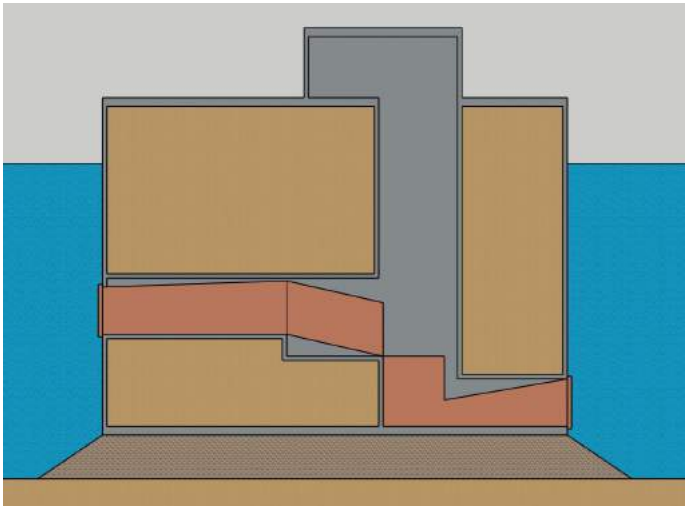

Figure J.7: Construction phase 5 of concept 'Unity'.

Phase 4 is when the caisson has arrived at the final location and shows relevant depths, while phase 5 shows the submerged (sunken) caisson, full with ballast material. In this case saturated sand.

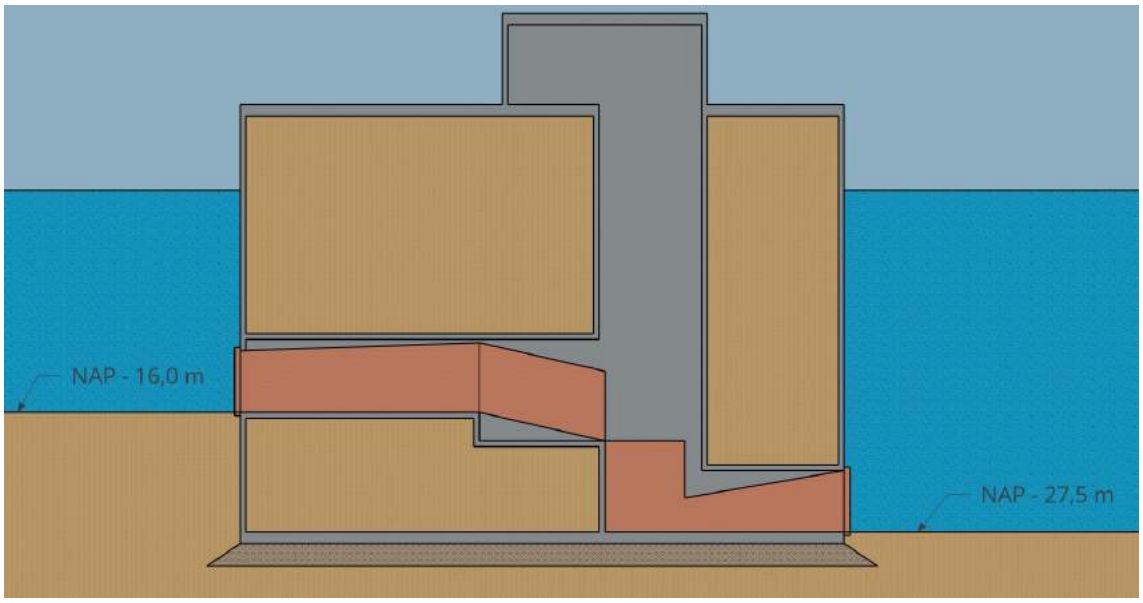

Figure J.8: Construction phase 6 of concept 'Unity'.

The final phase is phase 6, where the soil is placed back against the caisson at the required levels.

APPENDIX K

STABILITY OF CONCEPT 'UNITY'

In this appendix, the failure mechanisms that could undermine the stability of concept 'Unity' are worked out in more detail.

K.1 Internal Forces

Since the internal forces are equal for all failure mechanisms, these are treated here.

The internal forces are shown in Figure K.1. As a starting point, the width is set to 53 m, the height is 38,5 m and the length (along the division between sea and lake) of one single caisson room is 14,11 m (without partition wall). The thickness of the floor and the roof is set to 1 m and all the thickness of all other walls are assumed as 0,5 m.

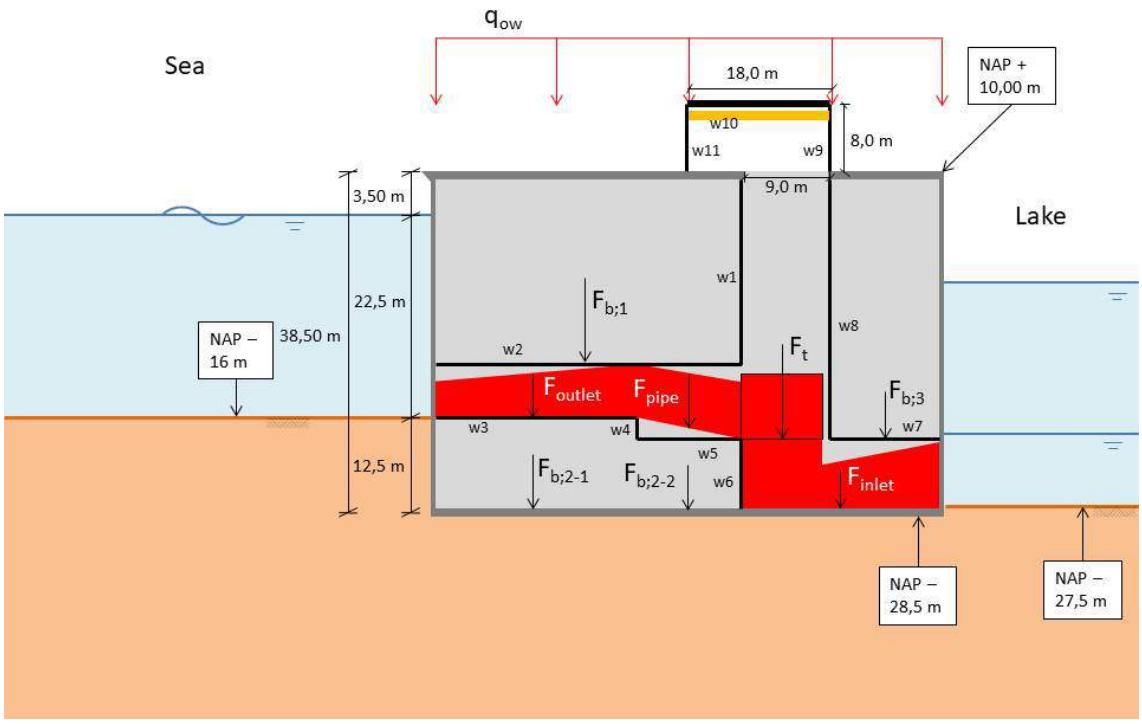

Figure K.1: Internal forces of concept 'Unity'.

Forces $F_{b;1}$ until $F_{b;3}$ are resulting forces from ballast material. Force F_t is from the pump-turbine weight, F_{outlet} = F_{inlet} and F_{pipe} are forces resulting from the water inside the pump-turbine system and F_c is the weight of the overhead crane (which is set to 0 for now, since the overhead crane can run over the entire length of the caisson). Lastly, q_{ow} results from all the concrete works (floor, roof, walls).

The specific weight of (reinforced) concrete is set to $\gamma_c = \rho_c \cdot g = 2,5 * 9,81$ = 24,52 kN/m^3 and as ballast material sand (γ_s = 19 kN/m^3) is assumed.

When Figure K.1 is combined with Figure 5.3 the following forces and arms are obtained in Table K.1.

Force	**Value**	**Unit**		**Arm**	**Value**	**Unit**
$F_{b;1;k}$	10 657,0	kN/m	|	$a_{b;1}$	37,25	m
$F_{b;2-1;k}$	4 180,0	kN/m	|	$a_{b;2-1}$	42,50	m
$F_{b;2-2;k}$	1 776,5	kN/m	|	$a_{b;2-2}$	27,00	m
$F_{b;3;k}$	6 686,1	kN/m	|	$a_{b;3}$	6,25	m
$F_{t;k}$	347,6	kN/m	|	a_t	16,23	m
$F_{outlet;k}$	701,6	kN/m	|	a_{outlet}	42,50	m
$F_{inlet;k}$	701,6	kN/m	|	a_{inlet}	10,50	m
$F_{pipe;k}$	230,0	kN/m	|	a_{pipe}	26,50	m
$F_{wall-sea;k}$	447,7	kN/m	|	$a_{wall-sea}$	52,75	m
$F_{wall-lake;k}$	447,7	kN/m	|	$a_{wall-lake}$	0,25	m
$F_{floor;k}$	1 300,1	kN/m	|	a_{floor}	26,50	m
$F_{roof;k}$	1 300,1	kN/m	|	a_{roof}	26,50	m
$F_{part-wall;k}$	1 649,9	kN/m	|	$a_{part-wall}$	26,50	m
$F_{w1;k}$	225,6	kN/m	|	a_{w1}	21,25	m
$F_{w2;k}$	380,2	kN/m	|	a_{w2}	36,50	m
$F_{w3;k}$	245,3	kN/m	|	a_{w3}	42,50	m
$F_{w4;k}$	30,7	kN/m	|	a_{w4}	32,75	m
$F_{w5;k}$	134,9	kN/m	|	a_{w5}	27,00	m
$F_{w6;k}$	110,4	kN/m	|	a_{w6}	21,25	m
$F_{w7;k}$	141,0	kN/m	|	a_{w7}	6,25	m
$F_{w8;k}$	381,4	kN/m	|	a_{w8}	12,25	m
$F_{w9;k}$	98,1	kN/m	|	a_{w9}	12,25	m
$F_{w10;k}$	220,8	kN/m	|	a_{w10}	25,50	m
$F_{w11;k}$	98,1	kN/m	|	a_{w11}	42,50	m

Table K.1: Summary of the acting internal forces on concept 'Unity'.

K.2 Rotational Stability

For this failure mechanism, first the loading situations are presented and then the checks are performed. A sketch of this failure mechanism is showed in Figure K.2.

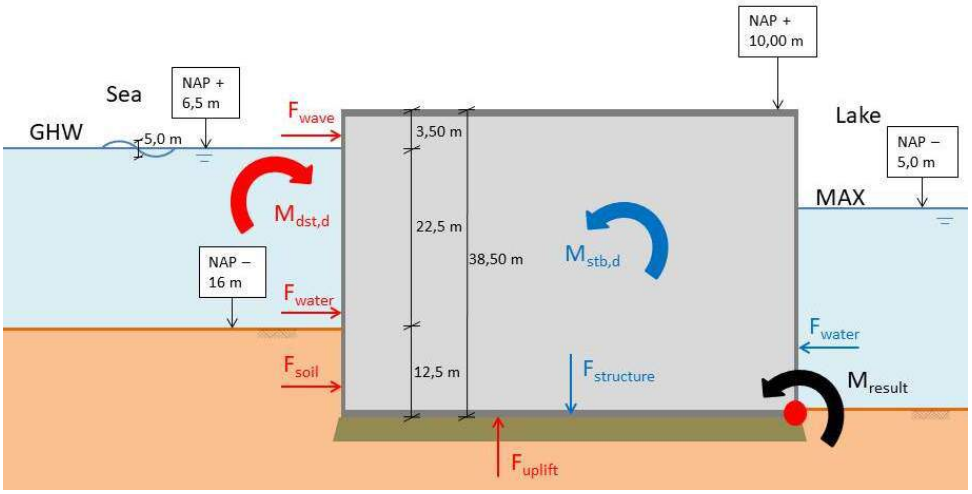

Figure K.2: Rotational stability of concept 'Unity'.

K.2.1 Loading situations

In Figure K.3 and K.4 the (characteristic) water pressures are shown. They are calculated by the well known equation $p_w = \gamma_{sw} \cdot h_w$, where $\gamma_{sw} = \rho_{sw} \cdot g = 1,025 * 9,81 = 10,06$ kN/m^3.

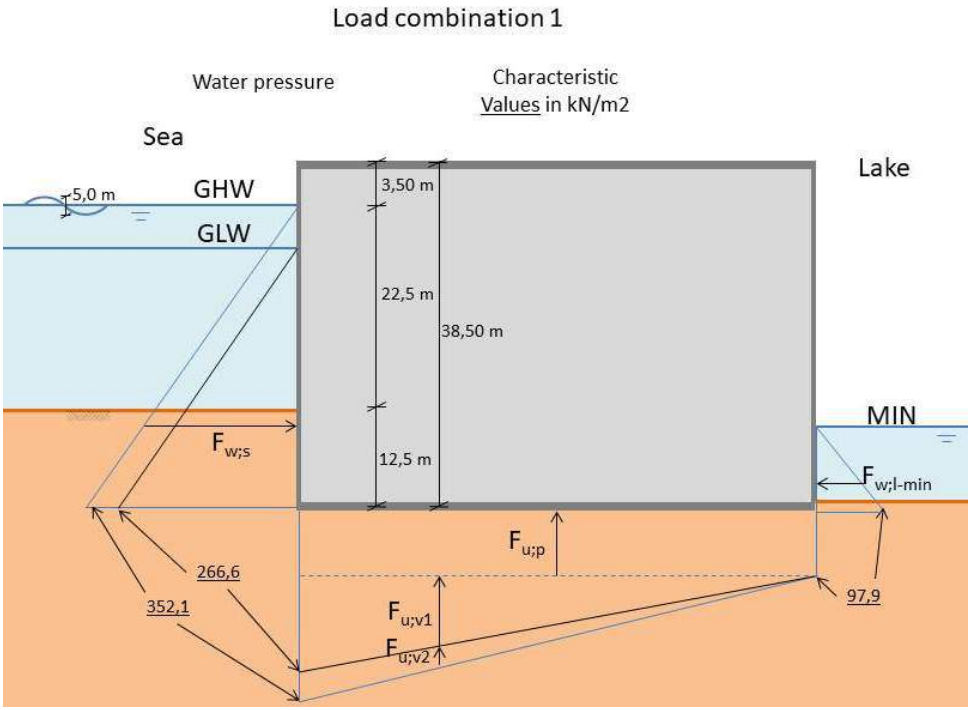

Figure K.3: Loading situation 1.

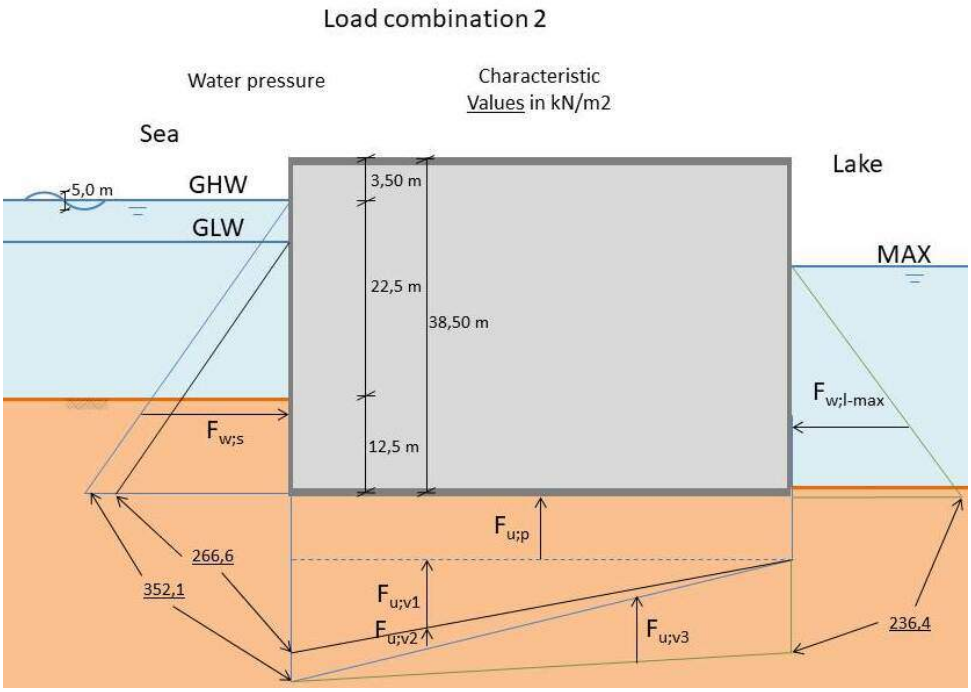

Figure K.4: Loading situation 2.

On the sea side the water pressure associated with GHW is $p_{w;s;h} = 22,5 + 12,5 * 10,06 = 352,1$ kN/m^2 and the water pressure associated with the (permanent) GLW is $p_{w;s;l} = 14 + 12,5 * 10,06 = 266,6$ kN/m^2.

The water pressure due to low water on the lake is $p_{w;l;h} = 8,73 + 1 * 10,06 = 97,9$ kN/m^2 and due to high water $p_{w;l;l} = 22,5 + 1 * 10,06 = 236,4$ kN/m^2. These pressures can also be assumed on the bottom side of the structure.

The wave pressures are determined according to the Goda wave model, see Appendix I. Resulting wave pressures are shown in Figure K.5.

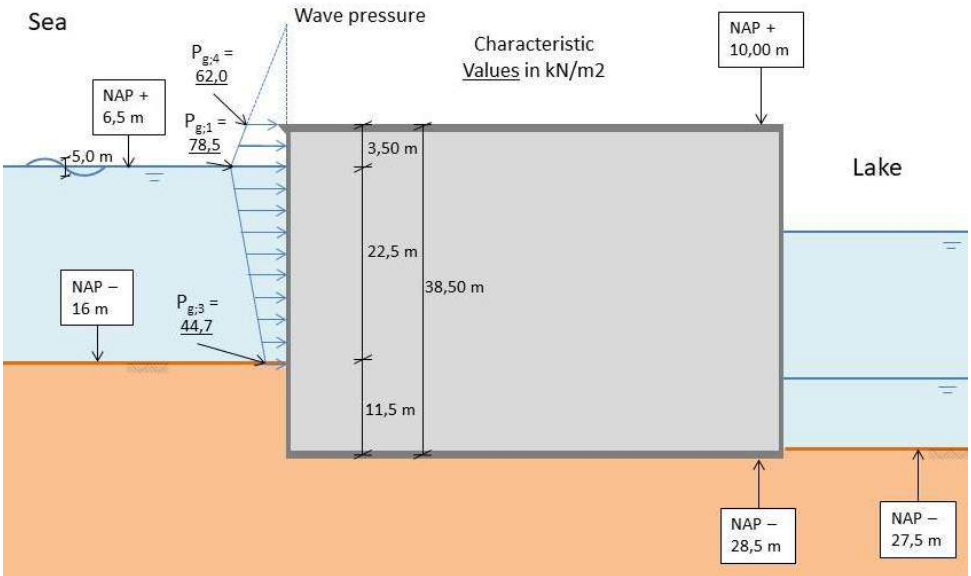

Figure K.5: Wave pressures on concept 'Unity'.

Lastly, the soil pressure has to be determined. For the soil pressure on the sea side the neutral soil parameter $K_{0;d}$ should be used, since there the soil and the caisson do not move relative to each other. The formula for the neutral soil pressure parameter is:

$$K_{0;d} = \left(1 - \sin \phi_d^{'}\right) \cdot \sqrt{OCR} \cdot (1 + \sin \beta) \tag{K.1}$$

Where for sand the $\phi_k^{'}$ = 30°and the $\phi_d^{'}$ = 25,7°, the OCR (over-consolidation rate) is assumed 1,0 and the β = 0, since there is no slope. So the $K_{0;d}$ = 0,566. On the lake side the passive soil parameter $K_{\gamma;p;d}$ has to be determined according to:

$$K_{\gamma;p;d} = \frac{\cos^2\left(\phi_d^{'} - \alpha\right)}{\cos^2(\alpha) \cdot \left(1 - \sqrt{\frac{\sin\left(\phi_d^{'} - \delta_{p;rep}\right) \cdot \sin\left(\phi_d^{'} - \beta_p\right)}{\cos\left(\alpha - \delta_{p;d}\right) \cdot \cos\left(\alpha + \beta_p\right)}}\right)^2} \tag{K.2}$$

With α = 0, since there is a vertical wall, and $\delta_d = 0,67 \cdot \phi_d^{'}$ = 17°. Which leads to a passive soil parameter $K_{\gamma;p;d}$ = 1,492. The acting soil pressure on the sea side then becomes $\sigma_{zz;s} = (\gamma_s - \gamma_{sw}) \cdot h_{seasoil} \cdot K_{0;d} = (19 - 10,06) * 12,5 * 0,566$ = 63,3 kN/m^2. The (resisting) soil pressure on the lake side is $\sigma_{zz;l} = (\gamma_s - \gamma_{sw}) \cdot h_{lakesoil} \cdot K_{\gamma;p;d} = (19 - 10,06) * 1,0 * 1,492$ = 13,3 kN/m^2.

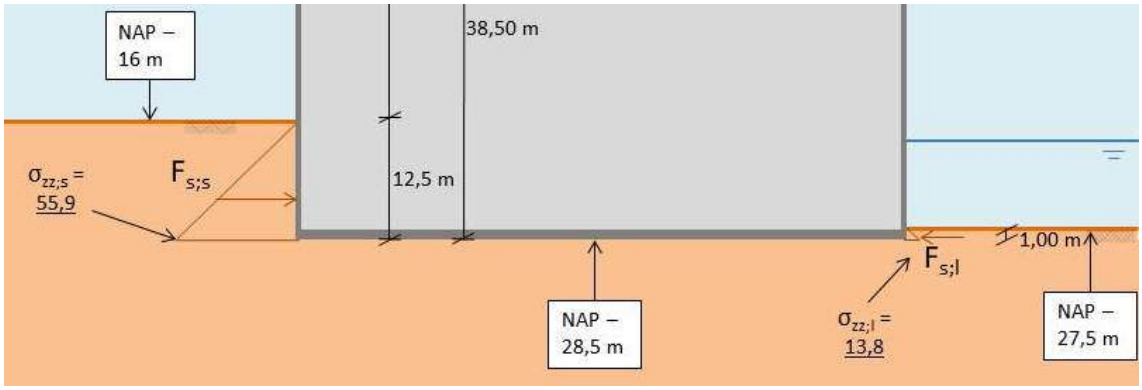

Figure K.6: Soil pressure acting on concept 'Unity'.

The wave forces are described as showed in Figure K.7.

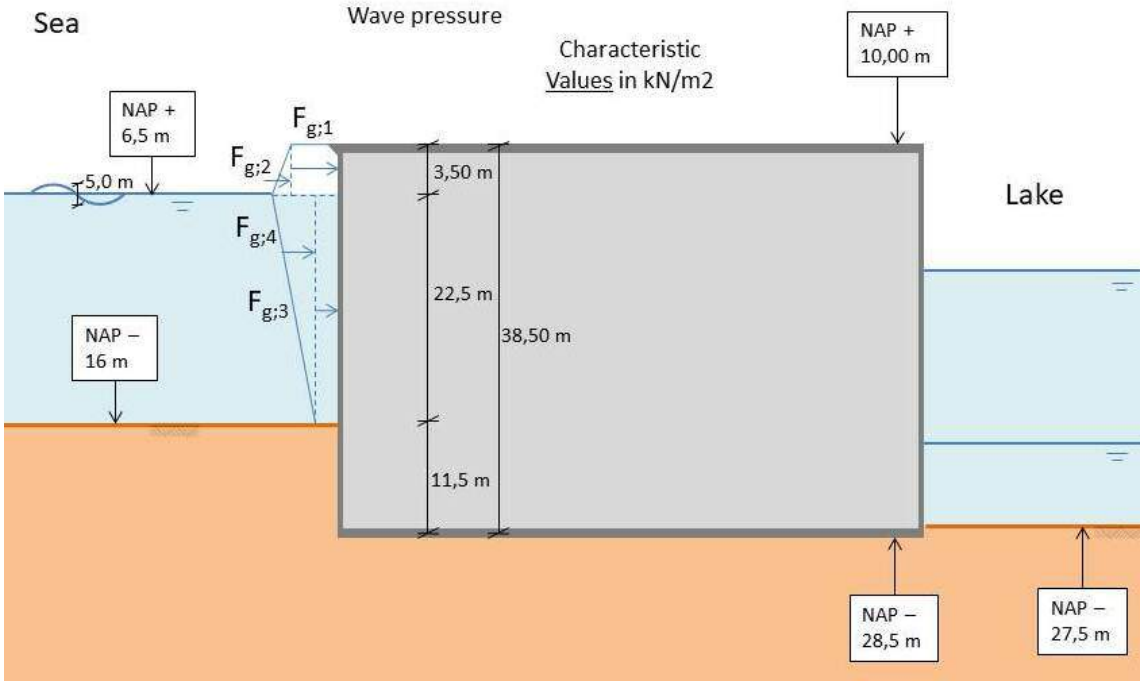

Figure K.7: Wave forces on concept 'Unity'.

To determine the characteristic value of the force the area of the acting pressure should be taken. Taking a width of 53 m as starting point, the forces are summarised in Table K.2, including the corresponding arm to the foot of the structure on the lake side.

Force	Value	Unit	|	Arm	Value	Unit
$F_{w;s;h;k}$	6 161,8	kN/m	|	$a_{w;s;h}$	11,67	m
$F_{w;s;l;k}$	3 532,5	kN/m	|	$a_{w;s;l}$	8,83	m
$F_{w;l-min;k}$	476,3	kN/m	|	$a_{w;l-min}$	3,24	m
$F_{w;l-max;k}$	2 777,7	kN/m	|	$a_{w;l-max}$	7,83	m
$F_{s;s;k}$	395,6	kN/m	|	$a_{s;s}$	4,17	m
$F_{s;l;k}$	6,7	kN/m	|	$a_{s;l}$	0,33	m
$F_{g;1;k}$	217	kN/m	|	$a_{g;1}$	36,75	m
$F_{g;2;k}$	28,9	kN/m	|	$a_{g;2}$	36,17	m
$F_{g;3;k}$	1 005,8	kN/m	|	$a_{g;3}$	23,75	m
$F_{g;4;k}$	380,3	kN/m	|	$a_{g;4}$	27,50	m
$F_{u;p;k}$	5 188,7	kN/m	|	$a_{u;p}$	26,50	m
$F_{u;v1;k}$	4 470,6	kN/m	|	$a_{u;v1}$	35,33	m
$F_{u;v2;k}$	2 265,8	kN/m	|	$a_{u;v2}$	35,33	m
$F_{u;v3;k}$	3 670,3	kN/m	|	$a_{u;v3}$	17,67	m

Table K.2: Summary of the acting external forces on concept 'Unity'.

K.2.2 Check for loading situation 1

Destabilising moments

The design overturning moment from the sea side equals:

$M_{sea,Q} = 1,25 * 6\ 161,8 * 11,67 + 217 * 36,75 + 28,9 * 36,17 + 1\ 005,8 * 23,75 + 380,3 * 27,50 + 1,0 * 395,6 * 4,17$ = 145 742 kNm/m.

And from the uplifting force under the structure:

$M_{uplift,Q} = 1,0 * 5\ 188,7 * 26,50 + 4\ 470,6 * 35,33 + 1,25 * 2\ 265,8 * 35,33$ = 395 510 kNm/m.

Consequently, the total destabilising moment is: $M_{dst,d} = M_{sea,Q} + M_{uplift,Q}$ = 541 252 kNm/m.

Stabilising moments

The stabilising moment from the lake side is:

$M_{lake,Q} = 1,25 * 476,3 * 3,24 + 1,0 * 6,7 * 0,33$ = 1 931 kNm/m.

The sum of the moment coming from the pump-turbine system:

$M_{pumpturbine,G} = 0,9 * 347,6 * 16,23 + 701,6 * 42,5 + 701,6 * 10,5 + 230 * 26,5$ = 44 029 kNm/m.

Lastly, the total moment coming from all concrete works equals:

$M_{concrete,G} = 0,9 * \Sigma F_{walls\ and\ floors} * a_{walls\ and\ floors} + \Sigma F_{ballast} * a_{ballast}$ = 766 914 kNm/m.

The total stabilising moment $M_{stb,d} = M_{lake,Q} + M_{pumpturbine,G} + M_{concrete,G}$ = 812 874 kNm/m.

Unity check The stabilising moment is bigger than the destabilising moment, when all chambers are filled completely with a sand ballast. The unity check gives: $uc = \frac{M_{dst,d}}{M_{stb,d}} = \frac{541\ 252}{812\ 874}$ = 0,67.

K.2.3 Check for loading situation 2

With high water on the lake, the resulting uplift moment increases with $1,25 * F_{u;v3;k} * a_{u;v3}$ to 476 578 kNm/m. The destabilising moment from the sea side remains the same.

The stabilising moment from the concrete works and from the pump-turbine system also stays the same as in load combination 1. The stabilising moment from the lake side becomes 27 189 kNm/m.

The total destabilising moment is now $M_{dst,d} = M_{sea,Q} + M_{uplift,Q} = 145\ 742 + 476\ 578$ = 622 320 kNm/m.

The stabilising moments are $M_{stb,d} = M_{lake,Q} + M_{concrete,G} + M_{pumpturbine,G} = 27\ 189 + 766\ 914 + 44\ 029$ = 838 132 kNm/m.

The unity check becomes $uc = \frac{M_{dst,d}}{M_{stb,d}} = \frac{622\ 320}{838\ 132}$ = 0,74.

K.3 Resistance Against Sliding

This failure mechanism is sketched in Figure K.8. The same loading situations apply as presented in Figure K.3 and Figure K.4.

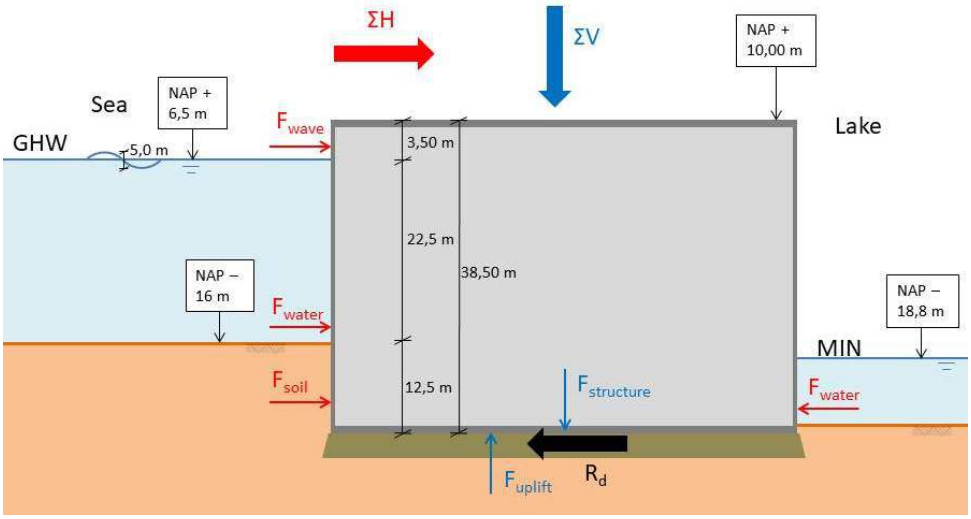

Figure K.8: Sliding Resistance of concept 'Unity'.

K.3.1 Acting loads

The resulting horizontal load in load combination 1 equals:

$$\Sigma H_1 = 1,25 \cdot \left(F_{g;1} + F_{g;2} + F_{g;3} + F_{g;4} + F_{w;s;h} - F_{w;l-min}\right) + 1,0 * \left(F_{s;s} - F_{s;l}\right) = 9\ 536 \text{ kN/m}$$

And the resulting vertical load:

$$\Sigma V_1 = 0,9 \cdot F_{structure} - 1,0 \cdot (F_{u;p} + F_{u;v1}) - 1,25 \cdot F_{u;v2} = 16\ 752 \text{ kN/m}$$

In load situation 2, the resulting horizontal load is:

$$\Sigma H_2 = 1,25 \cdot \left(F_{g;1} + F_{g;2} + F_{g;3} + F_{g;4} + F_{w;s;h} - F_{w;l-max}\right) + 1,0 * \left(F_{s;s} - F_{s;l}\right) = 6\ 659 \text{ kN/m}$$

And the resulting vertical load:

$$\Sigma V_2 = 0,9 \cdot F_{structure} - 1,0 \cdot (F_{u;p} + F_{u;v1}) - 1,25 \cdot (F_{u;v2} + F_{u;v3}) = 12\ 164 \text{ kN/m}$$

K.3.2 Sliding resistance

The resistance against sliding is given, in Eurocode 7, as:

$$R_d = V_d^{'} \cdot \tan \delta_d \tag{K.3}$$

Where δ_d = 22,2°for the present sill. Consequently, in load combination 1 the sliding resistance is R_d = 6 836 kN/m, which is 2 700 kN/m short, uc = 1,39.

In load combination 2 the sliding resistance R_d = 4 964 kN/m, which is 1 695 kN/m short, uc = 1,34.

K.3.3 Increasing the resistance

When the reduced δ_d can be increased to $\phi_k^{'}$, the sliding resistance in load combination 1 becomes R_d = 11 299 kN/m (which is 1 763 kN/m overcapacity) and the sliding resistance in load combination 2 becomes R_d = 8 205 kN/m (which is an overcapacity of 1 546 kN/m).

This can be achieved by roughening the bottom surface of the caisson.

K.4 Bearing Resistance

The bearing resistance failure mechanism is described as a slip circle, showed in Figure K.9.

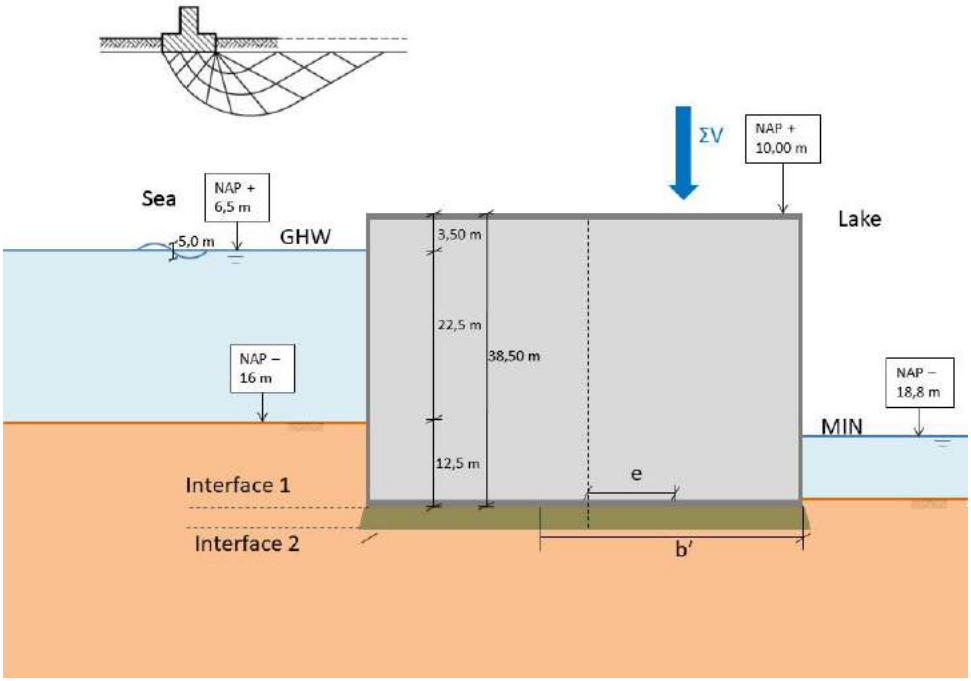

Figure K.9: Bearing capacity of concept 'Unity'.

The bearing capacity of the soil is described by:

$$\sigma^{'}_{max;d} = \sigma^{'}_{v;z;d} \cdot N_q \cdot s_q \cdot b_q \cdot i_q + 0,5 \cdot \gamma^{'}_{average} \cdot b' \cdot N_{\gamma'} \cdot s_{\gamma'} \cdot b_\gamma \cdot i_{\gamma'} \quad \text{(K.4)}$$

Where the first part of Equation K.4 (before the plus sign) describes the influence of the ground cover and the second part described the capacity of the soil under the structure. In these soils no cohesion is present and is left out of the equation.

K.4.1 Interface 1

The parameters of the 2 m high sill have been described in Section 5.6, so the effective width is;
$b' = W - 2 \cdot e_d = 53 - 2 * 10,29$ = 32,4 m.

The ground cover next to the sill is 1 m, so the effective vertical stress is;
$\sigma^{'}_{v;z;d} = 19 - 10,06 * 1 = 8,94$ kN/m^2

The load carrying factors for respectively the ground cover and the effective volumic weight are;
$N_q = \exp\left(\pi \cdot \tan \phi^{'}_{average;d}\right) \cdot \tan^2\left(45° + 0,5 \cdot \phi^{'}_{average;d}\right) = 29,4,$
$N_{\gamma'} = 2 \cdot (N_q - 1) \cdot \tan\left(\phi^{'}_{average;d}\right) = 38,3.$

Assuming 3 pump-turbines per element as starting point, gives a length of 3x(14,11+0,5)+0,5 = 44,33 m.
The shape factors for respectively the the ground cover and the volumic weight are;
$s_q = 1 + \frac{b'}{l'} \cdot \sin\left(\phi^{'}_{gem;d}\right) = 1 + \frac{32,4}{44,33} \cdot \sin(25,7) = 1,32,$
$s_{\gamma'} = 1 - 0,3 \cdot \frac{b'}{l'} = 1 - 0,3 * \frac{32,4}{44,33} = 0,78.$

Since the foundation slope is horizontal, no reduction factor should be applied; $b_\gamma = 1,0$.

The angle between the horizontal load and the longest side of the effective area is 90°, so the reduction factors for respectively the ground cover and the volumic weight are;
$i_q = \left(1 - \frac{0,7 \cdot H_d}{V_d}\right)^{m+1} = \left(1 - \frac{6\,675}{16\,752}\right)^{2,6}$ = 0,27,
$i_{\gamma'} = \left(1 - \frac{H_d}{V_d}\right)^{m+1} = \left(1 - \frac{9\,536}{16\,752}\right)^{2,6}$ = 0,11,
With: $m = m_B = [2 + (B'L')]\ /\ [1 + (B'L')] = 1,6.$

That gives as a result:
$\sigma^{'}_{max;d} = \sigma^{'}_{v;z;d} \cdot N_q \cdot s_q \cdot b_q \cdot i_q + 0,5 \cdot \gamma^{'}_{average} \cdot b' \cdot N_{\gamma'} \cdot s_{\gamma'} \cdot b_\gamma \cdot i_{\gamma'} = 8,94 * 29,4 * 1,34 * 0,27 + 0,5 * (20,3 - 10,06) * 32,4 * 38,3 * 0,78 * 1,0 * 0,11$ = 639 kN/m^2.

The acting soil pressure can be calculated according to:

$$q_d = \frac{\Sigma V}{b'} \tag{K.5}$$

The maximum acting stress under the caisson then becomes $q_d = \frac{16\,752}{32,4}$ = 517 kN/m^2.
The unity check for maximum occurring stress is $uc = \frac{517}{639}$ = 0,81.

K.4.2 Interface 2

For the second interface the weight of the 2m high sill has to be incorporated and the effective width has to be determined, following the spreading of forces by the sill. Assumed is that the sill distributes the loading with an angle equal to the internal angle of friction $\phi_d^{'}$ = 34°.

The extra width at the bottom is 2 x h_{sill} x $\tan\left(\phi_d^{'}\right)$ = $2 \cdot 2 \cdot \tan\left(34°\right)$ = 2,7 m, leading to a total (effective) width of 35,1 m.

The additional weight becomes (2 x 1/2 x h_{sill} x $\tan\left(\phi_d^{'}\right)$ + h_{sill} x b') x γ_{sill} = 733 kN/m.

$N_q = \exp\left(\pi \cdot \tan\phi_{average;d}^{'}\right) \cdot \tan^2\left(45° + 0,5 \cdot \phi_{average;d}^{'}\right) = 19,0,$
$N_{\gamma'} = 2 \cdot (N_q - 1) \cdot \tan\left(\phi_{average;d}^{'}\right) = 21,0,$
$s_q = 1 + \frac{b'}{l'} \cdot \sin\left(\phi_{gem;d}^{'}\right) = 1 + \frac{35,1}{44,33} \cdot \sin\left(25,7\right) = 1,34,$
$s_{\gamma'} = 1 - 0,3 \cdot \frac{b'}{l'} = 1 - 0,3 * \frac{35,1}{44,33} = 0,76,$
$b_\gamma = 1,0,$
$i_q = \left(1 - \frac{0,7 \cdot H_d}{V_d}\right)^{m+1} = \left(1 - \frac{6\,675}{16\,752+733}\right)^{2,6}$ = 0,27,
$i_{\gamma'} = \left(1 - \frac{H_d}{V_d}\right)^{m+1} = \left(1 - \frac{9\,536}{16\,752+733}\right)^{2,6}$ = 0,11.
That gives as a result:
$\sigma_{max;d}^{'}$ = 560 kN/m^2.

The maximum acting stress under the sill then becomes $q_d = \frac{16\,752+733}{35,1}$ = 498 kN/m^2.
The unity check for maximum occurring stress is $uc = \frac{498}{560}$ = 0,89.

K.5 Floating Stability

To assess the floating stability, the following method has been copied from the TU Delft reader "Hydraulic Structures - caissons" (Voorendt, Molenaar, and Bezuyen 2016). Indicated in Figure K.10 are three points, which are of importance in the evaluation of the stability:

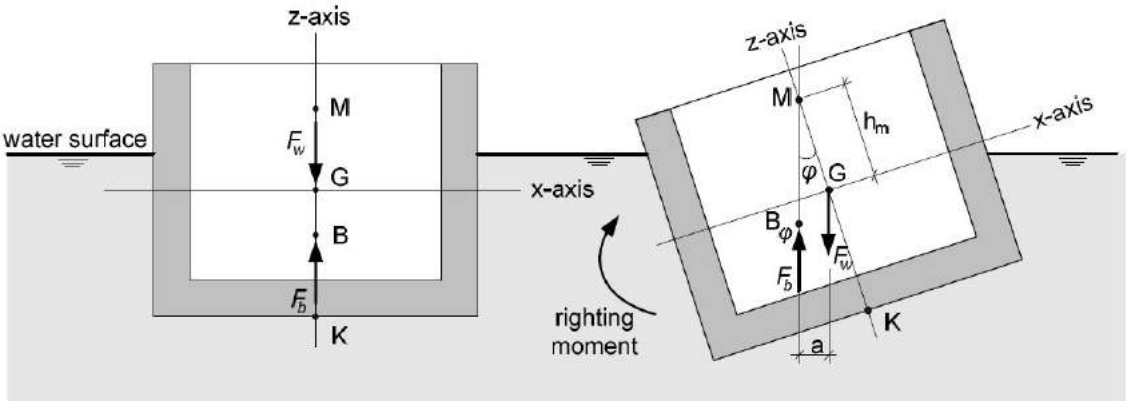

Figure K.10: Static stability of a floating element, SOURCE: (Molenaar and Voorendt 2019).

- B is the centre of buoyancy, the point of application of the buoyant force F_b in state of equilibrium (the state in which the axis of symmetry of the element is vertical). B is therefore the centre of gravity of the displaced water. In a rectangular container (caisson), B is found halfway between the water surface and the bottom of the element. In tilted position the centre of buoyancy shifts to a new position because the geometry of the displaced volume has changed. The shifted centre of buoyancy is indicated with $B\phi$ and the horizontal shift is a (m).
- G is the centre of gravity of the element. If the element is filled with a layer of gravel or water for the benefit of the immersing procedure (not shown in Figure 6.9), this weight should also be taken into account when calculating G. Not only will this ballast lower the centre of gravity, it will also increase the draught and will therefore raise B relative to the bottom. If the element heels over, the centre of gravity generally remains fixed with respect to the element because it just depends upon the position of the element's weight and ballast. The centre of gravity at the same time is the rotation point.
- M is the metacentre; the point of intersection of the axis of symmetry, the z-axis, and the action line of the buoyant force in tilted position. For small rotations ($\phi < 10°$) the metacentre is a fixed point (see lecture notes OE4652, 'Floating Structures' for a proof).

For static stability, rotation of the element should be compensated by a righting moment caused by the buoyant force and the weight of the element. This is the case if M is located over G: the line segment $\overline{GM}$, also known as the metacentric height h_m, must be positive.

The point of application of the buoyant force (F_b) in a state of rest, is the centre of pressure B. A rotation ϕ leads to a translation of the line of action of F_b over a distance a:

$$a = \frac{M}{F_b} = \frac{\phi \cdot \rho \cdot g \cdot I}{\rho \cdot g \cdot V} = \frac{\phi \cdot I}{V} \tag{K.6}$$

The distance between the centre of pressure and the metacentre therefore is $\overline{BM} = \frac{a}{\phi} = \frac{I}{V}$.

To check the static stability, the weight F_w and the position of the gravity centre G of the floating element has to be calculated., with reference to K ($\overline{KG}$). K is the interaction of the z-axis with the bottom line of the element:

$$\overline{KG} = \frac{\Sigma V_i \cdot e_i \cdot \gamma_i}{\Sigma V_i \cdot \gamma_i} = \frac{\Sigma V_i \cdot e_i}{\Sigma V_i} \tag{K.7}$$

Where V_i = volume of element i (m^3)

γ_i = specific weight of element i (kN/m^3)

e_i = distance between gravity centre of element i and a horizontal plane through point K (m)

No.	Element	Volume	Unit	|	Distance	Value	Unit
1.	Outer wall - sea	18,25	m^2/m	|	e1	19,25	m
2.	Outer wall - lake	18,25	m^2/m	|	e2	19,25	m
3.	Floor slab	53,00	m^2/m	|	e3	0,50	m
4.	Roof slab	53,00	m^2/m	|	e4	38,00	m
5.	Partition wall	67,26	m^2/m	|	e5	19,25	m
6.	Aw1	9,55	m^2/m	|	e6	27,95	m
7.	Aw2	15,50	m^2/m	|	e7	18,15	m
8.	Aw3	10,00	m^2/m	|	e8	11,25	m
9.	Aw4	1,25	m^2/m	|	e9	10,25	m
10.	Aw5	5,50	m^2/m	|	e10	8,75	m
11.	Aw6	4,00	m^2/m	|	e11	5,00	m
12.	Aw7	5,75	m^2/m	|	e12	6,65	m
13.	Aw8	15,55	m^2/m	|	e13	21,95	m
14.	Aw9	4,00	m^2/m	|	e14	42,50	m
15.	Aw10	9,00	m^2/m	|	e15	46,00	m
16.	Aw11	4,00	m^2/m	|	e16	42,50	m

Table K.3: Volume of elements versus distance from reference plane.

The data in Table K.3 results in $\overline{KG}$ = 20,20 m.

Furthermore, the draught *d* has to be determined. To do so, the total weight of the structure F_w has to be determined. From Table K.1 and a length of 4 times 44,33 = 177,3 m, the total weight of one caisson of 4 times 3 pump-turbine rooms (without ballast and pump-turbine system) F_w = 1 278 832 kN. This means that the draught of the structure can be determined as $d = \frac{F_w}{W \cdot L \cdot \gamma_{sw}}$ = 13,5 m.

The centre of buoyancy B and it's position above the bottom of the element has distance $\overline{KB} = \frac{1}{2}d$ = 6,8 m.

Lastly, the distance $\overline{BM} = \frac{I}{V}$ should be calculated. I (actually I_{yy}) is the area moment of inertia, relative to the y-axis, of the plane intersected by the waterline.

$I = 112 \cdot L \cdot W^3$ = 2 199 906 m^4 and the submerged volume V = $L \cdot W \cdot d$ = 127 154 m^3. This gives a distance $\overline{BM}$ = 17,3 m.

Stability

The static stability is described by $h_m = \overline{GM} = \overline{KB} + \overline{BM} - \overline{KG}$ = 6,8 + 17,3 - 20,2 = 3,9 m. This is more than the recommended 0,50 m (where theoretically $h_m > 0$ is stable).

APPENDIX L

CONSTRUCTION OF CONCEPT 'INTEGRATION'

In this appendix the construction sequence of the concept 'Integration' is elaborated. First the caisson on the sea side of the dyke is discussed and then the caisson on the lake side.

L.1 Construction of the Seaside Caisson

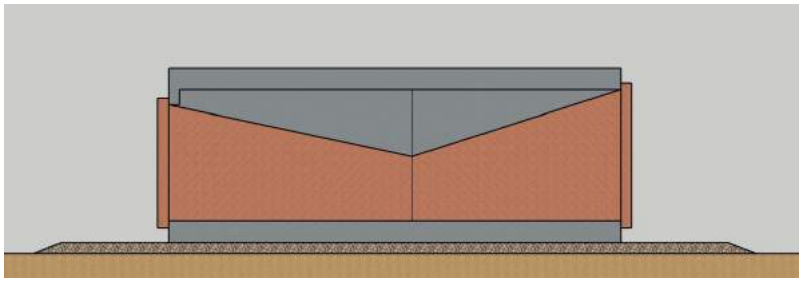

Figure L.1: Construction phase 1 of concept 'Integration', seaside.

As with concept 'Unity', the caisson is constructed in a building dock near the final location. The pump-turbine structure (metal body work) is already present within the structure and the openings on either side are closed off with gates.

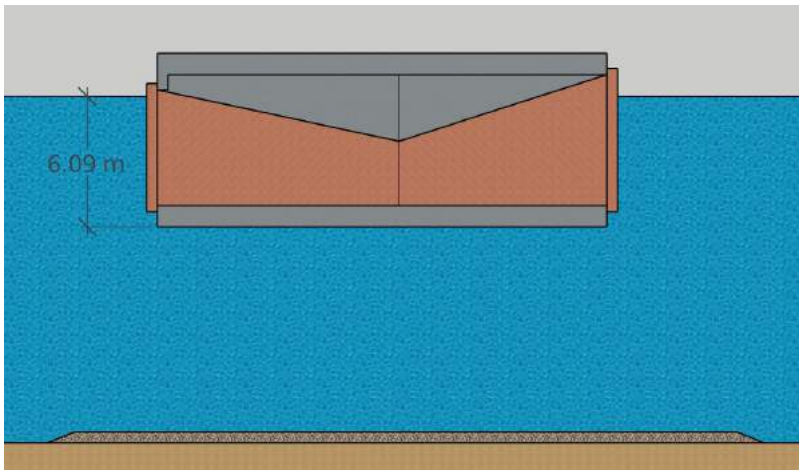

Figure L.2: Construction phase 2 of concept 'Integration', seaside.

When the structure is floating, the draught is 6,09 m.

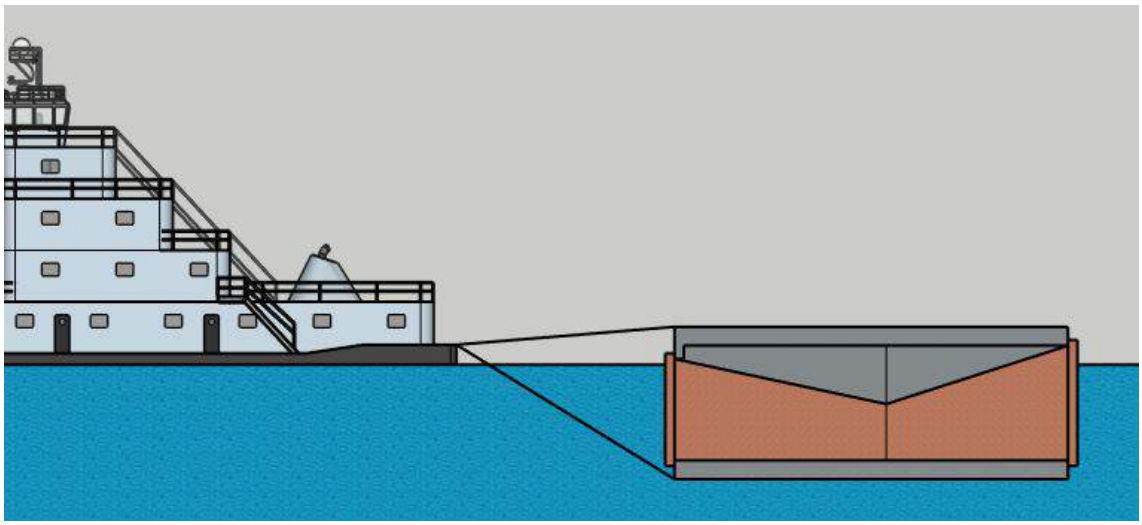

Figure L.3: Construction phase 3 of concept 'Integration', seaside.

Then the structure has to be towed to the final location.

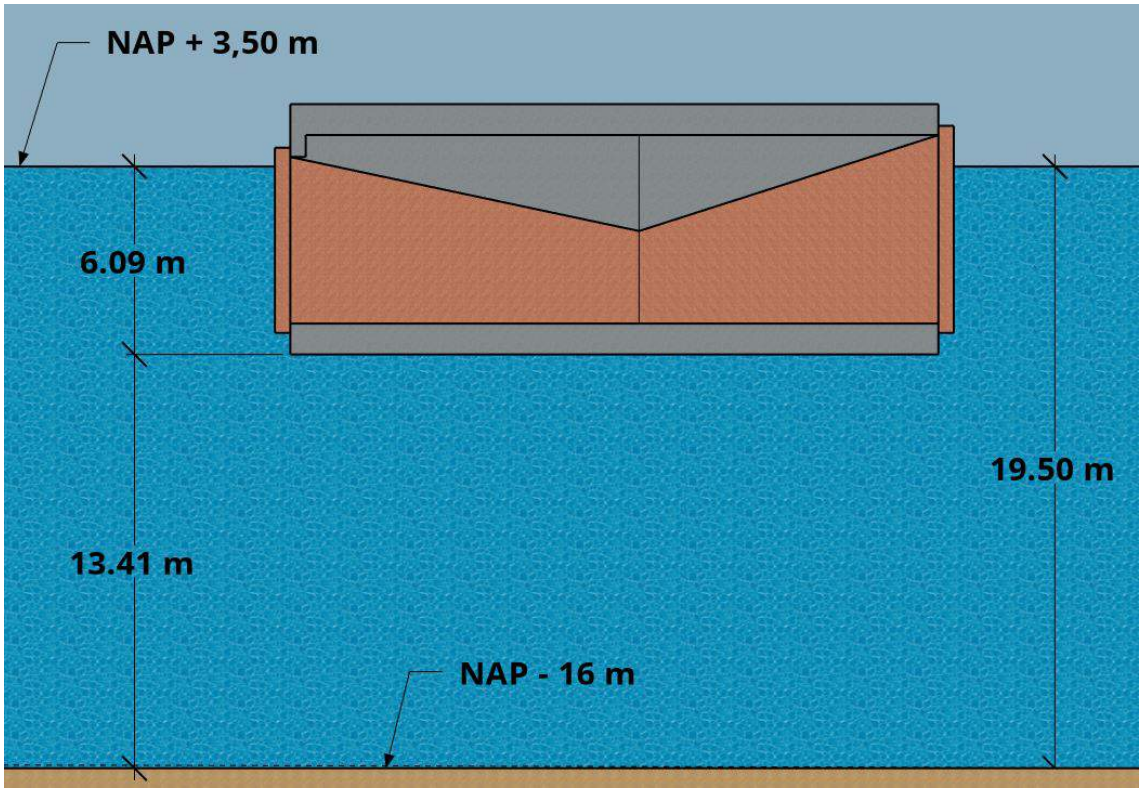

Figure L.4: Construction phase 4 of concept 'Integration', seaside.

At the final location, with the highest calculated water level (most probably) of NAP + 3,50 m, the required submerging distance to the bottom is 13,41 m. By opening the gates on either side and letting water flow in, in a controlled way, the caisson can gradually sink to the bottom.

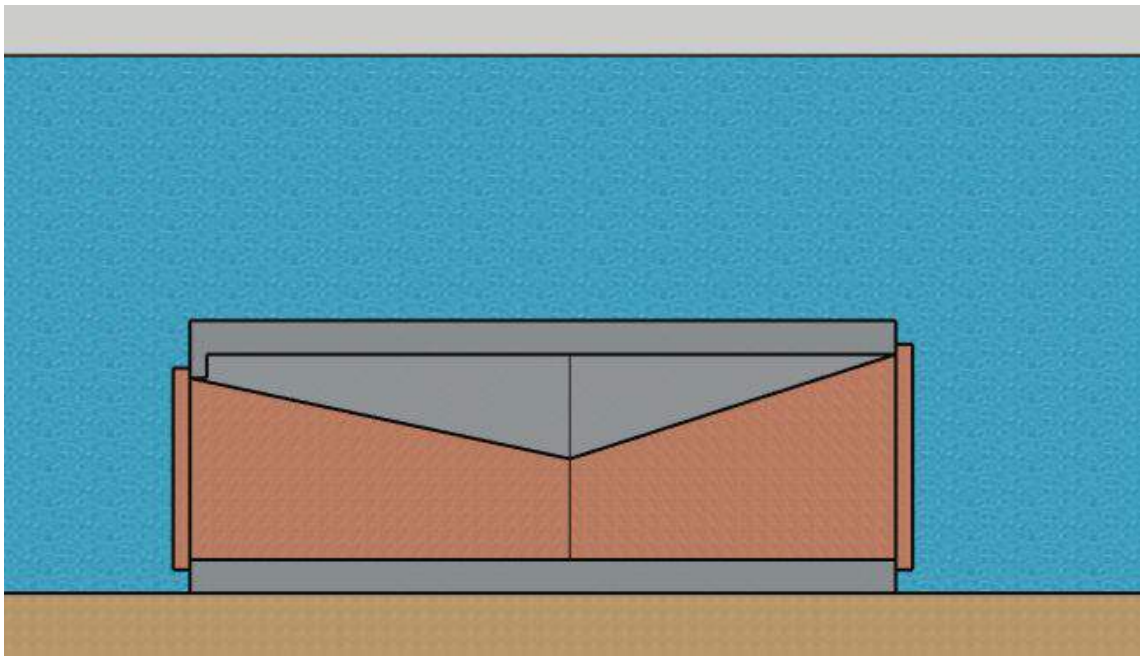

Figure L.5: Construction phase 5 of concept 'Integration', seaside.

Located at the bottom, the gates are still shown on either side, but the pump-turbine body work is completely filled with water. Also the ballast compartments can be filled with sand now.

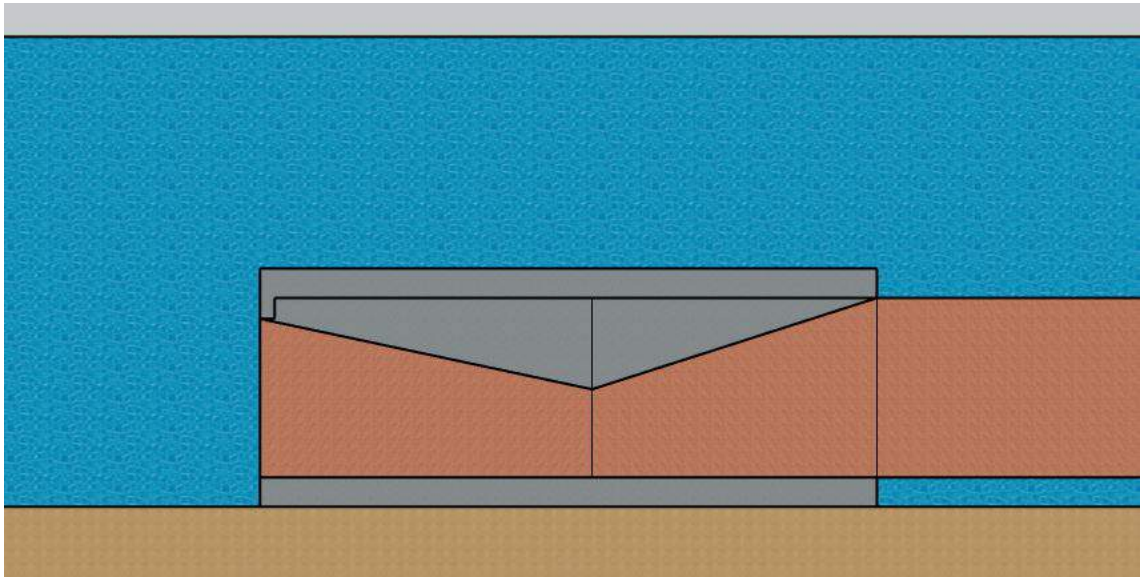

Figure L.6: Construction phase 6 of concept 'Integration', seaside.

Located at the bottom and fully ballasted, the pipe leading to the caisson on the lake side can be attached.

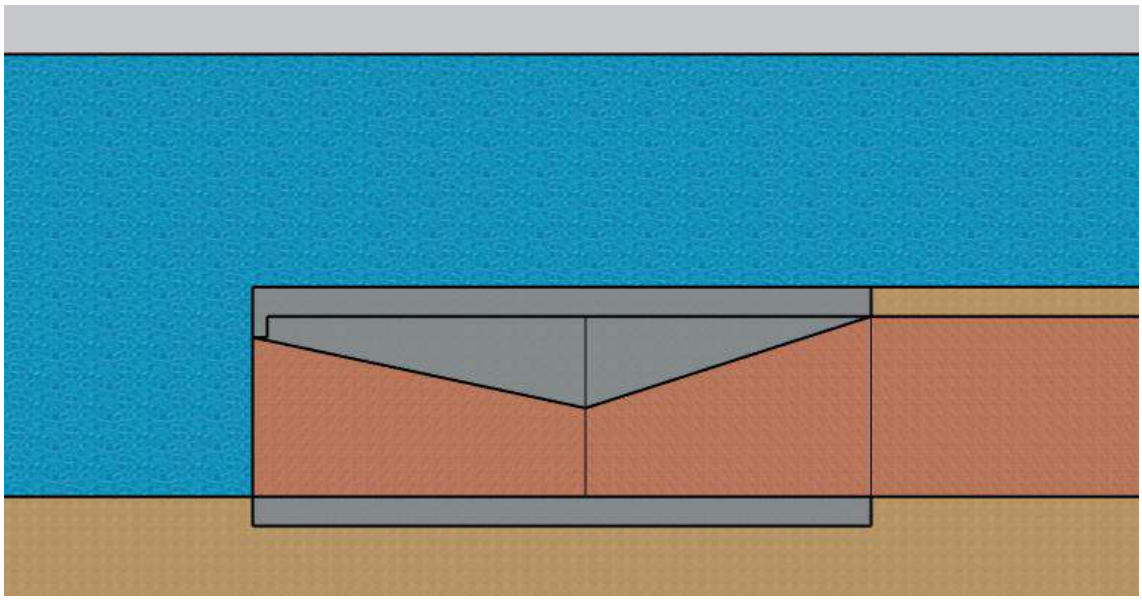

Figure L.7: Construction phase 7 of concept 'Integration', seaside.

And finally, the dyke body can be constructed and the bed protected in front of the caisson can be constructed.

L.2 Construction of the Lakeside Caisson

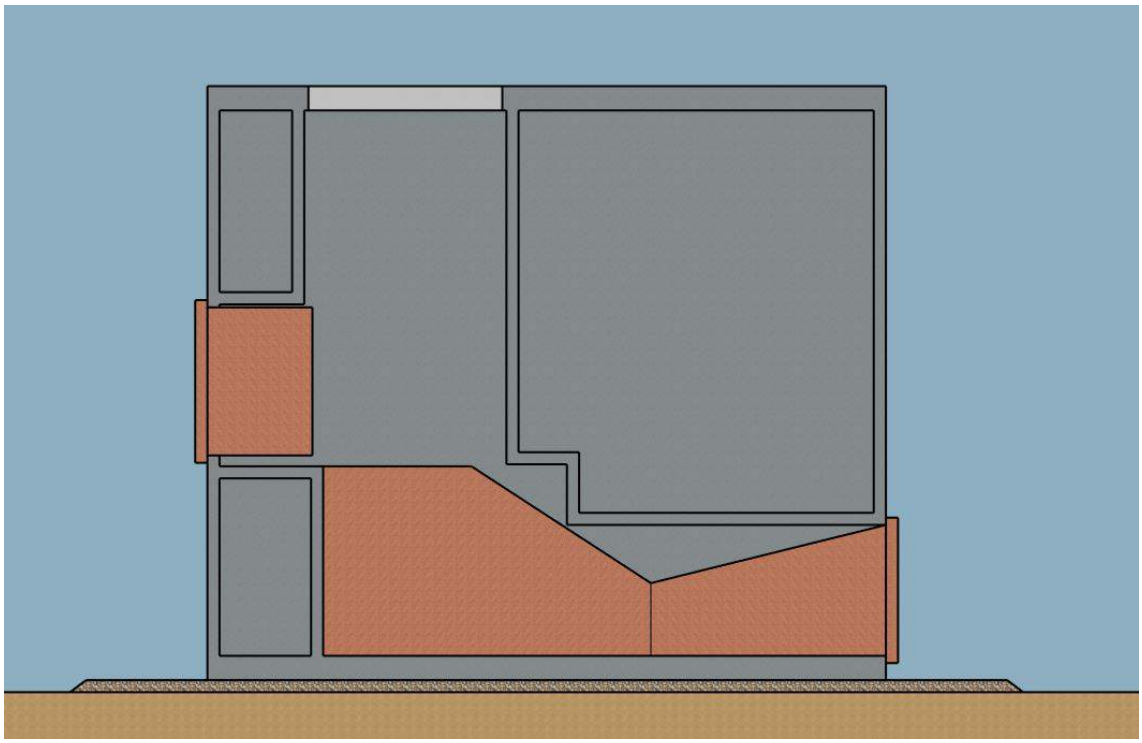

Figure L.8: Construction phase 1 of concept 'Integration', lakeside.

The described construction steps of the lake side caisson again starts after prefabrication has finished in the building dock.

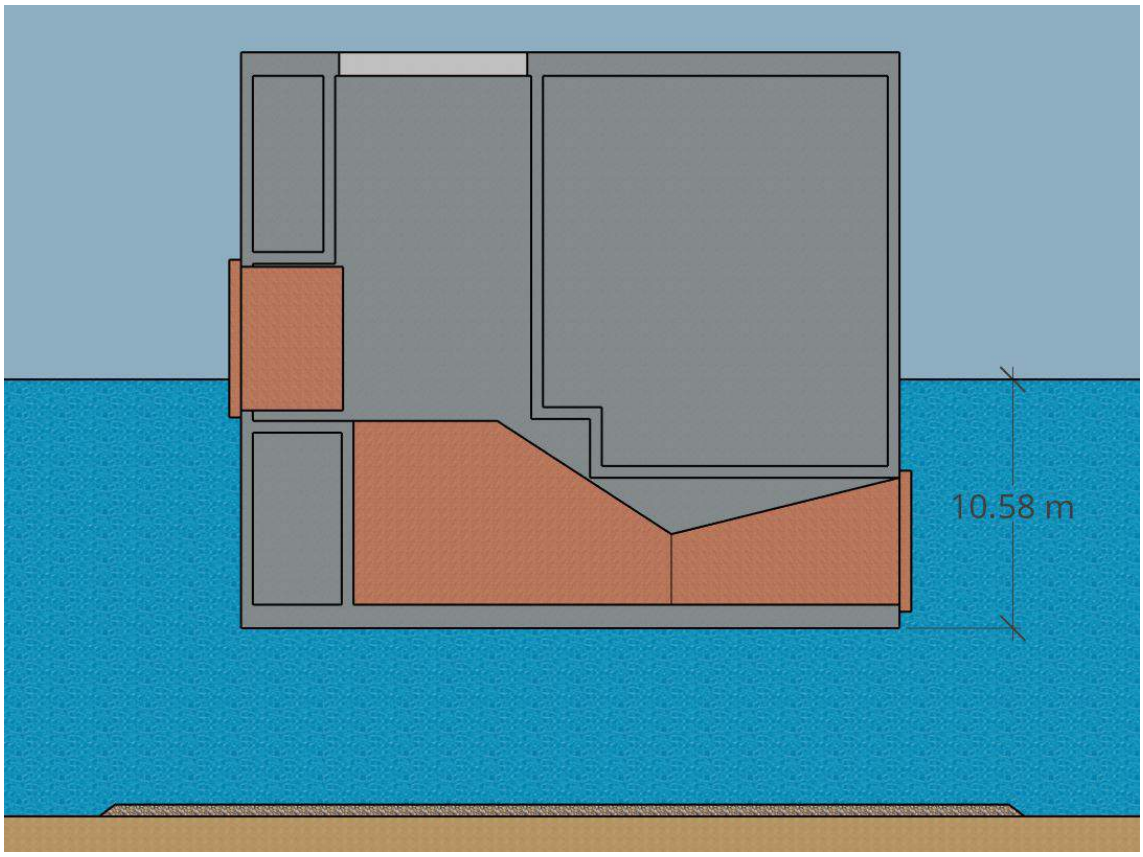

Figure L.9: Construction phase 2 of concept ‘Integration’, lakeside.

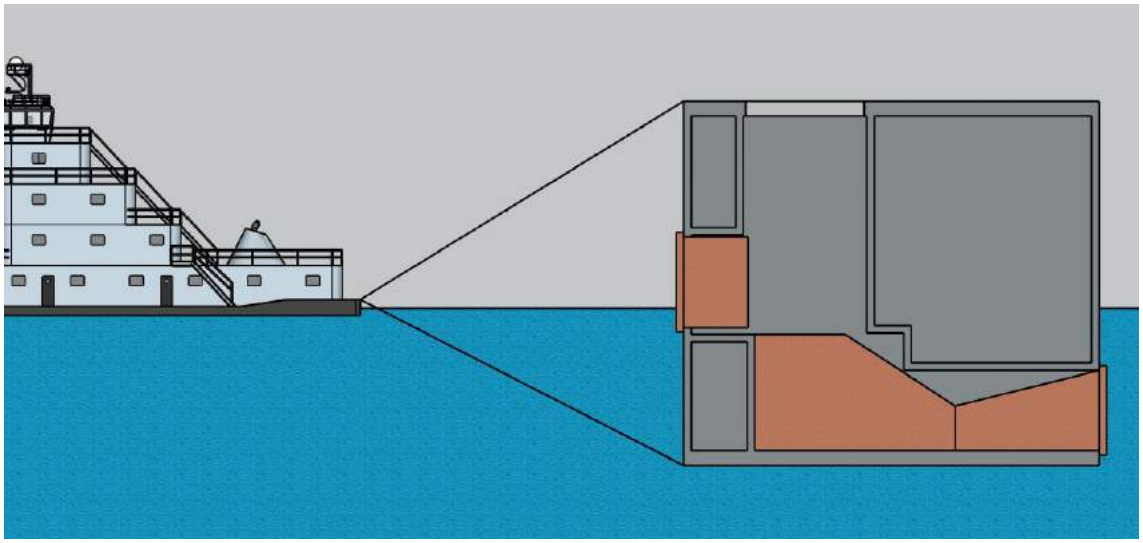

Figure L.10: Construction phase 3 of concept ‘Integration’, lakeside.

The floating caisson has a draught of 10,58 m, with which it is transported to the final location.

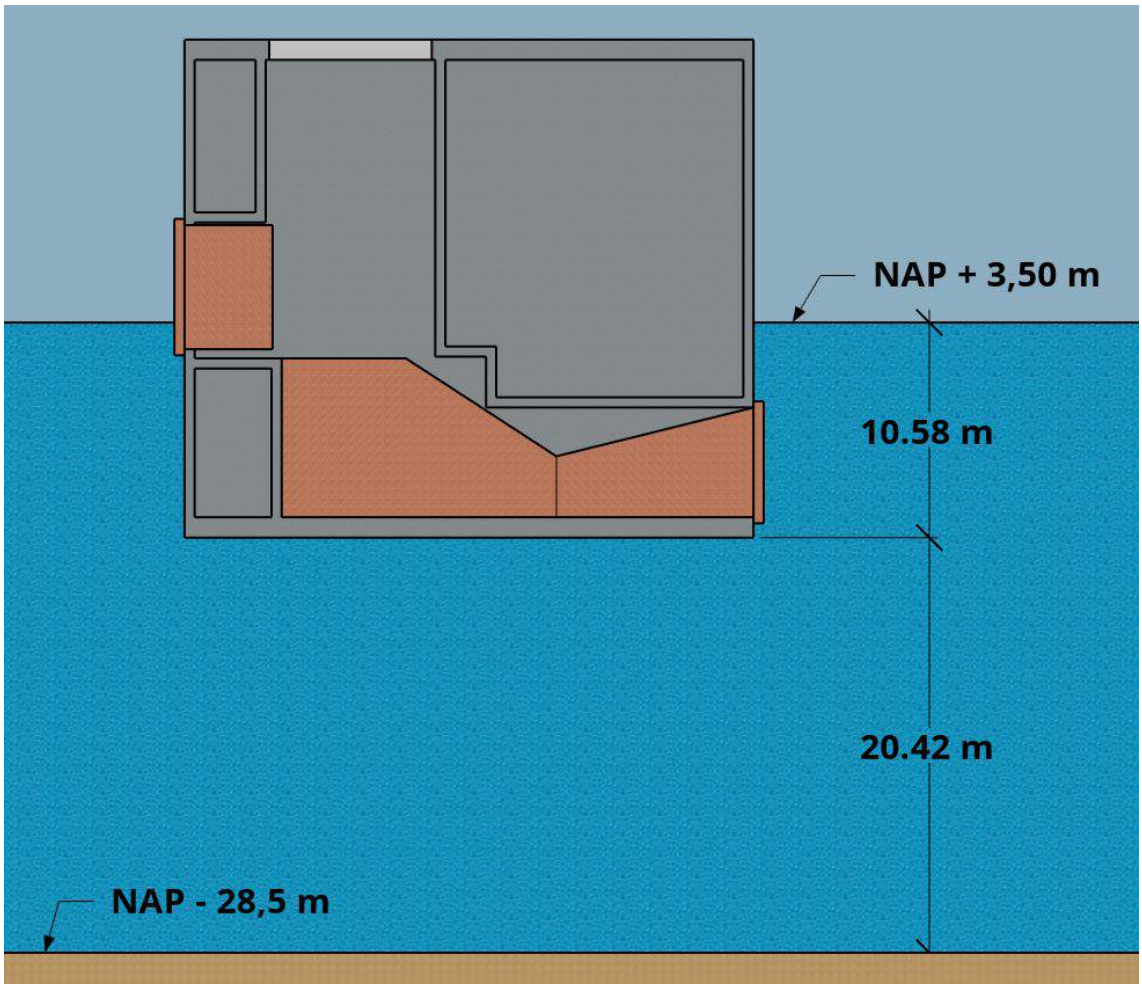

Figure L.11: Construction phase 4 of concept 'Integration', lakeside.

At the final location, the caisson has to be submerged a maximum of 20,42 m. The 0,5 m high sill has it's top level at NAP - 28,5 m, while the soil is dredged to a depth of NAP - 29 m. This means that the caisson will be, maximum, 6,50 m below the water level. The water pressure on the bottom side will, in this case, be 24,5 m x 10,06 kN/m^3 x 28 m = 6 901 kN/m. The weight of the filled caisson is 7 594 kN/m, so the caisson will sink to the bottom without extra measures required.

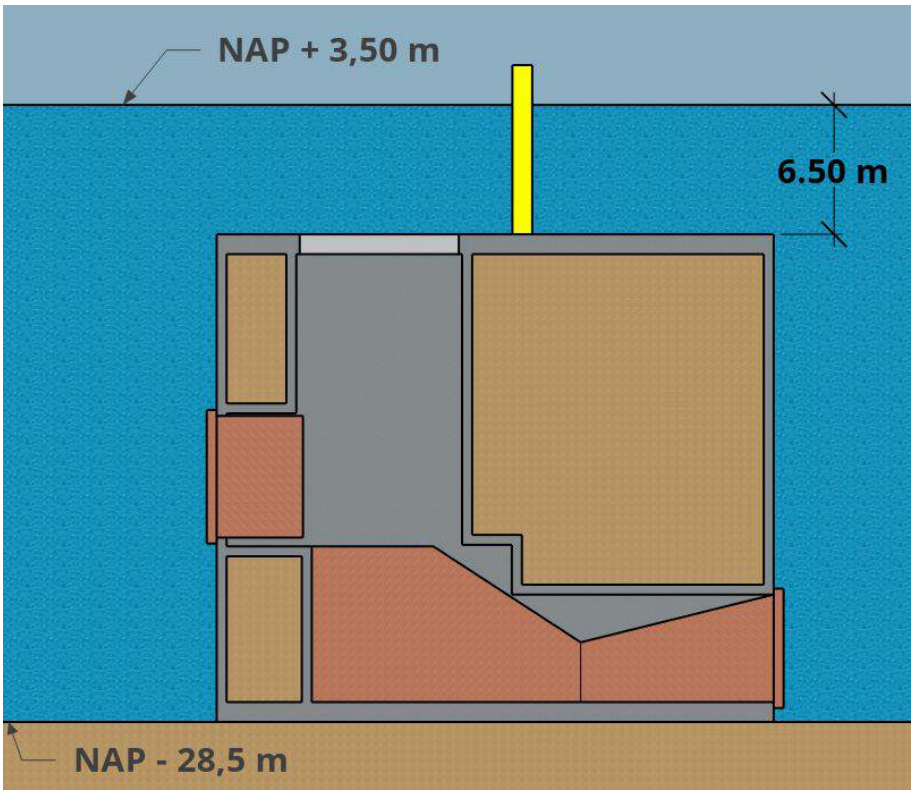

Figure L.12: Construction phase 5 of concept 'Integration', lakeside.

While fully submerged, a sand or gravel mixture is applied on top for navigational purposed. It is not required for ballast material.

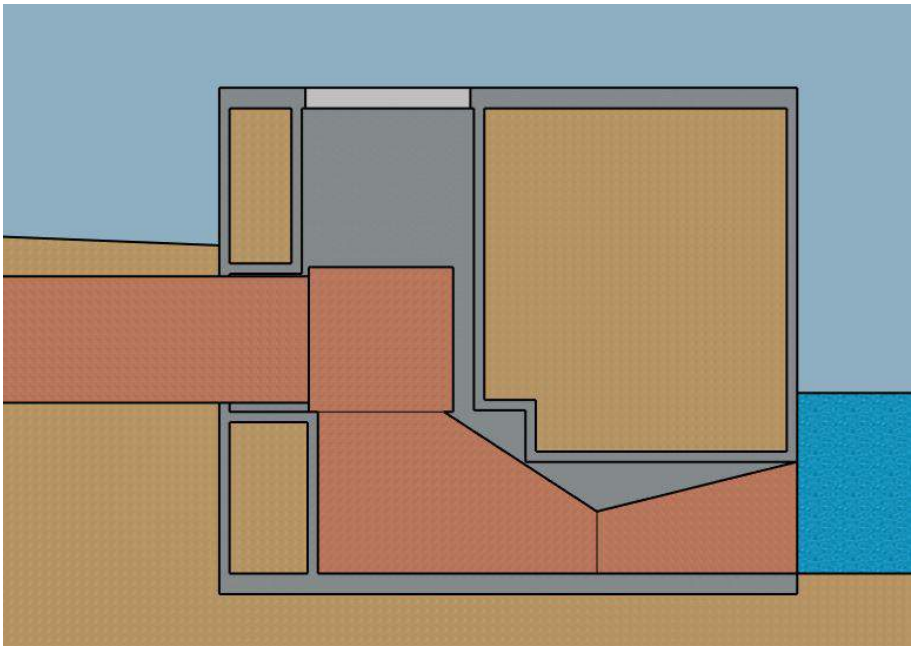

Figure L.13: Construction phase 6 of concept 'Integration', lakeside.

After being fully submerged, the pump-turbine pipe in between the caissons can be attached and the dyke structure can be completed.

L.3 Dredging Works

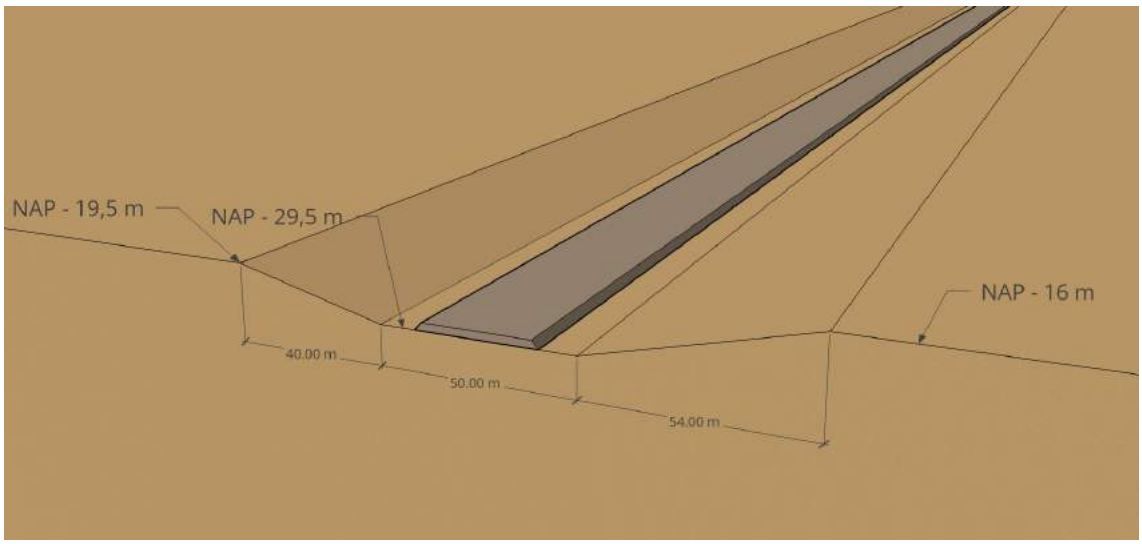

Figure L.14: Dredging works for concept 'Integration'.

Figure L.14 show the required dredging works. The sill showed is for the lake side caisson. The sea side caisson has to be constructed (out of sight) on the left hand side of the figure. The slope of the trench can be sloped up with 1V:4H until it meets the level of the pipe and then slopes gradually up along with the pipe. A total of 8,24 mln m^3 of sand should be dredged.

APPENDIX M

STABILITY OF CONCEPT 'INTEGRATION'

For the 'Integration' concept, showed again in Figure M.1, the stability is worked out in more detail in this appendix.

For this concept, please note that the design for the dyke body is left out of the scope of this master's thesis. A rough dyke design from Delta21 reports is taken as starting point for the design of this concept. Those starting points can be found in Figure 2.2.

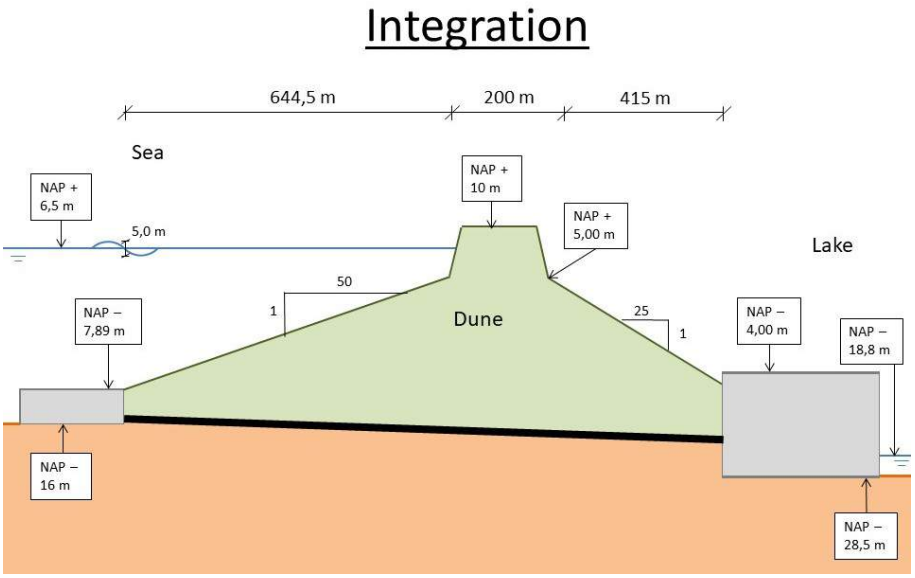

Figure M.1: Sketch of concept 'Integration'.

First the failure mechanisms for the seaside caisson are treated, then the failure mechanisms for the lakeside caisson are treated.

M.1 Failure Mechanisms for the Seaside Caisson

The failure mechanisms of the seaside caisson that require additional information to the main report are rotational stability and bearing capacity. First, the internal forces of the seaside caisson are presented, since these are equal for all failure mechanisms.

M.1.1 Internal forces

The internal forces follow from the cross section shown in Figure M.2 and the plan view shown in Figure M.3. As a starting point, the width is set to 21 m, the height is 8,11 m and the length (along the division between sea and dyke) of one single caisson room is 14,11 m (without partition wall). The thickness of the floor and the roof is set to 1 m and all the thickness of all other walls are assumed as 0,5 m.

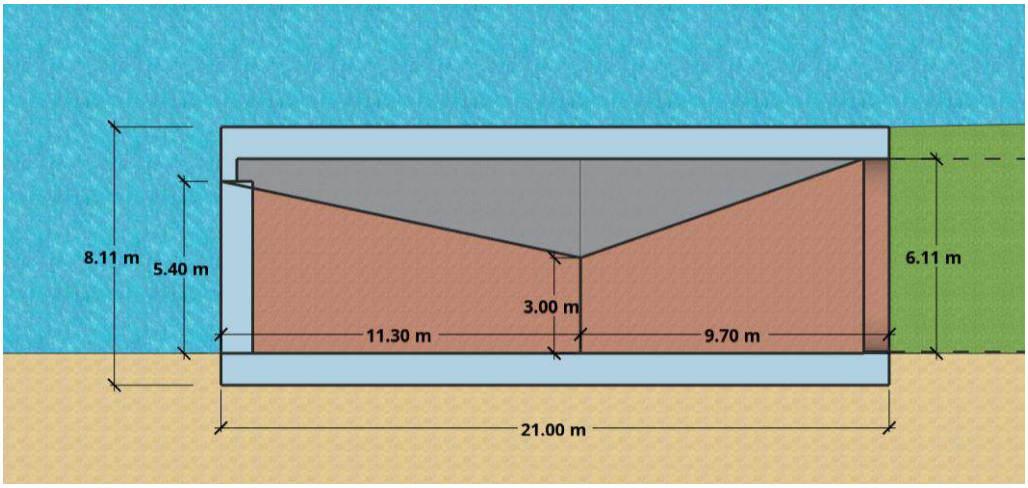

Figure M.2: Cross section of the seaside caisson of concept 'Integration'.

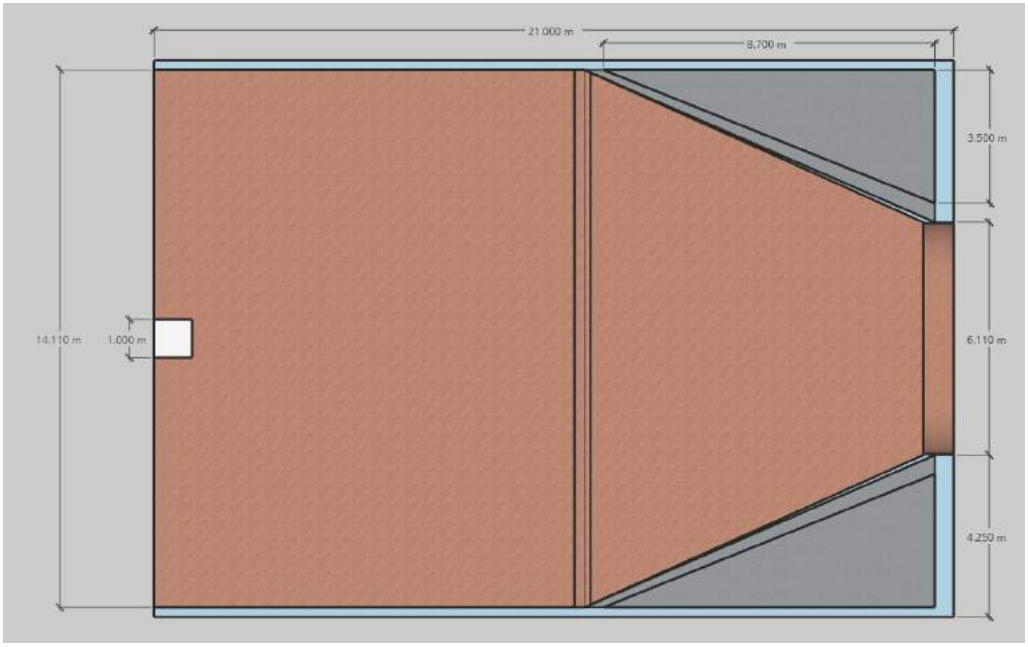

Figure M.3: Plan view of the seaside caisson of concept 'Integration'.

As can be seen in Figure M.3 near the pipe on the right side (the dyke side) there are two ballast chambers, with a combined volume of: $2 \cdot 12 \cdot 8,7 \cdot 3,5 \cdot 6,11 = 186,05$ m^3. Over the width of 14,11 m, this is 13,19 m^2. Furthermore the forces and their arms are summarized in Table M.1.

Force	Value	Unit	|	Arm	Value	Unit
$F_{b;1;k}$	250,6	kN/m	|	$a_{b;1}$	17,10	m
$F_{b;2;k}$	570,0	kN/m	|	$a_{b;2}$	10,50	m
$F_{outlet;k}$	701,6	kN/m	|	a_{oulet}	10,50	m
$F_{wall-dyke;k}$	56,4	kN/m	|	$a_{wall-dyke}$	20,75	m
$F_{floorroof;k}$	1 030,3	kN/m	|	$a_{floorroof}$	10,50	m
$F_{middle-floor;k}$	245,3	kN/m	|	$a_{middle-floor}$	10,50	m
$F_{part-wall;k}$	148,2	kN/m	|	$a_{part-wall}$	10,50	m
$F_{ballast-wall;k}$	103,0	kN/m	|	$a_{ballast-wall}$	16,15	m

Table M.1: Summary of the acting internal forces on the seaside caisson of concept 'Integration'.

M.1.2 Rotational stability

Loading

The loading on the seaside caisson is showed in Figure M.4.

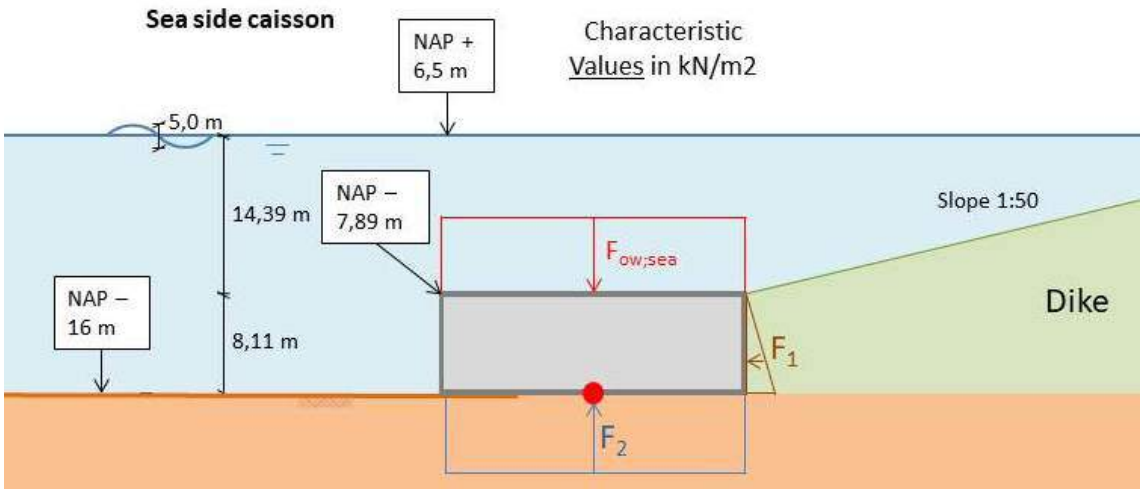

Figure M.4: Loading on seaside caisson of concept 'Integration'.

For the seaside caisson the neutral soil pressure parameter $K_{\gamma;0;d} = 0,578$. The soil pressure on the dyke side $s'_{zz} = 0,578 * 19 - 10,06 * 10,11 = 52,2$ kN/m^2, the water pressure on top of the caisson is $p_{w;top} = 10,06 * 12,39 = 124,6$ kN/m^2 and on the bottom side of the caisson $p_{w;bottom} = 10,06 * 23,5 = 236,4$ kN/m^2.

To determine the characteristic value of the force the area of the acting pressure should be taken. Taking a width of 21 m as starting point, the forces are summarised in Table M.2, including the corresponding arm to the foot of the structure on the sea side.

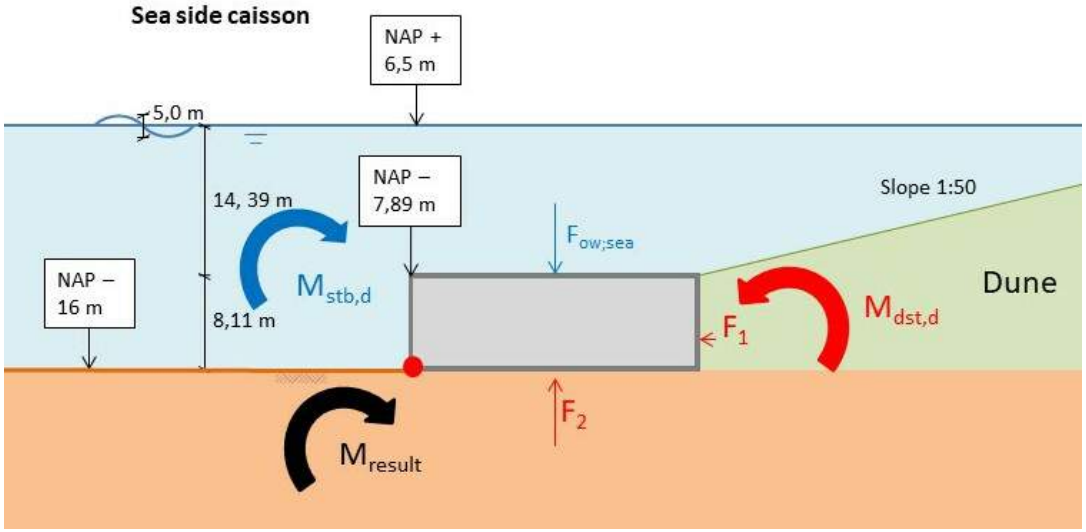

Figure M.5: Rotational stability for the seaside caisson.

Force	Value	Unit	|	Arm	Value	Unit
$F_{u;p;s;k}$	1 712,6	kN/m	|	$a_{u;p;s}$	10,5	m
$F_{s;d;k}$	37,0	kN/m	|	$a_{s;d}$	2,70	m
$F_{s;s;k}$	13,8	kN/m	|	$a_{s;s}$	0,33	m

Table M.2: Summary of the acting external forces on concept 'Integration'.

The failure mechanism rotational stability for the seaside caisson is indicated in Figure M.5.

Rotational stability check

Destabilising moments

The design overturning moment from the dyke equals:
$M_{dyke,Q} = 1,0 * 150,0 * 2,70$ = 405 kNm/m.

And from the uplifting force under the structure:
$M_{uplift,Q} = 1,0 * 1\ 712,6 * 10,5$ = 17 982 kNm/m.
Consequently, the total destabilising moment is: $M_{dst,d} = M_{dyke,Q} + M_{uplift,Q}$ = 18 387 kNm/m.

Stabilising moments

The sum of the stabilising moment coming from the pump-turbine system:
$M_{pumpturbine,G} = 0,9 * 701,6 * 10,5$ = 6 630 kNm/m.

Lastly, the total moment coming from all concrete works equals:
$M_{concrete,G} = 0,9 * \left(\Sigma F_{walls\ and\ floors} * a_{walls\ and\ floors} + \Sigma F_{ballast} * a_{ballast}\right)$ = 16 937 kNm/m.
The total stabilising moment $M_{stb,d} = M_{pumpturbine,G} + M_{concrete,G}$ = 23 567 kNm/m.

Unity check

The stabilising moment is bigger than the destabilising moment, when all chambers are filled completely with a sand ballast. The unity check gives: $uc = \frac{M_{dst,d}}{M_{stb,d}} = \frac{18\,387}{23\,567} = 0{,}78$.

Eccentricity

The line of action of resultant force is a distance from the toe of the structure: $x = \frac{M_{stb,d} - M_{dst,d}}{\Sigma V_d} = \frac{23\,567 - 18\,387}{303} = 17{,}10$ m. Which is $e_d = |W2 - x| = |212 - 17,10| = 6,60$ m from the centre line of the base.

M.1.3 Bearing capacity

This failure mechanism is visually presented in Figure M.6

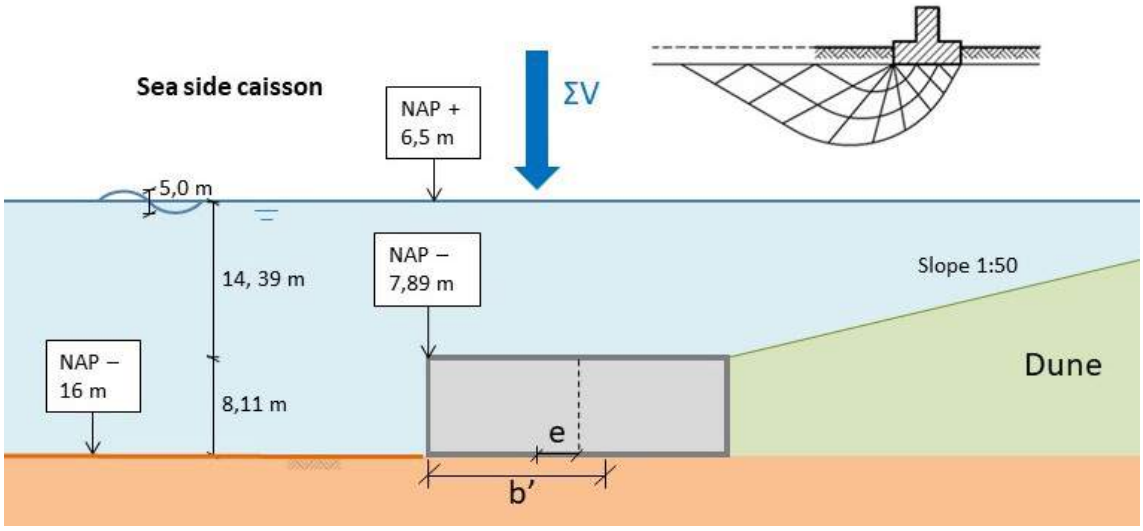

Figure M.6: Bearing capacity of the seaside caisson.

The previously described rule, from NEN-EN 1997-1 Eurocode 7, for the bearing capacity of the subsoil is:

$$\sigma'_{max;d} = \sigma'_{v;z;d} \cdot N_q \cdot s_q \cdot b_q \cdot i_q + 0,5 \cdot \gamma'_{average} \cdot b' \cdot N_{\gamma'} \cdot s_{\gamma'} \cdot b_\gamma \cdot i_{\gamma'} \qquad \text{(M.1)}$$

$N_q = \exp\left(\pi \cdot \tan \phi'_{average;d}\right) \cdot \tan^2\left(45° + 0,5 \cdot \phi'_{average;d}\right) = 19,0$
$N_{\gamma'} = 2 \cdot (N_q - 1) \cdot \tan\left(\phi'_{average;d}\right) = 21,0$

Assuming 3 pump-turbines per caisson as starting point, gives a length of 3x(14,11+0,5)+0,5 = 44,33 m.

$s_{\gamma'} = 1 - 0,3 \cdot \frac{b'}{l'} = 1 - 0,3 * \frac{7,8}{44,33} = 0,95$,
$b_\gamma = 1,0$.
The angle between the horizontal load and the longest side of the effective area is 90°:
$i_{\gamma'} = \left(1 - \frac{H_d}{V_d}\right)^{m+1} = \left(1 - \frac{143}{303}\right)^{2,9} = 0{,}16$,
With: $m = m_B = [2 + (B'L')]\ /\ [1 + (B'L')] = 1,9$.

That gives as a result:
$\sigma'_{max;d} = 0,5 \cdot \gamma'_{average} \cdot b' \cdot N_{\gamma'} \cdot s_{\gamma'} \cdot b_{\gamma} \cdot i_{\gamma'} = 0,5 * 20 - 10,06 * 7,8 * 21,0 * 0,95 * 1,0 * 0,16$ = 124 kN/m^2.

The acting soil pressure can be calculated according to:

$$q_d = \frac{\Sigma V}{b'} \tag{M.2}$$

The maximum acting stress under the caisson then becomes $q_d = \frac{303}{7,8}$ = 39 kN/m^2.

The unity check for maximum occurring stress is $uc = \frac{39}{124}$ = 0,31.

M.1.4 Floating stability

For the length $\overline{KB}$, the draught, d, is required. The draught of the seaside caisson is calculated by equalling the empty weight (while floating) to the weight of displaced water. So: $d = \frac{\text{Weight}}{W \cdot L \cdot \rho_w} = \frac{228\ 264 \text{ kN}}{21 \text{ m} * 4 * 44,33 \text{ m} * 10,06 \text{ kN/m}^3} = 6,09$ m. And $\overline{KB} = 0,5 \cdot d = 3,0$ m.

Where $I_{yy} = (1 / 12) \cdot L \cdot$ W^3 = 136 847 m^4 and $V_{uw} = W \cdot L \cdot d$ = 22 677 m^3, the length $\overline{BM} = 6,0$ m.

Lastly;

$$\overline{KG} = \frac{\Sigma V_i \cdot e_i \cdot \gamma_i}{\Sigma V_i \cdot \gamma_i} = \frac{\Sigma V_i \cdot e_i}{\Sigma V_i} \tag{M.3}$$

In which $\overline{KG}$ = 4,1 m.
This leads to a h_m of 4,9 m, which is stable.

M.2 Failure Mechanisms for the Lakeside Caisson

M.2.1 Internal forces

The internal forces follow from the cross section shown in Figure M.7. As a starting point, the width is set to 28 m, the height is 24,5 m, the dykes start 7,6 m below the top of the caisson (that leaves a cover above the pipe of 1,5 m) and the length (along the division between dyke and lake) of one single caisson room is 14,11 m (without partition wall). The thickness of the floor and the roof is set to 1 m and all the thickness of all other walls are assumed as 0,5 m.

A 0,5 m high sill is applied, with the same properties as the one described at concept 'Unity'.

The forces and their arms are summarized in Table M.3.

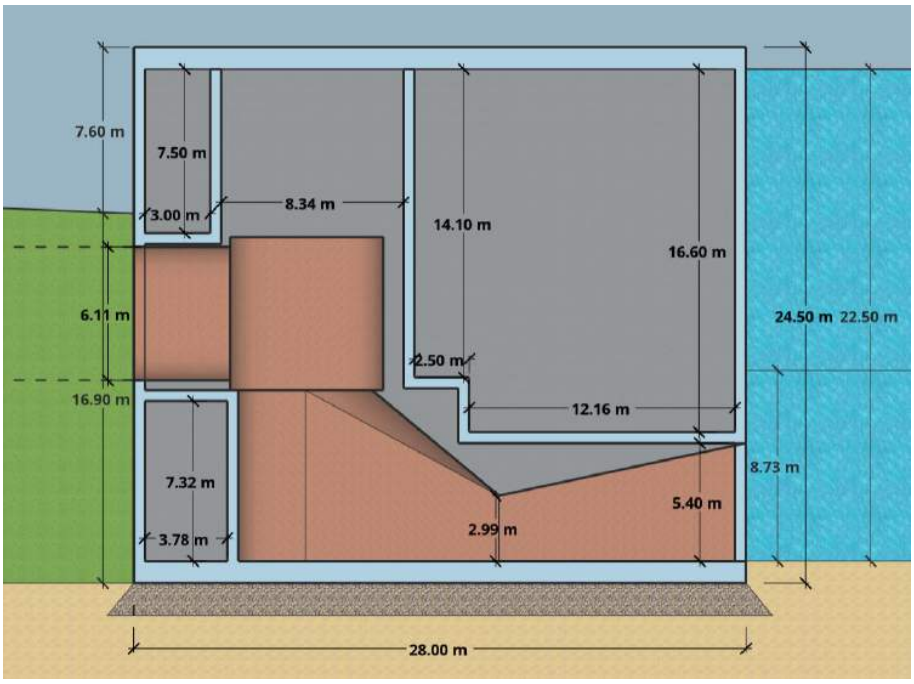

Figure M.7: Cross section of the lakeside caisson of concept 'Integration'.

Force	Value	Unit	|	Arm	Value	Unit
$F_{b;1;k}$	427,5	kN/m	|	$a_{b;1}$	26,00	m
$F_{b;2;k}$	525,7	kN/m	|	$a_{b;2}$	25,61	m
$F_{b;3-1;k}$	669,8	kN/m	|	$a_{b;3-1}$	13,91	m
$F_{b;3-2;k}$	570,0	kN/m	|	$a_{b;3-2}$	10,50	m
$F_{inlet;k}$	3 835,3	kN/m	|	a_{inlet}	6,58	m
$F_{t;k}$	347,6	kN/m	|	a_t	16,23	m
$F_{pipe;k}$	73,1	kN/m	|	a_{pipe}	26,25	m
$F_{wall-dyke;k}$	201,1	kN/m	|	$a_{wall-dyke}$	27,75	m
$F_{wall-lake;k}$	209,7	kN/m	|	$a_{wall-lake}$	0,25	m
$F_{floorroof;k}$	1 373,7	kN/m	|	$a_{floorroof}$	14,00	m
$F_{part-wall;k}$	528,1	kN/m	|	$a_{part-wall}$	14,00	m
$F_{w1;k}$	92,0	kN/m	|	$a_{w;1}$	24,25	m
$F_{w2;k}$	42,9	kN/m	|	$a_{w;2}$	26,00	m
$F_{w3;k}$	52,5	kN/m	|	$a_{w;3}$	25,61	m
$F_{w4;k}$	89,8	kN/m	|	$a_{w;4}$	23,47	m
$F_{w5;k}$	172,9	kN/m	|	$a_{w;5}$	15,41	m
$F_{w6;k}$	36,8	kN/m	|	$a_{w;6}$	13,91	m
$F_{w7;k}$	30,7	kN/m	|	$a_{w;7}$	12,91	m
$F_{w8;k}$	149,1	kN/m	|	$a_{w;8}$	6,58	m

Table M.3: Summary of the acting internal forces on the lakeside caisson of concept 'Integration'.

M.2.2 Rotational stability

The forces resulting from the water and soil pressures are indicated in Figure M.8. To determine the characteristic value of the force the area of the acting pressure should be

taken. Taking a width of 28 m as starting point, the forces are summarised in Table M.4, including the corresponding arm to the foot of the structure on the lake side.

The dyke is assumed as fully saturated with water, which is very unlikely, but gives the most severe loading combination.

Force	Value	Unit	|	Arm	Value	Unit
$F_{w;dyke;k}$	1 436,5	kN/m	|	$a_{w;dyke}$	5,63	m
$F_{w;l-min;k}$	467,3	kN/m	|	$a_{w;l-min}$	3,24	m
$F_{w;l-max;k}$	2 777,7	kN/m	|	$a_{w;l-max}$	7,83	m
$F_{s;dyke;k}$	752,1	kN/m	|	$a_{s;dyke}$	5,63	m
$F_{u;p;k}$	1 370,6	kN/m	|	$a_{u;p}$	9,33	m
$F_{u;v1;k}$	1 370,6	kN/m	|	$a_{u;v1}$	18,67	m
$F_{u;v2;k}$	1 009,4	kN/m	|	$a_{u;v2}$	18,67	m
$F_{s;s;k}$	6,9	kN/m	|	$a_{s;s}$	0,33	m

Table M.4: Summary of the acting external forces on the lakeside caisson of concept 'Integration'.

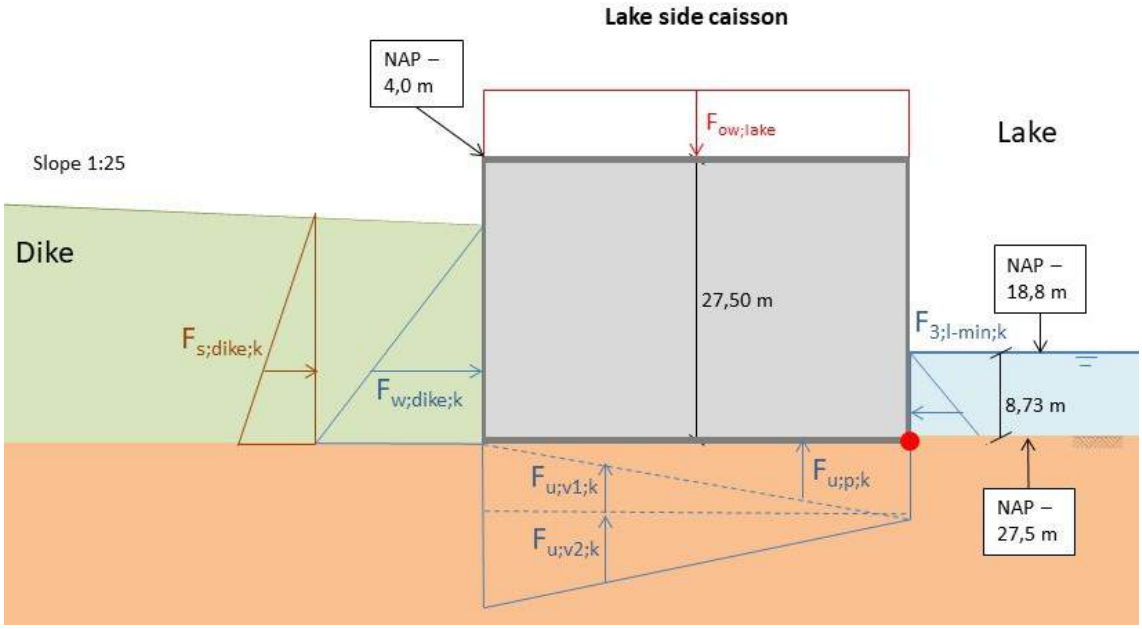

Figure M.8: Governing loading situation on the lakeside caisson.

In the determination of the neutral soil parameter $k_{\gamma;0;d}$ the slope of the dyke behind the caisson has to be included. Doing that results in $K_{\gamma;0;d} = \left(1 - \sin\left(\phi_d^{'}\right)\right) \cdot (1 + \sin(\beta))$ = 0,589 and $\sigma_{zz}^{'} = K_{\gamma;0;d} \cdot (\gamma_s - \gamma_w) \cdot h_{dyke} = 0,589 * (19 - 10,06) * 17,50 = 92,2$ kN/m^2.

The water pressure is easily calculated with $p_{w;dyke} = \gamma_w \cdot h_{dyke} = 10,06 * 17,50 = 176,1$ kN/m^2 and $p_{w;lake} = \gamma_w \cdot hesl = 10,06 * (8,73 + 1) = 97,9$ kN/m^2.

Only the force $F_{u;p;k}$ can be multiplied with a safety factor of 1,0, because that part is permanent, so no water inside the dyke and low water on the energy storage lake. The remaining upward water pressures should be multiplied with a safety factor of 1,25.

Destabilising moments

The design overturning moment from the soil of the dyke equals:
$M_{dyke;soil,Q} = 1,0 * 752,1 * 5,63$ = 4 153 kNm/m.

The design overturning moment from the water in the dyke equals:
$M_{dyke;water,Q} = 1,25 * 1\,540,9 * 5,83$ = 11 229 kNm/m.

And from the uplifting force under the structure:
$M_{uplift,Q}$ = $1,0 * 1\,370,6 * 9,33 + 1,25 * (1\,370,6 * 18,67 + 1\,094,8 * 18,67)$ = 70 324 kNm/m.
Consequently, the total destabilising moment is: $M_{dst,d} = M_{dyke,Q} + M_{uplift,Q}$ = 85 706 kNm/m.

Stabilising moments

The sum of the stabilising moment coming from the pump-turbine system:
$M_{pumpturbine,G} = 0,9 * (701,6 * 10,5 + 73,1 * 26,25 + 347,6 * 16,23)$ = 13 435 kNm/m.

The stabilising moment from the lake equals:
$M_{lake,Q} = 1,25 * 476,3 * 3,24 + 1,0 * 6,9 * 0,33$ = 1 931 kNm/m.

Lastly, the total moment coming from all concrete works equals:
$M_{concrete,G} = 0,9 * \left(\Sigma F_{walls\ and\ floors} * a_{walls\ and\ floors} + \Sigma F_{ballast} * a_{ballast}\right)$ = 92 468 kNm/m.
The total stabilising moment $M_{stb,d} = M_{pumpturbine,G} + M_{lake,Q} + M_{concrete,G}$ = 107 834 kNm/m.

Unity check

The stabilising moment is bigger than the destabilising moment, when all chambers are filled completely with a sand ballast. The unity check gives: $uc = \frac{M_{dst,d}}{M_{stb,d}} = \frac{85\,706}{107\,834}$ = 0,79.

Eccentricity

The line of action of resultant force is a distance from the toe of the structure: $x = \frac{M_{stb,d} - M_{dst,d}}{\Sigma V_d} = \frac{107\,834 - 85\,706}{3\,454}$ = 6,41 m. Which is $e_d = |W2 - x| = |282 - 6,41|$ = 4,09 m from the centre line of the base.

M.2.3 Bearing capacity

The bearing capacity of the lakeside caisson is presented in Figure M.9.

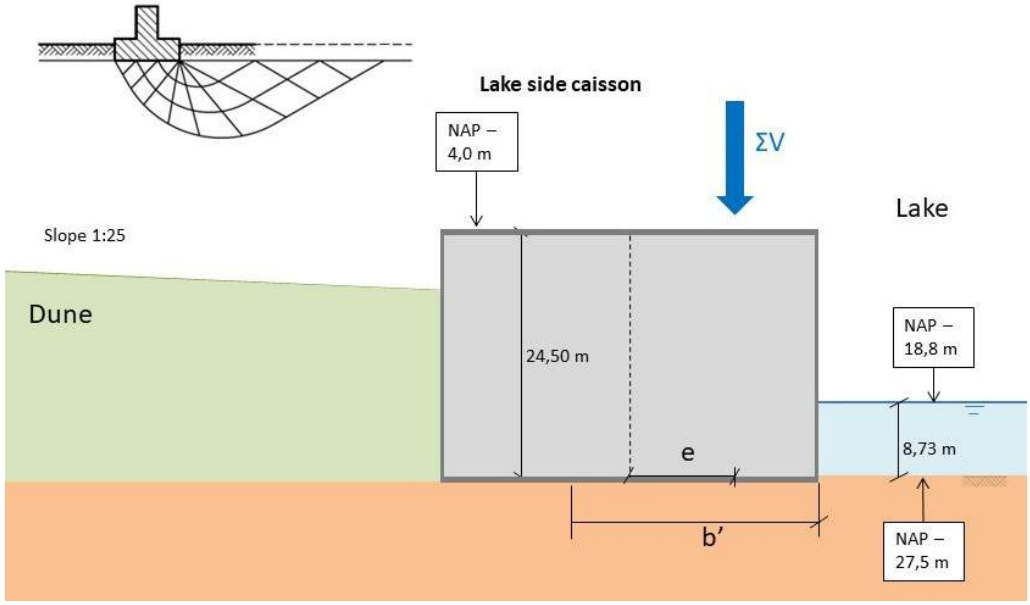

Figure M.9: Caption

The interfaces will be checked using the previously used rule from NEN-EN 1997-1, Eurocode 7:

$$\sigma'_{max;d} = \sigma'_{v;z;d} \cdot N_q \cdot s_q \cdot b_q \cdot i_q + 0,5 \cdot \gamma'_{average} \cdot b' \cdot N_{\gamma'} \cdot s_{\gamma'} \cdot b_\gamma \cdot i_{\gamma'} \qquad \text{(M.4)}$$

$N_q = \exp\left(\pi \cdot \tan \phi'_{average;d}\right) \cdot \tan^2\left(45° + 0,5 \cdot \phi'_{average;d}\right) = 19,0$
$N_{\gamma'} = 2 \cdot (N_q - 1) \cdot \tan\left(\phi'_{average;d}\right) = 21,0$

Assuming 3 pump-turbines per caisson as starting point, gives a length of 3x(14,11+0,5)+0,5 = 44,33 m.
$s_q = 1 + \frac{b'}{l'} \cdot \sin\left(\phi'_{gem;d}\right) = 1 + \frac{19,8}{44,33} \cdot \sin(25,7)$ = 1,19,
$s_{\gamma'} = 1 - 0,3 \cdot \frac{b'}{l'} = 1 - 0,3 * \frac{19,8}{44,33} = 0,87$
$b_\gamma = 1,0$
The angle between the horizontal load and the longest side of the effective area is 90°:
$i_q = \left(1 - \frac{0,7 \cdot H_d}{V_d}\right)^{m+1} = \left(1 - \frac{1\,425}{3\,454}\right)^{2,9}$ = 0,21,
$i_{\gamma'} = \left(1 - \frac{H_d}{V_d}\right)^{m+1} = \left(1 - \frac{2\,036}{3\,454}\right)^{2,9}$ = 0,08.
With: $m = m_B = [2 + (B'L')] \ / \ [1 + (B'L')] = 1,9$

That gives as a result:
$\sigma'_{max;d} = \sigma'_{v;z;d} \cdot N_q \cdot s_q \cdot b_q \cdot i_q + 0,5 \cdot \gamma'_{average} \cdot b' \cdot N_{\gamma'} \cdot s_{\gamma'} \cdot b_\gamma \cdot i_{\gamma'} = 8,94 * 19,0 * 1,19 * 1,0 * 0,21 + 0,5 * (20,3 - 10,06) * 19,8 * 21,0 * 0,87 * 1,0 * 0,08$ = 191 kN/m^2.

The acting soil pressure can be calculated according to:

$$q_d = \frac{\Sigma V}{b'} \tag{M.5}$$

The maximum acting stress under the caisson then becomes $q_d = \frac{3\,454}{19{,}8}$ = 174 kN/m^2.
The unity check for maximum occurring stress is $uc = \frac{174}{191}$ = 0,91.

M.2.4 Floating stability

For the length $\overline{KB}$, the draught, d, is required. The draught of the lakeside caisson is calculated by equalling the empty weight (while floating) to the weight of displaced water. So: $d = \frac{Weight}{W \cdot L \cdot \rho_w} = \frac{528\ 289 \text{ kN}}{28 \text{ m} * 4 * 44{,}33 \text{ m} * 10{,}06 \text{ kN/m}^3} = 10,58$ m. And $\overline{KB} = 0,5 \cdot d = 5,3$ m.

Where $I_{yy} = (1 / 12) \cdot L \cdot W^3$ = 324 377 m^4 and $V_{uw} = W \cdot L \cdot d$ = 26 314 m^3, the length $\overline{BM} = 12,3$ m.

Lastly;

$$\overline{KG} = \frac{\Sigma V_i \cdot e_i \cdot \gamma_i}{\Sigma V_i \cdot \gamma_i} = \frac{\Sigma V_i \cdot e_i}{\Sigma V_i} \tag{M.6}$$

In which $\overline{KG}$ = 12,1 m.
This leads to a h_m of 5,5 m, which is stable.

APPENDIX N

COSTS OF THE ALTERNATIVES

In this appendix, the costs sheets of the two alternatives are presented.

N.1 Alternative 'Unity'

The costs for the concrete works, ballast material, dredging works, sand refill and pump-turbines of alternative 'Unity' are shown in Figure N.1.

Description	Quantity	unit	Unit price	Deterministic price	
Building costs					
Construction caissons				€ **386.647.754,66**	**28,6%**
Porours bottom layer	129.150,00	m2	€ 25,00	€ 3.228.750,00	
Floor 46 x (53x44,33x1)	108.076,54	m3	€ 275,00	€ 29.721.048,50	
Outer walls 46 x (2*44,33+2*53)x38,5x0,5	172.371,43	m3	€ 820,00	€ 141.344.572,60	
Roof 46 x 53x44,33x1	108.076,54	m3	€ 550,00	€ 59.442.097,00	
Inner walls 46x3 x (10+18,39+30,6)x14,11x0,5 + 2 x 36,5x52x0,5	144.740,07	m3	€ 550,00	€ 79.607.040,76	
Inner floors 46 x (30,5+30,5+11,5)x14,11x0,5x3	70.585,28	m3	€ 675,00	€ 47.645.060,63	
Columns 46*6*1*1*5,4	1.490,40	m3	€ 1.600,00	€ 2.384.640,00	
Ballast material 46x(18,39*30,5+30,6*11,5+20*10+11*7,5)*14,11*3	2.327.454,52	m3	€ 10,00	€ 23.274.545,18	
			€ -	€ -	
Dredging + sand refill				€ **49.431.250,00**	**4%**
Dredging works	5.727.500,00		€ 5,00	€ 28.637.500,00	
Sand refill	2.079.375,00		€ 10,00	€ 20.793.750,00	
			€ -	€ -	
Installations				€ **791.430.000,00**	**59%**
Pump turbines	138,00	pc	€ 5.735.000,00	€ 791.430.000,00	
			€ -	€ -	
Total direct costs named				€ **1.227.509.004,66**	
to be further specified	10%	van Dir. costs named		€ **122.750.900,47**	**9,1%**
Total direct costs				€ **1.350.259.905,13**	**100%**

Figure N.1: Cost sheet of alternative 'Unity'.

N.2 Alternative ‘Integration’

The same cost aspects as for alternative ‘Unity’, but then for both the seaside and lakeside caissons and including the pipe in between, is shown in Figure N.2 and Figure N.3.

Description		Quantity	unit	Unit price	Deterministic price	
Building costs						
Construction seaside caissons					€ 237.985.553,64	5,8%
	Porours bottom layer	129.150,00	m2	€ 25,00	€ 3.228.750,00	
	Floor 46 x (21x44,33x1)	42.822,78	m3	€ 275,00	€ 11.776.264,50	
	Outer walls 46 x (2x44.33+2x21)x8,11x0,5	24.372,01	m3	€ 820,00	€ 19.985.048,04	
	Roof 46 x 21x44,33x1	42.822,78	m3	€ 550,00	€ 23.552.529,00	
	Inner walls 46x (3 x 2x6,11x9,7x0,5 + 2x6,11x20x0,5)	13.800,05	m3	€ 550,00	€ 7.590.026,30	
	Inner floors 0		m3	€ 675,00	€ -	
	Columns 46*3*1*1*6,11	843,18	m3	€ 1.600,00	€ 1.349.088,00	
	Ballast material 46x(2x0,5x8,7x3,5)*6,11*3	25.674,83	m3	€ 10,00	€ 256.748,31	
Construction lakeside caissons						
	Porours bottom layer	129.150,00	m2	€ 25,00	€ 3.228.750,00	
	Floor 46 x (28x44,33x1)	57.097,04	m3	€ 275,00	€ 15.701.686,00	
	Outer walls 46 x (2x44,33+2x28)x24,5x0,5	81.515,91	m3	€ 820,00	€ 66.843.046,20	
	Roof 46 x 28x44,33x1	57.097,04	m3	€ 550,00	€ 31.403.372,00	
	Inner walls 46x (3 x (7,5+7,32+16,6)x14,11x0,5 + 2 x 22,5x27x0,5)	58.535,20	m3	€ 550,00	€ 32.194.358,79	
	Inner floors 46 x (3+3,78+14,66)x14,11x0,5x3	20.873,77	m3	€ 675,00	€ 14.089.794,48	
	Columns 46*3*1*1*5,4	745,20	m3	€ 1.600,00	€ 1.192.320,00	
	Ballast material 46x(7,5x3 + 7,32x3,78 + 14,1x2,5 + 16,6x12,16)x14,11x3	559.377,30	m3	€ 10,00	€ 5.593.773,03	

Figure N.2: Cost sheet of alternative ‘Integration’ 1/2.

Dredging + dune					€ 2.421.981.937,50	64%
	Sand refill + dune	79.567.500,00	m3	€ 10,00	€ 795.675.000,00	
	Pipe	138,00	pc	€ 11.442.000,00	€ 1.578.996.000,00	
	Dredging works	9.462.187,50	m3	€ 5,00	€ 47.310.937,50	
				€ -	€ -	
Installations					€ 791.430.000,00	21%
	Pump turbines	138,00	pc	€ 5.735.000,00	€ 791.430.000,00	
				€ -	€ -	
Total direct costs named					€ 3.451.397.491,14	
to be further specified		10%	van Dir. costs named		€ 345.139.749,11	9,1%
Total direct costs					€ 3.796.537.240,26	100%

Figure N.3: Cost sheet of alternative ‘Integration’ 2/2.

N.3 Background of the Unit Prices

The unit prices of the cost sheets are obtained from the budget department of Ballast Nedam Infra Projects. The unit price of, for example, a concrete floor exists out of formwork, reinforcement and concrete costs.

The only self added cost is that of the pump-turbine pipe in between the caissons. For this, two alternatives were compared, fiberglass and steel. Since a supplier of fiberglass stated that the limitation in diameter is 4,0 m due to transport reasons, only steel is considered.

A diameter of 6,11 m is very large and monopile-like structures should be constructed. Usually, a monopile has a wall thickness of 5 - 6 cm, in this case 6 cm will be considered. According to (Bjerkseter and Agotnes 2013) the price of a monopile is approximately €2 000/ton.

The distance between the two caisson is 1 259,5 m, leading to a total steel volume of $V_{steel} = 0,25 \cdot \pi \cdot 6,17^2 - 0,25 \cdot \pi \cdot 6,11^2 \cdot 1259,5$ = 728,8 m^3. The density of steel is 7 850 kg/m^3, which then gives a steel weight of 5 721 tons per pipe and a price of €11,442 mln.

APPENDIX O

STRENGTH VERIFICATION

In this chapter the internal floors and walls will be structurally checked whether they can resist all imposed loading. A 3D cross-section, to give insight in how the plates look like, is given in Figure O.1.

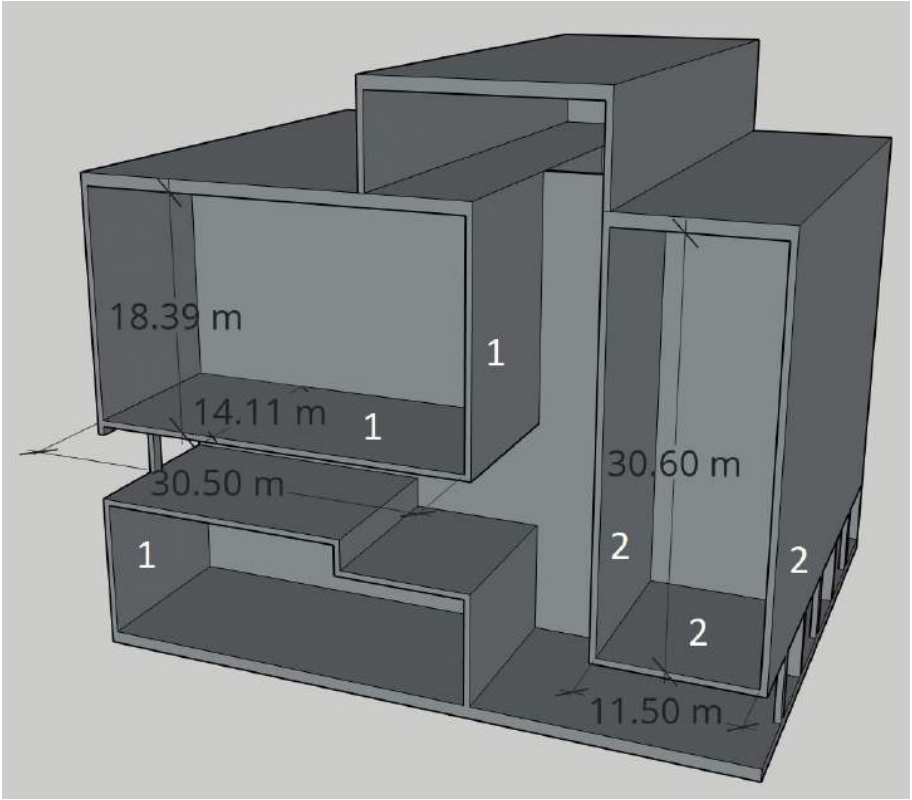

Figure O.1: Cross section in 3D of alternative 'Unity'.

Per plate in ULS, first, the governing loading is described, then the acting moments are calculated, the shear force is determined and finally, the required reinforcement and/or changes in plate thickness are determined. In SLS the occurring crack width is checked.

In the upper left ballast room in Figure O.1, the right wall is named 'Inner wall 1'. The bottom plate is called 'Inner floor 1'.

In the bottom (left) ballast room, the outer wall (on the left side) is named 'Outer wall 1'.

For the right ballast room, the (right) outer wall is named 'Outer wall 2', the (left) inner wall is named 'Inner wall 2' and the floor plate is named 'Inner floor 2'.

O.1 Inner Floor 1

The first plate to be checked is 'Inner floor 1', because a huge loading is present on this plate.

O.1.1 Loading on inner floor 1

The characteristic loading is shown in Figure O.2.

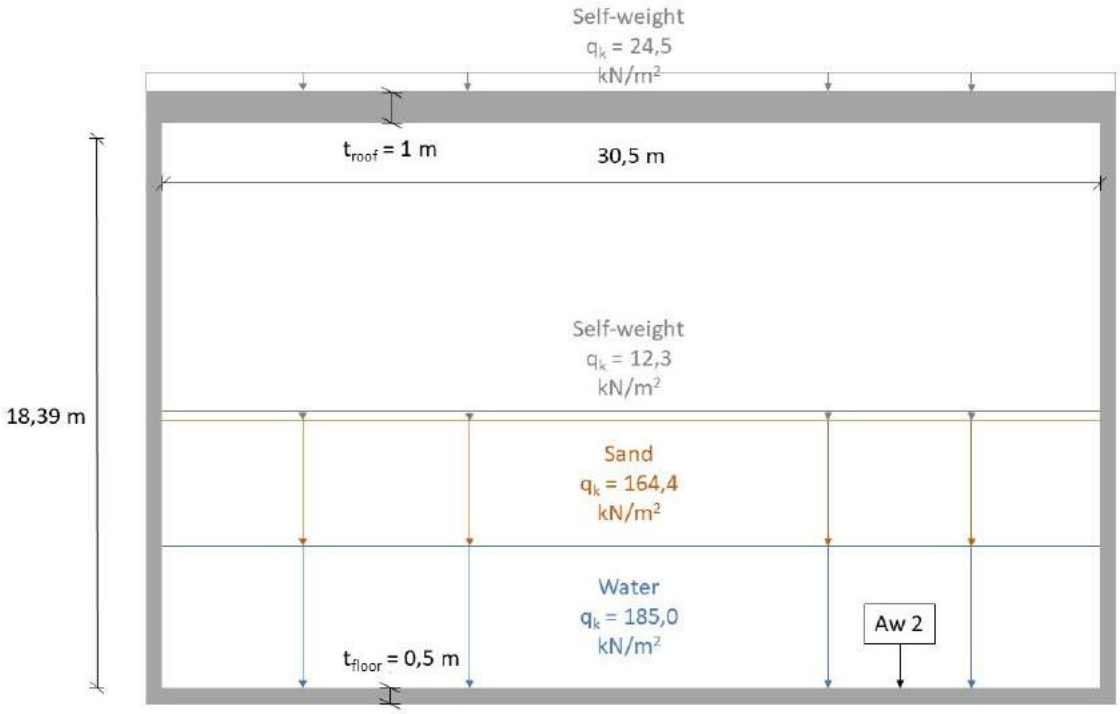

Figure O.2: Loading on inner floor 1.

For water the load is 18,39 x 10,06 = 185,0 kN/m^2. For sand the load is 18,39 x (19 - 10,06) x 0,566 = 164,4 kN/m^2.

The weight of reinforced concrete is assumed at 2 500 kg/m^3, converted 24,53 kN/m^3. This means the self-weight of the 0,5 m thick floor plate is 12,3 kN/m^2.

Since all loading is permanent, in ULS the design load equals $q_d = 1,35 \cdot q_{Gk}$.

O.1.2 ULS Bending moment distribution in inner floor 1

To calculate the bending moment distribution of inner floor 1, the support of the edges has to be determined. In reality, this will be somewhere between fully clamped and fully hinged. The old Dutch norm NEN6720 gives an indication for the bending moment distribution in plates for various line supports, see Figure O.3.

The design load on inner floor 1 equals $q_d = 1,35 * 185,0 + 164,4 + 12,3 = 488,3$ kN/m^2.

	l_y/l_x	1.0	1.2	1.4	1.6	1.8	2.0	2.5	3.0
I	$m_{vx} = 0.001\, p_d l_x^2$	41	54	67	79	87	97	110	117
	$m_{vy} = 0.001\, p_d l_x^2$	41	35	31	28	26	25	24	23
II	$m_{vx} = 0.001\, p_d l_x^2$	18	26	32	36	39	41	42	43
	$m_{vy} = 0.001\, p_d l_x^2$	18	16	12	10	10	10	10	10
	$m_{sx} = -0.001\, p_d l_x^2$	51	63	72	78	81	82	83	83
	$m_{sy} = -0.001\, p_d l_x^2$	51	54	55	54	54	53	51	49
	$a_x / l_x =$	0.18	0.19	0.19	0.19	0.19	0.19	0.19	0.19
	$a_y / l_y =$	0.18	0.16	0.15	0.13	0.11	0.10	0.07	0.06
III	$m_{vx} = 0.001\, p_d l_x^2$	25	36	45	53	58	62	67	69
	$m_{vy} = 0.001\, p_d l_x^2$	25	23	20	19	18	17	17	17
	$m_{sx} = -0.001\, p_d l_x^2$	68	84	97	106	113	117	122	124
	$m_{sy} = -0.001\, p_d l_x^2$	68	74	77	77	77	76	73	71
	$a_x / l_x =$	0.20	0.22	0.22	0.22	0.23	0.23	0.24	0.24
	$a_y / l_y =$	0.21	0.19	0.17	0.16	0.13	0.12	0.09	0.09
IV A	$m_{vx} = 0.001\, p_d l_x^2$	16	28	42	56	69	80	100	112
	$m_{vy} = 0.001\, p_d l_x^2$	29	32	32	30	27	24	20	18
	$m_{sy} = -0.001\, p_d l_x^2$	69	85	97	105	110	112	112	112
	$a_y / l_y =$	0.19	0.19	0.17	0.17	0.16	0.15	0.12	0.11
IV B	$m_{vx} = 0.001\, p_d l_x^2$	29	34	38	40	42	42	42	42
	$m_{vy} = 0.001\, p_d l_x^2$	16	14	13	13	13	13	13	13
	$m_{sx} = -0.001\, p_d l_x^2$	69	76	80	82	83	83	83	83
	$a_x / l_x =$	0.19	0.20	0.20	0.21	0.21	0.21	0.21	0.21

Figure O.3: NEN 6720 Table 18.

Plate types I, II, IV A and IV B will be checked, after which the maximum found bending moments will be assumed.

The ratio l_y / l_x for the inner floor 1 is 30,5 / 14,11 = 2,16. For a plate fully hinged against all line support (plate type I), the following bending moments are found:

$$m_{vx} = 0,10116 \cdot p_d \cdot l_x^2 = 0,10116 * 488,3 * 14,11^2 = 9\ 834 \text{ kNm/m}$$

$$m_{vy} = 0,02468 \cdot p_d \cdot l_x^2 = 2\ 399 \text{ kNm/m}$$

From basic engineering judgment one can conclude that the plate will never carry the loading in this way. Still, first the completely clamped situation is checked, to see how the moments will reduce due to this.

$$m_{vx} = 0,04132 \cdot p_d \cdot l_x^2 = 0,04132 * 488,3 * 14,11^2 = 4\ 017 \text{ kNm/m}$$

$$\begin{aligned} m_{vy} &= \quad 0,01 \cdot p_d \cdot l_x^2 = \quad 972 \text{ kNm/m} \\ m_{sx} &= -0,08232 \cdot p_d \cdot l_x^2 = -8\ 003 \text{ kNm/m} \\ m_{sy} &= -0,05236 \cdot p_d \cdot l_x^2 = -5\ 090 \text{ kNm/m} \end{aligned}$$

To optimize the load distribution, compartments are introduced in the upper left ballast room and the floor and wall thickness is increased to 0,75 m. This is shown in Figure O.4.

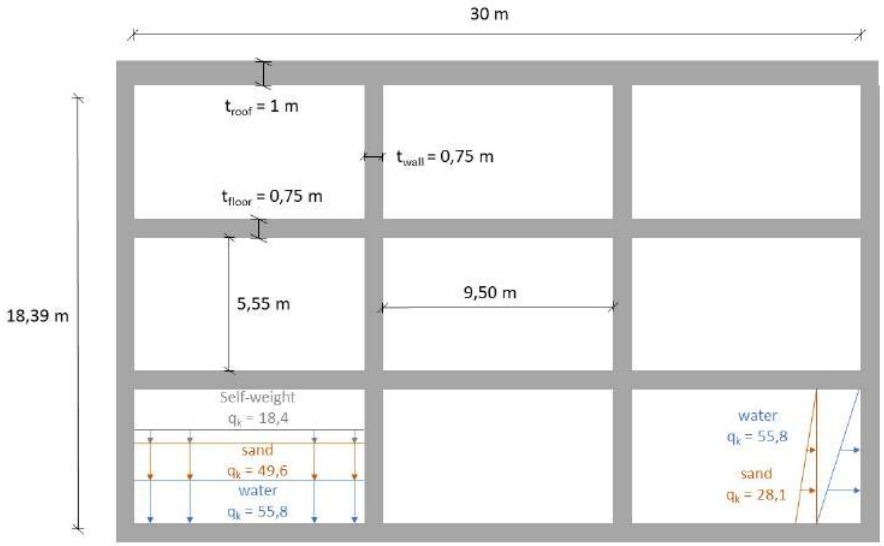

Figure O.4: Compartmentalised upper left ballast room.

For a floor, the design load now is $q_d = 1,35 * 55,8 + 49,6 + 18,4 = 167,1$ kN/m^2 and the ratio l_y / l_x = 14,63 / 14,11 = 1,04.

For the different support configurations, the bending moments are:

Plate type I:

$$m_{vx} = 0,0715 \cdot p_d \cdot l_x^2 = 1\ 078 \text{ kNm/m}$$
$$m_{vy} = 0,0297 \cdot p_d \cdot l_x^2 = \quad 447 \text{ kNm/m}$$

Plate type II:

$$m_{vx} = \quad 0,0338 \cdot p_d \cdot l_x^2 = \quad 510 \text{ kNm/m}$$
$$m_{vy} = \quad 0,0111 \cdot p_d \cdot l_x^2 = \quad 167 \text{ kNm/m}$$
$$m_{sx} = -0,0747 \cdot p_d \cdot l_x^2 = -1\ 127 \text{ kNm/m}$$
$$m_{sy} = -0,0546 \cdot p_d \cdot l_x^2 = - \quad 823 \text{ kNm/m}$$

$$a_x \text{ / } l_x = 0,19 \mid a_x = 1,81\ m$$

$$a_y \text{ / } l_y = 0,14 \mid a_y = 1,98\ m$$

Plate type IV A:

$$\begin{aligned} m_{vx} &= 0,0483 \cdot p_d \cdot l_x^2 = 728 \text{ kNm/m} \\ m_{vy} &= 0,0156 \cdot p_d \cdot l_x^2 = 469 \text{ kNm/m} \\ m_{sy} &= -0,0704 \cdot p_d \cdot l_x^2 = -1\,529 \text{ kNm/m} \end{aligned}$$

$$a_y \,/\, l_y = 0,17 \mid a_y = 2,40\ m$$

Plate type IV B:

$$\begin{aligned} m_{vx} &= 0,0389 \cdot p_d \cdot l_x^2 = 612 \text{ kNm/m} \\ m_{vy} &= 0,0130 \cdot p_d \cdot l_x^2 = 985 \text{ kNm/m} \\ m_{sx} &= -0,0809 \cdot p_d \cdot l_x^2 = -2\,402 \text{ kNm/m} \end{aligned}$$

$$a_x \,/\, l_x = 0,20 \mid a_x = 1,90\ m$$

This means that the maximum bending moment occurring at the bottom of the plate is 1 078 kNm/m and the maximum bending moment occurring at the top of the plate is 1 529 kNm/m.

O.1.3 Bending moment capacity

To check whether the 0,75 m thick floor can handle the imposed bending moment, the cross-section in Figure O.5, including reinforcement, is proposed. A section of 1 m wide is taken, so the obtained moment per unit length needs no conversion.

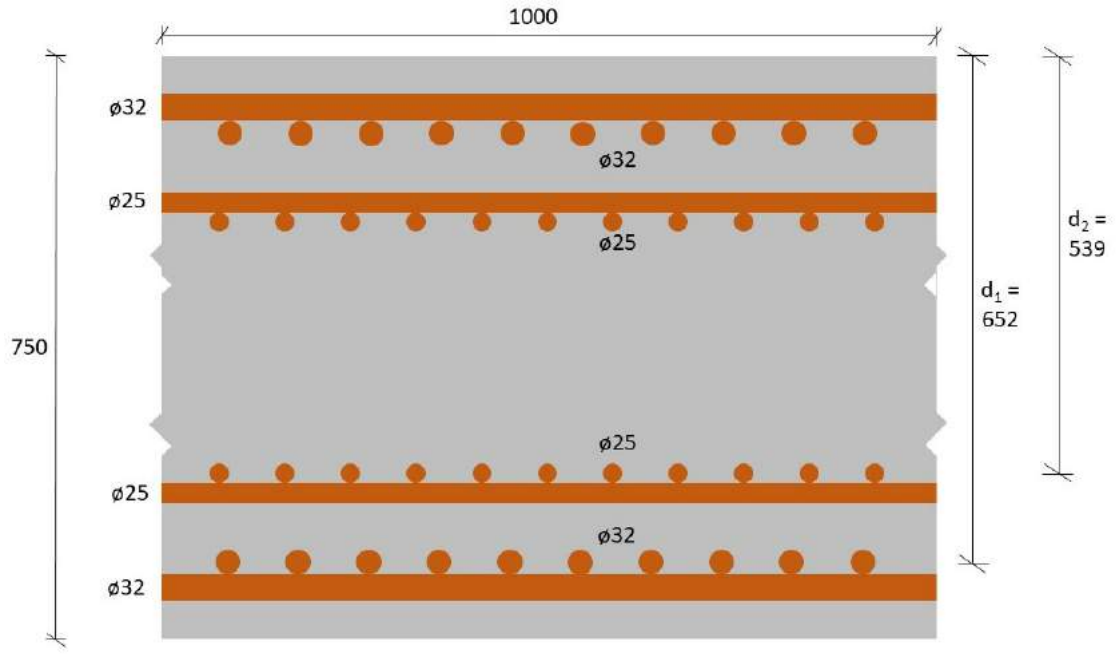

Figure O.5: Cross-section of inner floor 1.

Concrete cover
The concrete cover is determined by $c_{nom} = c_{min} + \Delta c_{dev}$ and Eurocode NEN-EN 1992-1-1+C2 (2011) is followed here.

$$c_{min} = MAX\{c_{min,b}; c_{min,dur} + \Delta c_{dur,\gamma} - \Delta c_{dur,st} - c_{dur,add}; 10\ mm\}$$

The $c_{min,b} = \phi$ = 32 mm.

With a lifetime of 100 years and being permanently exposed to salt water, the exposure class is XS2 and according to Eurocode Table 4.3N the construction class is S5. Construction class S5 and concrete class C50/60 leads to a $c_{min,dur}$ = 45 mm.

$\Delta c_{dur,\gamma}$ & $\Delta c_{dur,st}$ & $c_{dur,add}$ = 0 mm, according to the National Annex to NEN-EN-1992-1-1. From this it follows that c_{min} = 50 mm.

To compensate for construction tolerances, the Δc_{dev} = 5 mm, so the total concrete cover c_{nom} = 50 mm.

Arithmetic failure moment
To determine a general formula for the bending moment capacity, the stress-strain distributions for concrete and steel in the ultimate limit state should be known. For concrete C50/60 and steel B500, the arithmetic compressive strength of concrete f_{cd} = 50/1,5 = 33,3 N/mm^2 and the arithmetic tensile strength of the reinforcement steel f_{yd} = 500/1,15 = 435 N/mm^2. The ultimate tensile strain of concrete ϵ_{cu3} = 3,5 ‰. See Figure O.6.

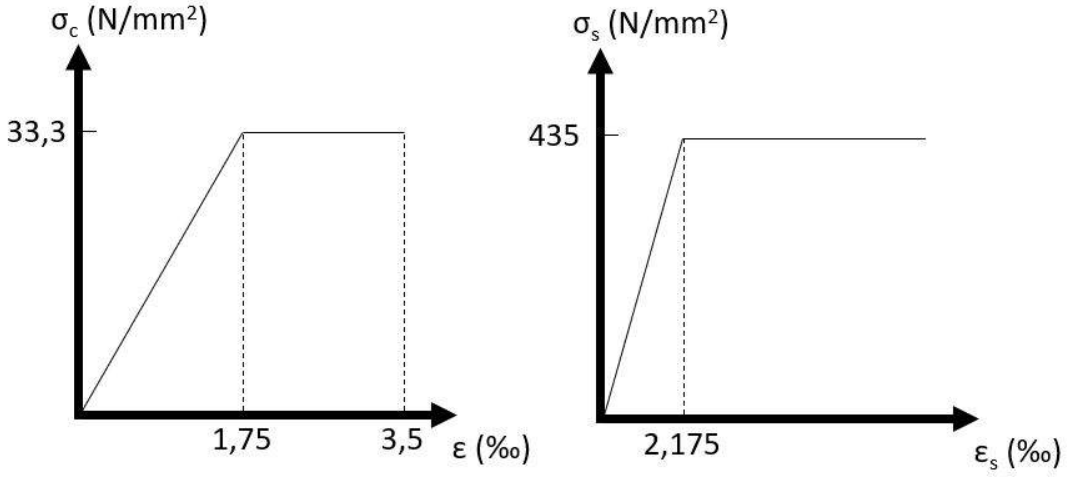

Figure O.6: Stress strain relations for concrete C50/60 and steel B500.

When the ultimate tensile strain of concrete is reached, the stress and strain distribution of the concrete compressive area are as in Figure O.7.

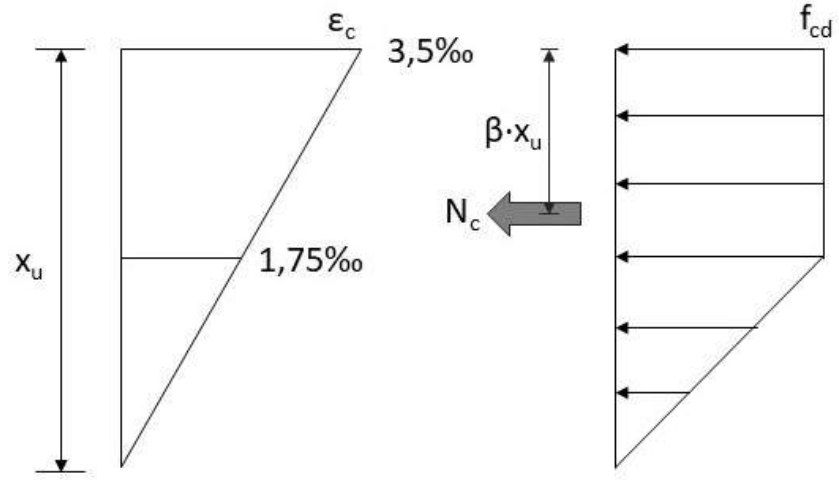

Figure O.7: Stress strain distributions in the concrete compressive area, after the ultimate tensile strain is reached.

Where;

$$N_c = \alpha \cdot b \cdot x_u \cdot f_{cd}$$

The fullness factor α = 0,75 and the distance factor β = 0,39. This concrete force should make an equilibrium with the steel yield force;

$$N_{yd} = A_s \cdot f_{yd}$$

This leads to;

$$x_u = \frac{A_s \cdot f_{yd}}{0,75 \cdot f_{cd} \cdot b}$$

Since we know the point of engagement of the concrete compressive force, the internal lever arm z equals;

$$z = d - 0,39x_u$$

The Eurocode gives for the bending moment capacity;

$$M_{Rd} = A_s \cdot f_{yd} \cdot z$$

Which becomes, with the herefore described relations, and $\rho = \frac{A_s}{b \cdot d}$;

$$M_{Rd} = A_s \cdot f_{yd} \cdot d \cdot \left(1 - 0,52 \cdot \rho \cdot \frac{f_{yd}}{f_{cd}}\right)$$

Bending moment resistance of the cross section
For the outer layer of reinforcement showed in Figure O.5, the steel cross section A_s = $10 \cdot 14 \cdot \pi \cdot 32^2$ = 8 042 mm^2. The spacing between the bars is 60 mm.

The effective height d = 750 - 50 - 32 - 0,5 * 32 = 652 mm. The reinforcement ratio $\rho = \frac{8\,042}{1000 \cdot 652} = 0,0123\ \ 1,23\%$. The reinforcement area is between the minimum and maximum value imposed by EC2;

$$A_{s,min} = 0,26 \cdot \frac{f_{ctm}}{f_{yk}} \cdot b_t \cdot d = 0,26 * \frac{4,1}{500} * 1\,000 * 652 = 1\,369\ mm^2$$

$$A_{s,max} = 0,04 \cdot A_c = 0,04 * 1000 * 652 = 26\,080\ mm^2$$

This leads to a bending moment resistance of
$M_{Rd;1} = 8\,042 * 435 * 652 * \left(1 - 0,52 * 0,0123 * \frac{435}{33,33}\right)$ = 2 090 E06 Nmm = 2 090 kNm.

The inner reinforcement layer has diameter ϕ 25 mm. The bending moment resistance of the second layer will be added to the first one, to determine the bending moment resistance of the cross section.

The effective height of the second row, ϕ 25 mm, is d = 750 - 50 - 2x32 - 60 - 25 - 0,5x25 = 539 mm. The bending moment resistance of the second row is then $M_{Rd;2}$ = 1 180 kNm. In total the bending moment resistance on top becomes 1 180 + 2 090 = 3 270 kNm. With an acting bending moment of 1 529 kNm/m, the unity check becomes 0,47.

O.1.4 ULS Shear force capacity

Secondly, in ULS, the shear force capacity has to be checked. According to Figure O.8 the shear force at the line supports (assumed there the maximum shear force occurs) has a maximum value of $\frac{167,1 \cdot 9,5}{2}$ = 794 kN/m.

The shear force capacity of concrete without shear reinforcement is given by:

$$V_{Rd,c} = \left[C_{Rd,c} \cdot k \cdot (100 \cdot \rho_l \cdot f_{ck})^{1/3} + k_1 \cdot \sigma_{cp}\right] \cdot b_w \cdot d$$

No normal force is assumed in the cross section, so σ_{cp} = 0. According to Eurocode 2, $C_{Rd,c} = \frac{0.18}{\gamma_c}$ = 0,12. The value k = $1 + \sqrt{\frac{200}{d}} \leq 2,0$, k = 1,55. The reinforcement ratio and area are already known, so $V_{Rd,c}$ = 583,7 kN/m, which is not sufficient.

The shear force capacity of a concrete cross section as shown in Figure O.5, after shear reinforcement is added, is the lowest value of either:

$$V_{Rd,s} = \frac{A_{sw}}{s} \cdot z \cdot f_{ywd} \cdot \cot(\theta)$$

$$V_{Rd,max} = \frac{\alpha_{cw} \cdot b_w \cdot z \cdot \nu_1 \cdot f_{cd}}{\cot(\theta) + \tan(\theta)}$$

No prestressing steel is present in the cross-section, meaning α_{cw} = 1. The considered width of the concrete section b_w = 1 000 mm and the internal lever arm z is determined by $z = d - 0,39 \cdot x$. Taking the two reinforcement layers, the total steel area A_s = 13 442 mm^2. The concrete compressive zone then equals $x = \frac{A_s \cdot f_{yd}}{0,75 \cdot f_{cd} \cdot b}$ = 234 mm. Resulting in z = 510 mm. The value of the angle between the pressure diagonal of concrete and the axis of the beam perpendicular to the shear force, θ, is between $1 \leq \cot\theta \leq 2,5$. The lower limit 45°is chosen as starting point. Lastly, ν_1 = 0,6 for this concrete class.

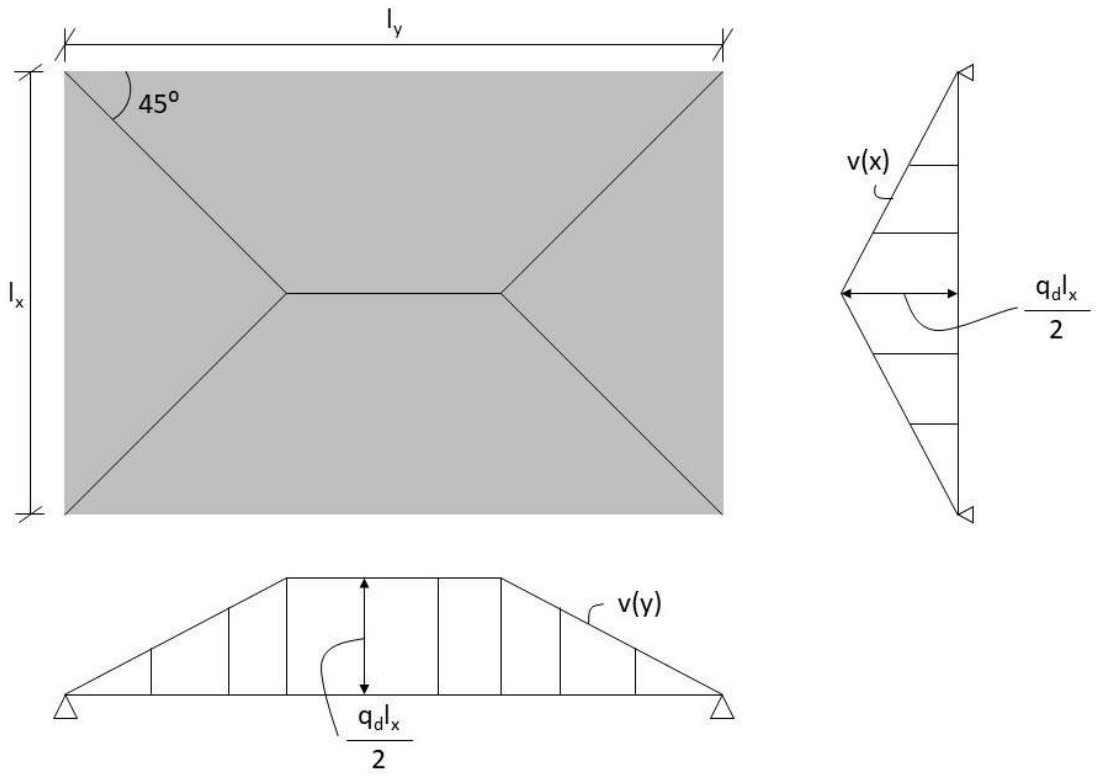

Figure O.8: Reaction forces on the line supports of a two-way spanning slab.

The above described values lead to $V_{Rd,max} = \frac{1{,}0*1\ 000*510*0{,}6*33{,}33}{\cot(45)+\tan(45)}$ = 5 100 kN/m. It is safe to assume that this will not be governing.

By setting the centre to centre spacing of the shear reinforcement to 200 mm, an area of 700 mm^2 of shear reinforcement is required to obtain $V_{Rd,s} = \frac{750}{200} \cdot 510 \cdot 435 \cdot \cot(45)$ = 832 kN/m.

O.1.5 SLS crack width check

EC2 Table 7.1N, national appendix, recommends for exposure class XS2 a maximum crack width $w_{max} \leq 0,20$ mm.

The EC proposed the following formula for crack width:

$$w_k = s_{r,max} \cdot (\epsilon_{sm} - \epsilon_{cm}) \tag{O.1}$$

In which: $s_{r,max}$ is the maximum crack distance;

ϵ_{sm} is the average elongation in the reinforcement under the applicable load combination, including the effect of imposed deformations and taking into account the effects of "tension stiffening". Only the elongation relative to the zero strain of the concrete on the same level is taken into account;

ϵ_{cm} is the average concrete strain between the cracks.

$\epsilon_{sm} - \epsilon_{cm}$ can be calculated according to:

$$\epsilon_{sm} - \epsilon_{cm} = \frac{\sigma_s - k_t \cdot \frac{f_{ct,eff}}{\rho_{p,eff}} \left(1 + \alpha_e \cdot \rho_{p,eff}\right)}{E_s} \geq 0,6 \cdot \frac{\sigma_s}{E_s} \tag{O.2}$$

And $s_{r,max}$ is given by:

$$s_{r,max} = k_3 \cdot c + k_1 \cdot k_2 \cdot k_4 \cdot \phi \,/\, \rho_{p,eff} \leq MAX\{(50 - 0,8 \cdot f_{ck}) \cdot \phi; 15 \cdot \phi\} \quad \text{(O.3)}$$

No prestressing steel is present, meaning α_{cw} = 1. The width assessed equals 1 m and the ν_1, a strength reduction factor for concrete cracked by shear force, is 0,6 for f_{ck} < 60 MPa.

Combining the two reinforcement layers $x_u = \frac{13\,442*435}{0{,}75*33{,}33*1\,000}$ = 234 mm. It follows that z = d - 0,39 x_u = 510 mm.

k_1 = 0,8
k_2 = 0,5
k_3 = 3,4
k_4 = 0,425

$\phi_{eq} = \frac{n_1 \cdot \phi_1^2 + n_2 \cdot \phi_2^2}{n_1 \cdot \phi_1 + n_2 \cdot \phi_2} = \frac{10*32^2 + 12*20^2}{10*32 + 12*20}$ = 26,86°

$s_{r,max} = 3,4 * 50 + 0,8 * 0,5 * 0,425 * 26,86 \,/\, 0,01841 \leq MAX\{(50 - 0,8 * 50) * 26,86 \;;\; 15 * 26,86\} = 402,9$ mm

For the steel tension σ_s in SLS, the characteristic load should be taken (without safety factor). According to the tables, with a load q_k = 123,8 N/mm^2 the maximum bending moment occurs on the top side and has a value of M_{Ed} = 1 780 kNm/m.

The stress present in the steel can be determined via:

$$\sigma_s = \frac{M_{Rd}}{A_s \cdot z}$$

Where z = d - (1/3)x

And $\frac{x}{d} = -\alpha_e \cdot \rho_{p,eff} + \sqrt{\left(\alpha_e \cdot \rho_{p,eff}\right)^2 + 2 \cdot \alpha_e \cdot \rho_{p,eff}}$

$\alpha_e = \frac{E_s}{E_{cm}} = \frac{200\,000}{37\,000} = 5,4$

$\rho_{p,eff} = 0,0123 + 0,0069 = 0,0192$

The effective height should be determined from the rebar closest to the surface, since this has the largest impact on the crack development. $d = \frac{684*0{,}0123 + 566*0{,}0069}{0{,}0123 + 0{,}0069}$ = 641,6 mm.

This means that x = 564 mm, and so the $\sigma_s = \frac{1\,780E06}{11\,812*564} = 267$ N/mm^2.

k_t is a factor depending on the duration of the load, where 0,6 is for short term loading and 0,4 is for long term loading. The latter should be used in this case.

$f_{ct,eff}$ depends on when the cracks are anticipated and equals either f_{ctm} or $f_{ctm}t$. Since the caisson is first constructed without ballast material, shipped to the final location and only then filled with ballast material, the value f_{ctm} = 4,1 N/mm^2 can be used.

This results into a $\epsilon_{sm} - \epsilon_{cm} = \frac{\sigma_s - k_t \cdot \frac{f_{ct,eff}}{\rho_{p,eff}}\left(1 + \alpha_e \cdot \rho_{p,eff}\right)}{E_s} \geq 0,6 \cdot \frac{\sigma_s}{E_s} = \frac{267 - 0{,}4 \cdot \frac{4{,}1}{0{,}0192}\left(1 + 5{,}4 \cdot 0{,}0192\right)}{200\,000} = 8,45E-04 \geq 0,6 \cdot \frac{267}{200\,000} = 8,01E-04$

The resulting crack width then becomes $w_k = 402,9 * 8,45E-04$ = 0,341 mm, which does not meet the criterion of 0,20 mm.

O.2 Outer Wall 1

The governing loading situation on 'outer wall 1' (on the seaside) is acting on the lowest part of the wall. It is presented in Figure O.9 and has dimensions l_x = 5,0 m and l_y = 14,11 m, giving a ratio of 2,82.

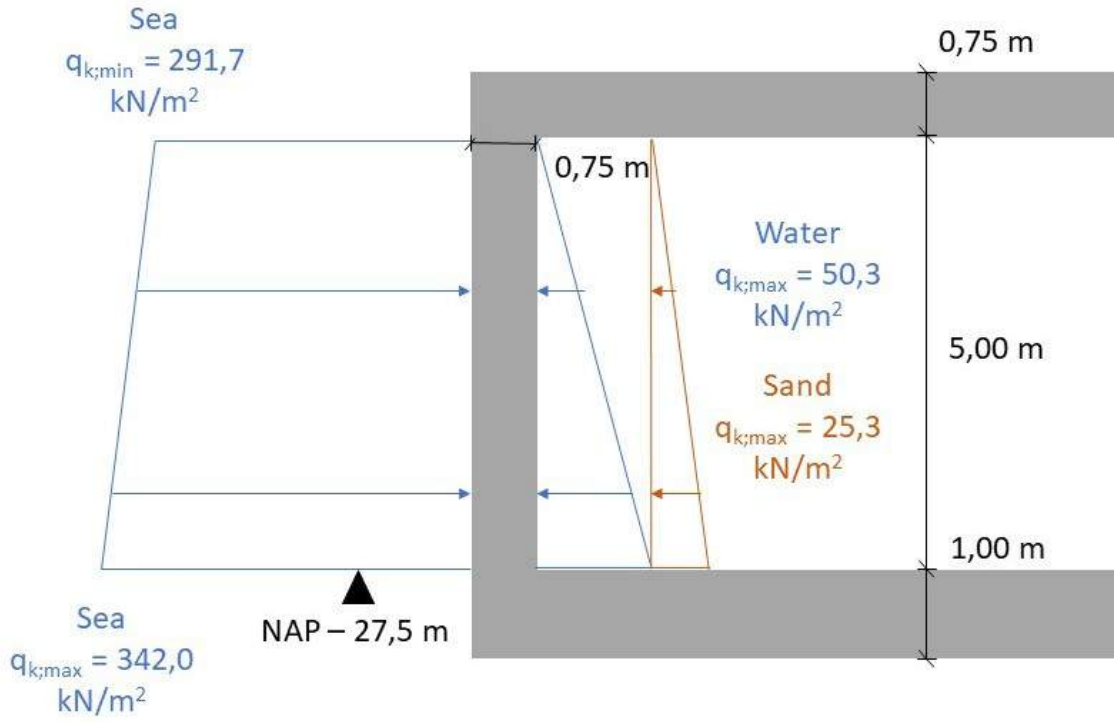

Figure O.9: Loading situation on 'outer wall 1'.

The characteristic loads on the wall are $q_{k,top}$ = 291,7 kN/m^2 and $q_{k,bottom}$ = 266,4 kN/m^2. This will be modelled by an evenly distributed load of q_k = 279,1 kN/m^2, leading to q_d = 376,9 kN/m^2.

The maximum positive bending moment comes from plate type I and m_{vx} = 232 kNm/m. The maximum negative bending moment follows from plate type IV A and m_{sy} = 235 kNm/m.

The shear force distribution is different from the evenly distributed load. When assessed as a simply supported beam, the maximum occurring shear force V_{Ed} = 956 kN/m. To be able to take up that force is to increase the area of shear reinforcement to 900 mm^2 per meter width. This increases the shear force capacity to $V_{Rd,s}$ = 999 kN/m.

O.3 Inner Wall 1

The loading on 'inner wall 1' is already displayed in Figure O.4. It is a triangular load that will be replaced by an evenly distributed load of q_k = 42 kN/m^2, leading to q_d = 68 kN/m^2.

The length l_x = 5,55 m and l_y = 14,11 m, leading to a ratio of 2,54. The governing bending moment follows from plate type IV A and is m_{sy} = 235 kNm/m. The maximum acting shear force is V_{Ed} = 189 kN/m. These values require no further checking.

O.4 Inner Wall 2

The loading on 'inner wall 2', 'inner floor 2' and 'outer wall 2' is presented in Figure O.10.

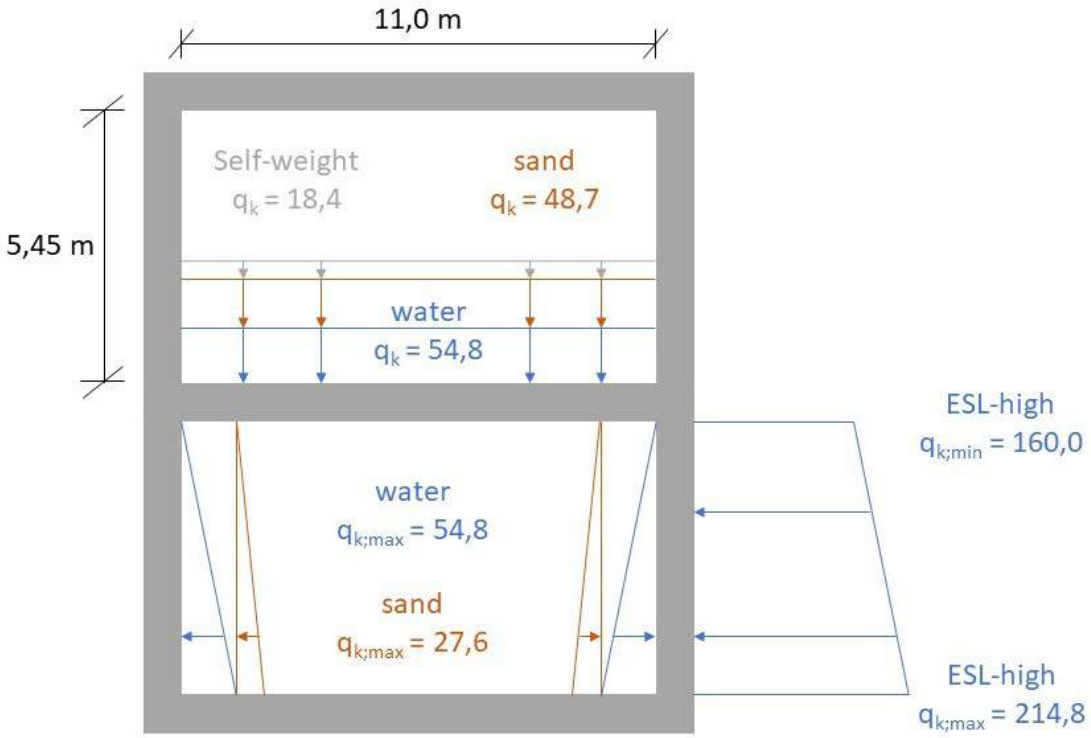

Figure O.10: Loading on the floor and walls for the governing elements on the lakeside.

In this section only 'inner wall 2' is treated. The length l_x = 5,45 m and l_y = 14,11 m, which gives a ratio of 2,59. The characteristic maximum load on the wall $q_{k,max}$ = 82,4 kN/m^2, which gives an evenly distributed load of q_k = 41,2 kN/m^2 and a design load of q_d = 55,6 kN/m^2.

The design load on 'inner wall 2' results in a maximum bending moment of m_{sy} = 185 kNm/m from plate type IV A and maximum occurring shear force V_{Ed} = 152 kN/m.

O.5 Inner Floor 2

As can be seen in Figure O.10, 'inner floor 2' has length l_x = 11,0 m and l_y = 14,11 m, meaning a ratio l_x/l_y = 1,28. The characteristic loading q_k = 121,9 kN/m^2, with design load q_d = 164,6 kN/m^2.

The maximum occurring bending moment results from plate type IV A and has as a value m_{sy} = 1 550 kNm/m. The shear force at the edge of the plate is V_{Ed} = 905 kN/m.

O.6 Outer Wall 2

Lastly, 'outer wall 2' has to be checked. Again, Figure O.10 shows the loading situation. The lengths and ratio are equally to 'inner wall 2'.

The resulting load on the top side is 160,0 kN/m^2 and on the bottom side 132,4 kN/m^2. The equal evenly distributed load then q_k = 146,2 kN/m^2 and the design load is q_d = 197,4 kN/m^2.

The maximum bending moment follows again from plate type IV A and is m_{sy} = 657 kNm/m and the maximum shear force V_{Ed} = 538 kN/m.

O.7 Stability Checks

In this section, the stability checks will be performed once more, but now for the improved design.

Rotational stability
The loading on the caisson has not changed, so in the governing loading situation the overturning moment $M_{overturning}$ = 622 320 kNm/m. Since the weight of the caisson has increased, due to thicker walls and floor (concrete is heavier than saturated sand), the stabilising moment increases to $M_{resisting}$ = 855 784 kNm/m. The result is an unity check of 0,70.

The highest eccentricity that in a loading situation is obtained is 7,05 m and so the effective width is 35,2 m.

Sliding resistance
The horizontal loading on the caisson remains H_{Ed} = 9 536 kN/m and the sum of the vertical forces increases to ΣV = 18 132 kN/m.

Then, the sliding resistance for the prefabricated caisson becomes $H_{Rd,prefab}$ = 7 400 kN/m. The sliding resistance for the in-situ constructed caisson is $H_{Rd,in-situ}$ = 12 230 kN/m. Resulting are unity checks of respectively 1,29 and 0,78.

Bearing capacity
Due to the increase of the effective width, compared to the original caisson, and the increase of the weight of the caisson, the bearing capacity becomes 850 kN/m^2 at interface 1 and 549 kN/m^2 at interface 2. Respectively, the design load equals 515 kN/m^2 and 499 kN/m^2 and the unity checks become 0,61 and 0,91.

APPENDIX P

SOFTWARE

Here all used software is discussed.

P.1 Hydra-NL

(RWS-WVL Waterkeringen 2018)

Hydra-NL is a probabilistic model at which the parameters (like sea water levels, wind speed, lake levels, discharge etc.) that lead to the hydraulic loading on water barriers (water levels and wave heights) are stochastic variables. For every loading system the databases 'physics' and 'statistics' are available. The databases 'physics' provide the link between the local water level and the basic stochastic variables (for example sea water level, discharge, wind speed). The statistics files describe the marginal statistics of the basic stochastic variables. Hydra-NL brings these marginal statistics together to the on-site loading statistics of the output locations, or the combined statistics of water level and waves. This takes into account the correlations between variables and the correlations over time. For an on-site calculation of a structure, a shore location must be chosen in Hydra-NL, after which the model generates the combined load statistics for the structure.

The current version 2.4.1 of Hydra-NL has three modes:

- Assessment mode, in which the databases 'physics' (these are the hydraulic boundary conditions databases) from the WBI2017 are calculated;
- design mode, in which years of vision 2050 and 2100 are calculated with adapted statistics files and sometimes also adapted databases 'physics'. The statistics files incorporate the effect of climate change on the statistics on discharge and/or sea water / lake level. For the upstream rivers, the databases 'physics' for design deviate from the databases for assessment due to a different discharge distribution over the split points. In addition, it is conceivable that people want to take spatial measures into account. Reference is made to the calculation recipes from OI2014 (Deltares 2018b) for the correct (combination of) physics and statistics databases;
- test mode, in which you can work with your own climate scenarios (to be processed by the user in customized statistics files).

For the purpose of the failure mechanism *height*, the program determines the Hydraulic Load Level (HLL), in other words the height of a dyke body or structure that corresponds to a specified overtopping / overflow discharge and associated probability of exceedance. The strength parameter - the critical overtopping or overflow discharge - is treated as a deterministic variable in the model. For designing, the program is therefore immediately suitable for determining the required crown height for the structure. Conversely, the program can also calculate the probability of failure if the crown height and overtopping / overflow discharge are specified. This is useful for the legal assessment.

In addition, Hydra-NL can, for the failure mechanisms *non-clusure*, *piping* and *structural failure*, based on marginal statistics calculate exceeding frequency lines of outside water level and waves for each output location. Using Hydra-NL 2.4.1, it is not possible to determine the combined water level and wave statistics required for *structural failure*.

For this project the WBI2017 database for the Dutch Coast - South (v03) is used from the ftp server of the WBI2017.

P.2 Riskeer (Ringtoets)

(RWS-WVL Waterkeringen 2018)

Riskeer (Ringtoets) is a software application that supports the WBI-2017 assessment. With Riskeer, hydraulic loads can be determined and a failure probability can be calculated for the failure mechanisms *height*, *non-closure* and *structural failure*. Here, the user enters into Riskeer a schematization of the strength of (parts of) the structure, after which with the failure mechanism model an analysis of the strength in relation to the loads can be performed. The result is a chance of failure for the relevant failure mechanism. The failure mechanism *piping* with structures is not included in Riskeer.

With the Riskeer version 17.2.1 currently in force, it is only possible to determine a chance of failure for a given construction. It is not possible to specify a target failure probability and thereby determine the required value of one of the input parameters (for example, the critical flow rate for the soil protection or the required strength of a structural component). In addition, it is not possible in Riskeer version 17.2.1 to calculate with a different year of vision than 2023 (the year of vision of the assessment). This means that Riskeer currently offers few options for carrying out a design verification.

For this project trajectories 20-1 and 25-1 are analyses, downloaded in July 2019.